EMEP Report 1/2013
Date: August 7, 2013

METEOROLOGISK INSTITUTT
Norwegian Meteorological Institute

Transboundary Acidification, Eutrophication and Ground Level Ozone in Europe in 2011

EMEP/MSC-W:	Michael Schulz, Michael Gauss, Anna Benedictow, Jan Eiof Jonson, Svetlana Tsyro, Ágnes Nyíri, David Simpson, Birthe Marie Steensen, Heiko Klein, Álvaro Valdebenito, Peter Wind, Alf Kirkevåg, Jan Griesfeller, Jerzy Bartnicki, Dirk Olivié, Alf Grini, Trond Iversen, Øyvind Seland, Valiyaveetil S. Semeena, Hilde Fagerli
EMEP/CCC:	Wenche Aas and Anne-Gunn Hjellbrekke
EMEP/CEIP:	Katarina Mareckova and Robert Wankmüller
NILU:	Philipp Schneider, Sverre Solberg, Tove Svendby, Li Liu
CCE/RIVM:	Maximilian Posch
CEH:	Massimo Vieno, Stefan Reis
UW:	Maciej Kryza, Malgorzata Werner, Kinga Walaszek

EMEP Status Report 2013; August 7, 2013

ISSN 1504-6109 (print)
ISSN 1504-6192 (on-line)

Executive Summary

This report has been prepared for the thirty-seventh session of the Steering Body to EMEP. It presents the progress of activities within EMEP in 2012 and 2013 with respect to acidification, eutrophication and ground level ozone. The status of transboundary depositions in Europe in 2011 is presented, and main differences compared to other years are discussed.

This report is accompanied by a series of other reports: i) Individual reports for each country in EMEP presenting calculated trends (2000-2011+2020), source-receptor relationships and comparison of model results and measurements in the actual country[1] (only on web); ii) supplementary, electronic format, source-receptor table data for all perturbation runs, including PM components (only on web); iii) a report describing EMEP/MSC-W model performance for acidifying and eutrophying components and photo-oxidants in 2011[2] (only on web); iv) a report documenting progress with respect to particulate matter modelling and measurements[3]; and v) a technical report documenting the performance of regional models (including the EMEP MSC-W model) on different resolutions [4].

Air pollution in Europe in 2011

Air concentrations, depositions and exceedances have been calculated for the year 2011 with the EMEP MSC-W model, based on the latest emission data submitted to CEIP (June 2013) and on comprehensive meteorological data from the European Centre for Medium-range Weather Forecasts. Large areas of the extended EMEP domain in 2011 remain at risk of eutrophication and critical load exceedances. In terms of acidification, less areas are at risk, although several regions of critical load exceedances have been identified. The inter-annual variability of air concentrations and depositions is mainly driven by changes in emissions and changes in meteorology. From 2010 to 2011, anthropogenic emissions of SO_x in the extended EMEP domain increased by 3.7%, although this is due to substantial increases in a small number of countries only. Decreases in volcanic emissions (not considering the Grímsvötn eruption) led to a total increase in SO_x emissions from 2010 to 2011 of 2.6%. In spite of this

[1]EMEP/MSC-W Data Note 1/13. Transboundary data by main pollutants (S, N, O3) and PM.

[2]Supplementary material to EMEP Status Report 1/13. EMEP/MSC-W model performance for acidifying and eutrophying components and photo-oxidants in 2011. Joint MSC-W & CCC Report

[3]EMEP Status Report 4/13. Transboundary Particulate Matter in Europe. Joint CCC & MSC-W & CEIP & CIAM Report

[4]EMEP/MSC-W Technical Report 1/13 Joint TFMM & MSC-W Report.

increase, the total deposition of sulphur in the extended EMEP domain decreased by 5.5%, which can be explained by (in this context) favourable meteorological conditions, such as the dryer conditions in large areas, effectively reducing the amount of wet deposition within the domain. NO_x emissions were reduced by 4.2% from 2010 to 2011, while the deposition of oxidized nitrogen, on average, decreased by as much as 9.3% during the same period, due to similar reasons as in the case of sulphur deposition. In the case of reduced nitrogen, emissions of NH_3 increased by 2.9% while the deposition of reduced nitrogen decreased slightly, by about 0.7%. As far as ozone is concerned, air quality indicators such as SOMO35 decreased on average, although this, too, was mainly a meteorological effect (e.g. due to the cooler summer in Western Russia and many parts of Europe in 2011, as compared to 2010). Nevertheless, the benefits of emission reductions in ozone precursors are shown in model calculations to contribute to the improvement of air quality in many countries. In comparison to the long-term average of 2000-2009, ozone levels during the summer of 2011 were fairly low, and even lower than in 2010.

Evolution of the EMEP MSC-W model system

The EMEP MSC-W model is continuously updated in order to incorporate new science, to improve structure or ease of use, and developed for different applications (e.g. forecasting, global modelling, nested model runs). The most updated version is used for this year's report, and this version is also released as open source code via the EMEP web page in April 2013. It appears that the quality of the model results is robust but that there also changes from year to year due to the evolution in meteorological conditions and observational data coverage. The performance of the model has been also compared through a trend run with earlier reported verification results. The trend study with this historical perspective also reveals, for the first time, that the model has clearly improved over time for most parameters investigated, and for most years. A training course for EMEP MSC-W model understanding and usage[5] was organised at MSC-W in April 2013 with 30 participants from 9 countries. The course shall be repeated in two years to support broader usage and joint development of this fundamental EMEP tool, as well as scientific collaboration among the parties of the LRTAP convention. A particular aspect of this year's model progress is the coupling to boundary conditions from different resolutions including usage of WRF meteorological input data. For better diagnostics regarding aerosol loads, optical depth calculations have been added to the standard model. Further work has been devoted to the foreseen modification of the EMEP grid. A trade-off has to be made between the wish for as high resolution as possible and the computational costs. A summarized argumentation, balancing between political needs, scientific needs and technical feasibility, as of 2013 and preparing for the years to come, suggests a 0.1×0.1–degree grid for reporting emissions and a slightly more flexible grid for application purposes.

Simulated and observed trends of air pollution from 1990-2011

Trends of eutrophying and nutrifying substances have been simulated with this report's EMEP MSC-W model version for 1990 and the period 2000–2011, using consistent meteorology from one ECMWF cycle version. The model data have been compared to European measurements at all sites contained in the EMEP/EBAS database for gases, aerosol components

[5] `https://wiki.met.no/emep/page1/emepmscw_opensource#training_course_presentations_24-26_april_2013`

and deposition, which consists in a considerable extension to the standard EMEP MSC-W model verification with daily data. This extended trend evaluation is consistent with the reported trend evaluation as discussed in chapter 3, indicating that the daily data verification of the EMEP MSC-W model is robust. From 2000 to 2011 both SO_2 concentrations and sulphur deposition seem to decrease more in the EMEP MSC-W model simulation than in the observations (modelled: SO_2: -59% versus observed -33%; modelled S-deposition: -45% versus obsvered -39%). For NO_2 and total nitrate (HNO_3+NO_3^-) the model bias decreases from +5% (NO_2), respectively +20% (total nitrate) in 2000 to being absent in recent years on annual average. Interestingly no significant trend in bias is found for deposition of oxidised nitrogen. For the oxidised N parameters only deposition has decreased by -15% from 2000 to 2011, consistently in model and observations. Gaseous ammonia trends are currently impossible to evaluate due to considerable network fluctuations and changes in measurement quality. Reduced nitrogen in deposition has almost no significant trend in the same ten–year period, while ammonium aerosol concentration seem to decline by ca. 10%. Seasonal bias in deposition has been found for oxidised nitrogen, with too high model values in summer and too low in winter, while reduced nitrogen deposition seems to be too low in summer in the model.

A particular study was done to demonstrate the effect of changing emissions and meteorology for deposition of nitrogen to the Baltic Sea, in support of the HELCOM convention. Source-receptor matrices from previous reports are used for all years from 1995 to 2010. Emissions from each year are multiplied with all source-receptor matrices, allowing to estimate a median deposition trend. Variation of N-deposition to the Baltic due to meteorological conditions can reach up to $\pm$15%. The reductions of the oxidised nitrogen deposition is relatively uniform among sub-basins and similar for the entire Baltic Sea basin, oscillating around 20%. For reduced nitrogen depositions, the reductions vary more among sub-basins, being significantly lower and of the order of 10%.

A particular comparison was carried out between SCIAMACHY NO_2 satellite data and the EMEP MSC-W model in order to test the data set's respective capabilities for estimating decadal trends in tropospheric NO_2 column over Europe. The EMEP MSC-W model trend map shows a much smaller number of grid cells with significantly increasing trends in eastern Europe. On the other hand, the areas of significantly decreasing NO_2 concentrations of around -4 % per year in most parts of central and western Europe have a more homogeneous and spatially contiguous structure in the EMEP-based trend map than in the SCIAMACHY trend map.

Finally a proposition is made in this report on how to further investigate and make use of observed and simulated trends, possibly in the framework of TFMM. Particular attention needs to be put on consistent observational data selection in the two recent decades. Model trends should be inspected with respect to such data selection. Inconsistency of instrumental records should be investigated for individual parameters, so that trends are not a result of changes in measurement method, or quality. Model bias trends with time or persistent seasonal bias over time should receive particular attention for a better understanding of trends and thus air quality policy achievements.

Global and regional model calculations

Within the framework of TF HTAP MSC/W is planning to run an extensive set of global (and partially regional) source receptor model runs later in 2013 as the HTAP emissions become available. In preparation several global and regional model test-runs have been made with this report's model version. The model runs have been made with 2010 emissions and with meteorological input data for 2008 and 2009. Additional global model runs have been made reducing the emissions in Europe, North America and China by 20%, demonstrating the effects of trans-continental pollution, focusing on surface ozone levels in Europe. Furthermore nested model runs have been made with future global 2030 emissions, utilizing the three latest European TSAP 2025 scenarios.

With lateral boundary concentrations nested from the global model calculations, regional model calculations have been made with present (2010) and the TSAP scenarios for future (2025) emissions. With present emissions CO and PM2.5 levels have been compared to measurements, demonstrating our modelling capability of attributing air pollution in Europe to sources outside the European continent. Compared to model calculations with present emission, the future emission scenarios result in marked improvements in European air quality. For boundary layer ozone the improvements are partially brought about by a decrease in future lateral boundary concentrations from the global model calculations as a result of future global emissions changes.

Interaction of short-lived climate forcers (SLCF) with air quality

Further work at MSC-W has been devoted to contribute to research on how the climate will change over the next decades, how air quality will be affected by the future climate change, and what measures are effective to mitigate air pollution and climate change? Emission estimates for the period from year 1850 to 2000 indicate that anthropogenic emissions of CO, NO_x, VOCs, and SO_2 have increased 10-fold or more, BC and NH_3 by a factor of 5, and OC by a factor of 2-3 (Lamarque et al., 2010). Although O_3 and aerosols exert a considerable radiative forcing on top of the atmosphere (RF), the largest anthropogenic impact on RF is still due to long-lived and well-mixed GHGs (CO_2, CH_4, and N_2O). For the period 1850-2000, Shindell et al. (2013) estimate a RF of +2.3 $\pm$0.2Wm^2 for well-mixed GHGs and +0.43$\pm$0.20Wm^2 for O_3, and an effective RF (including their indirect effects through clouds) of -1.2$\pm$0.5Wm^2 for aerosols. Global aerosol RF peaks in magnitude around year 1980 in most models. Published estimates of the aerosol forcing vary greatly, depending on what aerosol processes and components are accounted for, depending on the assumed pre-industrial and present-day reference year, etc. The uncertainty of RF and the climate impacts of the highly light absorbing Black Carbon aerosol (BC) is particularly large, firstly because there are huge uncertainties in the emissions of BC. Its atmospheric residence times and concentrations - especially as function of height, which is particularly important for the radiative effects - are also strongly dependent on the complex and not well understood interactions of BC with other aerosols and clouds. Results from 15 climate models submitted to CMIP5 and IPCC AR5 indicate that the global surface temperature will continue to increase towards year 2100, to in average ca. 2-5°C above the level of 1850, depending on the choice of scenario for emission of SLCF and GHG. Estimated warming over land areas is even higher. The equilibrium climate sensitivity (the temperature response to a sudden CO_2 doubling) of the Norwegian Earth System Model, NorESM, is in the lower range of the CMIP5 models. It therefore predicts a slightly weaker warming than the CMIP5 model average. The trend in the global historical temperature record is well captured in NorESM. This work enables further joint studies between EMEP and climate modelling to explore consequences of future emissions scenarios both for climate and air quality evolution.

Acknowledgments

This work has been funded by the EMEP Trust Fund. The development of the EMEP/MSC-W model has also been supported by the EU FP7 projects MACC-II, TRANSPHORM, ECLAIRE, ECLIPSE, PEGASOS, and IMPACT2C, the Nordic Council of Ministers, the Norwegian Space Centre and the Norwegian Ministry of the Environment.

The work presented here has benefited largely from the work carried out under the four EMEP Task Forces and in particular under TFMM.

The Working Group on Effects and its ICPs and Task Forces are acknowledged for their assistance in determining the risk of damage from air pollution. The Coordination Center for Effects (CCE) and Jean Paul Hettelingh have provided the latest data on critical loads.

Thanks are due to the Swedish SCARP programme for funding valuable contributions on the organic aerosol and dust modelling by Robert Bergström (University of Gothenburg, and SMHI, Sweden), and to the Swedish MERGE strategic project for funding work a Post-Doc (Abdulla Sakalli) working on improved biosphere treatment. Also to Massimo Vieno (CEH, UK) and Guus Velders (RIVM, Netherlands) for valuable comments on the EMEP MSC-W model code, and to Melissa Pfeffer (Icelandic Meteorological Office) for the advice on the volcanic emission estimates.

For development and application of the EMEP/WRF model, we are grateful for data provided by the MACC-II project, funded by the European Union under the 7th Framework Programme, the UK Department for the Environment, Food and Rural Affairs (Defra), the NERC Centre for Ecology and Hydrology (CEH), the EMEP programme under the UNECE LRTAP Convention, the Norwegian Meteorological Institute and the European Union projects NitroEurope IP and ECLAIRE. Support was also received from the University of Wroclav (UW) and the EU-China Environmental Governance Programme.

This work has received support from the Research Council of Norway (Programme for Supercomputing) through CPU time granted at the super computers at NTNU in Trondheim, the University of Tromsø, and the University of Bergen. IT infrastructure in general was available through the Norwegian Meteorological Institute. The CPU time made available by the ECMWF to generate meteorology has been of crucial importance for this year's status and trend calculations.

Contents

CHAPTER 1

Introduction

1.1 Purpose and structure of this report

The mandate of the European Monitoring and Evaluation Programme (EMEP) is to provide sound scientific support to the Convention on Long-range Transboundary Air Pollution (LRTAP), particularly in the areas of atmospheric monitoring and modelling, emission inventories, emission projections, and integrated assessment. Each year EMEP provides information on transboundary pollution fluxes inside the EMEP area, relying on information on emission sources and monitoring results provided by the Parties to the LRTAP Convention.

The purpose of the annual EMEP status reports is to provide an overview of the status of transboundary air pollution in Europe, tracing progress towards existing emission control Protocols and supporting the design of new protocols, when necessary. An additional purpose of these reports is to identify problem areas, new aspects and findings that are relevant to the Convention.

The present report is divided into four parts. Part I presents the status of transboundary air pollution with respect to acidification, eutrophication and ground level ozone in Europe in 2011. Part II summarizes recent development of the EMEP model system, while Part III deals with ongoing research work of relevance to the EMEP programme. Appendices A-C in Part IV contain basic information on 2011 emissions and emission trends in form of tables, and country-to-country source-receptor matrices with calculations of the transboundary contributions to pollution in different countries for 2011. Appendix D describes the country reports which are issued as a supplement to the EMEP status reports. Appendix E summarizes the changes of model performance between the current model version (rv4.4) and earlier model versions. Appendix F introduces the model evaluation report for 2011 (Gauss et al. 2013) which is available online and contains time-series plots of acidifying and eutrophying components (Nyíri et al. 2013), and ozone and NO_2 (Gauss and Hjellbrekke 2013). These plots are provided for all stations reporting to EMEP (with just a few exclusions due to data-capture or technical problems). This online information is complemented by numerical fields and other information on the EMEP website. The reader is encouraged to visit the website, `http://www.emep.int`, to access this additional information.

1.2 Definitions, statistics used

For sulphur and nitrogen compounds, the basic units used throughout this report are μg (S or N)/m^3 for air concentrations and mg (S or N)/m^2 for depositions. Emission data, in particular in some of the Appendixes, is given in Gg (SO_2) and Gg (NO_2) in order to keep consistency with reported values.

For ozone, the basic units used throughout this report are ppb (1 ppb = 1 part per billion by volume) or ppm (1 ppm = 1000 ppb). At 20°C and 1013 mb pressure, 1 ppb ozone is equivalent to 2.00 μg m^{-3} .

A number of statistics have been used to describe the distribution of ozone within each grid square:

Mean of Daily Max. Ozone - First we evaluate the maximum modelled concentration for each day, then we take either 6-monthly (1 April - 30 September) or annual averages of these values.

SOMO35 - The Sum of Ozone Means Over 35 ppb is the indicator for health impact assessment recommended by WHO. It is defined as the yearly sum of the daily maximum of 8-hour running average over 35 ppb. For each day the maximum of the running 8-hours average for O_3 is selected and the values over 35 ppb are summed over the whole year.

If we let A_8^d denote the maximum 8-hourly average ozone on day d, during a year with N_y days (N_y = 365 or 366), then SOMO35 can be defined as:

$SOMO35 = \sum_{d=1}^{d=N_y} \max\left(A_8^d - 35 \text{ ppb}, 0.0\right)$

where the `max` function evaluates $\max(A-B, 0)$ to $A-B$ for $A > B$, or zero if $A \leq B$, ensuring that only A_8^d values exceeding 35 ppb are included. The corresponding unit is ppb.days.

POD$_Y$ - Phyto-toxic ozone dose, is the accumulated stomatal ozone flux over a threshold Y, i.e.:

$$\text{POD}_Y = \int \max(F_{st} - Y, 0)\, dt \tag{1.1}$$

where stomatal flux F_{st}, and threshold, Y, are in nmol m^{-2} s^{-1}. This integral is evaluated over time, from the start of the growing season (SGS), to the end (EGS).

For the generic crop and forest species, the suffix gen can be applied, e.g. POD$_{Y,gen}$ (or $AF_{st}1.6_{gen}$) is used for forests. POD was introduced in 2009 as an easier and more descriptive term for the accumulated ozone flux. The definitions of AFst and POD are identical however, and are discussed further in Mills and Simpson (2010). See also Mills et al. (2011a) and Mills et al. (2011b).

AOT40 - is the accumulated amount of ozone over the threshold value of 40 ppb, i.e..

$AOT40 = \int \max(O_3 - 40 \text{ ppb}, 0.0)\, dt$

where the `max` function ensures that only ozone values exceeding 40 ppb are included. The integral is taken over time, namely the relevant growing season for the vegetation concerned. The corresponding unit are ppb.hours (abbreviated to ppb.h). The usage and definitions of AOT40 have changed over the years though, and also differ between UNECE and the EU. LRTAP (2009) give the latest definitions for UNECE work, and describes carefully how AOT40 values are best estimated for local conditions (using information on real growing seasons for example), and specific types of vegetation. Further, since O_3 concentrations can have strong vertical gradients, it is important to specify the height of the O_3 concentrations used. In previous EMEP work we have made use of modelled O_3 from 1 m or 3 m height, the former being assumed close to the top of the vegetation, and the latter being closer to the height of O_3 observations. In the Mapping Manual (LRTAP 2009) there is an increased emphasis on estimating AOT40 using ozone levels at the top of the vegetation canopy.

Although the EMEP/MSC-W model now generates a number of AOT-related outputs, in accordance with the recommendations of LRTAP (2009) we will concentrate in this report on two definitions:

AOT40$_f^{\mathbf{uc}}$ - AOT40 calculated for forests using estimates of O_3 at forest-top (uc: upper-canopy). This AOT40 is that defined for forests by LRTAP (2009), but using a default growing season of April-September.

AOT40$_c^{\mathbf{uc}}$ - AOT40 calculated for agricultural crops using estimates of O_3 at the top of the crop. This AOT40 is close to that defined for agricultural crops by LRTAP (2009), but using a default growing season of May-July, and a default crop-height of 1 m.

In all cases only daylight hours are included, and for practical reasons we define daylight for the model outputs as the time when the solar zenith angle is equal to or less than 89°. (The proper UNECE definition uses clear-sky global radiation exceeding 50 W m^{-2} to define daylight, whereas the EU AOT definitions use day hours from 08:00-20:00. Model outputs are also available using the EU definition, but not presented here).

The AOT40 levels reflect interest in long-term ozone exposure which is considered important for vegetation - critical levels of 3 000 ppb.h have been suggested for agricultural crops and natural vegetation, and 5 000 ppb.h for forests (LRTAP 2009). Note that recent UNECE workshops have recommended that AOT40 concepts are replaced by ozone flux estimates for crops and forests. (See also (Mills and Simpson 2010)).

This report includes also concentrations of particulate matter (PM). The basic units throughout this report are $\mu g/m^3$ for PM concentrations and the following acronyms are used for different components to PM:

SIA - secondary inorganic aerosols, defined as the sum of sulphate (SO_4^{2-}), nitrate (NO_3^-) and ammonium (NH_4^+). In the EMEP/MSC-W model SIA is calculated as the sum: SIA= SO_4^{2-} + NO_3^-(fine) + NO_3^-(coarse) + NH_4^+.

SS - sea salt.

PPM denotes primary particulate matter, originating directly from anthropogenic emissions. One usually distinguishes between fine primary particulate matter, $PPM_{2.5}$, with dry aerosol diameters below 2.5 μm and coarse primary particulate matter, PPM_{coarse} with dry aerosol diameters between 2.5 μm and 10 μm.

PM$_{2.5}$ denotes fine particulate matter, defined as the integrated mass of aerosol with dry diameters up to 2.5 μm. In the EMEP/MSC-W model PM$_{2.5}$ is calculated as PM$_{2.5}$ = SO_4^{2-} + NO_3^-(fine) + NH_4^+ + SS(fine) + PPM$_{2.5}$ + 0.27 NO_3^-(coarse).

PM$_{\mathbf{coarse}}$ denotes coarse particulate matter, defined as the integrated mass of aerosol with dry diameters between 2.5μm and 10μm. In the EMEP/MSC-W model PM$_{\text{coarse}}$ is calculated as PM$_{\text{coarse}}$ = 0.33 NO_3^-(coarse)+ SS(coarse) + PPM$_{coarse}$.

PM$_{10}$ denotes particulate matter, defined as the integrated mass of aerosol with dry diameters up to 10 μm. In the EMEP/MSC-W model PM$_{10}$ is calculated as PM$_{10}$ = PM$_{2.5}$+PM$_{\text{coarse}}$.

In addition to bias, correlation and root mean square the statistical parameter, index of agreement, are used to judge the model's agreement with measurements:

IOA - The index of agreement (IOA) is defined as follows (Elbir 2003, Willmott 1982):

$$IOA = 1 - \frac{\sum_{i=1}^{N}(m_i - o_i)^2}{\sum_{i=1}^{N}(|m_i - \bar{o}| + |o_i - \bar{o}|)^2} \tag{1.2}$$

where $\overline{o}$ is the average observed value. Similarly to correlation, IOA can be used to assess agreement either spatially or temporally. When IOA is used in a spatial sense, N denotes the number of stations with measurements at one specific point in time, and m_i and o_i are the modelled and observed values at station i. For temporal IOA, N denotes the number of time steps with measurements, while m_i and o_i are the modelled and observed value at time step i. IOA varies between 0 and 1. A value of 1 corresponds to perfect agreement between model and observations, and 0 is the theoretical minimum.

1.3 The EMEP extended domain

The EMEP domain defines the area where information on long-range transboundary air pollution is available from the EMEP centres. The information available concerns emissions, observations and modelling results. In 2007, the Steering Body adopted an extension of the official EMEP domain to facilitate the inclusion of countries in Eastern Europe, Caucasus and Central Asia (EECCA) in the EMEP calculations (ref. ECE/EB.AIR/GE.1/2007/9). Thus, in 2008, the official 50×50 km^2 polar stereographic EMEP grid was extended from 132×111 to 132×159 grid cells, following Stage 1 in ECE/EB.AIR/GE.1/2007/9. In geographical projection this led to an eastward extension. The extended EMEP domain is presented in Figure 1.1.

One of the drawbacks of the current extended EMEP domain is that it only partly covers the Russian Federation. It is also recognized that results on air pollution in central Asian countries are highly dependent on sources outside the calculation domain. Countries in Central Asia are contiguous with other Asian countries, like China, India, Pakistan and Iran, that significantly affect pollution levels over the EECCA territories but are not included directly in the calculations. Consequently, the current EMEP modelling capacity for EECCA countries and the related grid domain is only an interim solution.

At the 36th session of the EMEP Steering Body the EMEP Centres suggested to change the spatial resolution and projection of reported emissions from the 50×50 km^2 polar stereographic EMEP grid to 0.1° × 0.1° longitude-latitude grid in a geographic coordinate system

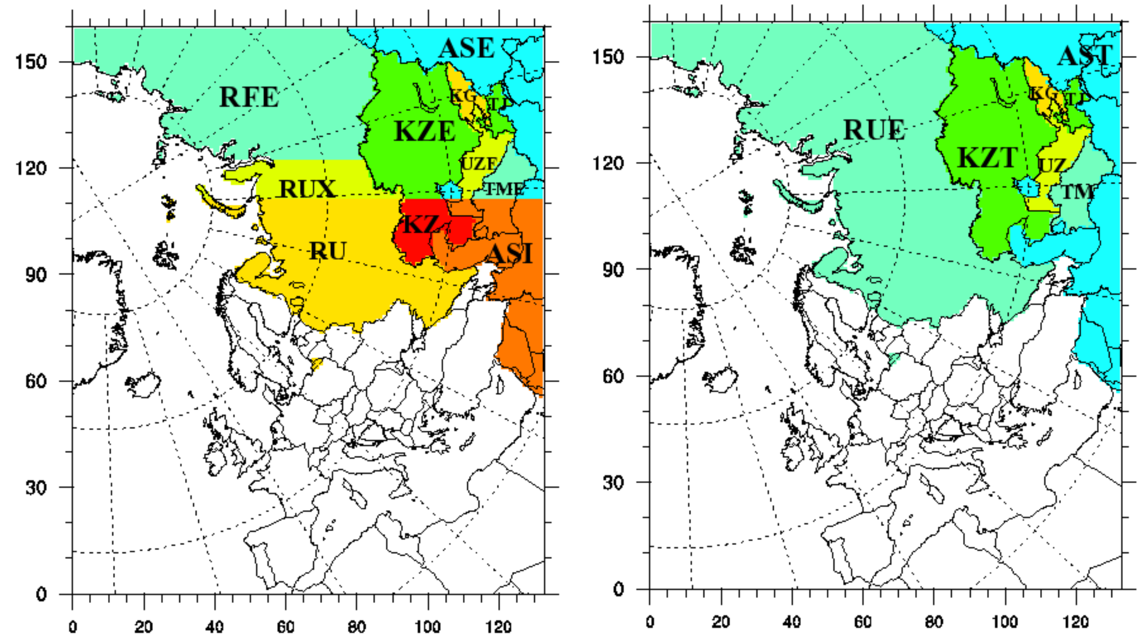

(a) (b)

Figure 1.1: Overview of the country/area codes in the extended EMEP domain. Panel (a) shows the previously defined areas in the official EMEP grid ('RU', 'KZ', 'ASI') together with the new areas in the grid extension ('RUX', 'RFE', 'KZE', 'UZE', 'TME', 'TJ', 'KG', 'ASE'). Panel (b) shows the countries/areas with their codes in the extended EMEP grid ('RUE', 'KZT', 'UZ', 'TM', 'TJ', 'KG', 'AST').

(WGS84). The new EMEP domain will cover the geographic area between 30°N-82°N latitude and 30°W-90°E longitude. This suggestion represents a balance between political needs, scientific needs and technical feasibility as of 2012 and for the next years. Countries are invited to report in the new system as soon as possible (on voluntary basis), but latest in 2017.

The extension of the official EMEP domain made it necessary to introduce new codes for the new countries and areas now included in the extended EMEP domain. The new country codes and their rationale are explained below.

Kyrgyzstan and Tajikistan were not included in the official EMEP domain in any part. These two countries are now included with their full area inside the extended EMEP domain. For these two countries, following UNECE nomenclature, ISO2 country codes are used. The codes are 'KG' for Kyrgyzstan and 'TJ' for Tajikistan.

In the case of the Russian Federation and Kazakhstan, their respective ISO2 codes, 'RU' and 'KZ', previously referred to the parts of their territories inside the official EMEP domain. To keep new model results consistent and comparable with the previous ones, we have kept these ISO2 country codes and use them to define the same areas as before in the official EMEP domain. Additional codes are used to identify parts of these countries' territories outside the official EMEP grid.

For Kazakhstan, the area of the country in the extension of the EMEP domain is denoted by 'KZE', as shown in Figure 1.1 (a). The total territory of Kazakhstan in the extended EMEP domain is then the sum of 'KZ' and 'KZE', and is denoted as 'KZT' in this report (see Figure 1.1 (b)).

For the Russian Federation, the territory in the extension of the domain is divided into two parts, 'RUX' and 'RFE', as shown in Figure 1.1 (a). The reason for this division is that the area called 'RUX' ('EMEP external part of Russian Federation') has been used in the modelling domain previously, although it was not included in the official EMEP domain. The combined territory of the Russian Federation inside the extended EMEP domain is denoted by 'RUE', which stands for 'Russian Federation in the extended EMEP domain' and is presented in Figure 1.1 (b).

Until 2008 Turkmenistan and Uzbekistan were not included in the official EMEP domain as individual countries. However, parts of their territories were inside the official EMEP domain and included in the region called 'Remaining Asian Areas', denoted by country code 'ASI'. As indicated in Figure 1.1 (a), 'ASI' also includes Syria, Lebanon, Israel, parts of Iran, Iraq and Jordan. In the extended EMEP domain, the 'ASI' area has been redefined, and the areas of Turkmenistan and Uzbekistan inside the old 'ASI' have been extracted.

The territories of Turkmenistan and Uzbekistan in the domain extension are denoted by 'TME' and 'UZE', respectively, as in Figure 1.1 (a). The whole territories of Turkmenistan and Uzbekistan in the extended EMEP domain are the sum of the 'extended' and 'official' parts of the countries, namely the sum of 'TME' and 'TMO', and 'UZE' and 'UZO'. The respective ISO2 codes are 'TM' for Turkmenistan and 'UZ' for Uzbekistan.

The region code 'ASE' in Figure 1.1 (a) denotes Asian countries in the extension of the EMEP domain and includes parts of Afghanistan, India, Pakistan, China and Mongolia. The 'ASE' area together with those parts of 'ASI' which are left after the exclusion of the Turkmenistan and Uzbekistan territories forms 'AST' in Figure 1.1 (b) referring to all Asian areas in the extended EMEP domain.

1.4 Country Codes

Many tables and graphs in this report make use of codes to denote countries and regions in the EMEP area. Results are presented for both the official and the extended EMEP domains. All through the report an effort is made to distinguish results from these two different domains. Table 1.1 provides an overview of these codes and lists the countries and regions included, with explicit mention whether the code refers to the official or the extended EMEP domain.

All 51 Parties to the LRTAP Convention, except four, are included in the analysis presented in this report. The Parties that are excluded of the analysis are: Canada and the United States of America, Monaco and Liechtenstein. Canada and USA are excluded because they lie outside the EMEP domains, both the official and the extended domains. Monaco and Liechtenstein are excluded because their emissions and geographical extents are below the accuracy of the present source-receptor calculations in $50\times50km^2$.

Malta is introduced as a receptor country. However, the estimated emissions from Malta are below the accuracy limit of the source-receptor calculations and do not justify a separate study of Malta as an emitter country.

1.5 Other Publications

This report is complemented by EMEP Status Report 4/2013 on Transboundary Particulate Matter in Europe (EMEP CCC & MSC-W 2013) and by the country specific reports on the 2011 status of transboundary acidification, eutrophication, ground level ozone and PM (see

Code	Country/Region
AL	Albania
AM	Armenia
ASI	Remaining Asian areas (official)
AST	Remaining Asian areas (extended)
AT	Austria
ATL	Remaining N.-E. Atlantic Ocean
AZ	Azerbaijan
BA	Bosnia and Herzegovina
BAS	Baltic Sea
BLS	Black Sea
BE	Belgium
BG	Bulgaria
BIC	Boundary and Initial Conditions
BY	Belarus
CH	Switzerland
CY	Cyprus
CZ	Czech Republic
DE	Germany
DK	Denmark
EE	Estonia
EMC	EMEP land areas (official)
EXC	EMEP land areas (extended)
ES	Spain
EU	European Union (EU27)
FI	Finland
FR	France
GB	United Kingdom
GE	Georgia
GL	Greenland
GR	Greece
HR	Croatia
HU	Hungary

Code	Country/Region
IE	Ireland
IS	Iceland
IT	Italy
KG	Kyrgyzstan
KZ	Kazakhstan (official)
KZT	Kazakhstan (extended)
LT	Lithuania
LU	Luxembourg
LV	Latvia
MD	Republic of Moldova
ME	Montenegro
MED	Mediterranean Sea
MK	The FYR of Macedonia
MT	Malta
NL	Netherlands
NO	Norway
NOA	North Africa
NOS	North Sea
PL	Poland
PT	Portugal
RO	Romania
RS	Serbia
RU	Russian Federation (official)
RUE	Russian Federation (extended)
SE	Sweden
SI	Slovenia
SK	Slovakia
TJ	Tajikistan
TM	Turkmenistan
TR	Turkey
UA	Ukraine
UZ	Uzbekistan

Table 1.1: Country/region codes used throughout this report:'official' refers to the area of the country/region which is inside the official EMEP grid domain, while 'extended' refers to the area of the country/region inside the extended EMEP grid domain.

Apendix D). Both English and Russian versions of the country reports are available to the twelve EECCA countries.

As noted above, time series plots of acidifying and eutrophying components (Nyíri et al. 2013), and ozone and NO_2 (Gauss and Hjellbrekke 2013) have been made available online, at `www.emep.int` along with much other material.

A list of all associated technical reports and notes by the EMEP centres in 2013 follows at the end of this section.

Peer-reviewed publications

The following scientific papers of relevance to transboundary air pollution and involving EMEP/MSC-W, EMEP/MSC-E and CCC staff have become available in 2012 and 2013:

Aas, W., Tsyro, S., Bieber, E., Bergström, R., Ceburnis, D., Ellermann, T., Fagerli, H., Frölich, M., Gehrig, R., Makkonen, U., Nemitz, E., Otjes, R., Perez, N., Perrino, C., Prévôt, A. S. H., Putaud, J.-P., Simpson, D., Spindler, G., Vana, M., and Yttri, K. E.: Lessons learnt from the first EMEP intensive measurement periods, Atmos. Chem. Physics, 12, 8073–8094, doi:10.5194/acp-12-8073-2012, 2012.

Aleksandropoulou, V., Tørseth, K., Lazaridis, M.: The effect of forest fires in emissions of biogenic volatile organic compounds and windblown dust over urban areas, Air Qual. Atmos. Health, 6, 277-294, doi:10.1007/s11869-012-0170-y, 2012.

Alterskjær, K., Kristjánsson, J. E., Seland, Ø.: Sensitivity to deliberate sea salt seeding of marine clouds - observations and model simulations, Atmos. Chem. Phys., 12 (5), 2795-2807, 2012.

Asmi, A., Collaud Coen, M., Ogren, J. A., Andrews, E., Sheridan, P., Jefferson, A., Weingartner, E., Baltensperger, U., Bukowiecki, N., Lihavainen, H., Kivekäs, N., Asmi, E., Aalto, P. P., Kulmala, M., Wiedensohler, A., Birmili, W., Hamed, A., O'Dowd, C., G Jennings, S., Weller, R., Flentje, H., Fjæraa, A. M., Fiebig, M., Myhre, C. L., Hallar, A. G., Swietlicki, E., Kristensson, A., Laj, P.: Aerosol decadal trends - Part 2: In-situ aerosol particle number concentrations at GAW and ACTRIS stations, Atmos. Chem. Phys., 13, 895-916. doi:10.5194/acp-13-895-2013, 2013.

Bentsen, M., Bethke, I., Debernard, J. B., Iversen, T., Kirkevåg, A., Seland, Ø., Drange, H., Roelandt, C., Seierstad, I. A., Hoose, C., Kristjánsson, J. E.: The Norwegian Earth System Model, NorESM1-M - Part 1: Description and basic evaluation of the physical climate, Geosci. Model Dev., 6, 687-720, GMD - Special Issue, 2013.

Bergström, R., Denier van der Gon, H. A. C., Prévôt, A. S. H., Yttri, K. E., and Simpson, D.: Modelling of organic aerosols over Europe (2002–2007) using a volatility basis set (VBS) framework: application of different assumptions regarding the formation of secondary organic aerosol, Atmos. Chem. Physics, 12, 8499–8527, doi:10.5194/acp-12-8499-2012, 2012.

Björkman, M. P., Kühnel, R., Partridge, D. G., Roberts, T. J., Aas, W., Mazzola, M., Viola, A., Hodson, A., Ström, J., Isaksson, E.: Nitrate dry deposition in Svalbard, Tellus B, 65, 19071, doi:10.3402/tellusb.v65i0.19071, 2013.

Bond, T. C., Doherty, S. J., Fahey, D. W., Forster, P. M., Berntsen, T., DeAngelo, B. J., Flanner, M. G., Ghan, S., Kärcher, B., Koch, D., Kinne, S., Kondo, Y., Quinn, P. K., Sarofim, M. C., Schultz, M. G., Schulz, M., Venkataraman, C., Zhang, H., Zhang, S., Bellouin, N., Guttikunda, S. K., Hopke, P. K., Jacobson, M. Z., Kaiser, J. W., Klimont, Z., Lohmann, U., Schwarz, J. P., Shindell, D., Storelvmo, T., Warren, S. G. and Zender, C. S.: Bounding the role of black carbon in the climate system: A scientific assessment, J. Geophys. Res., doi:10.1002/jgrd.50171, 2013.

Büker, P., Morrissey, T., Briolat, A., Falk, R., Simpson, D., Tuovinen, J.-P., Alonso, R., Barth, S., Baumgarten, M., Grulke, N., Karlsson, P. E., King, J., Lagergren, F., Matyssek, R., Nunn, A., Ogaya, R., Peñuelas, J., Rhea, L., Schaub, M., Uddling, J., Werner, W., and Emberson, L. D.: DO_3SE modelling of soil moisture to determine ozone flux to forest trees, Atmos. Chem. Physics, 12, 5537–5562, doi:10.5194/acp-12-5537-2012, 2012.

Colette, A., Granier, C., Hodnebrog, Ø., Jakobs, H., Maurizi, A., Nyiri, A., Rao, S., Amann, M., Bessagnet, B., D'Angiola, A., Gauss, M., Heyes, C., Klimont, Z., Meleux, F., Memmesheimer, M., Mieville, A., Rouïl, L., Russo, F., Schucht, S., Simpson, D., Stordal, F., Tampieri, F., and Vrac, M.: Future air quality in Europe: a multi-model assessment of projected exposure to ozone, Atmos. Chem. Physics, 12, 10 613–10 630, doi:10.5194/acp-12-10613-2012, 2012.

Collaud Coen, M., Andrews, E., Asmi, A., Baltensperger, U., Bukowiecki, N., Day, D., Fiebig, M., Fjæraa, A. M., Flentje, H., Hyvärinen, A., Jefferson, A., Jennings, S. G., Kouvarakis, G., Lihavainen, H., Lund Myhre, C., Malm, W. C., Mihapopoulos, N., Molenar, J. V., O'Dowd, C., Ogren, J. A., Schichtel, B. A., Sheridan, P., Virkkula, A., Weingartner, E., Weller, R., Laj, P.: Aerosol decadal trends - Part 1: In-situ optical measurements at GAW and IMPROVE stations, Atmos. Chem. Phys. Discuss., 13, 869-894, doi:10.5194/acp-13-869-2013, 2013.

Flechard, C. R., Massad, R.-S., Loubet, B., Personne, E., Simpson, D., Bash, J. O., Cooter, E. J., Nemitz, E., and Sutton, M. A.: Advances in understanding, models and parameterisations of biosphere-atmosphere ammonia exchange, Biogeosciences, doi:10.5194/bg-10-5183-2013, 2013.

Gudmundsson, M. T., Thordarson, T., Höskuldsson, A., Larsen, G., Björnsson, H., Prata, F. J., Oddsson, B., Magnússon, E., Högnadóttir, T., Petersen, G. N., Hayward, C. L., Stevenson, J. A., Jónsdóttir, I.: Ash generation and distribution from the April-May 2010 eruption of Eyjafjallajökull, Iceland, Sci. Rep., 2, 572, doi:10.1038/srep00572, 2012.

Gusev, A., MacLeod, M., Bartlett, P.: Intercontinental transport of persistent organic pollutants: a review of key findings and recommendations of the task force on hemispheric transport of air pollutants and directions for future research, Atmospheric Pollution Research 3, 463-465, 2012.

Halse, A. K., Eckhardt, S., Schlabach, M., Stohl, A., Breivik, K.: Forecasting long-range atmospheric transport episodes of polychlorinated biphenyls using FLEXPART, Atmos. Environ., 71, 335-339. doi:10.1016/j.atmosenv.2013.02.022, 2013.

Halse, A. K., Schlabach, M., Sweetman, A., Jones, K. C., Breivik, K.: Using passive air samplers to assess local sources versus long range atmospheric transport of POPs, J. Environ. Monit., 14, 2580-2590, doi:10.1039/C2EM30378G, 2012.

Healy, R. M., Sciare, J., Poulain, L., Kamili, K., Merkel, M., Mller, T., Wiedensohler, A., Eckhardt, S., Stohl, A., Sarda-Estève, R., McGillicuddy, E., O'Connor, I. P., Sodeau, J. R., Wenger, J. C.: Sources and mixing state of size-resolved elemental carbon particles in a European megacity: Paris, Atmos. Chem. Phys., 12, 1681-1700, doi:10.5194/acp-12-1681-2012, 2012.

Hertel, O., Skjøth, C. A., Reis, S., Bleeker, A., Harrison, R. M., Cape, J. N., Fowler, D., Skiba, U., Simpson, D., Jickells, T., Kulmala, M., Gyldenkærne, S., Sørensen, L. L., Erisman, J. W., and Sutton, M. A.: Governing processes for reactive nitrogen compounds in the European atmosphere, Biogeosciences, 9, 4921–4954, doi:10.5194/bg-9-4921-2012, 2012.

Hilboll, A., Richter, A., Rozanov, A., Hodnebrog, Ø., Heckel, A., Solberg, S., Stordal, F., Burrows, J. P.: Improvements to the retrieval of tropospheric NO2 from satellite - stratospheric correction using SCIAMACHY limb/nadir matching and comparison to Oslo CTM2 simulations, Atmos. Meas. Tech., 6, 565-584, doi:10.5194/amt-6-565-2013, 2013.

Hodnebrog, Ø., Berntsen, T. K., Dessens, O., Gauss, M., Grewe, V., Isaksen, I. S. A., Koffi, B., Myhre, G., Olivié, D., Prather,M. J., Stordal, F., Szopa, S., Tang, Q., van Velthoven, P., Williams, J. E.: Future impact of traffic emissions on atmospheric ozone and OH based on two scenarios, Atmos. Chem. Phys., 12, 12211-12225, doi:10.5194/acp-12-12211-2012, 2012.

Hodnebrog, Ø., Solberg, S., Stordal, F., Svendby, T. M., Simpson, D., Gauss, M., Hilboll, A., Pfister, G. G., Turquety, S., Richter, A., Burrows, J. P., and Denier van der Gon, H. A. C.: Impact of forest fires, biogenic emissions and high temperatures on the elevated Eastern Mediterranean ozone levels during the hot summer of 2007, Atmos. Chem. Physics, 12, 8727–8750, doi:10.5194/acp-12-8727-2012, 2012.

Iversen, T., Bentsen, M., Bethke, I., Debernard, J. B., Kirkevåg, A., Seland, Ø., Drange, H., Kristjánsson, J. E., Medhaug, I., Sand, M., Seierstad, I. A.: The Norwegian Earth System Model, NorESM1-M. Part 2: Climate Response and Scenario Projections, Geosci. Model Dev., 6, 389-415, GMD - Special Issue, 2013.

Jeričević, A., Fagerli, H., Grisogono, B.: Exploring the properties of local and non-local vertical diffusion schemes in the EMEP model using 222Rn data, Int. J. of Environment and Pollution, 48 (1/2/3/4), 231-243, Special Issue, 2012.

Karlsson, P.E., Ferm, M., Tømmervik, H., Hole, L.R., Karlsson, G.P., Ruoho-Airola, T., Aas, W., Hellsten, S., Akselsson, C., Mikkelsen, T. N., Nihlgård, B.: Biomass burning in eastern Europe during spring 2006 caused high deposition of ammonium in northern Fennoscandia, Environ. Pollut., 176, 71-79, doi:10.1016/j.envpol.2012.12.006, 2013.

Keywood, M., Kanakidou, M., Stohl, A., Dentener, F., Grassi, G., Meyer, C. P., Tørseth, K., Edwards, D., Thompson, A.M., Lohmann, U., Burrows, J.: Fire in the air - biomass burning impacts in a changing climate, Crit. Rev. Environ. Sci. Tech., 43, 40-83, doi:10.1080/10643389.2011.604248, 2013.

Kirkevåg, A., Iversen, T., Seland, Ø, Hoose, C., Kristjánsson,J. E., Struthers, H., Ekman, A., Ghan, S., Griesfeller, J., Nilsson, D., Schulz, M.: Aerosol-climate interactions in the Norwegian Earth System Model – NorESM1-M, Geosci. Model Dev., 6, 207-244. GMD - Special Issue, 2013.

Koffi, B., Schulz, M., Bréon, F.-M., Griesfeller, J., Winker, D., Balkanski, Y., Bauer, S., Berntsen, T., Chin, M., Collins, W. D., Dentener, F., Diehl, T., Easter, R., Ghan, S., Ginoux, P., Gong, S., Horowitz, L. W., Iversen, T., Kirkevåg, A., Koch, D., Krol, M., Myhre, G., Stier, P., Takemura, T.: Application of the CALIOP layer product to evaluate the vertical distribution of aerosols estimated by global models: AeroCom phase I results, J. Geophys. Res., 117, D10201, doi:10.1029/ 2011JD016858, 2012.

Kopanakis, I., Chatoutsidou, S.E., Tørseth, K., Glytsos, T., Lazaridis, M.: Particle number size distribution in the Eastern Mediterranean: Formation and growth rates of ultrafine airborne atmospheric particles, Atmos. Environ., Available online 8 June 2013, doi:10.1016/j.atmosenv.2013.05.066, 2013.

Langner, J., Engardt, M., Baklanov, A., Christensen, J. H., Gauss, M., Geels, C., Hedegaard, G. B., Nuterman, R., Simpson, D., Soares, J., Sofiev, M., Wind, P., and Zakey, A.: A multi-model study of impacts of climate change on surface ozone in Europe, Atmos. Chem. Physics, 12, 10 423–10 440, doi:10.5194/acp-12-10423-2012, 2012.

Mazzola, M., Stone, R. S., Herber, A., Tomasi, C., Lupi, A., Vitale, V., Lanconelli, C., Toledano, C., Cachorro, V. E., O'Neill, N. T., Shiobara, M., Aaltonen, V., Stebel, K., Zielinski, T., Petelski, T., Ortiz de Galisteo, J. P., Torres, B., Berjon, A., Goloub, P., Li, Z., Blarel, L., Abboud, I., Cuevas, E., Stock, M., Schulz, K. H., Virkkula, A.: Evaluation of sun photometer capabilities for retrievals of aerosol optical depth at high latitudes: The POLAR-AOD intercomparison campaigns, Atmos. Environ., 52, 4-17, doi:10.1016/j.atmosenv.2011.07.042, 2012.

Myhre, G., Samset, B. H., Schulz, M., Balkanski, Y., Bauer, S., Berntsen, T. K., Bian, H., Bellouin, N., Chin, M., Diehl, T., Easter, R. C., Feichter, J., Ghan, S. J., Hauglustaine, D., Iversen, T., Kinne, S., Kirkevåg, A., Lamarque, J.-F., Lin, G., Liu, X., Luo, G., Ma, X., Penner, J. E., Rasch, P. J., Seland, Ø., Skeie, R. B., Stier, P., Takemura, T., Tsigaridis, K., Wang, Z., Xu, L., Yu, H., Yu, F., Yoon, J.-H., Zhang, K., Zhang, H., Zhou, C.: Radiative forcing of the direct aerosol effect from AeroCom Phase II simulations, Atmos. Chem. Phys., 13, 1853-1877, doi:10.5194/acp-13-1853-2013, 2013.

Olivié, D., Cariolle, D., Teyssèdre, H., Salas, D., Voldoire, A., Clark, H., Saint-Martin, D., Michou, M., Karcher, F., Balkanski, Y., Gauss, M., Dessens, O., Koffi, B., Sausen, R.: Modeling the climate impact of road transport, maritime shipping and aviation over the period 1860-2100 with an AOGCM, Atmos. Chem. Phys.,12 (3), 1449-1480, 2012.

Pikridas, M., Riipinen, I., Hildebrandt, L., Kostenidou, E., Manninen, H., Mihalopoulos, N., Kalivitis, N., Burkhart, J. F., Stohl, A., Kulmala, M., Pandis, S. N.: New particle formation at a remote site in the eastern Mediterranean, J. Geophys. Res., 117, D12205, doi:10.1029/2012JD017570, 2012.

Quennehen, B., Schwarzenboeck, A., Matsuki, A., Burkhart, J. F., Stohl, A., Ancellet, G., Law, K. S.: Anthropogenic and forest fire pollution aerosol transported to the Arctic: observations from the POLARCAT-France spring campaign, Atmos. Chem. Phys., 12, 6437-6454, doi:10.5194/acp-12-6437-2012, 2012.

Sakalli, A. and Simpson, D.: Towards the use of dynamic growing seasons in a chemical transport model, Biogeosciences, 9, 5161–5179, doi:10.5194/bg-9-5161-2012, 2012.

Samset, B. H., Myhre, G., Schulz, M., Balkanski, Y., Bauer, S., Berntsen, T. K., Bian, H., Bellouin, N., Diehl, T., Easter, R. C., Ghan, S. J., Iversen, T., Kinne, S., Kirkevåg, A., Lamarque, J.-F., Lin, G., Liu, X., Penner, J., Seland, Ø., Skeie, R. B., Stier, P., Takemura, T., Tsigaridis, K., Zhang, K.: Black carbon vertical profiles strongly affect its radiative forcing uncertainty, Atmos. Chem. Phys., 13, 2423-2434, doi:10.5194/acp-13-2423-2013, 2013.

Schulz, M. , Prospero, J. M., Baker, A. R., Dentener, F., Ickes, L., Liss, P. S., Mahowald, N. M., Nickovic, S., Pérez García-Pando, C., Rodríguez, S., Sarin, M., Tegen, I., Duce, R. A.: Atmospheric Transport and Deposition of Mineral Dust to the Ocean: Implications for Research Needs, Environ. Sci. Technol., 46 (19), 10390-10404, 2012.

Schuster, J. K., Gioia, R., Harner, T., Lee, S. C., Breivik, K., Jones, K. C.: Assessment of sorbent impregnated PUF disks (SIPs) for long-term sampling of legacy POPs, J. Environ. Monit., 14, 71-78, doi:10.1039/C1EM10697J, 2012.

Shatalov, V., Johansson, J. H., Wiberg, K., Cousins, I. T.: Tracing the origin of dioxins in Baltic air using an atmospheric modeling approach, Atmospheric Pollution Research 3, 408-416, 2012.

Simpson, D., Benedictow, A., Berge, H., Bergström, R., Emberson, L. D., Fagerli, H., Flechard, C. R., Hayman, G. D., Gauss, M., Jonson, J. E., Jenkin, M. E., Nyíri, A., Richter, C., Semeena, V. S., Tsyro, S., Tuovinen, J.-P., Valdebenito, A., and Wind, P.: The EMEP MSC-W chemical transport model – technical description, Atmos. Chem. Physics, 12, 7825–7865, doi:10.5194/acp-12-7825-2012, 2012.

Stjernberg, A.-C. E., Skorokhod, A., Paris, J. D., Elansky, N., Nédélec, P., Stohl, A.: Low concentrations of near-surface ozone in Siberia, Tellus B, 64, 11607, doi:10.3402/tellusb.v64i0.11607, 2012.

Struthers, H., Ekman, A. M. L., Glantz, P., Iversen, T., Kirkevåg, A., Seland, Ø., Mårtensson, E. M., Noone, K., Nilsson, E. D.: Climate-induced changes in sea salt aerosol emissions: 1870 to 2100, JGR Atmospheres, 118, 2, 670-682, 2013.

Sutton, M. A., Reis, S., Riddick, S. N., Dragosits, U., Nemitz, E., Theobald, M. R., Tang, Y. S., Braban, C. F., Vieno, M., Dore, A. J., Mitchell, R. F., Wanless, S., Daunt, F., Fowler, D., Blackall, T. D., Milford, C., Flechard, C. R., Loubet, B., Massad, R., Cellier, P., Personne, E., Coheur, P. F., Clarisse, L., Van Damme, M., Ngadi, Y., Clerbaux, C., Skjth, C. A., Geels, C., Hertel, O., Wichink Kruit, R. J., Pinder, R. W., Bash, J. O., Walker, J. T., Simpson, D., Horvth, L., Misselbrook, T. H., Bleeker, A., Dentener, F., and de Vries, W.: Towards a climate-dependent paradigm of ammonia emission and deposition, Philosophical Transactions of the Royal Society B: Biological Sciences, 368, doi:10.1098/rstb.2013.0166, 2013.

Szopa S., Balkanski, Y., Schulz, M., Bekki, S., Cugnet, D., Fortems-Cheiney, A., Turquety, S., Cozic, A., Déandreis, C., Hauglustaine, D., Idelkadi, A., Lathiére, J., Lefevre, F., Marchand, M., Vuolo, R., Yan, N., Dufresne, J.-L.: Aerosol and Ozone changes as forcing for Climate Evolution between 1850 and 2100, Climate Dynamics, 40 (9-10), 2223-2250, 2012.

Tjiputra, J. F., Roelandt, C., Bentsen, M., Lawrence, D. M., Lorentzen, T., Schwinger, J., Seland, Ø., Heinze, C.: Evaluation of the carbon cycle components in the Norwegian Earth System Model (NorESM), Geosci. Model Dev. , 6, 301-325. GMD - Special Issue, 2013.

Toledano, C., Cachorro, V., Gausa, M., Stebel, K., Aaltonen, V., Berjón, A., Ortiz de Galisteo, J.P., de Frutos, A.M., Bennouna, Y., Blindheim, S, Myhre, C.L., Zibordi, G., Wehrli, C., Kratzer, S., Hakansson, B., Carlund, T., de Leeuw, G., Herber, A., Torres, B.: Overview of sun photometer measurements of aerosol properties in Scandinavia and Svalbard, Atmos. Environ., 52, 18-28. doi:10.1016/j.atmosenv.2011.10.022, 2012.

Tørseth, K., Aas, W., Breivik, K., Fjæraa, A. M., Fiebig, M., Hjellbrekke, A. G., Lund Myhre, C., Solberg, S., Yttri, K. E.: Introduction to the European Monitoring and Evaluation Programme (EMEP) and observed atmospheric composition change during 1972-2009, Atmos. Chem. Phys., 12, 5447-5481. doi:10.5194/acp-12-5447-2012, 2012.

Ubl, S., Scheringer, M., Stohl, A., Burkhart, J. F., Hungerbuhler, K.: Primary source regions of polychlorinated biphenyls (PCBs) measured in the Arctic, Atmos. Environ., 62, 391-399, doi:10.1016/j.atmosenv.2012.07.061, 2012.

Wiedensohler, A., Birmili, W., Nowak, A., Sonntag, A., Weinhold, K., Merkel, M., Wehner, B., Tuch, T., Pfeifer, S., Fiebig, M., Fjæraa, A. M., Asmi, E., Sellegri, K., Depuy, R., Venzac, H., Villani, P., Laj, P., Aalto, P., Ogren, J. A., Swietlicki, E., Williams, P., Roldin, P., Quincey, P., Hüglin, C., Fierz-Schmidhauser, R., Gysel, M., Weingartner, E., Riccobono, F., Santos, S., Grüning, C., Faloon, K., Beddows, D., Harrison, R. M., Monahan, C., Jennings, S. G., O'Dowd, C. D., Marinoni, A., Horn, H.-G., Keck, L., Jiang, J., Scheckman, J., McMurry, P. H., Deng, Z., Zhao, C. S., Moerman, M., Henzing, B., de Leeuw, G., Löschau, G., Bastian, S.: Mobility particle size spectrometers: harmonization of technical standards and data structure to facilitate high quality long-term observations of atmospheric particle number size distributions. Atmos. Meas. Tech., 5, 657-685, doi:10.5194/amt-5-657-2012, 2012.

Worton, D. R., Sturges, W. T., Reeves, C. E., Newland, M. J., Penkett, S. A., Atlas, E., Stroud, V., Johnson, K., Schmidbauer, N., Solberg, S., Schwander, J., Barnola, J.-M.: Evidence from firn air for recent decreases in non-methane hydrocarbons and a 20th century increase in nitrogen oxides in the northern hemisphere. Atmos. Environ., 54, 592-602, doi:10.1016/j.atmosenv.2012.02.084, 2012.

Associated EMEP reports and notes in 2013

Joint reports

Transboundary acidification, eutrophication and ground level ozone in Europe in 2011. Joint MSC-W & CCC & CEIP Report. EMEP Status Report 1/2013.

Ilyin, I., Rozovskaya, O., Travnikov, O., Varygina, M., Aas, W., Uggerud, H.T. Heavy Metal Transboundary Pollution of the Environment. EMEP Status Report 2/2013.

Gusev, A., Rozovskaya, O., Shatalov, V., Sokovykh, V., Vulykh, N., Aas, W., Breivik, K., Katsogiannis, A. A. Persistent Organic Pollutants in the Environment. EMEP Status Report 3/2013.

Transboundary Particulate Matter in Europe. Joint CCC & MSC-W & CEIP & CIAM Report. EMEP Status Report 4/2013.

ScaleDep: Performance of European chemistry-transport models as function of horizontal spatial resolution. Joint TFMM & MSC-W Report. EMEP Technical Report 1/2013.

CCC Technical and Data reports

Cavalli, F., Putaud, J-P., Yttri, K.E. Availability and quality of the EC and OC measurements within EMEP, including results of the fourth interlaboratory comparison of analytical methods for carbonaceous particulate matter within EMEP (2011). EMEP/CCC-Report 1/2013.

Hjellbrekke, A.-G., Fjæraa, A. M. Data report 2011. Acidifying and eutrophying compounds and particulate matter. EMEP/CCC-Report 2/2013.

Hjellbrekke, A.-G., Solberg, S., Fjæraa, A. M. Ozone measurements 2011. EMEP/CCC-Report 3/2013.

Aas, W., Breivik, K. Heavy metals and POP measurements 2011. EMEP/CCC-Report 4/2013.

Solberg, S. VOC measurements 2011. EMEP/CCC-Report 5/2013.

CEIP Technical and Data reports

Mareckova, K., Wankmüller, R., Moosman, L., Pinterits, M. Inventory Review 2013; Review of emission data reported under the LRTAP Convention and NEC Directive, Stage 1 and 2 review and review of gridded data. EEA/CEIP Technical report (Vienna, August 2013)

MSC-E Technical and Data reports

Shatalov, V., Ilyin, I., Gusev, A., Rozovskaya, O., Sokovykh, V., Travnikov, O. Heavy Metals and Persistent Organic Pollutants: Model Assessment of Pollution and Research Activities. EMEP/MSC-E Technical report 1/2013.

MSC-W Technical and Data reports

Gauss, M., Nyíri, Á., Semeena, V. S., Benedictow, A. C., Klein, H. Transboundary air pollution by main pollutants (S, N, O_3) and PM in 2011, Country Reports. EMEP/MSC-W Data Note 1/2013.

Bartnicki, J., Gusev, A., Aas, W., Semeena, V. S. Atmospheric Supply of Nitrogen, Lead, Cadmium, Mercury and Dioxins/Furans to the Baltic Sea in 2011. EMEP/MSC-W Technical Report 2/2013.

References

Elbir, T.: Comparison of model predictions with the data of an urban air quality monitoring network in Izmir, Turkey, Atmos. Environ., 37, 21492157, 2003.

EMEP CCC & MSC-W: Transboundary Particulate Matter in Europe. EMEP Status Report 4/2013, EMEP Report 4/2013, The Norwegian Institute for Air Research (NILU), Kjeller, Norway, 2013.

Gauss, M. and Hjellbrekke, A.-G.: Photo-oxidants: validation and combined maps, Supplementary material to EMEP Status Report 1/2013, available online at `www.emep.int`, The Norwegian Meteorological Institute, Oslo, Norway, 2013.

Gauss, M., Nyíri, Á., Semeena, V. S., and Hjellbrekke, A.-G.: EMEP Unified model performance for acidifying and eutrophying components and photo-oxidants in 2011., Supplementary material to EMEP Status Report 1/2013, available online at `www.emep.int`, The Norwegian Meteorological Institute, Oslo, Norway, 2013.

LRTAP: Mapping critical levels for vegetation, in: Manual on Methodologies and Criteria for Mapping Critical Loads and Levels and Air Pollution Effects, Risks and Trends. Revision of 2009, edited by Mills, G., UNECE Convention on Long-range Transboundary Air Pollution. International Cooperative Programme on Effects of Air Pollution on Natural Vegetation and Crops, updated version available at `www.icpmapping.com/`, 2009.

Mills, G. and Simpson, D.: The Mediterranean region, in: Transboundary acidification, eutrophication and ground level ozone in Europe. EMEP Status Report 1/2010, pp. 37–48, The Norwegian Meteorological Institute, Oslo, Norway, 2010.

Mills, G., Hayes, F., Simpson, D., Emberson, L., Norris, D., Harmens, H., and Büker, P.: Evidence of widespread effects of ozone on crops and (semi-)natural vegetation in Europe (1990-2006) in relation to AOT40- and flux-based risk maps, Global Change Biology, 17, 592–613, doi:10.1111/j.1365-2486.2010.02217.x, 2011a.

Mills, G., Pleijel, H., Braun, S., Büker, P., Bermejo, V., Calvo, E., Danielsson, H., Emberson, L., Grünhage, L., Fernández, I. G., Harmens, H., Hayes, F., Karlsson, P.-E., and Simpson, D.: New stomatal flux-based critical levels for ozone effects on vegetation, Atmos. Environ., 45, 5064 – 5068, doi:10.1016/j.atmosenv.2011.06.009, 2011b.

Nyíri, Á., Gauss, M., Semeena, V. S., and Hjellbrekke, A.-G.: Acidifying and eutrophying components: validation and combined maps, Supplementary material to EMEP Status Report 1/2013, available online at `www.emep.int`, The Norwegian Meteorological Institute, Oslo, Norway, 2013.

Willmott, C. J.: Some Comments on the Evaluation of Model Performance, Bulletin American Meteorological Society, 63, 1309–1313, doi:10.1175/1520-0477(1982)063<1309:SCOTEO>2.0.CO;2, 1982.

Part I

Status in 2011

CHAPTER 2

Status of transboundary pollution in 2011

Michael Gauss, Anna Benedictow, Anne -Gunn Hjellbrekke, Katarina Mareckova, Ágnes Nyíri and Robert Wankmüller

This chapter describes the status of transboundary pollution in 2011. It starts by reviewing the main input data to the EMEP MSC-W air quality model, i.e. the meteorological conditions and pollutant emissions in the EMEP domain in 2011. Thereafter, the status of air pollution and exceedances in 2011, as well as changes with respect to previous years, will be presented in maps covering the EMEP domain.

2.1 Meteorological data for 2011

Since 2008 the meteorological data to drive the EMEP MSC-W air quality model have been generated by the Integrated Forecast System model (IFS) of the European Centre for Medium-Range Weather forecasts (ECMWF), hereafter referred to as ECMWF-IFS model. In the meteorological community the ECMWF-IFS model is considered as state-of-the-art, and MSC-W has been using this model in hindcast mode to generate accurate meteorological reanalyses for the year to be studied.

The meteorological fields used for 2011 are based on ECMWF-IFS model cycle 36r1, initialised by ECMWF Interim Reanalysis (ERA) data. The meteorological fields have been interpolated from longitude latitude coordinates with a resolution of $0.22° \times 0.22°$ to the polar-stereographic 50×50 km^2 grid of EMEP. This section describes the meteorological data for 2011 and discusses their main features in comparison to previous years.

2.1.1 2011 compared to 2010

When investigating the causes of changes in air pollution from year to year it is important not only to look at increases or reductions in emissions but also at changes in meteorology. Meteorological conditions have a significant effect on air concentrations and depositions of pollutants, controlling their transport, diffusion and dry and wet removal. Figure 2.1 shows annual-mean differences in surface temperature and precipitation from 2010 to 2011. The warmer winter in Europe in the beginning and at the end of 2011 (except for Northeastern Europe) explains most of the positive temperature change revealed in the figure (left panel). The lower temperatures in the Southeastern part of the model domain, including southern regions of the Russian Federation are partly explained by the absence of a heatwave comparable to the one experienced in 2010. Although also western and central Europe had a relatively cool summer in 2011, this negative contribution to the annual mean was overcompensated by abnormally warm spring and autumn seasons in these regions. The dry spring and autumn in central, eastern and southeastern Europe, but wet conditions in northwestern Europe explain the changes seen in annual precipitation from 2010 to 2011 over Europe (right panel). The relatively high precipitation over western Russia and Caucasus, compared to the dry summer conditions of 2010, is also visible.

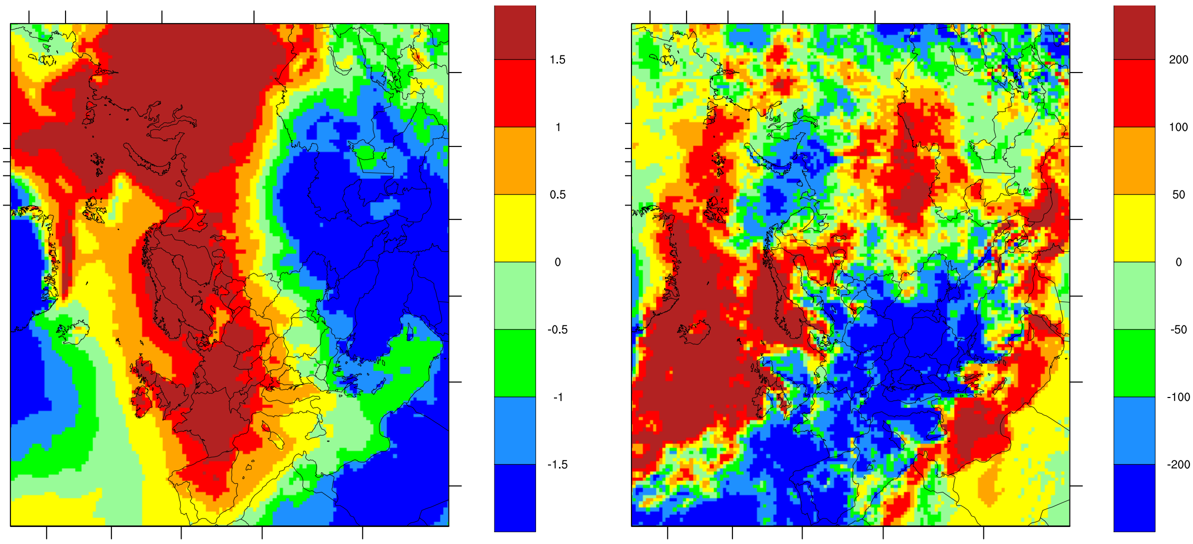

(a) ΔT2m [2011–2010] (b) Δprecipitation [2011–2010]

Figure 2.1: Meteorological change from 2010 to 2011. Left: Annual mean temperature at 2m [K], right: Annual precipitation [mm].

2.1.2 2011 compared to the 2000–2009 average

When investigating particularities of the year 2011 in general it is illustrative to compare it to a multi-annual average. In order to present a consistent picture, we use data generated in the same way as the data used for 2010 and 2011 EMEP MSC-W simulations, i.e. derived from the same version of the ECMWF-IFS model and using the same model setup (model resolution, initial conditions, etc.). The longest period of consistent meteorological input data at our disposal for this comparison is the 2000-2009 period (2000s). Figure 2.2 shows the difference between 2011 and the climatological average of the 2000s. Figure 2.3 shows these differences for the summer months only. On annual average, 2011 was rather warm and dry in France, Germany, large parts of Spain, Switzerland, and the southern part of the United Kingdom. As this feature is not seen during the summer months, it must be mainly explained by the relatively mild and dry spring, autumn and winter of 2011. Another striking feature in

the annual mean is the relatively high temperature over Siberia, the relatively low temperature over Central Asia, and the relatively dry conditions over Southeast Europe.
When looking at summer conditions only, the western part of Russia had a rather hot and dry summer (though not as hot and dry as in 2010), while most parts of Central Russia and Western Europe had a cooler and wetter summer compared to the 2000s average.

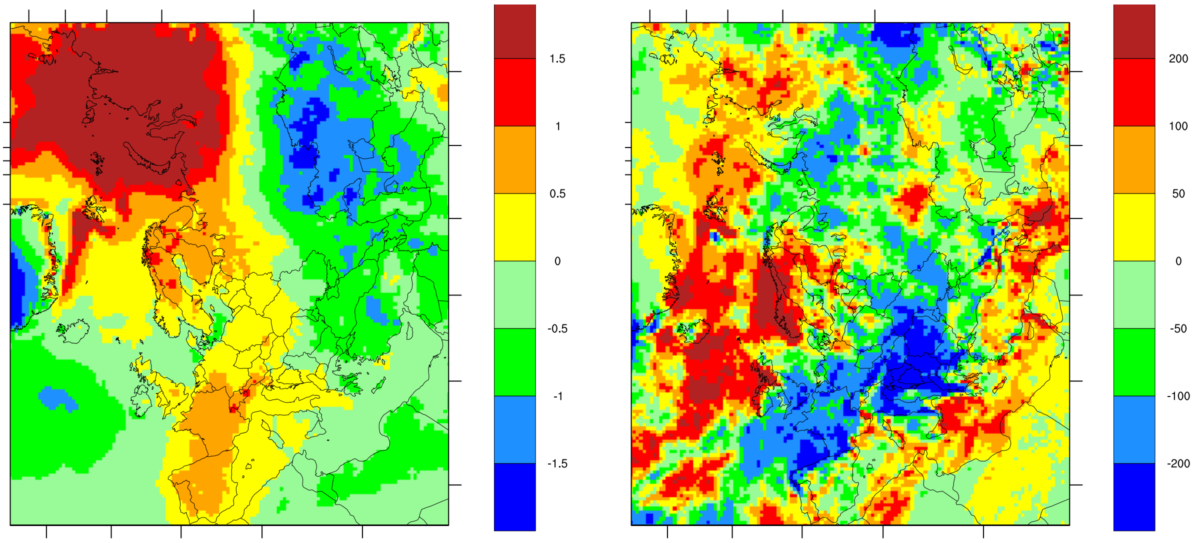

(a) ΔT2m [2011–2000s] (b) Δprecipitation [2011–2000s]

Figure 2.2: Meteorological conditions in 2011 compared to the 2000-2009 average. Left: Annual mean temperature at 2m [K], right: Annual precipitation [mm].

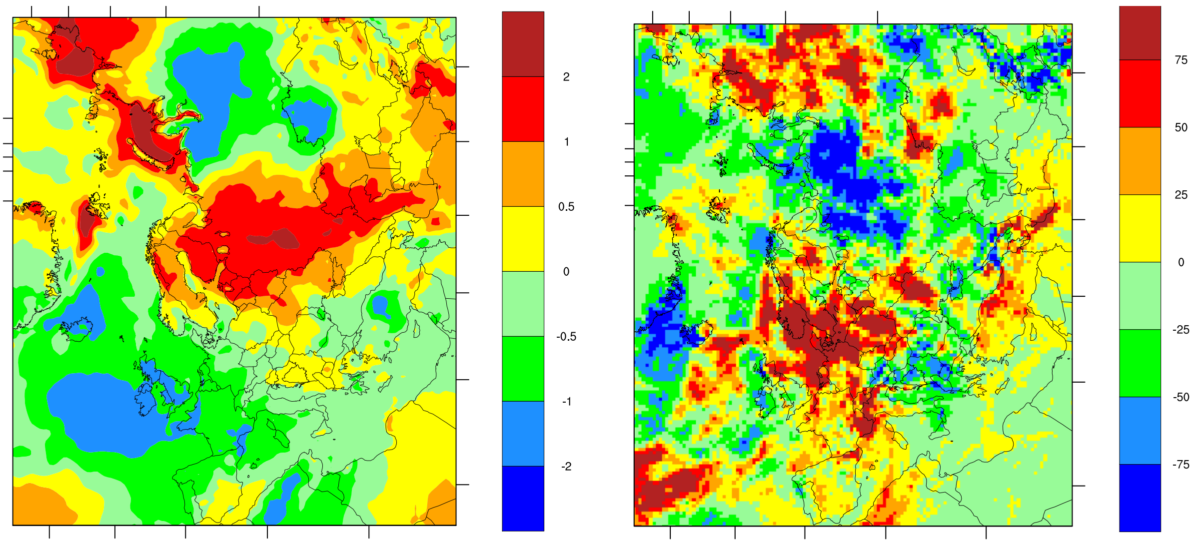

(a) ΔT2m [JJA 2011–JJA 2000s] (b) Δprecipitation [JJA 2011–JJA 2000s]

Figure 2.3: Same as Figure 2.2, but only for summer (June, July, August).

2.2 Emission data for 2011

In addition to meteorological variability, changes in the emissions affect the interannual variability of air pollution, deposition and and transboundary transport. The main changes in emissions in 2011 with respect to previous years are documented in the following sections.

2.2.1 Emission reporting under the LRTAP Convention in 2013

Parties to the LRTAP Convention submit air pollution emission data (SO_x, NO_x, NH_3, CO, NMVOCs, HMs, POPs and PM) annually to the EMEP Centre on Emission Inventories and Projections (CEIP) and notify the LRTAP Convention Secretariat thereof. Parties are requested to report emission inventory data using standard formats in accordance with the EMEP Reporting guidelines (UNECE 2009). The deadline for the submission of 2013 data was 15 February 2013.

This section refers to the most recent emissions and projections reported under the LRTAP Convention and emissions as used in the EMEP models. The original submissions by the Parties can be accessed via the CEIP homepage at `http://www.ceip.at/status-of-reporting/2013-submissions/`. Emissions used in EMEP models can be accessed at `http://www.ceip.at/webdab-emission-database/emissions-as-used-in-emep-models/`.

Reporting of emission inventories in 2013

Completeness and consistency of submitted inventories have improved significantly over the last 10 years but there are still areas for improvement. In 2013, 45 (88%) of the 51 Parties to the Convention submitted inventories. Of the 45 submissions, 34 Parties reported emission data by the due date (15 February 2013) as shown in Figure 2.4. Six Parties (Albania, Azerbaijan, Bosnia and Herzegovina, Kazakhstan, Montenegro and the Russian Federation) did not submit any data in 2013.

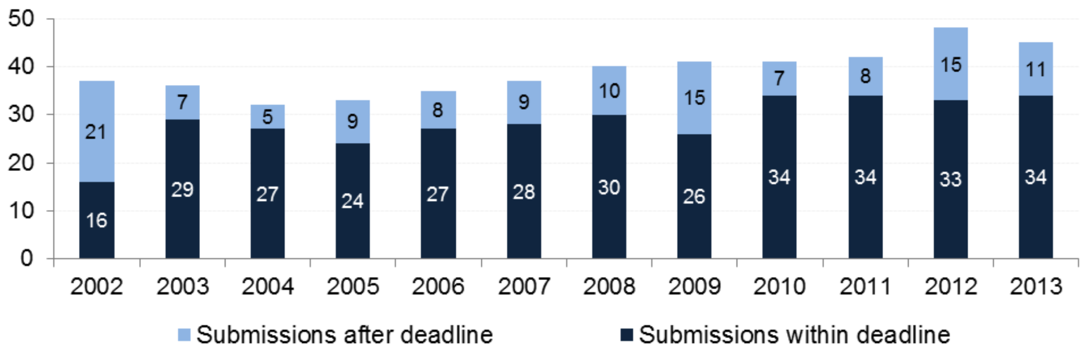

Figure 2.4: Number of Parties reporting emission data to EMEP since 2002 (as of 31 May 2013).

All 45 Parties submitted data on the main pollutants, but only 40 Parties provided data on PM emissions. Armenia submitted an inventory which is not consistent with the standard formats. All submitted inventories have been checked, and details on the completeness and consistency of submitted data can be found in Mareckova et al. (2013).

Reporting of gridded emissions in 2013

Gridded data form part of the five year reporting obligation and was not due for reporting in 2013. Nevertheless, gridded emissions of main pollutants and PM for 2011 were submitted by Cyprus, Finland and Spain. The United Kingdom submitted gridded data for 2010, calculated on the resolution of the new EMEP grid (0.1°x0.1° long-lat), on a voluntary basis. Spain submitted gridded emissions for the whole timeline from 1990 to 2011. All gridded sectoral data was submitted in GNFR sectors.

In total, only 23 of the 48 countries which are considered to be part of the extended EMEP area reported sectoral gridded emissions for the main pollutants and PM for the year 2010, and 22 countries for the year 2005. Twenty countries reported sectoral gridded data on the main pollutants and only 19 countries on PM for the year 2000.

19 countries (out of 48) did not report gridded sectoral data, neither for 2000 nor for 2005 and 2010 (Albania, Armenia, Azerbaijan, Bosnia and Herzegovina, Georgia, Greece, Kazakhstan, Kyrgyzstan, Liechtenstein, Luxembourg, TFY Republic of Macedonia, Malta, Republic of Moldova, Monaco, Montenegro, Romania, Serbia, Slovakia and Turkey). Italy, Iceland and the Russian Federation did not provide gridded sectoral data for 2005. Hungary, Lithuania, Belarus and Ukraine did not provide gridded sectoral emissions for 2000.

An overview of the reporting of gridded emissions is shown in Figure 2.5).

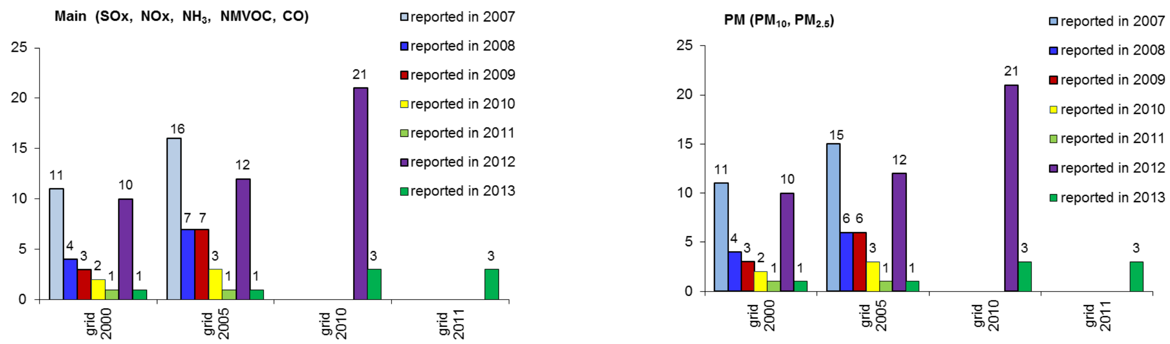

Figure 2.5: Number of Parties reporting gridded sectoral data to EMEP (as of 31 May 2013). Left: Main pollutants (SO_x, NO_x, NH_3, NMVOC, CO), Right: Particulate matter ($PM_{2.5}$,PM_{10}).

2.2.2 Uncertainty of reported data

It is very difficult to quantify the uncertainty of reported emissions, as countries in general do not provide such information. Variations observed in the 2005 emissions reported in subsequent years (2007-2013) are therefore regarded as a potential indicator of uncertainty. Figures 2.6–2.12) illustrate the variations observed in the individual countries' reported 2005 emissions, with 0% corresponding to 2005 emissions being the same as reported in 2013. Negative values indicate that 2005 emission levels reported in 2013 are higher than the values reported in previous years.

Significant fluctuations are visible in NMVOC, CO and PM 2005 emissions. A decrease of about 40% in 2005 emissions reported between 2007 and 2013 was observed rather frequently in the case of NMVOC and CO.

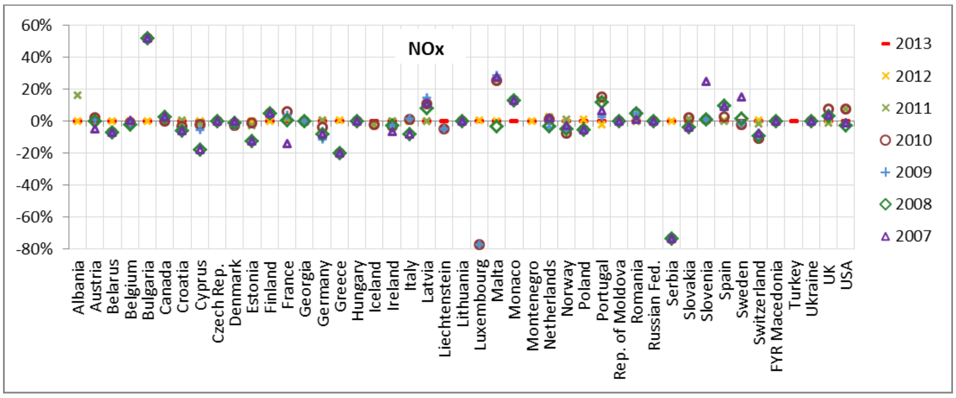

Figure 2.6: Variations in NO_x 2005 emissions reported between 2007 and 2013 (negative values indicate that emissions were lower in comparison to the value reported in 2013).

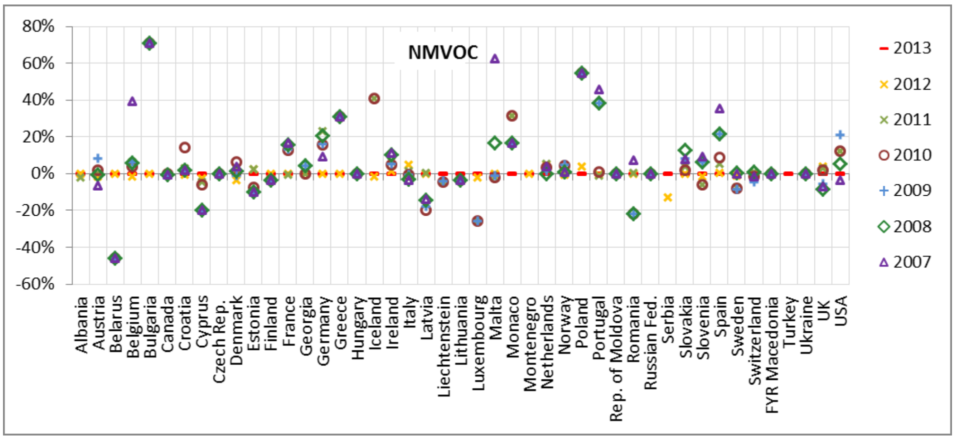

Figure 2.7: Variations in NMVOC 2005 emissions reported between 2007 and 2013 (negative values indicate that emissions were lower in comparison to the value reported in 2013).

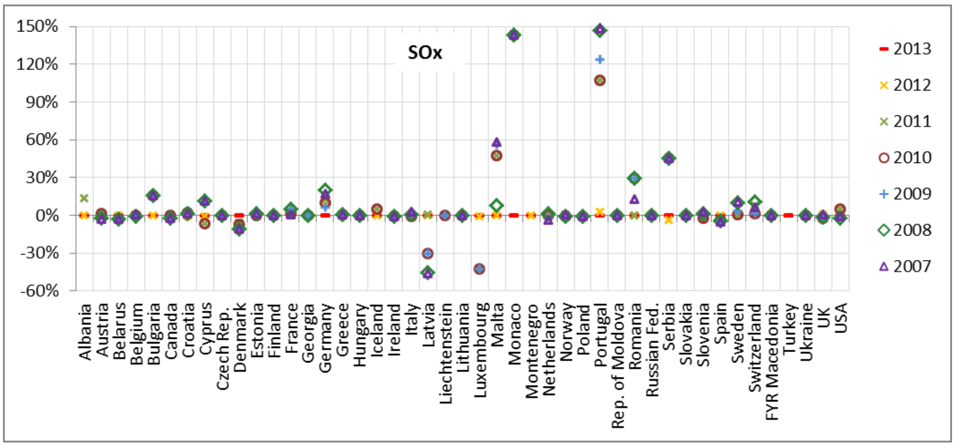

Figure 2.8: Variations in SO_x 2005 emissions reported between 2007 and 2013 (negative values indicate that emissions were lower in comparison to the value reported in 2013).

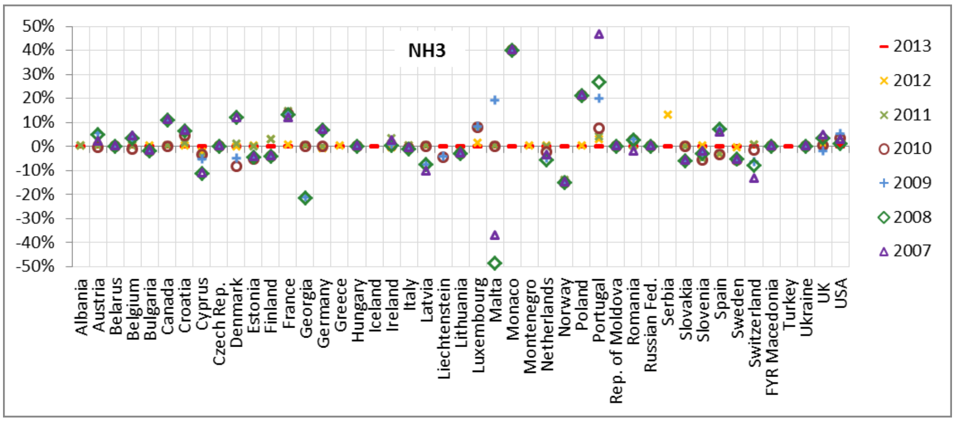

Figure 2.9: Variations in NH_3 2005 emissions reported between 2007 and 2013 (negative values indicate that emissions were lower in comparison to the value reported in 2013).

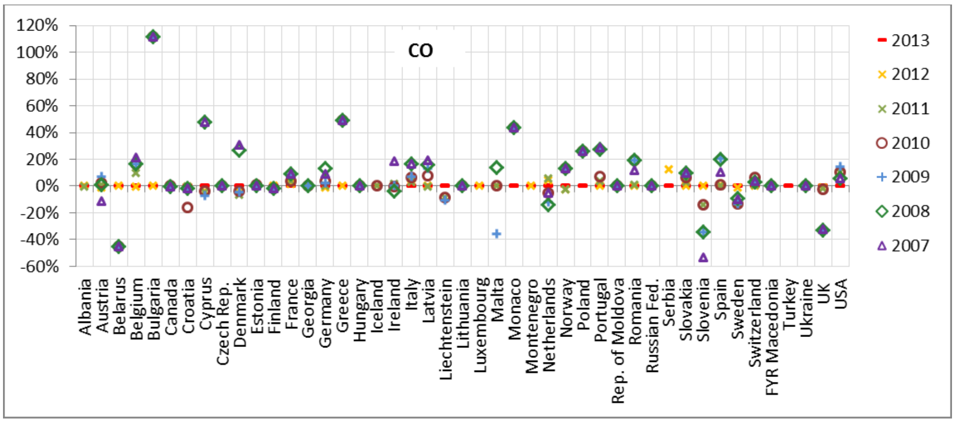

Figure 2.10: Variations in CO 2005 emissions reported between 2007 and 2013 (negative values indicate that emissions were lower in comparison to the value reported in 2013).

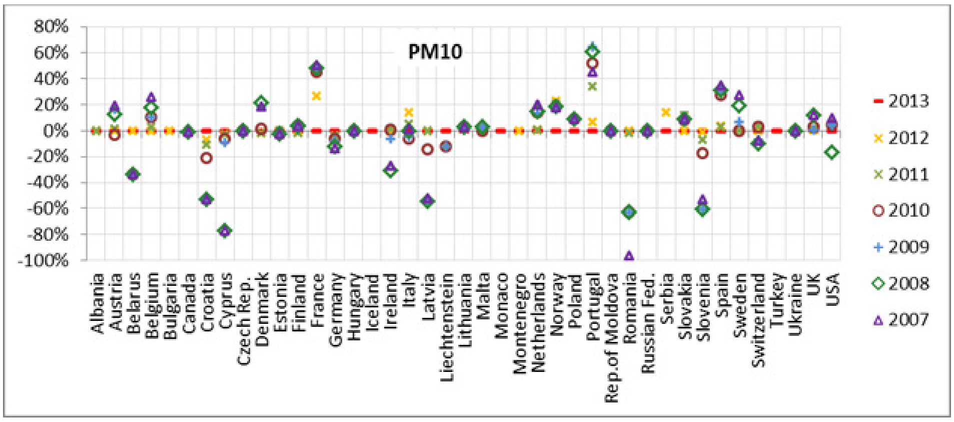

Figure 2.11: Variations in PM_{10} 2005 emissions reported between 2007 and 2013 (negative values indicate that emissions were lower in comparison to the value reported in 2013).

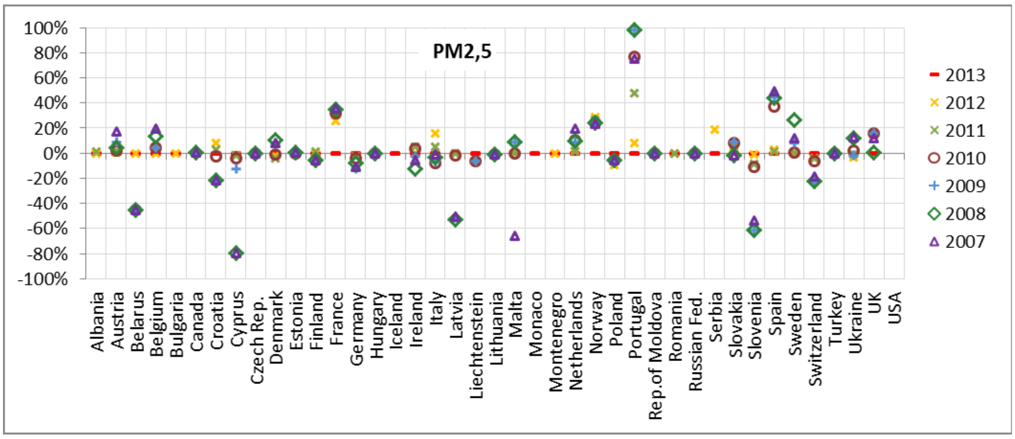

Figure 2.12: Variations in $PM_{2.5}$ 2005 emissions reported between 2007 and 2013 (negative values indicate that emissions were lower in comparison to the value reported in 2013).

Variations in SO_x and NO_x emissions are less frequent and mostly do not exceed $\pm$ 20%, although we also have a few extreme recalculations here. In addition, there are some countries (e.g. Belgium, Bulgaria, Malta, Monaco, Liechtenstein, Poland and Portugal) which reported 2005 emissions in 2007 that were more than twice as high as in 2012 or 2013, respectively.

An increase in 2005 emissions might indicate an improved completeness of the data, particularly on PM emissions, but to be able to prove this additional analysis would be needed.

The observed fluctuations in 2005 data during the last six years seem to indicate a relatively high level of uncertainty in PM and NMVOC and partly also CO and NH_3 emissions.

2.2.3 Emission Trends

The emission trends of air pollutants (NO_x, NMVOC, SO_x, NH_3, CO and PM) presented in Figure 2.13 and in Appendix B indicate that total emissions of all reported pollutants decreased in the EMEP area since 1990. These trends are partly based on reported data and partly on expert estimates. However, the situation in individual countries is different, as illustrated in Figures 2.14–2.16. In 11 countries emissions of at least one pollutant have increased during this period. Monaco reports almost constant data for the entire time series.

Overview tables with reported emission trends for individual countries have been published on the CEIP website at `http://www.ceip.at/status-of-reporting/2013-submissions`, while detailed information on the sectoral level can be accessed in WebDab (`http://www.ceip.at/webdab-emission-database/`).

The uncertainty of individual country data, particularly for PM trends, might be quite significant, while a number of countries do not update historical data.

Thirty-tree Parties[1] to the Convention defined 2010 targets for NO_x, NMVOC, SO_x and NH_3 in the Gothenburg Protocol (GP). These targets should not be exceeded in subsequent years either. However, Figures 2.14 and 2.15 indicate that a number of countries were not

[1]Parties with 2010 GP targets: Armenia, Austria, Belgium, Bulgaria, Belarus, Croatia, Cyprus, Czech Republic, Denmark, Finland, France, Germany, Greece, Hungary, Ireland, Italy, Liechtenstein, Lithuania, Luxembourg, Latvia, Republic of Moldova, Netherlands, Norway, Poland, Portugal, Romania, Slovakia, Slovenia, Spain, Sweden, Switzerland, United Kingdom and Ukraine. Of these, Armenia, Austria, Belarus, Greece, Ireland, Italy, Liechtenstein, Republic of Moldova, Poland and Ukraine have not signed/ratified the GP yet.

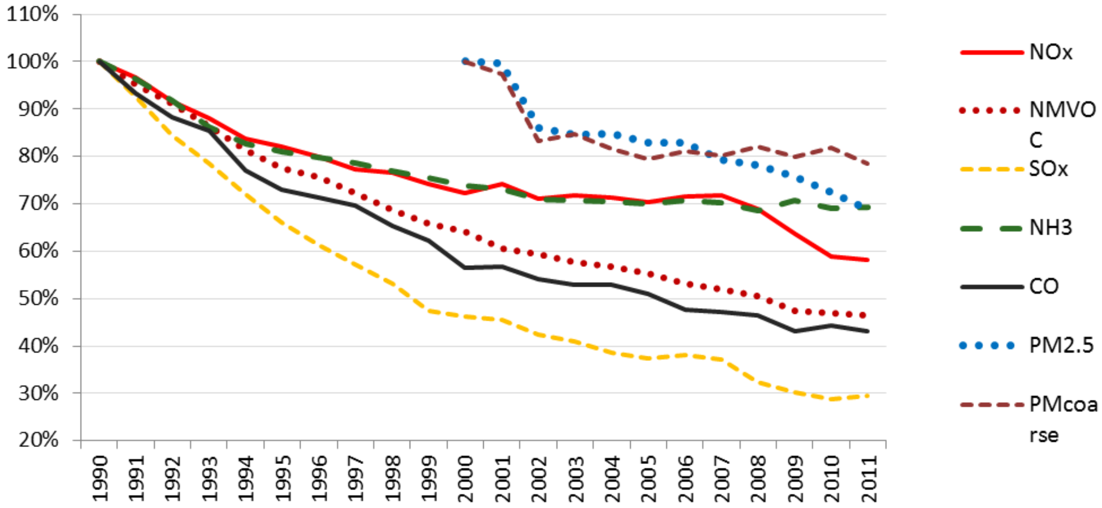

Figure 2.13: Emission trends [%] in the EMEP area for 1990–2011 based on data reported by countries (gap-filled with expert estimates). Shipping emissions are not included.

fully successful in reducing their emissions. These countries exceeded their individual ceilings also in 2011.

NO_x emissions

On the basis of reported data, the total reduction of NO_x emissions in the EMEP countries for the period 1990–2011 was estimated to be -42%. Emissions decreased in 41 countries and increased in six countries (Figure 2.14). The strongest increase was reported by Turkey (+98%). Nine countries still exceed their NO_x ceilings stipulated in the GP, e.g. Austria[2], Luxembourg and Liechtenstein by more than 70%.

NMVOC emissions

Compared to 1990, NMVOC emissions decreased in 43 countries and increased in four countries (Figure 2.14). The strongest NMVOC increase can be observed in Georgia[3], where emissions more than doubled. NMVOC emissions in the EMEP area have decreased since 2010 by another 2%, in total -53% compared to 1990 levels. GP emission targets are not reached by 3 countries; the exceedances reported by Germany and Luxembourg are minor (about 1%), while being more significant in Belarus (12%).

SO_x emissions

Of all reported pollutants, SO_x emissions decreased most substantially (-71%) between 1990 and 2011. However, it should be noted that SO_x emissions within the overall EMEP region have increased by 4% compared to last year. Compared to 1990, SO_x emissions have decreased in 44 countries and increased in three countries (Figure 2.15); Iceland (+283%), Turkey (+52%) and the FYR of Macedonia (+4%). No country exceeded its SO_x GP target, neither in 2010 nor in 2011.

[2]Calculations are based on fuel sold.

[3]Based on gap-filled reported data for 2010 and expert estimates for 1990

NH_3 emissions

Compared to 1990, NH_3 emissions decreased in 39 countries and increased in 8 countries (Figure 2.15). The strongest increases are reported by Malta (+118%) and Spain (+14%). The total decrease in national total emissions from 1990 to 2011 amounted to -31%. Seven countries (2 more than in 2010) exceeded their GP targets also in 2011.

CO emissions

Compared to 1990, CO emissions in 2011 decreased in all Parties except Turkey, where they increased by 51% (Figure 2.16). The total decrease of CO emissions in the EMEP area from 1990 to 2011 amounted to -57%.

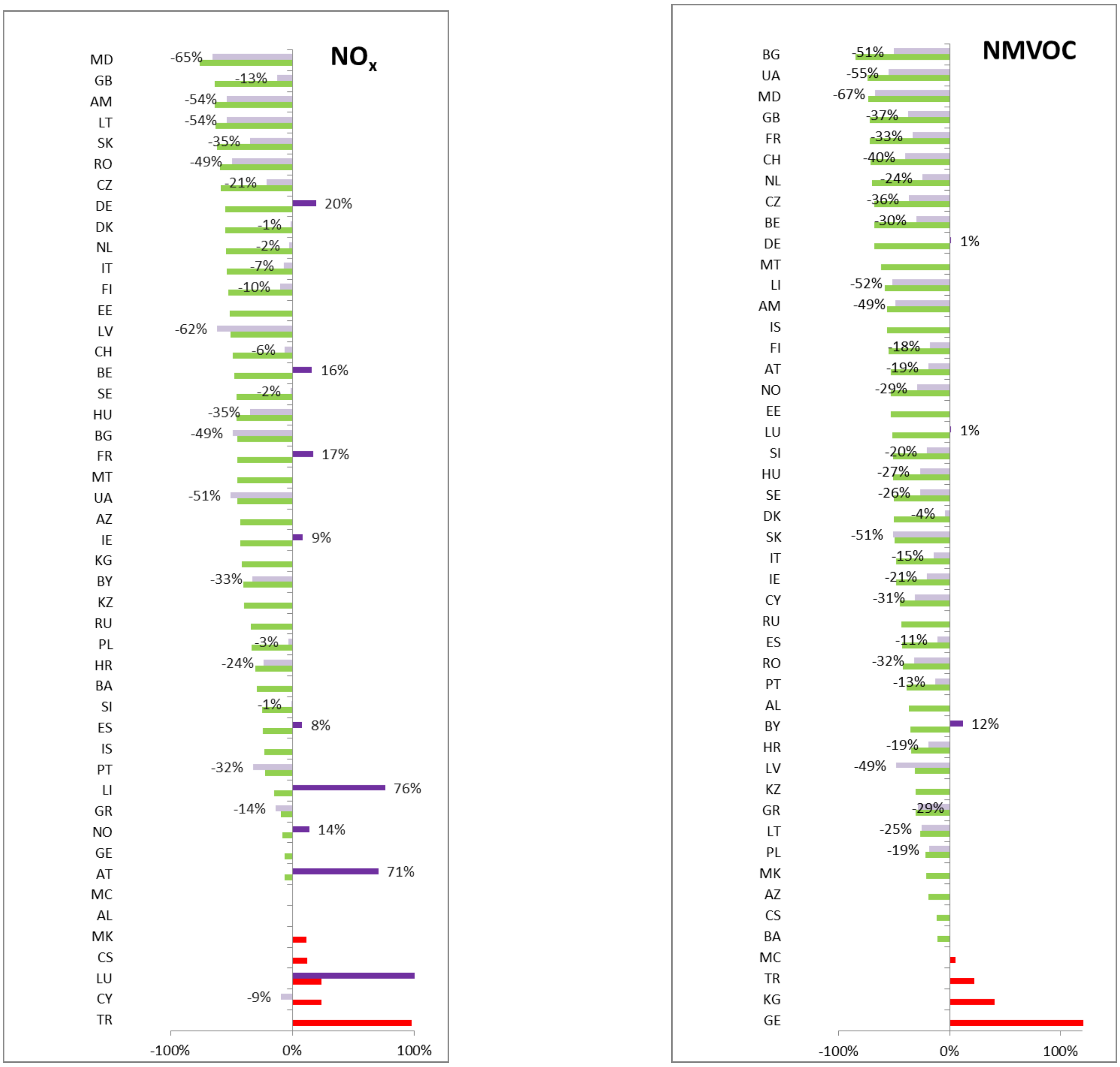

Figure 2.14: Differences in individual countries emissions reported for 1990 and 2011 (Green: 2011 emissions are lower than in 1990, Red: 2011 emissions are higher than in 1990), and the distance of 2011 emissions from the GP targets (Light purple: 2011 emissions were below the GP target, Dark purple: 2011 emissions were above the GP target). NO_x (left) and NMVOC (right).

PM emissions

PM emissions have been reported only from 2000 onwards and since that time the values are decreasing. However biggest decrease of emissions observed between 2001 and 2002 does not correspond to emission trends of other pollutants (Figure 2.13) and may rather indicate incomplete PM reporting for the year 2001.

The total decrease in $PM_{2.5}$ emissions from 2000 to 2011 amounted to -31%. Compared to the year 2000, $PM_{2.5}$ emissions decreased in 29 countries and increased in 18 countries (Figure 2.16). Increases by 30% or more are reported by the Republic of Moldova (+126%), Belarus (+99%) and Bulgaria (+30%). Part of these increases might be due to an improved completeness of the reported data.

Figure 2.15: Differences in individual countries emissions reported for 1990 and 2011 (Green: 2011 emissions are lower than in 1990, Red: 2011 emissions are higher than in 1990), and the distance of 2011 emissions from the GP targets (Light purple: 2011 emissions were below the GP target, Dark purple: 2011 emissions were above the GP target). SO_x (left) and NH_3 (right).

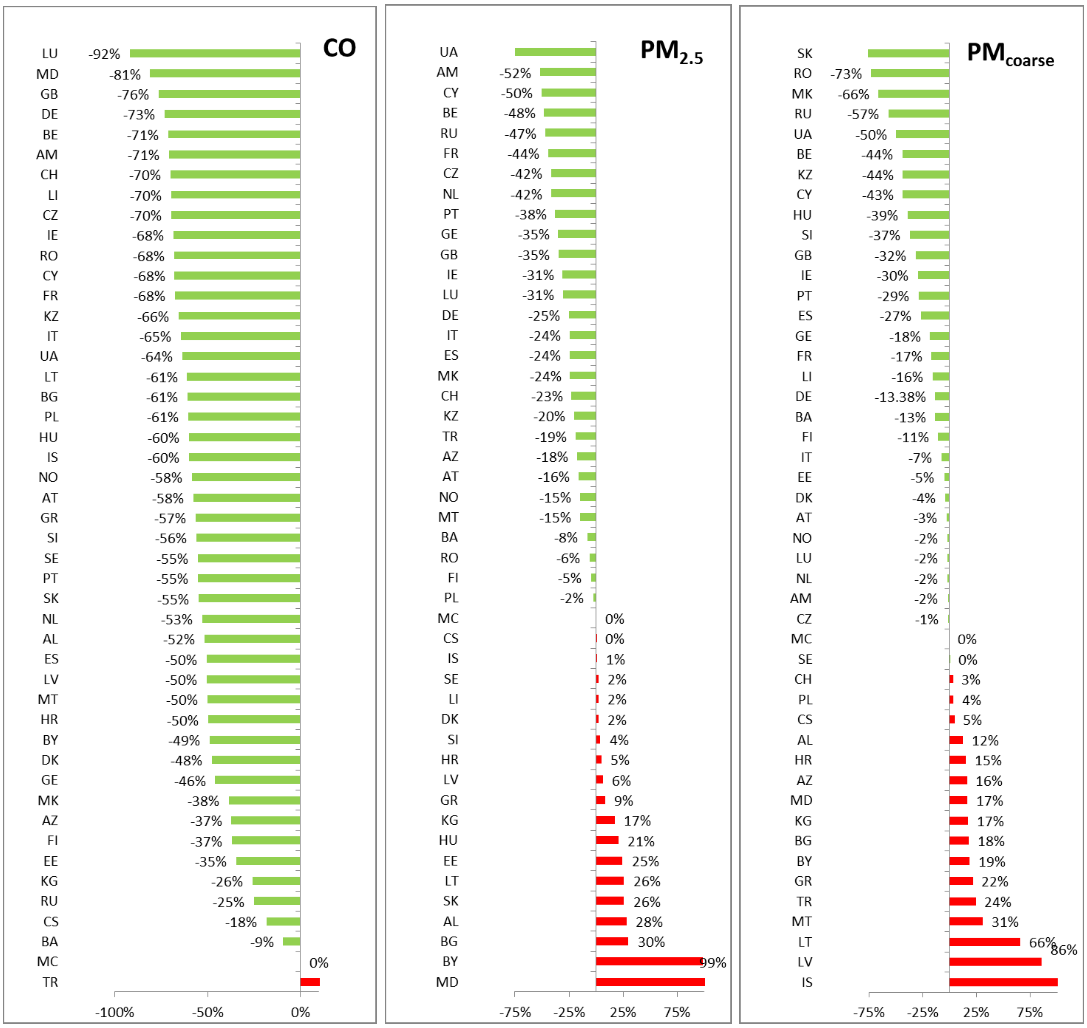

Figure 2.16: Differences in individual countries emissions reported for 1990 and 2011. (Green: 2011 emissions are lower than 1990. Red: 2011 emissions are higher than 1990). CO (left), $PM_{2.5}$ (middle) and PM_{coarse} (right).

Compared to 2000, PM_{coarse} emissions decreased in 30 countries and increased in 17 countries (Figure 2.16). The strongest increases are reported by Iceland (+103%), Latvia (+86%), Lithuania (+ 66%) and Malta (+31%). The total decrease of PM_{coarse} emissions from 2000 to 2010 is amounted to -22%.

2.2.4 Emission data used for modelling in 2013

In order to create emission data for the modellers, reported sectoral (NFR09) emissions are aggregated to 10 SNAP sectors[4]. If countries do not report complete sectoral timeseries, the aggregated emissions are gap filled. To gap-fill the missing sectoral emissions, CEIP applies three methods:

a) linear extrapolation of the last five years (three years as a minimum)

[4]A table showing the conversion between NFR09 and SNAP is available on the CEIP website. `http://www.ceip.at/fileadmin/inhalte/emep/pdf/nfr09_to_snap.pdf`

b) copy of previous years emissions (data from 2009 or 2008)

c) other sources (e.g. IIASA, ENTEC, UNFCCC, NECD, etc.)

The gap-filled sectoral SNAP emissions are distributed across an extended EMEP grid using the 'base grid'. The base grid defines the distribution of emissions in the extended EMEP area and was calculated by using gridded sectoral emissions if reported by countries and/or proxy data such as large point sources, population data and data from different models if no or incomplete data were reported by countries. The overview information on gap-filled sectors is listed in Table 2.1.

The gap-filled data are imported to WebDab and are available on the CEIP website under "Emissions as used in EMEP models" (`http://www.ceip.at/webdab-emission-database/emissions-as-used-in-emep-models/`).

Table 2.1: List of countries and pollutants for which expert estimates were used in the 2011 data set. The table lists only countries/areas for which expert estimates were used for at least one sector. x means that the data are gap-filled.

Parties	NO_x	NMVOC	SO_x	NH3	$PM_{2.5}$	PM_{coarse}	CO
Albania	x	x	x	x	x	x	x
Armenia	x	x	x	x	x	x	x
Azerbaijan	x	x	x	x	x	x	x
Belgium		x					
Bosnia and Herzegovina	x	x	x	x	x	x	x
Bulgaria					x	x	
Czech Republic		x	x				x
Georgia	x	x	x	x	x	x	x
Greece	x	x	x	x	x	x	x
Iceland					x	x	
Kazakhstan	x	x	x	x	x	x	x
Kyrgyzstan	x	x	x	x	x	x	x
Lithuania					x	x	
Luxembourg		x			x	x	
FYR of Macedonia					x	x	
Montenegro	x	x	x	x	x	x	x
Republic of Moldova	x	x	x	x	x	x	x
Russian Federation	x	x	x	x	x	x	x
Switzerland			x			x	x
Tajikistan	x	x	x	x	x	x	x
Turkey					x	x	
Turkmenistan	x	x	x	x	x	x	x
Ukraine			x		x	x	
Uzbekistan	x	x	x	x	x	x	x
Other areas	**NO_x**	**NMVOC**	**SO_x**	**NH_3**	**$PM_{2.5}$**	**PM_{coarse}**	**CO**
Asian Areas	x	x	x	x	x	x	x
N-E Atlantic Ocean	x	x	x		x	x	x
Baltic Sea	x	x	x		x	x	x
Black Sea	x	x	x		x	x	x
Caspian Sea	x	x	x		x	x	x
Mediterranean Sea	x	x	x		x	x	x
North Sea	x	x	x		x	x	x
North Africa	x	x	x	x	x	x	x

For 2011 shipping data, interpolated NO_x, SO_x and PM emissions were used based on recent estimates by IIASA for year 2010 and 2015. CO and NMVOC emissions were interpolated using ENTEC/IIASA estimates from the 2007 shipping study “Analysis of Policy Measures to Reduce Ship Emissions in the Context of the Revision of the National Emissions Ceilings Directive” (Cofala et al. 2007) for years 2010 and 2020. The activity levels for the new NO_x, SO_x and PM estimates are the same as the ones used in this shipping study, but the baseline from 2007, which is still used for CO and NMVOC, is now outdated because it does not include SECAs for the Baltic Sea and the North Sea.

Emission data for the “extended EMEP area” (e.g. Kazakhstan, the Asian part of Russia, Kyrgyzstan, Uzbekistan, Turkmenistan and North Africa) were not reported to CEIP. As a consequence, expert estimates were used for the gridding[5] process.

[5]In 2009, CEIP considered the extended EMEP domain in the gap-filling and gridding process for the first time. Since emission data was missing from a number of countries in this area, MSC-W estimates from 2009 were used and gridded together with current population data in specific countries. For the Russian areas in the extended EMEP domain, these estimates were adjusted according to the reported emission trends for the European part of the Russian Federation. The source of population data used by CEIP for gridding was IIASA.

2.3 Main changes in concentrations and depositions in 2011

The differences between the reported concentrations and depositions for 2010 (reported last year) and 2011 (reported this year) are mainly due to changes in emissions and meteorological variability. Furthermore, the EMEP MSC-W model has been updated since last year (see chapter 3). Here we discuss briefly the effects caused by emission changes and changes in meteorological conditions.

2.3.1 Changes in sulphur and nitrogen deposition

We have calculated air concentrations and depositions for the years 2010 and 2011 with the same EMEP MSC-W model version (rv4.4), using consistent meteorological data and the most updated set of emission data.

In Figure 2.17 we show first the modelled total changes in depositions of sulphur, oxidized nitrogen and reduced nitrogen (top row). Changes due to emission change only, and changes due to meteorological change only, are shown in the middle and bottom rows, respectively.

The effects of emissions only are consistent with the emission data used by the EMEP MSC-W model. In most countries these changes are small from one year to another, although there are notable exceptions.

Even when annually averaged, as in this figure, the influence of meteorology is quite substantial and in many areas overwhelms the effect of the small emission change. This, of course, does not mean that emission changes are not important. Where meteorological change counteracts the benefits of emission reductions we can safely assume that without emission reduction, pollution levels would be even worse. In cases where meteorology is favourable to air quality, emission reductions would improve air quality even further. From 2010 to 2011, anthropogenic emissions of SO_x in the extended EMEP domain increased by 3.7%, although this is due to substantial increases in a small number of countries only (e.g. Bulgaria, Turkey, Ukraine, Spain). Decreases in volcanic emissions (not considering the Grímsvötn eruption [6]) led to a total increase in SO_x emissions from 2010 to 2011 of 2.6%. In spite of this increase, the total deposition of sulphur in the extended EMEP domain decreased by 5.5%, which can be explained by (in this context) favorable meteorological conditions, such as the dryer conditions in large areas of the domain, effectively reducing the amount of wet deposition and increasing export out of the EMEP domain. A model calculation shows that, with the meteorological conditions of 2010, the total deposition of sulphur would have indeed increased by about 2.5%, reflecting the increase in emissions.

NO_x emissions were reduced by 4.2% from 2010 to 2011, while the deposition of oxidized nitrogen, on average, decreased by as much as 9.3% during the same period, due to larger export as in the case of sulphur. Without meteorological change, deposition would have decreased by about 4.3% only, closely matching the emission change. In another model experiment we have kept the emissions constant and changed only meteorology, resulting in a reduction in deposition of reduced nitrogen by about 5%, i.e. clearly short of the total change (–9.3%), thus illustrating the additional benefit from emission reductions. In the case of reduced nitrogen, emissions of NH_3 increased by 2.9% while the deposition of reduced nitrogen decreased

[6]The eruption at Grímsvötn volcano in Iceland in May 2011 has not been included in the model simulations. The reason for this is that the eruption plume reached heights up to 16 km, which is currently above the top layer of the EMEP MSC-W model, thus the plume and its transport can not be simulated by the current version of the model. As described in chapter 3, extension of the model's vertical domain is currently under development.

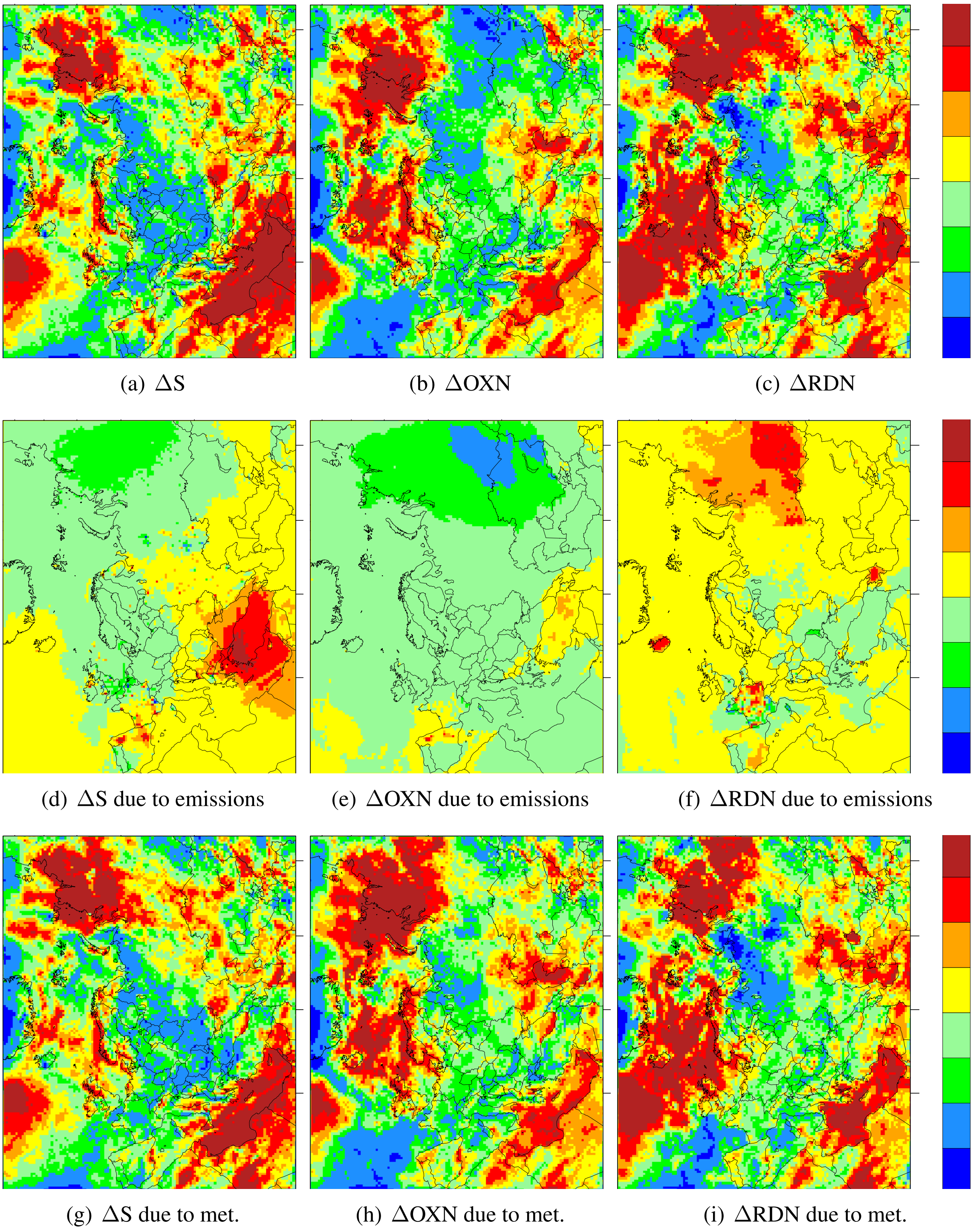

(a) ΔS (b) ΔOXN (c) ΔRDN

(d) ΔS due to emissions (e) ΔOXN due to emissions (f) ΔRDN due to emissions

(g) ΔS due to met. (h) ΔOXN due to met. (i) ΔRDN due to met.

Figure 2.17: Changes from 2010 to 2011 (annual values in %) for: sulphur deposition (left column), oxidized nitrogen deposition (middle column), and reduced nitrogen deposition (right column). The top panels show the total effect, while the middle and bottom rows show, respectively, the contribution from emission change only, and the contribution from meteorological change only.

slightly, by about 0.7%. Also in this case, meteorological change has acted favourably. Without this change, depositions would have increased by more than 3%.

2.3.2 Changes in ozone

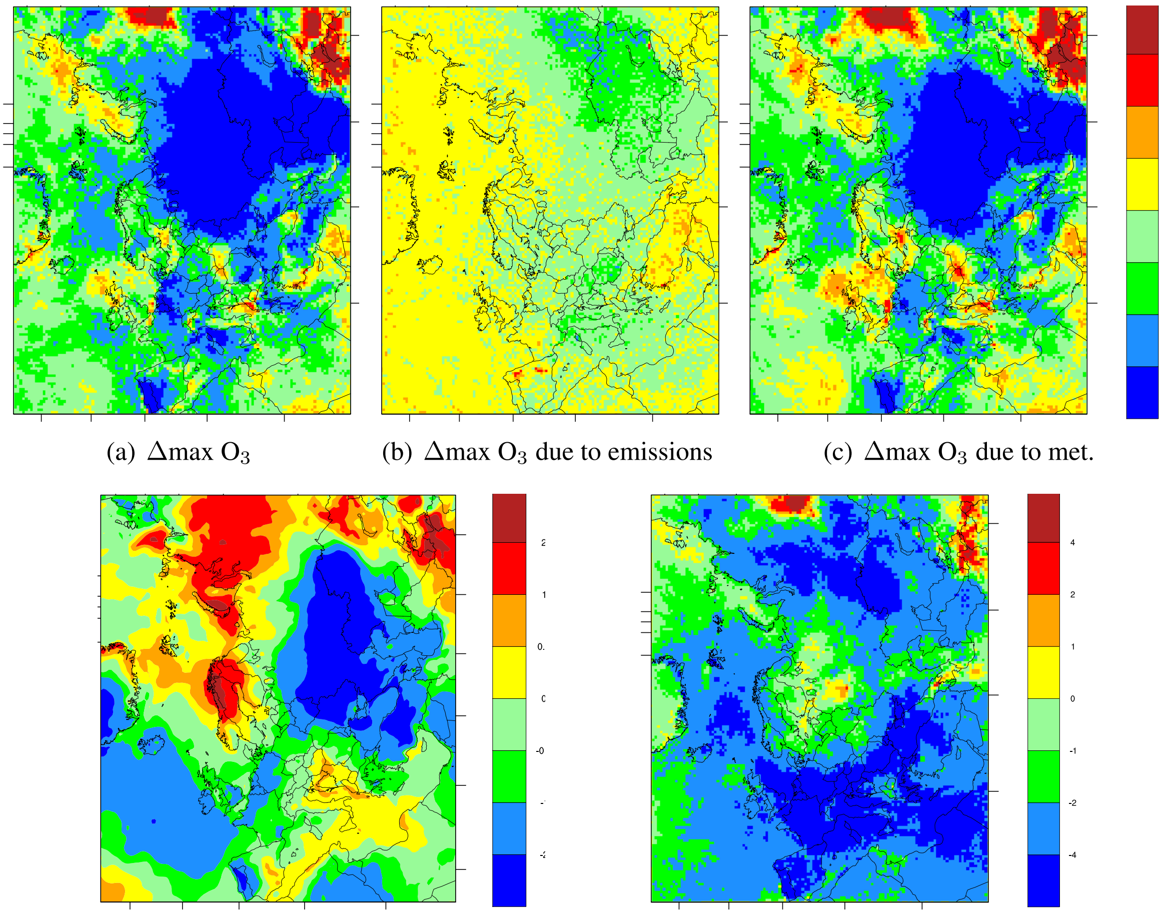

(a) Δmax O_3 (b) Δmax O_3 due to emissions (c) Δmax O_3 due to met.

(d) ΔT_{2m} (e) Δmax O_3 (wrt 2000s)

Figure 2.18: Differences between 2011 and 2010 summer values for: (a) max ozone [ppb], (b) max ozone due to emissions, (c) max ozone due to meteorology, (d) Temperature at 2m [K], e) Difference in max ozone [ppb] between 2011 and the average of 2000-2009 summer values.

The upper left panel of Figure 2.18 shows changes in summer ozone maxima from 2010 to 2011 as calculated by the EMEP MSC-W model. Maximum ozone levels decreased almost everywhere from 2010 to 2011, with values more than 4 ppbv lower than in 2010 over large parts of Russia and Central Asia, but also in Europe (e.g. Portugal, Central Europe, Greece). As can be seen in the upper middle panel only a small part of this change can actually be explained by changes in emissions, although it can be noted that emissions have led to some reduction in maximum ozone in most areas of the model domain, except Turkey, Northern Spain and some areas that are influenced by the boundary conditions (import from outside the model domain), e.g. the North Atlantic and the Arctic. Emission change has led to maximum ozone reductions by more than 1 ppb, e.g., in Northern Italy, Hungary, Romania and large areas of Central Asia. The upper right panel in Figure 2.18 shows the change in maximum ozone which is due to changes in meteorology. Indeed it explains most of the total change in maximum ozone, partly due to cooler summer temperatures (e.g. Portugal, Russia) as seen in the left panel of the second row, although temperature change can not explain the ozone change at all. A more detailed analysis of meteorological change is beyond the scope of this section, but it is interesting to note that most of the change in maximum ozone between 2010 and 2011 appears to be related to meteorological conditions. The bottom right panel of the figure shows the difference in maximum summer time ozone between 2011 and the multi-year average for the 2000–2009 period. Judging from this figure 2011 had relatively low maximum ozone also compared to the multi-year average (and not only compared to 2010). Air quality indicators such as SOMO35 (not shown) decreased on average from 2010 to 2011, although this, too, was mainly a meteorological effect (e.g. due to the cooler summer in Western Russia and many parts of Europe in 2011, as compared to 2010). Nevertheless, the benefits of emission reductions in ozone precursors can be assessed in model calculations and are shown to contribute to the improvement of air quality in many countries.

2.4 Combined model results and observations for 2011

As in previous years, we have combined EMEP measurements with model data regarding air concentrations and depositions for 2011, not only to calculate normalized differences between model and observations, but also, and more importantly, to obtain data that are as close to reality as possible. The results of this effort are shown in the next sections.

2.4.1 Acidification and eutrophication

In this section, we present the 'best estimates' for air concentrations of SO_2, SO_4^{2-}, NH_3+NH_4^+ and HNO_3+NO_3^- as well as concentrations of oxidized sulphur, oxidized nitrogen and reduced nitrogen in precipitation. The 'best estimates' have been created by using a combination of model results and observations from the EMEP network for 2011. For all measurement points, the difference between the measured value at that point and the modelled value in the corresponding grid cell is calculated. This difference is interpolated spatially using radial basis functions, giving a continuous two-dimensional function describing the difference at any point within the modelled grid. For the interpolated normalized differences (observations-model/(observations+model)), positive values show where the model underpredicts the values, whilst negative values show where the model overpredicts values. The combined maps are derived by adjusting the model results with the interpolated differences, giving large weight to the observed values close to stations, and using the modelled values in areas with no observations. The range of influence of the measured values depends on the component, and has been set to 300 km for NH_3+NH_4^+ and HNO_3+NO_3^- in air, and to 500 km for all other components. For each of the components, we present four different figures, visualizing the different steps of the procedure (Figures 2.19 to 2.22). In general, there is good agreement between model results and measurements for 2011 as for previous years. Thus, the combined results are rather similar to the model results. Please note that a more detailed evaluation of the performance of the EMEP MSC-W model, version rv4.4, for 2011 is not included in this chapter, but is available on the EMEP website (Nyíri et al. 2013) and in summarized form in chapter 3.

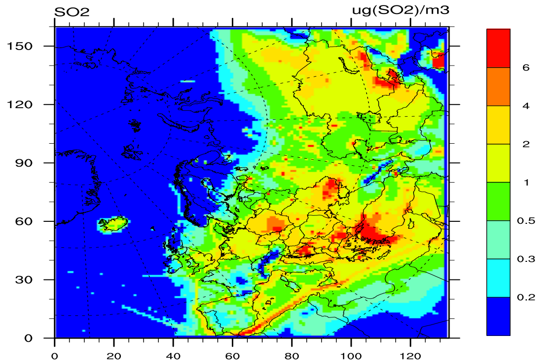

(a) Modelled SO_2 in air

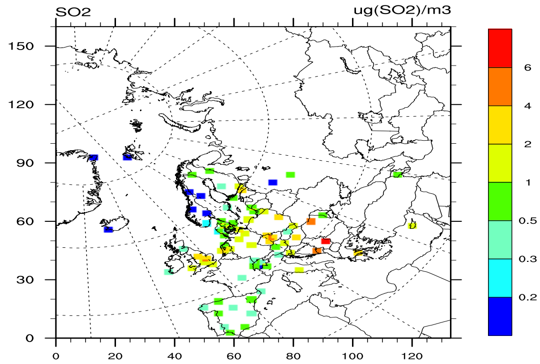

(b) Measured SO_2 in air

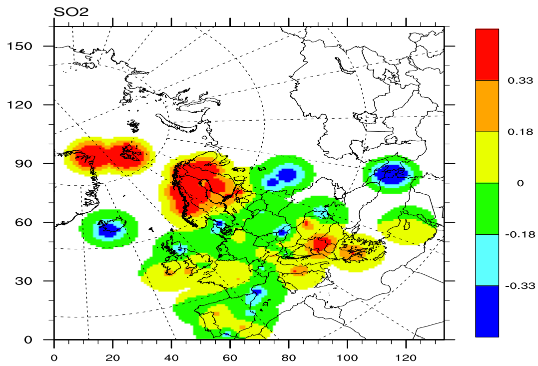

(c) Interpolated normalized differences

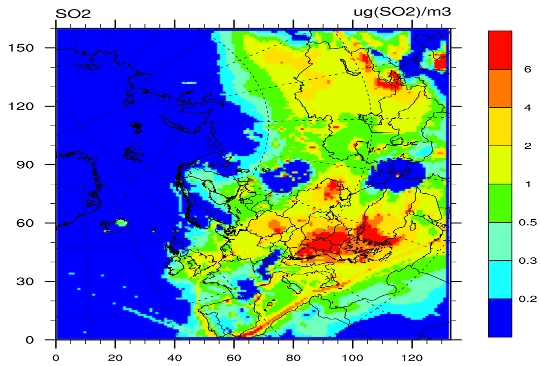

(d) Combined SO_2 in air

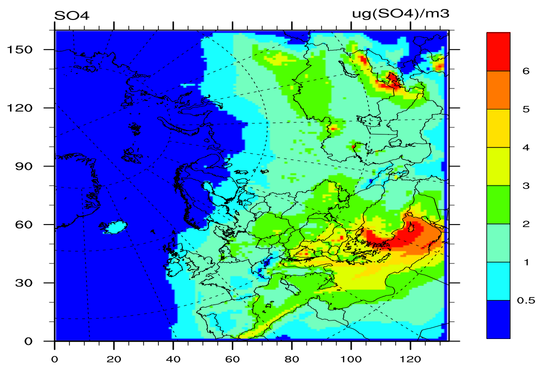

(e) Modelled SO_4^{2-} in air

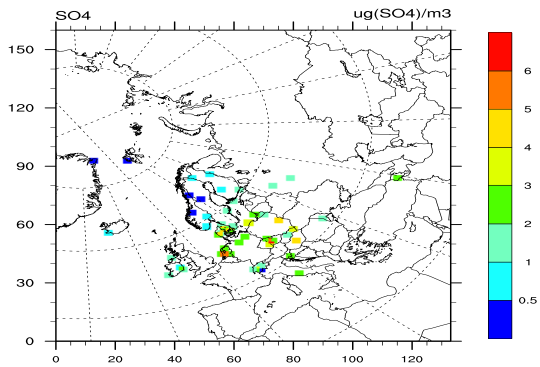

(f) Measured SO_4^{2-} in air

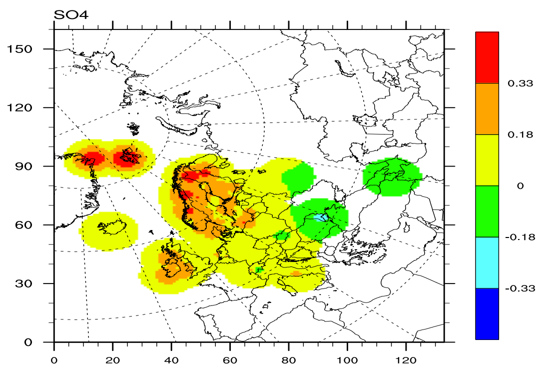

(g) Interpolated normalized differences

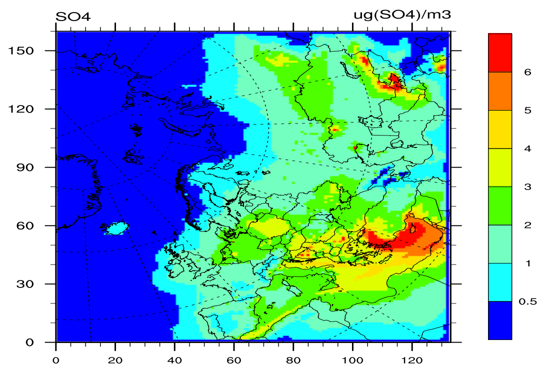

(h) Combined SO_4^{2-} in air

Figure 2.19: Yearly averaged SO_2 (a)-(d) and SO_4^{2-} (e)-(h) concentrations in air [μg m^{-3}] in 2011.

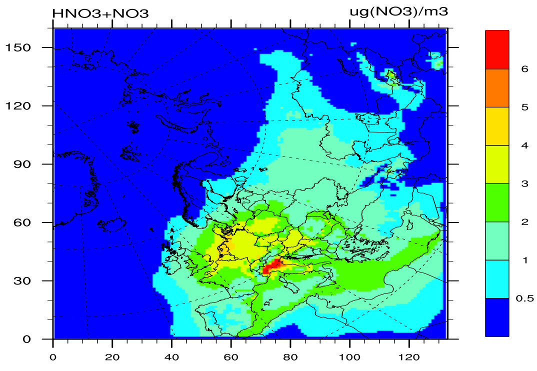

(a) Modelled total nitrate in air

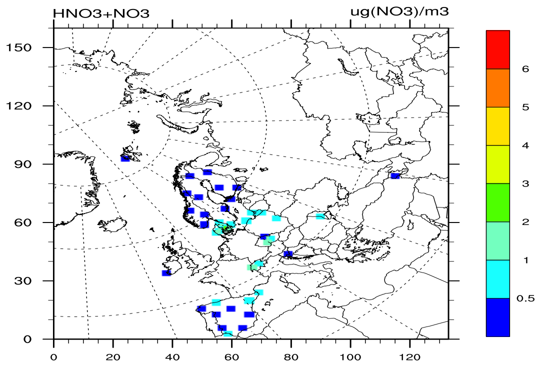

(b) Measured total nitrate in air

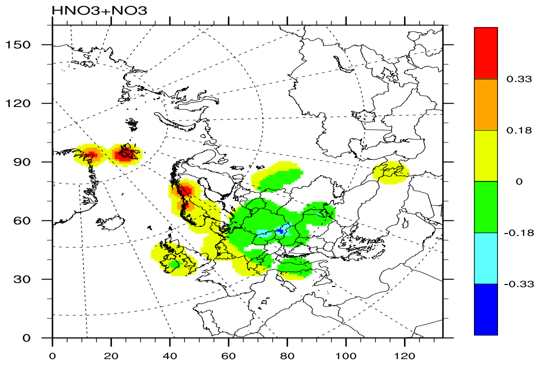

(c) Interpolated normalized differences

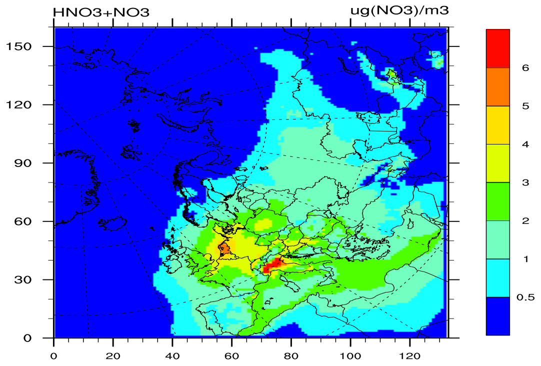

(d) Combined total nitrate in air

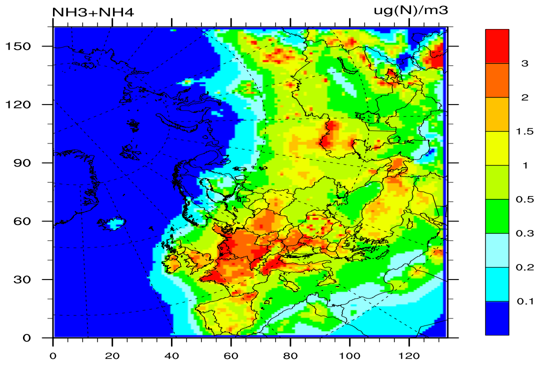

(e) Modelled ammonia+ammonium in air

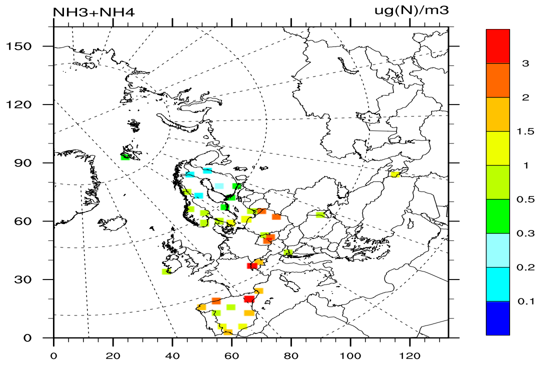

(f) Measured ammonia+ammonium in air

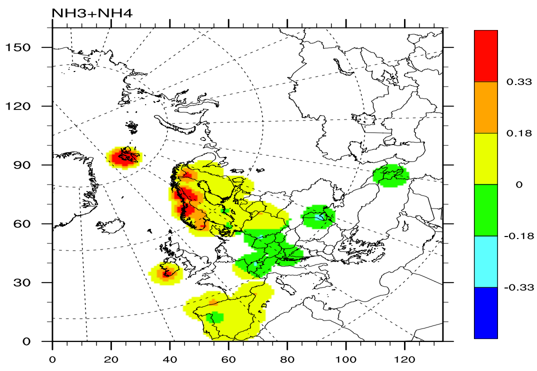

(g) Interpolated normalized differences

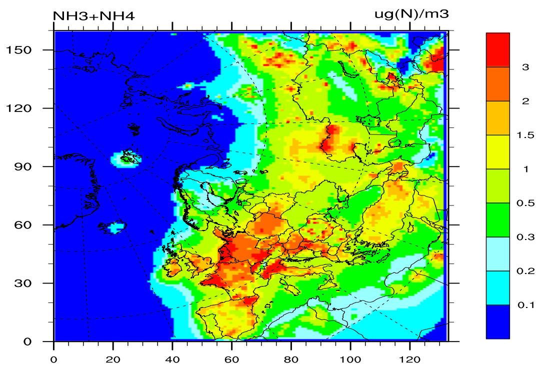

(h) Combined ammonia+ammonium in air

Figure 2.20: Yearly averaged HNO_3+NO_3^- (a)-(d) and NH_3+NH_4^+ (e)-(h) concentrations in air in 2011. Units: [μg(NO_3) m^{-3}] for HNO_3+NO_3^- and [μg(N) m^{-3}] for NH_3+NH_4^+.

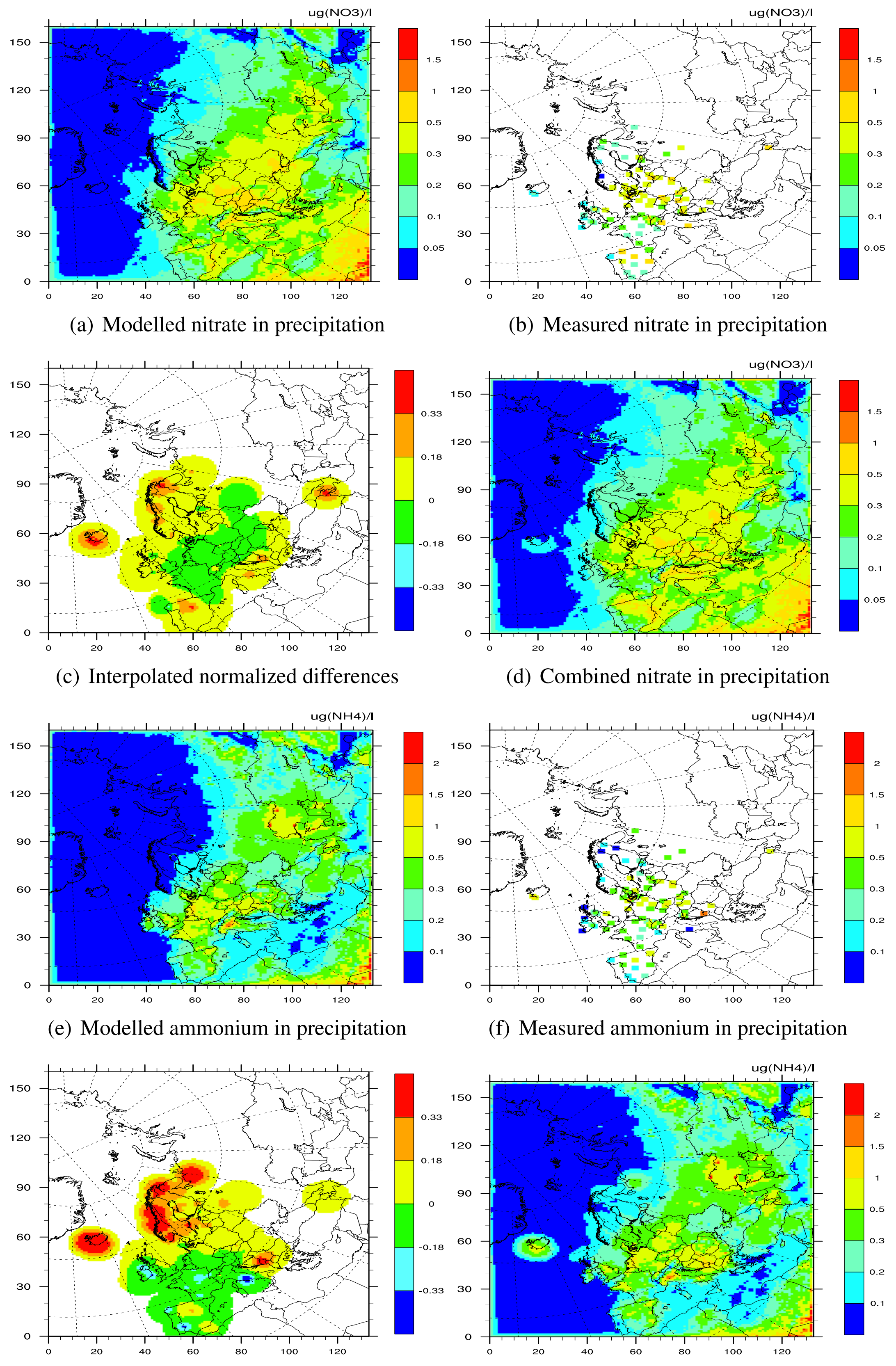

(a) Modelled nitrate in precipitation
(b) Measured nitrate in precipitation
(c) Interpolated normalized differences
(d) Combined nitrate in precipitation
(e) Modelled ammonium in precipitation
(f) Measured ammonium in precipitation
(g) Interpolated normalized differences
(h) Combined ammonium in precipitation

Figure 2.21: Yearly averaged oxidized nitrogen (a)-(d) and reduced nitrogen (e)-(h) concentrations in precipitation [μg/l] in 2011.

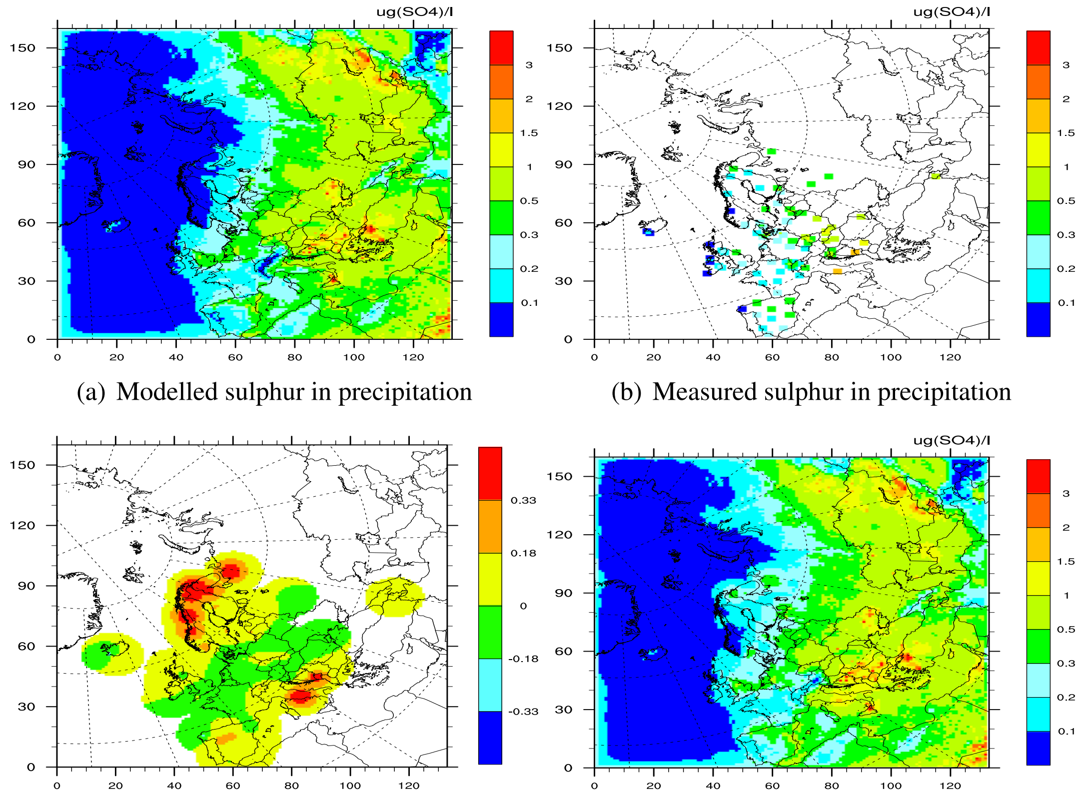

(a) Modelled sulphur in precipitation
(b) Measured sulphur in precipitation
(c) Interpolated normalized differences
(d) Combined sulphur in precipitation

Figure 2.22: Yearly averaged sulphur concentrations in precipitation [μg/l] in 2011.

2.4.2 Ozone and nitrogen dioxide

'Best estimates' have also been calculated for air concentrations of ozone and NO_2, using a combination of model results and observations from the EMEP network for 2011. The technique is the same as described in section 2.4.1.

There is good agreement between model results and observation in 2011, thus the maps of combined results look very similar to those of the model results. Therefore we show only the combined results and the normalized error in Figure 2.23. For ozone the normalised errors are relatively small, within $\pm 5\%$ over large parts of Europe, and almost always within $\pm 10\%$, although some areas of more severe underestimation remain, e.g. in Northern Italy and the BeNeLux area. NO_2 is a more difficult compound to model, as it has a short lifetime in the atmosphere and the variability within a 50×50 km^2 grid cell can be large. Normalised errors are larger than for ozone, but still most areas of Europe show normalised errors within the $\pm 18\%$ range as shown in Figure 2.23(f).

A detailed evaluation of the EMEP MSC-W model, version rv4.4, in terms of ozone and NO_2 for 2011 is available on the EMEP website (Gauss and Hjellbrekke 2013).

2.5 Exceedances of critical loads

The calculated exceedances of critical loads and the ecosystem areas at risk in 2011 are presented in Figure 2.24 both for Europe in the old EMEP domain (a)-(d) and for EECCA countries in the extended EMEP domain (e)-(h). The calculations for Europe in the old EMEP

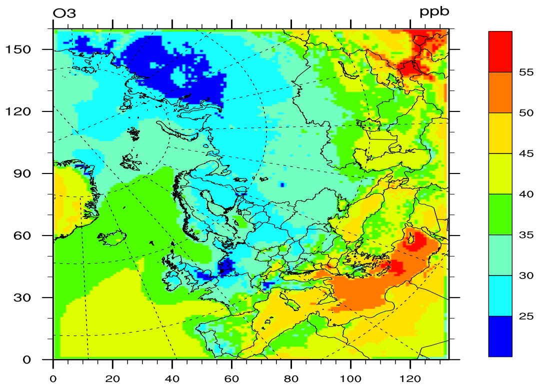

(a) Combined (model+obs)

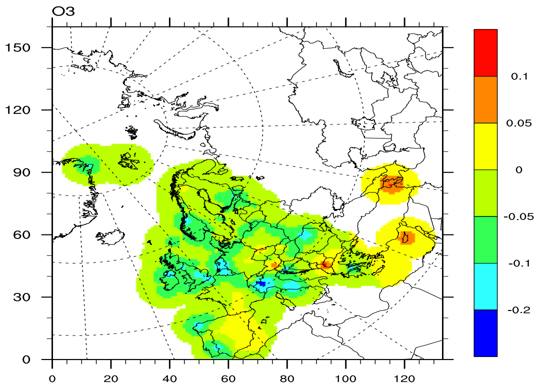

(b) Interpolated normalized differences

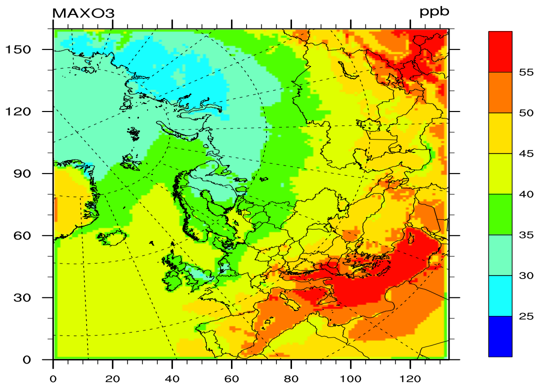

(c) Combined (model+obs)

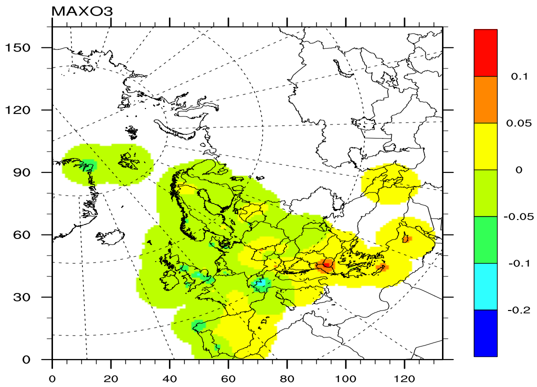

(d) Interpolated normalized differences

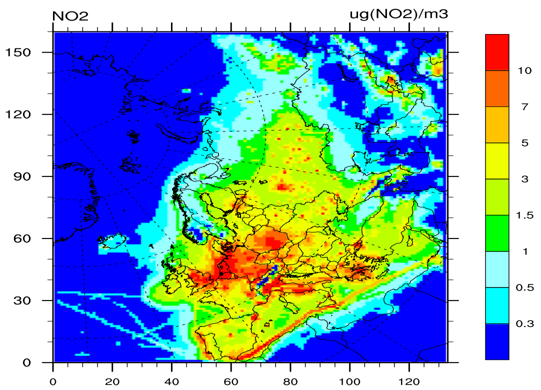

(e) Combined (model+obs)

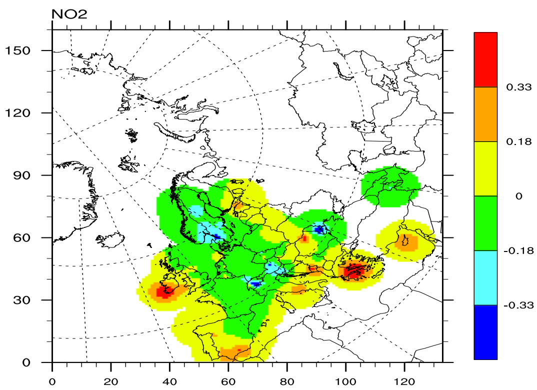

(f) Interpolated normalized differences

Figure 2.23: Yearly averages, and interpolated differences, for: daily mean ozone (a+b), daily maximum ozone (c+d) and mean NO_2 (e+f). Units: [ppb] for ozone, [$\mu g(NO_2)\ m^{-3}$] for NO_2.

domain are based on official critical load data as described in Hettelingh et al. (2008), while those for EECCA countries are based on non-official critical load data by CCE's background database (Reinds et al. 2008). In terms of acidification, 'hot spots' of relatively high exceedance and risk percentage are seen, e.g. in Northwest France, the BeNeLux area, the Southern tip of Norway, Denmark, the Czech Republic, Poland and Lithuania. An even more striking feature, however, are the large exceedances of critical loads and areas at risk in terms of eutrophication. In this respect it has to be noted that not only in Europe, but also in a large part of the EECCA area, the percentage of area at risk is above 90%. While acidification is

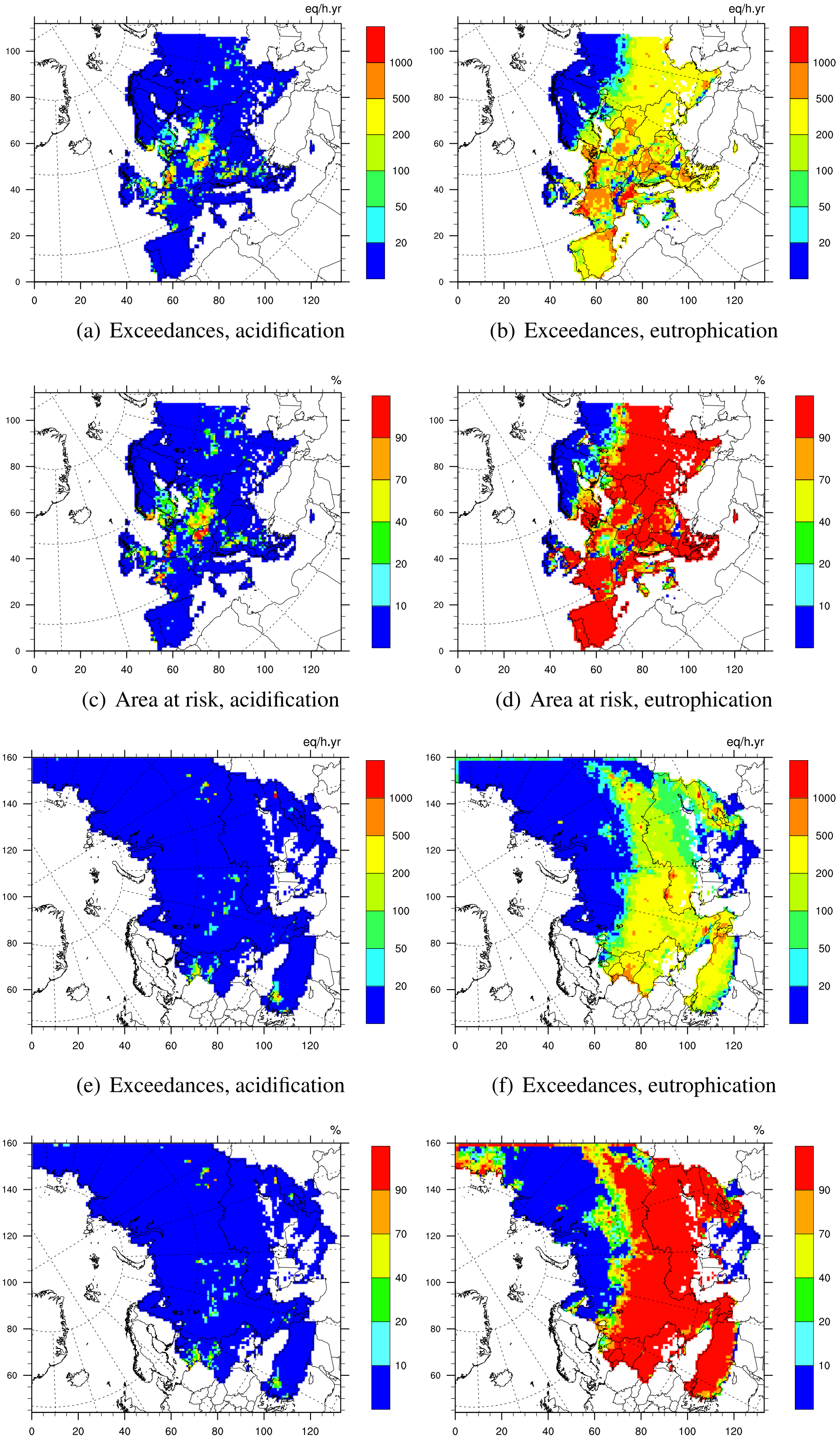

(a) Exceedances, acidification

(b) Exceedances, eutrophication

(c) Area at risk, acidification

(d) Area at risk, eutrophication

(e) Exceedances, acidification

(f) Exceedances, eutrophication

(g) Area at risk, acidification

(h) Area at risk, eutrophication

Figure 2.24: Exceedances of critical loads [eq h^{-1} yr^{-1}] and % ecosystem areas at risk for 2011 in Europe (a)-(d) and in EECCA countries (e)-(h).

low in the EECCA area, eutrophication is potentially a severe problem also there. In Western Europe, the situation in terms of eutrophication (areas at risk) has also not improved substantially from 2010 to 2011. In some areas (e.g. Portugal and Southern England) it has become worse, while in other areas (e.g. Southern Finland and Southern Germany) it has improved. Again, it has to be noted that such year-to-year changes are partly explained by changes in meteorology.

References

Cofala, J., Amann, M., Heyes, C., Wagner, F., Klimont, Z., Posch, M., Schöpp, W., Tarrasón, L., Jonson, J., Whall, C., and Stavraki, A.: Analysis of Policy Measures to Reduce Ship Emissions in the Context of the Revision of the National Emissions Ceiling Directive, Final Report, Tech. Rep. IIASA Contract No 06-107, CIAM, 2007.

Gauss, M. and Hjellbrekke, A.-G.: Photo-oxidants: validation and combined maps, Supplementary material to EMEP Status Report 1/2013, available online at `www.emep.int`, The Norwegian Meteorological Institute, Oslo, Norway, 2013.

Hettelingh, J.-P., Posch, M., and Slootweg, J.: Critical load, dynamic modelling and impact assessment in Europe, Status Report 2008, Tech. rep., Coordination Centre for Effects, Bilthoven, The Netherlands, 2008.

Mareckova, K., Wankmüller, R., Pinterits, M., and Moosman, L.: Inventory review 2013 stage 1 and 2 and review of gridded data, EMEP/CEIP Technical Report 1/2013, EEA/CEIP Vienna, 2013.

Nyíri, Á., Gauss, M., Semeena, V. S., and Hjellbrekke, A.-G.: Acidifying and eutrophying components: validation and combined maps, Supplementary material to EMEP Status Report 1/2013, available online at `www.emep.int`, The Norwegian Meteorological Institute, Oslo, Norway, 2013.

Reinds, G. J., Posch, M., De Vries, W., Slootweg, J., and Hettelingh, J.-P.: Critical loads of sulphur and nitrogen for terrestrial ecosystems in Europe and Northern Asia using different soil chemical criteria, Water, Air and Soil Pollution, 193, 269–287, doi:10.1007/s11270-008-9688-x, 2008.

UNECE: Guidelines for reporting emission data under the Convention on Long-range Transboundary Air Pollution, Tech. Rep. ECE/EB.AIR/97, UNECE, URL `http://www.ceip.at/fileadmin/inhalte/emep/reporting_2009/Rep_Guidelines_ECE_EB_AIR_97_e.pdf`, 2009.

Part II

Model system development

CHAPTER 3

EMEP model development and performance changes

David Simpson, Michael Schulz, Valiyaveetil Shamsudheen Semeena, Svetlana Tsyro, Álvaro Valdebenito, Peter Wind and Birthe Marie Steensen

3.1 Introduction

The EMEP MSC-W group takes part in a large number of activities involving both application and development of the model. Such development can be either scientific, for example to improve process descriptions, or technical, for example to ease the use of the model for different scales and map-projections. Over 2012–2013 most of the changes made in the standard model were of the technical type, but research-versions of the model have explored possible process improvements.

In section 3.2 we briefly review some of the developments of the model, section 3.3 summarises a user-training course given in spring 2013, and in section 3.4 we illustrate how model performance has changed over the years with different model versions, demonstrating the improvements associated with recent model versions.

3.2 Development activities

Much of the development work over the last years has focused on making the EMEP model more flexible in its ability to explore the interactions between climate change, air pollution, and ecosystems. As well as through EMEP funding, much of this work has been supported by the following research projects:

- The EU project ECLAIRE (Effects of climate change on air pollution impacts and response strategies for European ecosystems) is a cooperation between 39 partner Institutes looking at a whole host of processes, from soil microbiology to large scale atmospheric modelling. The EMEP MSC-W model is supporting ECLAIRE through the provision of long-term calculations of nitrogen deposition and ozone, data which is being used as inputs to several ecosystem models. In turn, these models and their results will be used to develop more realistic, and climate-sensitive, treatments of biosphere-atmosphere exchange. A second EU project, PEGASOS, will also provide improvements in the model's dry deposition parameterisations

- The Nordic Council of Ministers funded project EnsClim is working towards establishing both the changes in air pollutants brought about by climate change, and the uncertainty of such predictions as represented by a small ensemble of chemical transport models. Langner et al. (2012) presented results of this project for ozone, and also illustrated the large uncertainty in the biogenic VOC emissions still found in such modelling studies (Fig. 3.1).

- The Swedish funded strategic project MERGE (ModElling the Regional and Global Earth system) has similar aims, with a very strong ecosystem component. (MERGE funded a Post-Doc at Chalmers University of Technology to work with the EMEP MSC-W model.)

- The Norwegian Space agency has been encouraging and funding works aiming at the use of satellite data. Within the projects AeroKval and PM-VRAE, the EMEP MSC-W model has been developed to calculate aerosol optical parameters, such as Aerosol Optical Depth (AOD) and 3-dimensional aerosol extinction coefficients. Comparison of model calculations with multi-year satellite observations of AOD and extinction profiles provides additional information on the model performance, especially valuable for the regions not presently covered by air quality monitoring networks, and also on the global scale.

- Within the TFMM Eurodelta-3 activities, the EMEP MSC-W model is compared with five state-of-art air quality models and with observations from the EMEP and Airbase data bases, with particular focus on extended and highly resolved EMEP intensive measurements. The differences between model results and their discrepancies with observations are systematically analysed and the findings shall be used as a basis for model improvements.

Within these projects we have explored for example the use of more realistic (temperature-sensitive) growing seasons in the EMEP model (Sakalli and Simpson 2012), as illustrated in Fig. 3.2. This work showed that even simple temperature-based methods offered more realistic growing seasons compared to the default latitude-based approach. These results were found for birch, and further work is needed to explore methods for other species, perhaps based upon ecosystem-model approaches (e.g. Smith et al. 2011).

The parameterisation of the surface exchange of ammonia has also been a focus topic, with new ideas being reviewed and explored in Flechard et al. (2013) and Sutton et al. (2013). This work also draws attention to the need for more dynamic estimates of NH_3 emissions in future, with the possibility of significantly increased emissions being caused by the temperature increases associated with climate change.

An initiative to improve the vertical structure and resolution of the model can be mentioned. The model has been limited to 20 vertical sigma levels since the original formulation of Berge and Jakobsen (1998). We are currently developing the model using flexible and general hybrid coordinates (levels defined by $P(k) = A(k) + B(k)P_{\text{surf}}$). In a first phase we are

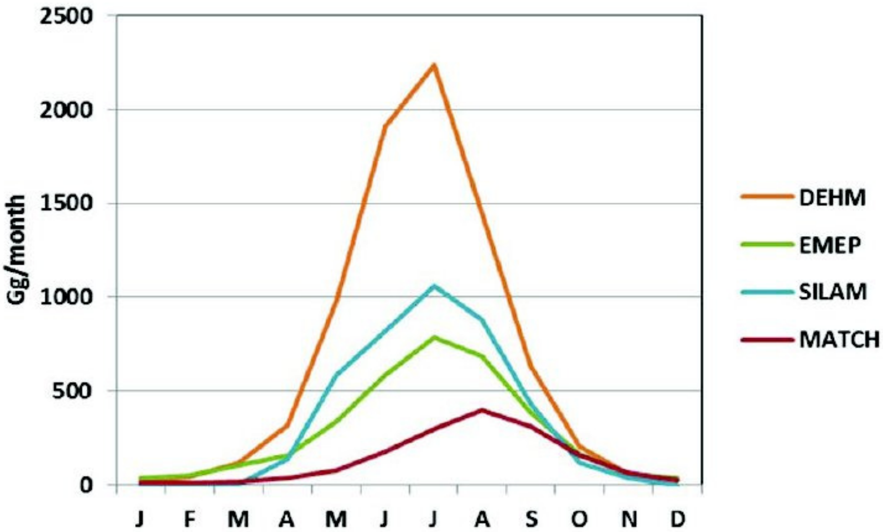

Figure 3.1: Simulated seasonal variation in biogenic isoprene emissions as an average for 2000–2009, from four different chemical transport models (DEHM, EMEP, MATCH, SILAM). Units Gg/month. From Langner et al. (2012), where details can also be found of the models and of the climate-model based meteorology.

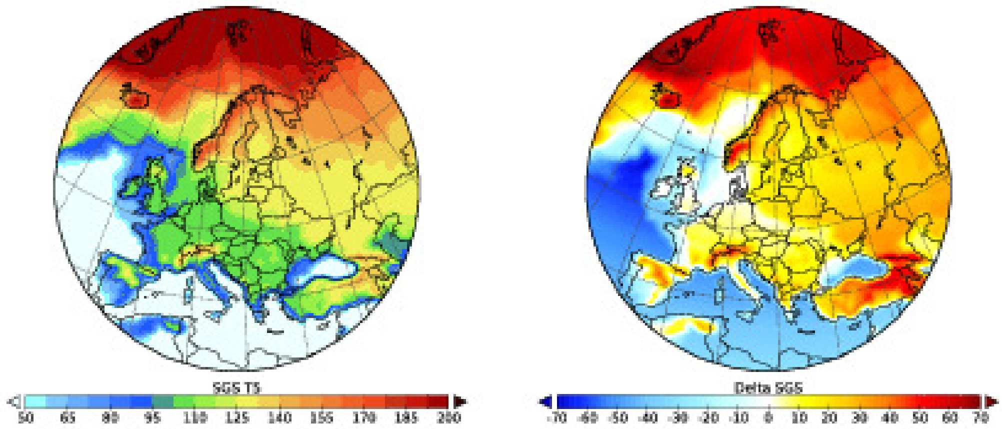

(a) $d_{SGS,T5}$ (b) $d_{SGS,T5} - d_{SGS,LAT}$

Figure 3.2: **(a)** Estimated start of the growing season (day number) using a temperature-based method ('T5'), and **(b)** the difference between the T5 and default latitude-based method. From Sakalli and Simpson 2012.

testing an extension of the levels at high altitudes using 42 hybrid levels and a top at 9 hPa (about 30 km). This version is used to simulate the ash dispersion from high volcano eruptions. Figure 3.3 shows a snapshot of the Grimsvötn eruption in 2011. The eruption started on May 21, and during the first 24 hours there was more ash release than during the entire 2010 Eyjafjallajökull release, and the plume reached up to 18 km altitude . The standard 20 layer vertical sigma level grid has a top at 100 hPa. From Figure 3.3 one can see that parts of the ash plume were found above 100 hPa.

Finally, a related exercise is going on to improve the vertical resolution of the surface layer (in the present model version the lowest layer is appr. 90 m thick). However before the

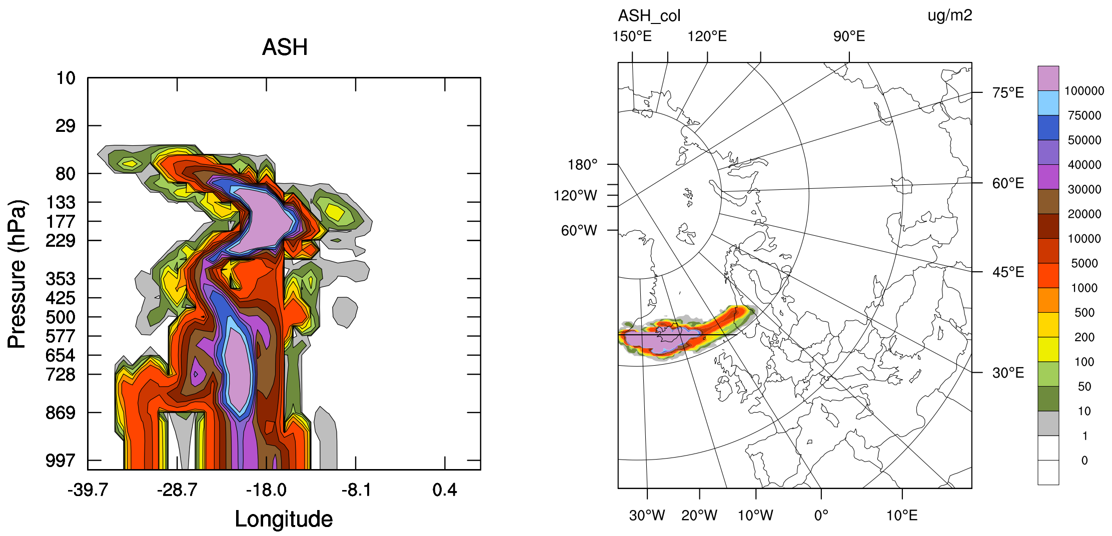

Figure 3.3: Grimsvötn ash plume at 12 UTC 23 May 2011, as simulated by top-extended EMEP MSC-W model: a cross section (left) of the vertical distribution of the ash plume; horizontal distribution (right) of the ash plume, the black line represents where the cross section is taken. Same scale on both plots.

model is fully adapted to such higher vertical resolution, we still need to define photolysis rates for the stratosphere, develop a deposition scheme for thinner layers close to the surface, and generalise the scheme for distribution of emitted pollutants vertically. This work should also enable a better representation of near-source dispersion in the model, which is especially important as grid-sizes are reduced.

3.2.1 Model updates

The EMEP MSC-W model, version rv4.0, released as open-source in September 2012, was described in detail in Simpson et al. (2012). In March 2013 version rv4.3 was released on the EMEP web site, just prior to the Training course (Sec. 3.3), and in summer 2013 rv4.4 used for this report will be similarly released. Table 3.1 summarises the main model versions from rv1.7 in 2003 to rv4.4 in 2013. The 'smoothed MARS' modification in rv4.3 requires some explanation. This refers to changes in the EMEP coding of the MARS module (Binkowski and Shankar 1995) which computes the equilibrium for SO_4, HNO_3-NO_3 and NH_3-NH_4. MARS has two main regimes, depending on the ammonium to sulphate ratio. At the transition between the two regimes the low and high ratio algorithms gave different answers, resulting in a discontinuity of the results even when the input concentrations varies smoothly. The new routines defines a transition regime where a linear combination of the two previous regimes is applied. The physical interpretation being that in these cases, both regimes are present in different parts of a single grid cell.

3.3 Training

In order to help users of the EMEP MSC-W model, a training course was organised in Oslo, 24-26 April 2013. Thirty researchers from 9 European countries - Austria, Belgium, Croatia, Estonia, Hungary, Italy, Norway, Poland and United Kingdom - participated in the course. The course was organised in such a way that both new and experienced model-users would benefit from the course. The course started with an introduction about the philosophy, concepts and principles of the EMEP MSC-W model followed by the structure, computational requirements and the input data needed to work with the model. Simple exercises to run the model with different set ups were given. Tools to visualise, post-process and analyse the model outputs were also introduced in the course. The agenda of the training course in 'pdf' format can be found on the EMEP web site at: `http://www.emep.int/meetings/EMEP_Training_2013/Agenda_EMEP_TrainingCourse2013_MS.pdf` The course materials were uploaded to the EMEP web site after the course and can be found at: `https://wiki.met.no/emep/page1/emepmscw_opensource` under the section 'Training Course Presentations (24-26 April 2013)'. The feedback from the participants indicated that the course was very informative, with suggestions to make such a course (possibly bi-annual) more to the needs of absolute beginners. The intensive discussions with the participants throughout the course provided important points to be focused upon in future development of the EMEP MSC-W model.

3.4 Model performance - status and changes

EMEP MSC-W model performance is reported each year in the appropriate status reports, providing an ongoing documentation of the model as compared to observations collected from the EMEP monitoring network. However, such results cannot be compared in a consistent manner from year to year – there are typically changes in the meteorological year used, in the emissions data-sets, and sometimes in the EMEP model version. There was also a major change of meteorological driver in May 2011 (when the ECMWF-IFS model replaced the previous PARLAM/HIRLAM), which also resulted in changed model performance even when using the same EMEP MSC-W chemical transport model.

It is however useful to illustrate how the current model is performing compared to earlier reported model results. In this section, we compare the 'original' model results (as documented in previous EMEP reports) with a new multi-year evaluation using the latest (rv4.4, 'current model') version of the model, and latest measurement data for all sites.

The aim of this multi-year model evaluation is threefold: (1) to demonstrate the continued good (and sometimes improved) skills of the present model version rv.4.4 relative to the earlier ones, and (2) to illustrate some features of the robustness of model results in changing meteorological and chemical regimes, and (3) to compare the performance of the current model version to previous performance evaluations from peer-reviewed papers featuring the EMEP model.

An important complication with the original reported results is that even 'observations' change, as older results are corrected and updated by the data-providers and EMEP CCC. Indeed, some of the differences to be discussed below will be due to a comprehensive update of the observational data for all years used at MSC-W in 2012. As even the number of stations may change between earlier and recent comparisons (and it would be a huge task to work out which stations were included in each annual report for each pollutant), and individual sites can make a big difference to statistical measures, we cannot unfortunately use these comparisons to trace specific reasons for changes in model performance; we can only give an illustration of current model performance compared to earlier versions. At MSC-W we have begun a more systematic analysis, rerunning the older model versions with current emissions, meteorological driver, and observations, and in time this will allow a more informative comparison of model development.

The model has been evaluated for concentrations of all traditional pollutants, both in air and precipitation, for which an appropriate suite of statistical parameters relevant for analysis of model performance have been calculated. Here, we discuss only two of them, namely the annual mean 'Relative bias' and 'Correlation' (R-values). Original model results are available for the years 1980, 1985, 1990-2011. Current model results are available for the years 1990, and 2000-2011 (the years reflect availability of data from the newer ECMWF-IFS meteorological driver). The summary of the results is provided in Figs 3.4–3.5, and Tables E:1-E:15.

The EMEP reports giving information on the 'original' model performance can be found at: `http://emep.int/mscw/mscw_publications.html` in the supplementary material to EMEP reports for the years 2009–2012, and in the Status Report of respective years for all other years. These model versions are shown in the 'Original Results' column of Tables E:1-E:15. The data in 'Original Results' tell us about the evolution of the model system in time, where model system refers to EMEP model version, meteorological driver, meteorological year, and the status of the emissions and observational databases at the time of reporting. The data in 'Updated Results' illustrate more systematically the effect of meteorology and emissions on the accuracy of calculations, with the same EMEP model and meteorological driver used throughout, and current databases for emissions and observations (the same runs are also described as Trend runs in chapter 6). The Updated Results in Tables E:1-E:15 use all the available stations with observations for the meteorological years except 2011.

Given the many variables which change when comparing results, we will not go through all comparisons in detail, but rather give some examples to demonstrate both features and complications of such a comparison.

Considering first SO_2 and sulphate SO_4^{2-}, Tables E:1-E:2, some differences between the two compounds are readily apparent. For SO_2 the correlation coefficient changes significantly from year to year, e.g. ranging from 0.32 to 0.7 in the 2000s with rv4.4, whereas for SO_4^{2-} much higher correlations are found, with lower year to year variation (from 0.67 to 0.85 for the 2000s). The latest model version is sometimes better, sometimes worse, than earlier results, but with again sulphate showing more consistency than SO_2.

Given the variability in year-to-year performance for the consistent rv4.4 results, it is not easy to compare the rv4.4 findings against the original model versions. At first sight for example, the older rv1.7 model seems superior for sulphate and inferior for SO_2, but significantly more observational data are included in the current evaluation compared to the original one (e.g. for SO_4^{2-} 87 sites for rv4.4 but only 47 for rv1.7).

In general we can only conclude that these sulphur species are captured within 20-30%, and for both species results seem to be better for earlier years rather than later. This likely reflects the rapidly changing nature of SO_2 emissions, where today's emissions stem from a relatively wide range of sources, whereas in earlier years power-stations completely dominated the S-emissions.

Results for NO_2 from rv4.4 (Table E:3) are rather consistent from year to year, with R-values of about 0.6-0.8. The model bias is low, and seems even to be improving for recent

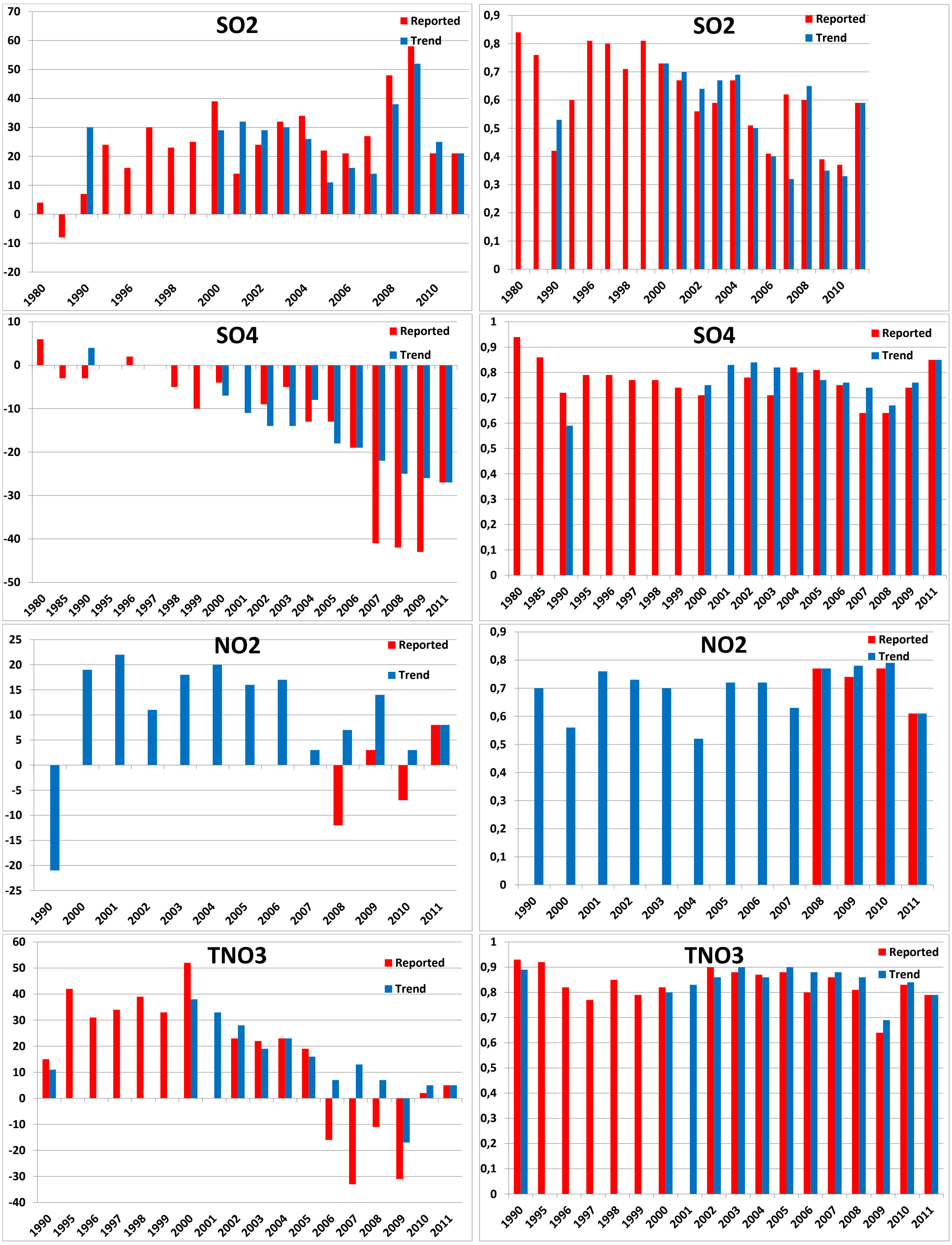

Figure 3.4: Calculated bias (left) and correlation (right) between the model and observations for the components SO_2, SO_4, NO_2 and total nitrate (TNO3).Here the 'Reported' model results represent values as given in original EMEP runs, 'Trend' results give updated calculations with current rv4.4 model version.

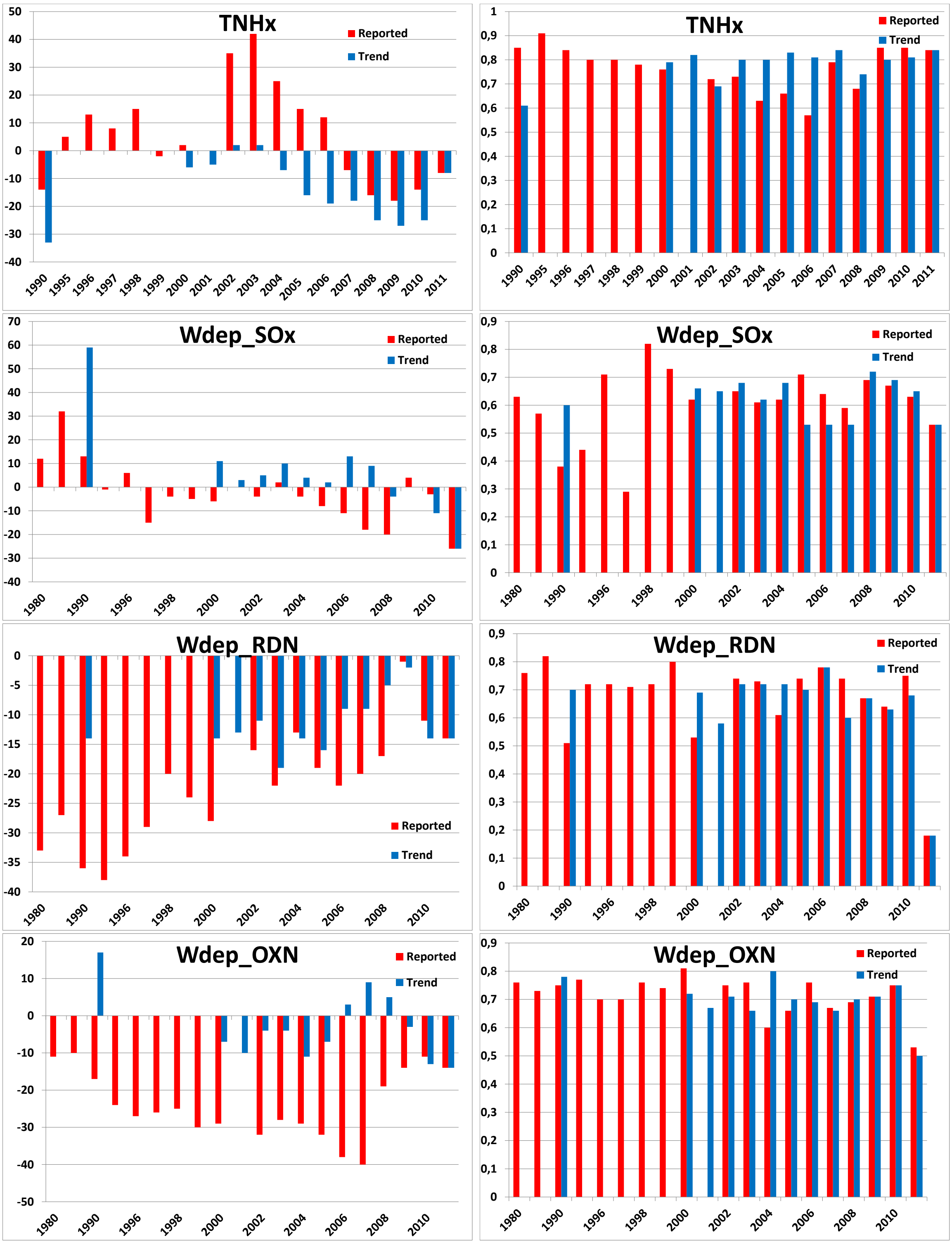

Figure 3.5: Calculated bias (left) and correlation (right) between the model and observations for the components total ammonia (TNHx), wet deposition of SO_x (Wdep_SOx), wet deposition of reduced nitrogen (Wdep_RDN) and wet deposition of oxidised nitrogen (Wdep_OXN).

years, from ca. 20% in 1990 and 2000 to less than 10% in recent years.

Original model results are only available for four years, but are essentially comparable with the rv4.4 results. In summary, the model performance for NO_2 is rather satisfactory, and among the more robust outputs from the EMEP MSC-W model.

NH_3 (Table E:4) offers possibly the most complex example of model performance interpretation. The comparisons are often dominated very strongly by individual sites or clusters of sites in terms of concentrations, for example high-NH_3 sites from the Netherlands in one region of the scatter plot (Nyíri et al. 2013), and very low concentration Nordic sites on another region. Inclusion or removal of individual sites (especially the high concentration ones) from these comparisons can strongly affect the statistics. Another unique feature for NH_3 is the very high correlations (R>0.97) in the earlier years. This does not represent near-perfect model performance, but rather is a statistical result of the clustering of sites in high or low NOx regions of the scatter plots. The large bias (underprediction) in these high R-value statistics are a result of the model not reproducing some very high observations, but some such underpredictions are to be expected for NH_3 – measurements of NH_3 can be strongly affected by local sources, something which the model can not be expected to capture.

Ammonium (NH_4^+, Table E:5) is expected to be better captured due to its secondary nature, with the measurements being more representative of larger areas. The number of measurements is also greater than for NH_3, although much lower than for S-compounds or NO_2. Correlation coefficients are rather good (R∼0.8) for all years with around 20 sites or more, and bias is small, from almost zero to around 20% with rv4.4. The current model has both better correlation and lower bias than the older codes, which is likely related to generally lower deposition velocities in recent versions.

As has been discussed in detail elsewhere (e.g. Aas et al. 2012, Fagerli and Aas 2008, and references cited therein) the measurements of N-compounds made with filter packs are complicated by partitioning (especially of ammonium nitrate) and condensation processes; measurements of gaseous compounds (e.g. HNO_3) or particulate compounds alone are likely biased. The sum of nitrate and nitric acid (TNO_3 in Figure 3.4) of ammonia and ammonium (TNHx) are far more reliable than measurements of the gas or aerosol compound alone.

Considering TNHx in air, the recent model still shows significant under-prediction (up to 27%, although often less than 20%) compared to measurements, especially in recent years, but the R-values are uniformly high, mostly around 0.8. The current model version has lower concentrations, but typically higher R-values, compared to the earlier reported results. For TNO_3 in air, the model shows even better performance in both older and the current code, with R-values reaching up to 0.9, and low bias of the current model in recent years. Again, it is easy to find examples of year to year variability, with the current code showing underpredictions in some years and overpredictions in others.

Table 3.2 compares precipitation results for the EMEP sites. Precipitation is one of the key input parameters to the EMEP model, and this Table makes it clear that this input is also both imperfect, and changing in time. Indeed, the tendency in recent years seems to be for lower bias compared to the measurements, but also somewhat lower correlations compared to earlier years. Again though, the number of stations changes between the current analysis and the originally reported ones, and there were clearly more sites with precipitation data in the 1990 case than in later years.

Tables E:10-E:15 provide results for both concentrations in precipitation and wet deposition amounts, and Figure 3.5 illustrates the changes in wet deposition. Results for sulphate are seen to be generally good (bias usually less than 20%, high R-values) for all model versions and years. The year 1990 with the current model stands out with far higher bias than found with later years or with earlier model codes; this needs to be investigated. For ammonium, current model results are similarly good (often better) than for sulphate, also for the year 1990. The current model results seem to show lower bias, although somewhat lower R-values, compared to earlier runs. The year 2011 results stand out with remarkably low R-values; this seems to be an artefact caused by one or two sites and will be investigated further. R-values for other years are usually around 0.6–0.8.

In conclusion:

- The comparisons discussed here give an overview of how model performance has changed over the years. However, a systematic comparison has not been possible, since many other factors have also changed. Not least, the observational database available for the recent comparisons has been improved compared to those available for older EMEP reports. Further, emission data-bases are continually evolving, with again hopefully better data available today, also for previous years.
- Year-to-year variations in model evaluation can be large, so evaluation statistics determined for one year cannot be assumed to be representative for general model performance.
- Differences between pollutants are also large, and often not correlated. For example, model changes that improved SO_4^{2-} were associated with reduced performance for SO_2. Again, evaluation needs to be performed over many years and in different pollutant regimes.
- Model performance is (as expected) generally better for secondary than for primary pollutants.
- A more systematic evaluation is needed, with all model-inputs and observations held constant as model version is changed, in order to identify key factors behind changes in model performance.
- The latest model version shows a good level of performance across pollutants and years, generally better than older codes when all pollutants are considered together.

Table 3.1: Summary of major EMEP MSC-W model versions from 2003–2013. Extended from Table S1 of Simpson et al. 2012.

Revision	Date	Main changes
rv1.7	Jul 2003	First 'unified' model, with both acidification and photochemical scheme, documented in Simpson et al. (2003).
rv2.0	Apr 2004	Pseudo-H_2O_2 added in aqueous oxidation, revised VOC speciation, boundary-layer physics modified, N_2O_5 hydrolysis improved inclusion of sea-salt. Used for Nr-evaluations in Simpson et al. (2006a), Simpson et al. (2006b) and O_3, NO_2 in Jonson et al. (2006) .
rv2.5	Jul 2006	Used for IIASA (GAINS) source-receptor matrices. Changes in: N_2O_5 hydrolysis, EQSAM scheme for nitrate formation, PM-water added, land-cover parameters changed, ozone-flux outputs added, move to netcdf file format. Global modelling capability added. Similar to codes used by Fagerli and Aas (2008), Huijnen et al. (2010) and Jonson et al. (2010) (rv2.6).
rv3.0	Feb 2008	**First public-domain release.** Included various small changes, e.g. to vegetation parameters, and numerous technical changes. Similar to rv3.1 codes used by Colette et al. (2011) and Bartnicki and Fagerli (2008).
rv3.2		Improved deposition scheme, including co-deposition for SO_2 (cf Fowler et al. 2009), revised particle deposition scheme, daily snow instead of climatological. Code revisions for more flexible grids and global scale.
rv3.4	2009	Additional chemical schemes implemented, EmChem09 scheme developed, Forecast model versions implemented.
rv3.6	2010	Boundary layer physics updates (Hmix from Jeričevič et al. 2010), convection routine added.
rv3.7	2010	BVOC emissions updated, aerosol deposition and sea-salt revised, dust added, global soil NO emissions.
rv3.8	May 2011	**Second public-domain.** Major revisions in: Aerosol dry deposition methodology, also revised sub-cloud scavenging; Biogenic VOC emission methods, rates; added cumulus scheme; ECMWF IFS model replaces PARLAM/HIRLAM NWPs as default meteorological driver. Similar code used for Colette et al. (2012).
rv3.9	Nov 2011	Major revisions in: pH dependence of sulphate formation; added organic aerosol and SOA formation; use of daily FINNv1 forest fire module; changed temporal variations for sectors SNAP-1 (changing winter/summer ratios) and SNAP-2 (degree-days).
rv4β	Mar 2012	Soil NO emissions, preliminary road-dust production added, use of soil moisture index from ECMWF IFS fields. As used in Aas et al. (2012).
rv4.0	Aug 2012	**Third public-domain.** Hourly emission variations replaced former day/night emission factors, more flexible handling of volcanic emissions, increased MMD of coarse nitrate to 3μm, small change in vertical distribution of emissions. As documented in Simpson et al. (2012).
rv4.3	Mar 2013	**Fourth public-domain.** AOD scheme was improved to implicitly account for aerosol effective extinction cross-section and for aerosol hygroscopic growth due to relative humidity. Smoothing of MARS results for inorganic aerosol (see text). Introduction of an Emergency module for volcanic ash and other emergency scenarios. For example, with the appropriate input and the new Emergency module it is possible to simulate the transport and deposition of radioactive material from a nuclear power plant accident, such as the Fukushima 2011 disaster. A start was made to simplify the model configuration system by using Fortran namelist inputs to define setup-variables and various run options, instead of these being given in the code. The new system will be gradually expanded, and should result in considerable simplifications for users of the EMEP model. Dust and road-dust options added as defaults Advection algorithm changed, to solve some problems with extreme divergence cases (Clappier (1998)).
rv4.4	Summer 2013	gfortran compatibility improved following comments received on the EMEP model course. Further use of namelist inputs. The coding of AOD parameterisations was improved.

Table 3.2: Comparison of modelled and observed precipitation (mm) at EMEP sites for the years 1980–2011. Original results refer to evaluations as given in earlier EMEP reports, with model version as given in left column. Updated results are derived from model version rv4.4 and latest EMEP CCC data base for observations.

Original Results					Year	Updated Results (rv4.4)			
Rev.	N_{stat}	Obs.	Bias(%)	Corr.		N_{stat}	Obs.	Bias(%)	Corr.
rv1.7	29	24475	-2	0.57	1980				
rv1.7	40	34828	0	0.66	1985				
rv1.7	60	47344	20	0.49	1990	84	63593	25	0.86
rv1.7	73	64077	2	0.49	1995				
rv1.7	74	60248	9	0.48	1996				
rv1.7	73	62201	14	0.54	1997				
rv1.7	75	68630	15	0.48	1998				
rv1.7	77	66917	14	0.62	1999				
rv1.7	64	54508	12	0.65	2000	68	58277	14	0.86
rv1.8					2001	66	56226	11	0.80
rv2.0	61	53215	9	0.53	2002	67	58072	13	0.78
rv2.3	57	43468	7	0.68	2003	65	46370	10	0.83
rv2.6	44	38072	0	0.64	2004	59	50795	7	0.83
rv2.7	54	41571	7	0.73	2005	57	43505	7	0.75
rv3.1	55	22967	-4	0.64	2006	60	49164	11	0.86
rv3.4	50	41862	-4	0.65	2007	59	52492	12	0.76
rv3.6	64	63989	2	0.72	2008	62	60928	8	0.73
rv3.8	62	56367	5	0.71	2009	63	56960	5	0.70
rv4.0	57	49067	-1	0.64	2010	57	49067	-1	0.64
rv4.4	51	39208	4	0.78	2011	51	39208	4	0.78

References

Aas, W., Tsyro, S., Bieber, E., Bergström, R., Ceburnis, D., Ellermann, T., Fagerli, H., Frölich, M., Gehrig, R., Makkonen, U., Nemitz, E., Otjes, R., Perez, N., Perrino, C., Prévôt, A. S. H., Putaud, J.-P., Simpson, D., Spindler, G., Vana, M., and Yttri, K. E.: Lessons learnt from the first EMEP intensive measurement periods, Atmos. Chem. Physics, 12, 8073–8094, doi:10.5194/acp-12-8073-2012, 2012.

Bartnicki, J. and Fagerli, H.: Airborne load of nitrogen to European seas, Ecological Chemistry and Engineering S- Chemia i Inzynieria Ekologiczna S, 15, 297–313, 2008.

Berge, E. and Jakobsen, H. A.: A regional scale multi-layer model for the calculation of long-term transport and deposition of air pollution in Europe, Tellus, 50, 205–223, 1998.

Binkowski, F. and Shankar, U.: The Regional Particulate Matter Model .1. Model description and preliminary results, J. Geophys. Res., 100, 26 191–26 209, 1995.

Clappier, A.: A Correction Method for Use in Multidimensional Time-Splitting Advection Algorithms: Application to Two- and Three-Dimensional Transport, Monthly Weather Review, 126, 232–242, 1998.

Colette, A., Granier, C., Hodnebrog, Ø., Jakobs, H., Maurizi, A., Nyiri, A., Bessagnet, B., D'Angiola, A., D'Isidoro, M., Gauss, M., Meleux, F., Memmesheimer, M., Mieville, A., Rouïl, L., Russo, F., Solberg, S., Stordal, F., and Tampieri, F.: Air quality trends in Europe over the past decade: a first multi-model assessment, Atmos. Chem. Physics, 11, 11 657–11 678, doi:10.5194/acp-11-11657-2011, 2011.

Colette, A., Granier, C., Hodnebrog, Ø., Jakobs, H., Maurizi, A., Nyiri, A., Rao, S., Amann, M., Bessagnet, B., D'Angiola, A., Gauss, M., Heyes, C., Klimont, Z., Meleux, F., Memmesheimer, M., Mieville, A., Rouïl, L., Russo, F., Schucht, S., Simpson, D., Stordal, F., Tampieri, F., and Vrac, M.: Future air quality in Europe: a multi-model assessment of projected exposure to ozone, Atmos. Chem. Physics, 12, 10 613–10 630, doi:10.5194/acp-12-10613-2012, 2012.

Fagerli, H. and Aas, W.: Trends of nitrogen in air and precipitation: Model results and observations at EMEP sites in Europe, 1980-2003, Environ. Poll., 154, 448–461, 2008.

Flechard, C. R., Massad, R.-S., Loubet, B., Personne, E., Simpson, D., Bash, J. O., Cooter, E. J., Nemitz, E., and Sutton, M. A.: Advances in understanding, models and parameterizations of biosphere-atmosphere ammonia exchange, Biogeosciences, 10, 5183–5225, doi:10.5194/bg-10-5183-2013, 2013.

Fowler, D., Pilegaard, K., Sutton, M., Ambus, P., Raivonen, M., Duyzer, J., Simpson, D., Fagerli, H., Fuzzi, S., Schjoerring, J., Granier, C., Neftel, A., Isaksen, I., Laj, P., Maione, M., Monks, P., Burkhardt, J., Daemmgen, U., Neirynck, J., Personne, E., Wichink-Kruit, R., Butterbach-Bahl, K., Flechard, C., Tuovinen, J., Coyle, M., Gerosa, G., Loubet, B., Altimir, N., Gruenhage, L., Ammann, C., Cieslik, S., Paoletti, E., Mikkelsen, T., Ro-Poulsen, H., Cellier, P., Cape, J., Horváth, L., Loreto, F., Niinemets, Ü., Palmer, P., Rinne, J., Misztal, P., Nemitz, E., Nilsson, D., Pryor, S., Gallagher, M., Vesala, T., Skiba, U., Brüeggemann, N., Zechmeister-Boltenstern, S., Williams, J., O'Dowd, C., Facchini, M., de Leeuw, G., Flossman, A., Chaumerliac, N., and Erisman, J.: Atmospheric composition change: Ecosystems-Atmosphere interactions, Atmos. Environ., 43, 5193–5267, doi:10.1016/j.atmosenv.2009.07.068, 2009.

Huijnen, V., Eskes, H. J., Poupkou, A., Elbern, H., Boersma, K., Foret, G., Sofiev, M., Valdebenito, A., Flemming, J., Stein, O., Gross, A., Robertson, L., D'Isidoro, M., Kioutsioukis, I., Friese, E., Amstrup, B., Bergstrom, R., Strunk, A., Vira, J., Zyryanov, D., Maurizi, A., Melas, D., Peuch, V.-H., and Zerefos, C.: Comparison of OMI NO_2 tropospheric columns with an ensemble of global and European regional air quality models, Atmos. Chem. Physics, 10, 3273–3296, doi:10.5194/acp-10-3273-2010, 2010.

Jeričevič, A., Kraljevič, L., Grisogono, B., Fagerli, H., and Večenaj, v.: Parameterization of vertical diffusion and the atmospheric boundary layer height determination in the EMEP model, Atmos. Chem. Physics, 10, 341–364, doi:10.5194/acp-10-341-2010, 2010.

Jonson, J., Simpson, D., Fagerli, H., and Solberg, S.: Can we explain the trends in European ozone levels?, Atmos. Chem. Physics, 6, 51–66, sRef-ID: 1680-7324/acp/2006-6-51, 2006.

Jonson, J., Stohl, A., Fiore, A., Hess, P., Szopa, S., Wild, O., Zeng, G., Dentener, F., Lupu, A., Schultz, M., Duncan, B., Sudo, K., Wind, P., Schulz, M., Marmer, E., Cuvelier, C., Keating, T., Zuber, A., Valdebenito, A., Dorokhov, V., De Backer, H., Davies, J., Chen, G., Johnson, B., Tarasick, D., Stübi, R., Newchurch, M., von der Gathen, P., Steinbrecht, W., and Claude, H.: A multi-model analysis of vertical ozone profiles, Atmos. Chem. Physics, 10, 5759–5783, doi:10.5194/acp-10-5759-2010, 2010.

Langner, J., Engardt, M., Baklanov, A., Christensen, J. H., Gauss, M., Geels, C., Hedegaard, G. B., Nuterman, R., Simpson, D., Soares, J., Sofiev, M., Wind, P., and Zakey, A.: A multi-model study of impacts of climate change on surface ozone in Europe, Atmos. Chem. Physics, 12, 10 423–10 440, doi:10.5194/acp-12-10423-2012, 2012.

Nyíri, Á., Gauss, M., Semeena, V. S., and Hjellbrekke, A.-G.: Acidifying and eutrophying components: validation and combined maps, Supplementary material to EMEP Status Report 1/2013, available online at `www.emep.int`, The Norwegian Meteorological Institute, Oslo, Norway, 2013.

Sakalli, A. and Simpson, D.: Towards the use of dynamic growing seasons in a chemical transport model, Biogeosciences, 9, 5161–5179, doi:10.5194/bg-9-5161-2012, 2012.

Simpson, D., Fagerli, H., Jonson, J., Tsyro, S., Wind, P., and Tuovinen, J.-P.: The EMEP Unified Eulerian Model. Model Description, EMEP MSC-W Report 1/2003, The Norwegian Meteorological Institute, Oslo, Norway, 2003.

Simpson, D., Butterbach-Bahl, K., Fagerli, H., Kesik, M., Skiba, U., and Tang, S.: Deposition and Emissions of Reactive Nitrogen over European Forests: A Modelling Study, Atmos. Environ., 40, 5712–5726, doi:10.1016/j.atmosenv.2006.04.063, 2006a.

Simpson, D., Fagerli, H., Hellsten, S., Knulst, J., and Westling, O.: Comparison of modelled and monitored deposition fluxes of sulphur and nitrogen to ICP-forest sites in Europe, Biogeosciences, 3, 337–355, 2006b.

Simpson, D., Benedictow, A., Berge, H., Bergström, R., Emberson, L. D., Fagerli, H., Hayman, G. D., Gauss, M., Jonson, J. E., Jenkin, M. E., Nyíri, A., Richter, C., Semeena, V. S., Tsyro, S., Tuovinen, J.-P., Valdebenito, A., and Wind, P.: The EMEP MSC-W chemical transport model – technical description, Atmos. Chem. Physics, 12, 7825–7865, doi:10.5194/acp-12-7825-2012, 2012.

Smith, B., Samuelsson, P., Wramneby, A., and Rummukainen, M.: A model of the coupled dynamics of climate, vegetation and terrestrial ecosystem biogeochemistry for regional applications, Tellus A, 63A, 87–106, URL `http://dx.doi.org/10.1111/j.1600-0870.2010.00477.x`, 2011.

Sutton, M. A., Reis, S., Riddick, S. N., Dragosits, U., Nemitz, E., Theobald, M. R., Tang, Y. S., Braban, C. F., Vieno, M., Dore, A. J., Mitchell, R. F., Wanless, S., Daunt, F., Fowler, D., Blackall, T. D., Milford, C., Flechard, C. R., Loubet, B., Massad, R., Cellier, P., Personne, E., Coheur, P. F., Clarisse, L., Van Damme, M., Ngadi, Y., Clerbaux, C., Skjth, C. A., Geels, C., Hertel, O., Wichink Kruit, R. J., Pinder, R. W., Bash, J. O., Walker, J. T., Simpson, D., Horvth, L., Misselbrook, T. H., Bleeker, A., Dentener, F., and de Vries, W.: Towards a climate-dependent paradigm of ammonia emission and deposition, Philosophical Transactions of the Royal Society B: Biological Sciences, 368, doi:10.1098/rstb.2013.0166, 2013.

CHAPTER 4

The new EMEP Grid

Michael Schulz, Katarina Mareckova, Robert Wankmüller, Maximilian Posch, Ágnes Nyíri, Anna Benedictow, Michael Gauss

At the 36th session of the EMEP Steering Body the EMEP Centres suggested to increase spatial resolution of reported emissions from 50 $\times$ 50 km EMEP grid to 0.1°$\times$ 0.1°, with a lon-lat projection in the geographic coordinate system WGS84. The new domain will cover the geographic area between 30°N-82°N latitude and 30°W-90°E longitude (see Figure 4.1). This suggestion represents a balance between political needs, scientific needs and technical feasibility as of 2012 and for the next years.

Here we summarize recent argumentation in favor of a new grid and projection, provide some information for the upcoming changes for emission reporting, and report from first work to document the impact of utilizing such a new grid for critical load exceedances used in integrated assessments.

4.1 Argumentation for a new grid and projection

Emissions are basic information for any air pollution modelling. Only emissions regridded from sufficiently fine resolution lead to exact results. In the recent years MSC-W the EMEP MSC-W model was asked to perform simulations for different assessments and projects, including in support of the revision of the Gothenborg protoal and TSAP, on several new grids. Because of the problematic regridding procedure from the standard 50$\times$50 km EMEP grid such work has often been done with other emission data sets. This leads to an inconsistency between different simulations and does not allow for a straight forward comparability of simulations performed e.g. for TSAP and EMEP. Assuming that regulatory work and the supporting assessments for different international bodies should be rather consistent with respect to input data, it would be of general advantage to set an adequate grid standard through EMEP.

The grid used in EMEP simulations up to now has served its purpose. However, the 50$\times$50 km grid is becoming old and is no longer state-of-the-art. The grid used in the EMEP model system has not changed since 15 years, since 1999. Also, the earlier 150×150 km grid had been in use for ca. 15 years from 1984 to 1998. As of today, the MACC project, using a model ensemble of 6 regional models including the EMEP model, performs regular chemical weather forecasts for EUROPE every day on a grid of approximately 0.2×0.2 degrees on a lat-lon grid, producing a model ensemble on a 0.1×0.1 degrees. EMEP MSC-W model simulations on a similar grid would be thus just state-of-the-art.

Today's fine-scale ecosystem data can only be used to their full potential if atmospheric data are available on equivalently finer scales. By using a finer grid the simulation of atmospheric deposition and the exceedances of critical loads can be quantified with higher accuracy for more patchy vegetation units. At the same time the simulation of biospheric emissions of VOC's, NH_3 and dust can make use of highly resolved land-cover category information and any coupling between the biosphere and atmosphere can be simulated more accurately.

A lon-lat projection of the EMEP grid can be more easily integrated with other geo-data and boundary conditions. In particular problematic is the regridding from a polar-stereographic grid to a lon-lat grid, where uncertain overlap functions have to be defined. Global chemistry transport models, as used for example in the TFHTAP, provide boundary conditions on lon-lat grids. The foreseen studies on the impact of hemispheric air pollution on regional air quality scenarios require that global and regional models can operate easily together. Exchange of boundary conditions is more easy and precise with a lon-lat grid. Other input data, such as meteorological data from ECMWF or climate models (IPCC-CMIP5) and land use data are mainly available on lon-lat grids.

Simulations of surface concentrations and deposition are improved when utilizing a higher resolved grid. This is in particular the case if the underlying emissions are reported in a better quality and finer resolution. In coastal and mountaineous areas an improvement exists even if the refinement of the real emission patterns is not as certain as the change in resolution suggests. A joint TFMM & MSC-W attempt to assess the performance of regional models as a function of scale and resolution has shown that all models show a better performance when using a finer grid, in particular for primary substances and near agglomerations [1].

Technically the foundations have been laid to utilize a higher resolved grid and associated input data. Computing resources and the parallelization of the model code have greatly developed and allow today for multiple simulations with finer grids. This has been demonstrated by the EMEP MSC-W model simulations in support of the TSAP revision, spanning hundreds of years simulated, exploring a range of different scenarios using the new MET Norway supercomputer, installed in 2012. However, technical work is needed to prepare the emission data in the countries, but also to keep the EMEP model system in a state, that it can process massive data streams in an efficient way.

Integrated assessments of air-quality and climate change scenarios require consistent simulations from urban to global scales. Regional scale assessments of eutrophying and nutrifying substances such as done by EMEP can serve as an efficient link between local urban and global scales. Several processes, such as vertical mixing in highly polluted areas, can only be described on a higher resolved grid with more vertical levels than in the current 50×50 km grid. The new EMEP grid offers the possibility to study air-quality-climate interactions in an adequate manner.

Harmonized model input data are needed across the EMEP domain and model system to

[1] EMEP/MSC-W Technical Report 1/13 Joint TFMM & MSC-W.

serve the future needs of the UNECE convention. Certainly a new balance has to be sought between efforts to increase the spatial detail in emission inventories and other research to improve air quality assessments. Some emission data may be best produced with gap-fill methods, which use expert judgements. Other data are readily available on higher resolution. Suggesting and shifting to a finer EMEP grid at this point in time would ensure that relevant scientific results can be produced for the next decade in support of the implementation of the UNECE air pollution protocols.

The new grid will make it also easier to utilize the EMEP model for regulatory purposes for any party to the convention. Countries may utilize the emissions and model system for finer scale applications and assessments. They can then improve these studies by using regional and global EMEP model simulations (readily available at emep.int) to have consistent and coherent boundary conditions.

4.2 Changes to reporting of emission and projections

Apart from the change in grid and projection and correcting for minor errors, the rationale for amending the 2009 Emission Reporting Guidelines (ECE/EB.AIR/97) is to allow for:

- changes to be incorporated from the 2012 amendment of the Gothenburg protocol and Heavy Metal protocol, as well as from the 2009 amendment of the Persistent Organic Pollutant (POPs) protocol
- continued consistency between the CLRTAP Nomenclature for Reporting (NFR) and the UNFCCC Common Reporting Format (CRF). Changes to the latter shall be followed for reporting from 2015 onward
- restructuring of the document by bringing together all definitions into one section that previously were provided throughout the Guidelines text and its annexes;
- incorporation of a new section on Inventory Adjustments.

In practice this would mean, that there will be also a change in NFR source categories (some will be replaced, some will be added other deleted) and a total of 13 categories (GNFR) used for reporting of gridded data (instead of 10 SNAP sectors) plus memo items.

The Revised Guidelines will be presented at the EMEP Steering Body for adoption (Sept 2013), followed by the CLRTAP Executive Body (Dec 2013). It is anticipated that a final and translated version will be published by the Convention Secretariat in early 2014 for use in 2015 and subsequent years. There will be no temporary reporting templates for the new EMEP grid in the transition period. If countries plan to prepare gridded data in the new resolution before 2015, it should be reported in current templates by replacing 50km^2 EMEP grid coordinates ”i” and ”j” with the long-lat coordinates.

More information about the new grid can be downloaded from the CEIP website (`http://www.ceip.at/the-new-emep-grid`); a document prepared by the EMEP centres for the SB which summarizes the main points of the new EMEP grid and a short presentation about the changes in the EMEP grid and the grid development over time. Parties are invited to download data defining the new grid cells and fractions of grid cells (as text and Excel file) also from the CEIP website at `http://www.ceip.at/the-new-emep-grid`. Country specific ESRI shape files with the new 0.1°$\times$ 0.1°(lon-lat) grid definition can be downloaded as well.

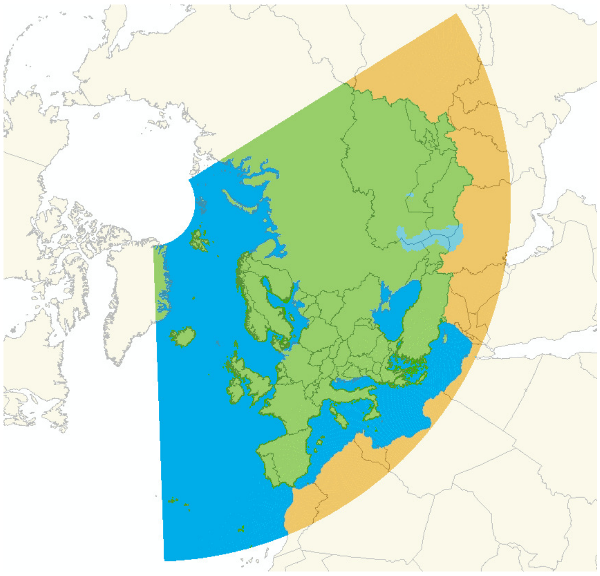

Figure 4.1: The new EMEP domain covering the geographic area between 30°N-82°N latitude and 30°W-90°E longitude.

4.3 Changes of critical load exceedances in different resolutions

One of the applications of modelled European depositions of sulphur (S) and total nitrogen (N) is the computation of critical load (CL) exceedances, often within the framework of integrated assessment. In the following paragraphs we assess the influence of the resolution of deposition fields on the exceedances of CLs.

For this purpose two EMEP model simulations and output for analysis of critical loads were prepared at two different resolutions (ca 14 km and 56 km grid size). Emissions were the same as used for the scale dependency report [2]. The CL data base used is the most recent held at the Coordination Centre for Effects (CCE) of the ICP Modelling and Mapping and described in Posch et al. (2011), with updates in Posch et al. (2012). This data base is also implemented in CIAM's GAINS model and currently used in scenario analyses for the European Commission's revision of the Thematic Strategy on Air Pollution. The database consists of about 2.5 million sites for which critical loads of acidity and/or nutrient N (eutrophication) have been computed (both CLs are available for most sites), covering an area of about 3.9 million km^2.

A critical load (CL) characterises the sensitivity of an ecosystem to S and/or N deposition, and if the deposition is greater than the CL, the CL is said to be exceeded (with harmful effects in the long run). For a single site the exceedance of the nutrient N, CL is simply the difference between the total N deposition and the critical load value. In the case of acidity, to which both S and N contribute, the CL is characterised by a so-called critical load function, and the exceedance is defined as the distance to this function; for details see ICP Mapping and Modelling (2010) (Umweltbundesamt). Note that non-exceedance is assigned the value zero (not a negative number). To characterise the exceedance with a single number for a region (grid cell, country, group of countries), the so-called average accumulated

[2]EMEP/MSC-W Technical Report 1/13 Joint TFMM & MSC-W.

exceedance (AAE) has been defined: If Ex_k is the (zero or positive) exceedance and A_k the area of site k, and there are N sites in the region of interest, then the AAE is defined as: $AAE = (A_1 Ex_1 + ... + A_N Ex_N)/(A_1 + ... + A_N)$, i.e., the area-weighted exceedances within the whole region.

On average, using output from the two different resolutions, exceedances are little different but consistently lower for the finer grid. The ecosystem area at risk, where the exceedance is greater than zero, and the AAE for acidity and nutrient N on the European and EU28 territory is shown in Table 4.1. The differences are consistent with the differences in the depositions: the average deposition onto the European ecosystem area is slightly higher for the TNO56 grid output than for the TNO14 output (390 vs. 383 mgS/m^2 and 719 vs.702 mgN/m^2). It shows that for a European-wide assessment the deposition on the 56 km grid is of sufficient quality and will not change with a change in grid. This might be different, however, when looking at a regional or local level.

Table 4.1: Ecosystem area exceeded and average exceedance (AAE) for acidity and nutrient N critical loads in the EU28 region and in the whole of Europe using depositions modelled on the TNO56 and TNO14 grid, using meteo and emissions from 2009. Corresponding results from this years report of 2011 conditions are given for comparison.

Region	Grid	Acidity Critical Loads		Nutrient N Critical Loads	
		Area exc. (%)	AAE (mol ha^{-1}a^{-1})	Area exc. (%)	AAE (mol ha^{-1}a^{1})
EU28	TNO56	8.54	30.0	65.4	260.0
	TNO14	8.18	28.2	64.4	243.7
	EMEP-2011	6.8	19.9	63.4	230.5
Europe	TNO56	5.90	18.6	58.8	193.6
	TNO14	5.78	17.4	58.1	184.1
	EMEP-2011	4.8	12.9	59.5	180.0

To investigate whether there are significant differences on a local (grid) scale we compare European maps of exceedances (Figs. 4.2 and 4.3). Different combinations of deposition data at TNO56 and TNO14 and displaying the CL in respectively the three resolutions (including also the intermediate TNO28 resolution) have been tested. The most straight-forward results are those in the top-left (deposition at TNO56 and CL at TNO56) and bottom-right corners (deposition at TNO14 and CL at TNO14) of the figures. Obviously, the TNO56 map gives a much cruder picture; and the TNO14 map reveals the variability of both the critical loads and (potentially) the depositions within the larger grid cells. To reveal the influence of the difference in the depositions alone, one has to look at maps using deposition on two resolutions but CL displayed on the same resolution: Either both displayed on a TNO56 grid, i.e. the exceedances on the 4 $\times$ 4 TNO14 grid cells aggregated to a single number on the corresponding TNO56 cell; or both mapped on the TNO14 grid, i.e. all 4 $\times$ 4 grid cells receiving the same deposition in case of the TNO56 model output. It appears in both cases there are differences, but they are small. The TNO56 grid display overemphasises high exceedances, i.e. large black grid cells, although the high exceedances are constraint to a few small cells within the larger one, as can be seen when looking at the TNO14 maps (e.g. in the Po-valley in northern Italy).

Finally, in the centre rows of both figures the TNO56 and TNO14 model results are displayed on the TNO28 grid, the one for which source-receptor matrices were available, e.g. for the revision of the TSAP, and which is currently used in integrated assessment. A look at the TNO28 maps shows, that they are quite comparable, with the TNO14 model output still showing a better spatial differentiation. Possibly the TNO28 model output (not available for comparison here in this chapter) is the right compromise between accuracy and ease of use (in terms of resources) for assessments on a European scale.

The corresponding results from 2011, as reported in this status report, are given as well in Table 4.1 to illustrate that emissions (different in TNO56 than in EMEP) and meteorological conditions (2011 vs 2009) have a similarly large influence on average exceedance indicators than a grid change. It is interesting to note that especially for the critical nitrogen exceedances the grid change has a relatively large impact though, at least as compared to the difference between the TNO56 and standard EMEP emission based simulation result.

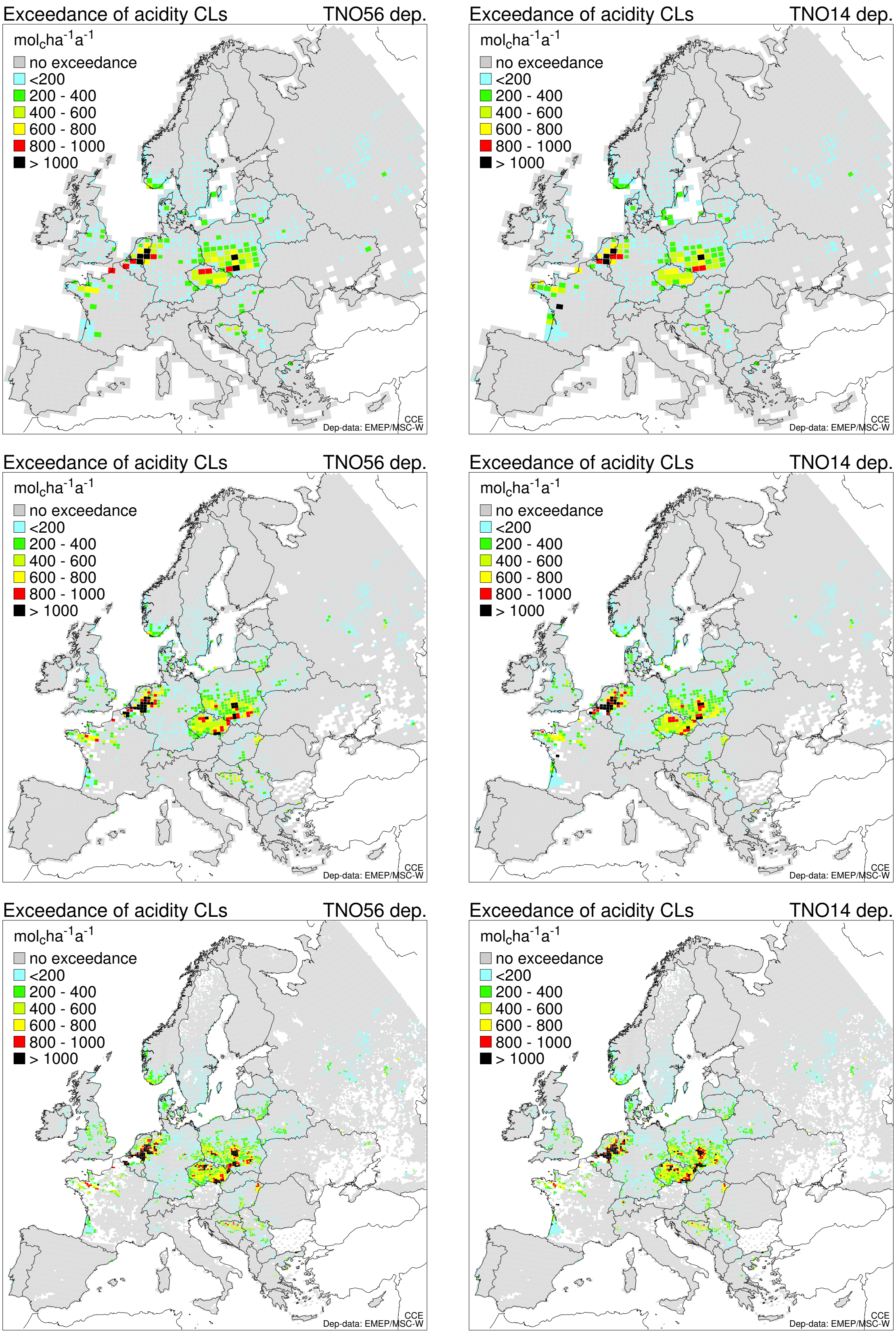

Figure 4.2: Average accumulated exceedance (AAE, in molc ha^{-1} a^{-1}) of acidity critical loads, using the TNO56 deposition (left column) and the TNO14 deposition (right column). The AAE is displayed on the TNO56 (top) TNO28 (centre) and TNO14 (bottom) grid. Note that the size of the coloured grid cells is proportional to the ecosystem area exceeded in the respective cell

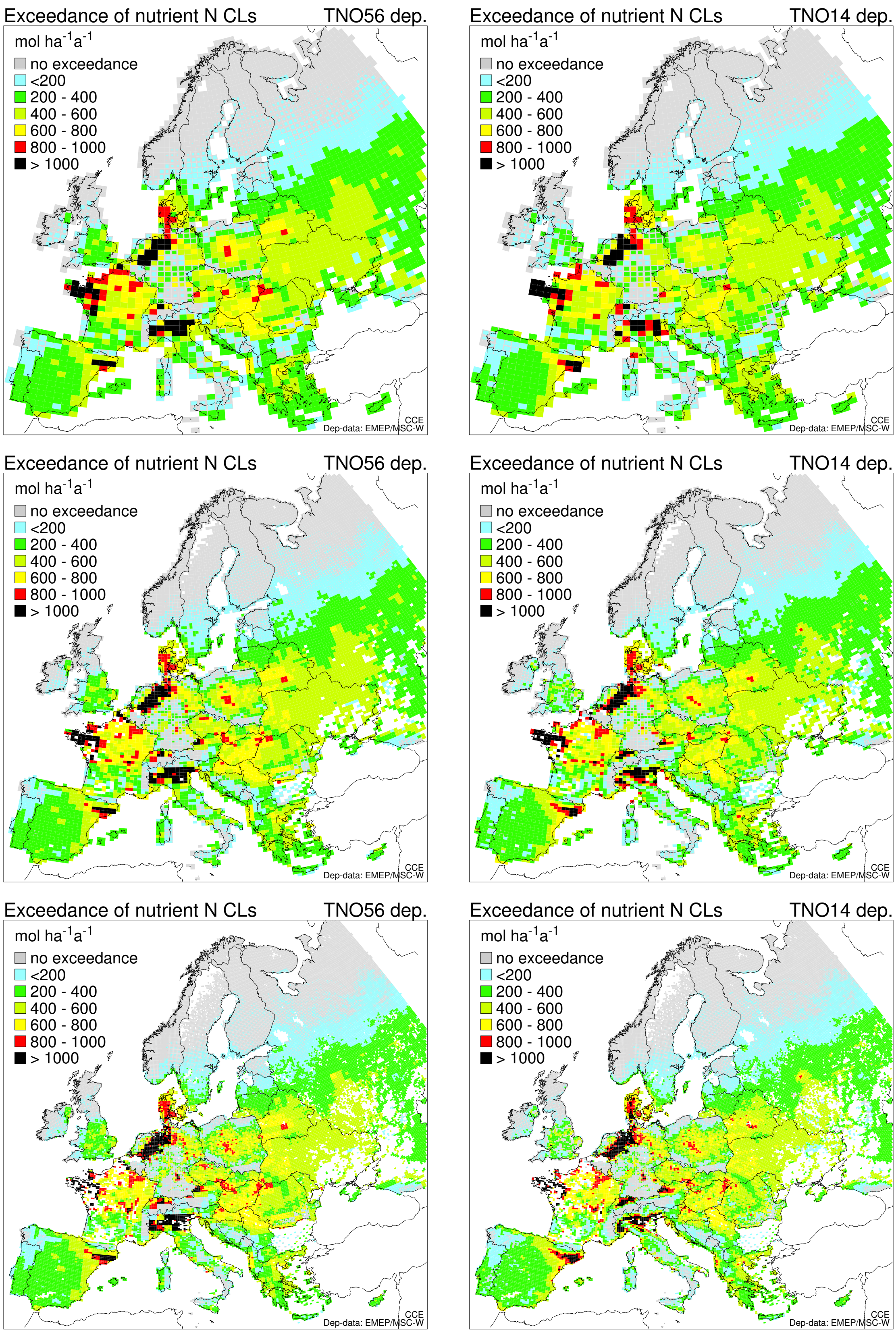

Figure 4.3: Average accumulated exceedance (AAE, in mol ha^{-1} a^{-1}) of nutrient N critical loads, using the TNO56 deposition (left column) and the TNO14 deposition (right column). The AAE is displayed on the TNO56 (top) TNO28 (centre) and TNO14 (bottom) grid. Note that the size of the coloured grid cells is proportional to the ecosystem area exceeded in the respective cell

References

Posch, M., Slootweg, J., , and Hettelingh, J.-P.: Modelling critical thresholds and temporal changes of geochemistry and vegetation diversity, in: CCE Status report 2011, RIVM Report 680359003, edited by Hettelingh, J.-P., p. 186 pp, Coordination Centre for Effects, RIVM, Bilthoven, The Netherlands, URL `http://www.wge-cce.org`, 2011.

Posch, M., Slootweg, J., , and Hettelingh, J.-P.: Modelling and mapping of atmospherically-induced ecosystem impacts in Europe, in: CCE Status report 2011, RIVM Report 680359004, edited by Hettelingh, J.-P., p. 141 pp, Coordination Centre for Effects, RIVM, Bilthoven, The Netherlands, URL `http://www.wge-cce.org`, 2012.

(Umweltbundesamt), F. E. A.: ICP Modelling and Mapping 2010, Manual on Methodologies and Criteria for Modelling and Mapping Critical Loads and Levels and Air Pollution Effects, Risks and Trends, UBA-Texte 52/04, revised version of 2010, URL `http://www.icpmapping.org`, 2010.

CHAPTER 5

Application of a coupled WRF/EMEP MSC-W model

Massimo Vieno, Stefan Reis, Tove Svendby, Sverre Solberg, Philipp Schneider, Li Liu, Maciej Kryza, Malgorzata Werner, Kinga Walaszek and Peter Wind.

5.1 Introduction

In recent years the EMEP MSC-W model (Simpson et al. 2012) has been extended and upgraded to allow it to operate with different projections and meteorological drivers. This enables the EMEP MSC-W model to be applied at regional scale (i.e. for the country or landscape) with horizontal resolutions varying from 50 km $\times$ 50 km to 5 km $\times$ 5 km and to 1 km $\times$ 1 km.

Currently the EMEP MSC-W model is applied for regional studies in the UK, Croatia, Denmark, Norway, Peoples Republic of China, and Sweden. Although not all EMEP regional applications are using the Weather Research and Forecast model (WRF) as meteorological driver this section will solely focus on the EMEP-WRF model setup, specifically on the examples of the UK, Peoples Republic of China, and Poland.

The easy availability, with a GNU General Public Licence (GPL), as well as the global coverage of the initial and boundary conditions (IC, BC) makes the WRF model an excellent choice as an alternative meteorological driver for non-standard and country domain applications of the EMEP MSC-W model where the preparation of ECMWF meteorological fields is too cumbersome.

5.2 The WRF model Setup

The WRF model is a mesoscale numerical weather prediction model designed to serve both operational forecasting and atmospheric research needs. WRF is freely available and has a large and active user base all over the world. It is designed to be a flexible, state-of-the-art non hydrostatic numerical weather prediction model (NWP) suitable for use in a broad range of applications across scales ranging from meters to thousands of kilometres. The model consists of the WRF Pre-processor System WPS (used to create the necessary input files for the WRF model) and the meteorological model WRF (`http://www.wrf-model.org`).

The work discussed here is based on WRF version 3.xx with input data from NCEP (National Centers for Environmental Prediction) which is part of the US National Oceanic and Atmospheric Administration (NOAA). For the forecast application the NCEP Global Forecast System (GFS) data, which are provided on a grid with 1.0°× 1.0°resolution in GRIB2 format are used with a 3-hour forecast data frequency. For historical model runs the final "FNL" Operational Global Analysis data (computed with the same model as GFS) are used.

The WRF model options allow to use the same vertical resolution, coordinate system (sigma coordinates) and number of layers in WRF as in the EMEP model. Thus, there is no need for vertical interpolation of meteorological data.

5.3 EMEP-WRF model application for the UK

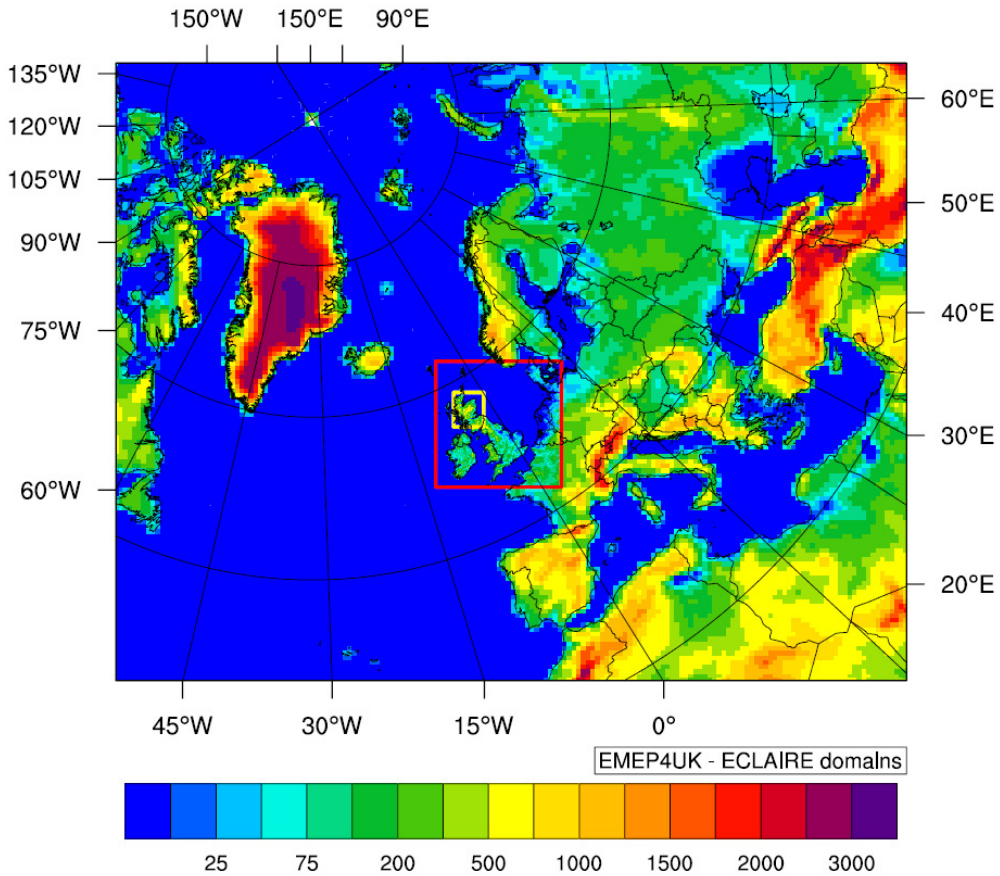

Figure 5.1: The EMEP4UK Greater European domain, modelled at 50 km × 50 km horizontal resolution, outlined in red, the nested British Isles domain, modelled at 5 km × 5 km horizontal resolution, and finally outlined in yellow, the nested Scottish domain, modelled at 1 km × 1 km. The colour scale indicates grid-average altitude in meters.

This section presents the results of a nested EMEP-WRF model system for the European domain at 50 km × 50 km, the UK domain at 5 km × 5 km, and for the Scottish at 1 km × 1 km horizontal resolution.

The UK application of the EMEP MSC-W model is in short known as the EMEP4UK model (Vieno et al. 2010). The EMEP4UK model domain is shown in Figure 5.1. The EMEP4UK model uses the EMEP polar stereographic (`www.emep.int`) as geographical projection. The horizontal and vertical grid is the same as the EMEP grid described in the EMEP website (`http://emep.int/mscw/index_mscw.html`) of the EMEP 50 km × 50 km grid European model domain (prior to 2008 `www.emep.int`). Two nested domain (5 km × 5 km and 1 km × 1 km) in a telescopic configuration are then used for the UK and Scotland, respectively, as illustrated in Figure 5.1.

An example of the spatial distribution of the 2008 NO_x total annual emissions used in the EMEP4UK model for all 3-model domains (Figure 5.1) is shown in Figure 5.2. Only the Scottish area of the EMEP4UK model domain covered by the high resolution nest is shown here to highlight the impact of horizontal resolution of emission input data on the spatial concentration variability. The emissions inputs are created using the 1 km × 1 km UK National Atmospheric Emissions Inventory (NAEI), 5 km × 5 km shipping emissions generated by ENTEC (ENTEC 2010) and 50 km × 50 km EMEP emissions (where no higher resolution data is readily available) from the EMEP Centre for Emission Inventories and Projections (CEIP).

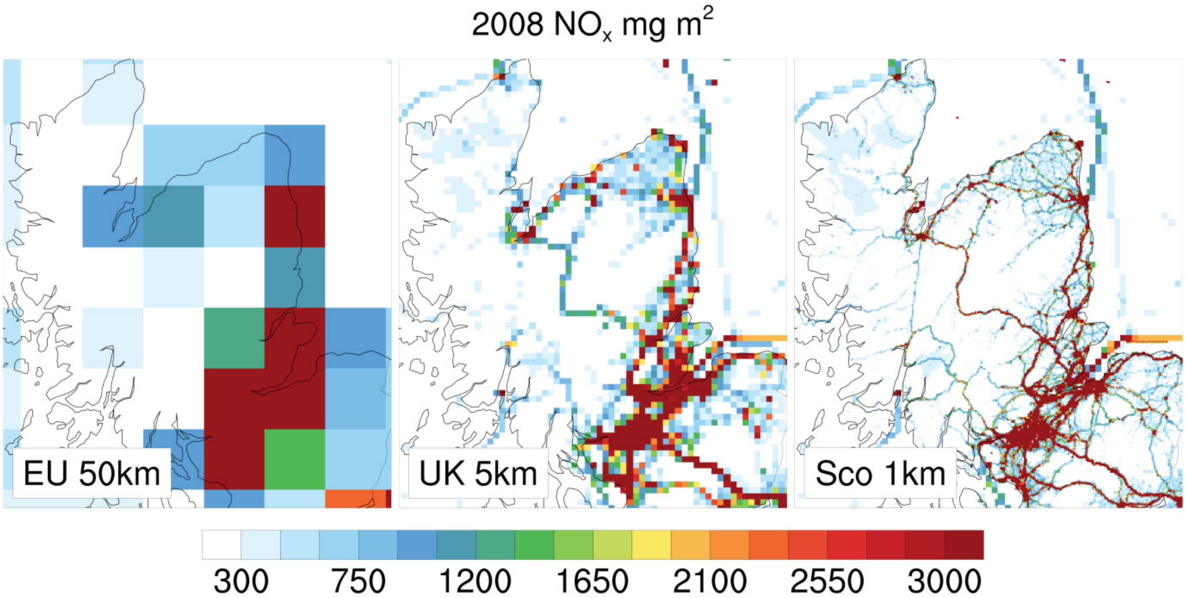

Figure 5.2: EMEP4UK 2008 annual gridded NO_x emission estimates for the Scottish zoom-in for each resolution: European (50 km × 50 km), UK (5 km × 5 km), and Scotland (1 km × 1 km).

To illustrate what can be done, we show some preliminary results of the surface 2008 NO_2 concentrations calculated by the EMEP4UK model. For each of the three domains the field is shown in Figure 5.3. For NO_2 the spatial distribution of surface concentrations is very similar to the emissions pattern, as it is expected for trace gases mainly emitted by road transport sources. In the European 50 km × 50 km domain, two grid squares cover the whole Scottish Central Belt (Edinburgh-Glasgow area). The resolution effect is even more pronounced when we zoom in the Edinburgh-Glasgow area as shown in Figure 5.4.

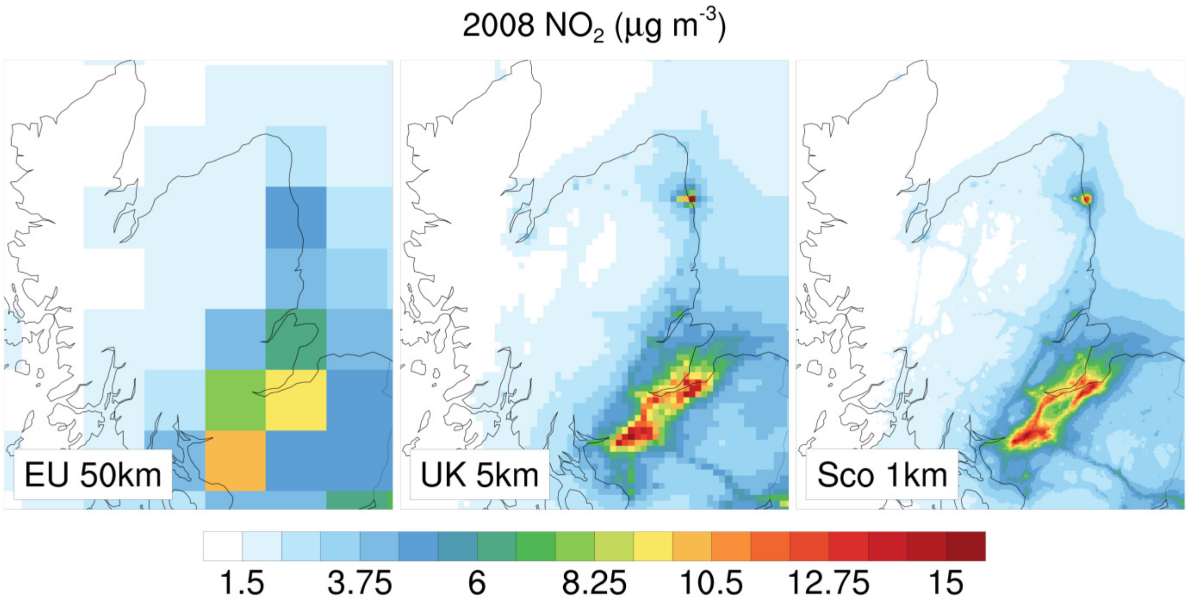

Figure 5.3: EMEP4UK 2008 annual average NO_2 surface concentrations for the Scottish zoom in of the three domains: European (50 km × 50 km), UK (5 km × 5 km), and Scotland (1 km × 1 km).

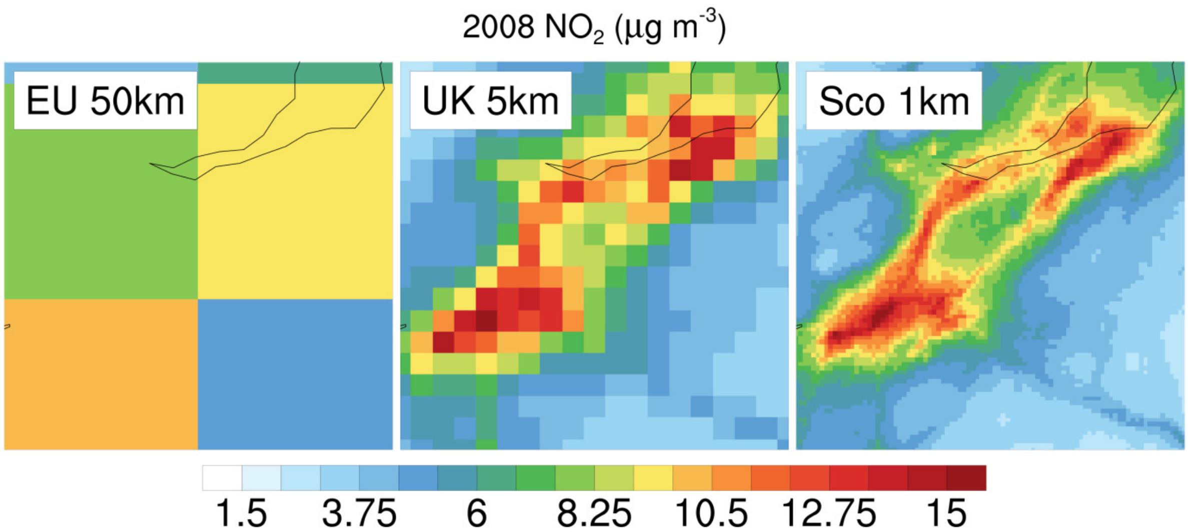

Figure 5.4: EMEP4UK 2008 annual average NO_2 surface concentrations for the Glasgow-Edinburgh area.

The effect of resolution on a secondary pollutant such as ozone is illustrated in Figure 5.5. The hourly observations from the UK automatic monitoring network are used to validate the calculated hourly surface ozone by the EMEP4UK model. The summary analysis shown in Figure 5.5 highlights how increasing the resolution of the EMEP4UK model may reduce the bias in the predicted ozone when compared with observations in urban areas, whereas for truly rural areas the model performances are similar at different scales.

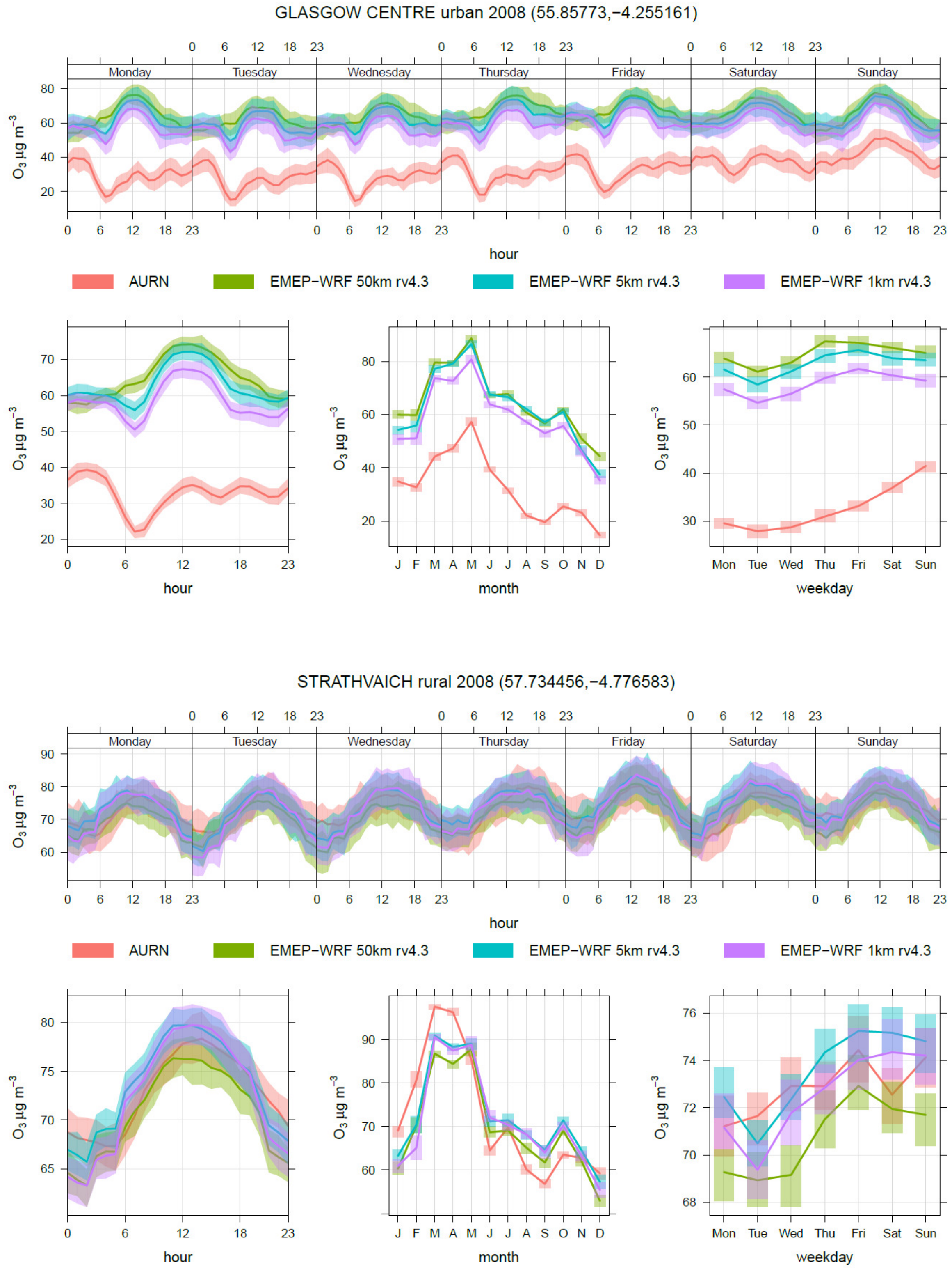

Figure 5.5: EMEP4UK and U.K. Automatic Urban and Rural Network (AURN) hourly surface ozone for the year 2008 for two sites: Glasgow city centre (urban traffic) and Strathvaich (rural).

5.3.1 EMEP4UK projects

The EMEP4UK model framework is funded under the contract AQ0727 by the UK Department for Environment, Food and Rural Affairs (Defra) with the aim to develop a photochemistry transport model which can be applied both for scientific research and for policy decision support.

The EMEP4UK modelling framework is currently being deployed within other research projects, such as the AWESOME project (`http://awesome.lshtm.ac.uk/`) to examine the effects of air quality and climate policies on air pollutant exposures and human health in the UK. Six-hourly, global, meteorological fields from the NCEP final analysis are downscaled with WRF and used to drive EMEP4UK for the period 2001 to 2010. This generates a decade-long self-consistent estimate of a suite of potentially health-related weather indices, gaseous concentrations and particulate loadings over the whole UK on a 5 km $\times$ 5 km grid at sub-daily temporal resolution with no data gaps. Application of this full data set together with similarly spatio-temporally disaggregated health metrics enables epidemiological studies based on a multi-pollutant approach. This focus on pollution (and weather) mixtures enables a more comprehensive characterisation of the complexity of exposures and health effects compared to a traditional single pollutant focus. The potential health impacts of various climate and emission policies are examined in further studies using WRF-EMEP-EMEP4UK driven by climate model output instead of meteorological reanalysis, as well as the interaction between air pollution and climate change and effects on ecosystem services. The application of the EMEP4UK model in research projects includes, but is not limited to, the EU FP7 funded research project ECLAIRE (`http://www.eclaire-fp7.eu`), the UK Integrated Assessment Modelling project (AQ0947) and the Global Challenge Network on Groundlevel Ozone (Science and Technology Facilities Council, FUTURES programme, `http://www.ozone-net.org.uk`).

5.4 EMEP-WRF forecast model system for Hubei/China

This section presents the development of a nested EMEP-WRF forecast model system for a geographical domain outside Europe (Peoples Republic of China). The aim is to highlight the flexibility of the EMEP model and to show the possibilities, limitations and challenges when applying the nested EMEP model outside the standard domains.

Through a European project, NILU is developing an air quality forecast modelling system for the province of Hubei in Peoples Republic of China (Figure 5.6). The system is based on a combined EMEP-WRF model, with NILUs urban model EPISODE (Slørdal et al. 2003) applied in the innermost EMEP-WRF model domain, thus the end-product will be an EMEP-WRF-EPISODE model system. The model setup has many similarities to EMEP4UK (Vieno et al. 2010) with two major exceptions: The model domain is outside the traditional EMEP/EECCA region and, secondly, the models are run in forecast mode. As in EMEP4UK the WRF model (Skamarock and Klemp 2008) is used to produce data for meteorology and land-use on various scales and these fields are used as input to the EMEP model.

In the following, we discuss model modifications that are needed as well as the challenges related to emissions, boundary conditions and other input files. The main purpose is to present the model structure. Modelling results, comparisons with measurements etc are not analysed here. We stress that the model set-up is preliminary and in a developing phase and that major changes may be applied before the system is put into operation.

5.4.1 Model set-up and geographical domains

Figure 5.6: The EMEP-WRF model domains in the Hubei project. The two nests (0.5°and 0.1°resolution) are marked as red rectangles.

For the model runs presented in this chapter we have used the EMEP/MSC-W model version 4.3 with lat/lon projection for a region covering most of Peoples Republic of China. Both the EMEP and WRF models are compiled with gfortran on a Linux cluster locally at NILU.

In the current project WRF is run with two nests in the lat/lon projection. For the mother domain covering most of Peoples Republic of China we use a 0.5°grid resolution whereas the 2nd domain is centred on Hubei with a resolution of 0.1°($\sim$11 km $\times$ 11 km), as shown in Figure 5.6. The mother domain has 122 $\times$ 70 grid cells in longitudinal and latitudinal directions, respectively, whereas the inner domain contains 90 $\times$ 50 grid cells.

The main requirements applying for the EMEP-WRF model outside the EMEP/EECCA region are:

Anthropogenic emissions Running the model outside the EMEP/EECCA domain normally requires emission data other than the standard data set. If the emission is prepared in NetCDF format the data dont necessarily need to be specified in the exact grid domains/resolution. The EMEP MSC-W model contains routines for automatic regridding and interpolation of input emission data.

Landuse Software for conversion of WRF landuse data to EMEP input data is needed (unless the global EMEP landuse data are used). Since the landuse categories differ between WRF and EMEP, various assumptions for scaling and lumping are needed. We have used a conversion program developed for the EMEP4UK system (Vieno et al. 2010).

Boundary values Lateral and top boundary concentrations of gases and aerosols are needed as input to the EMEP MSC-W model. Whereas the standard EMEP boundary data are developed for Europe, alternative boundary values for other regions can be read from separate files.

We also refer to the presentation of the nested EMEP-WRF system in last years EMEP Status report (Solberg and Svendby 2012).

5.4.2 Boundary conditions

Boundary concentrations of the chemical trace species are obtained from the EU FP7 project MACC-II (Monitoring Atmospheric Composition and Climate). This project provides various services and data products for free, including global day-to-day forecasts of ozone and related species. For the Hubei project we extract daily forecasts from the MOZART model (experiment "fnyp", `http://join.iek.fz-juelich.de/macc/workspace`). The MOZART model provides 5 days forecasts from 00 UTC. The data has a spatial resolution of 1.125°× 1.125 °with 47 vertical layers with a hybrid coordinate system (η-coordinates).

In the latest version of the EMEP MSC-W model version 4.3 the use of external boundary data has been simplified. Thus, input of MACC-II/MOZART data on η-levels are done in a fairly simple way by including an ascii file containing the definition of the hybrid levels, and in addition the proper settings in the namelist file (config_emep.nml) have to be supplied. Internal routines in the EMEP MSC-W take care of vertical and horizontal interpolation of the boundary input data. The units of the boundary species may need special attention. If the units dont match the standard units in the EMEP MSC-W, it may be necessary to include certain changes in the EMEP MSC-W model code (i.e. in the routine Units_ml.f90).

So far 15 species from MACC-II/MOZART have been included as boundary values to the EMEP MSC-W model: O_3, NO, NO_2, CO, CH_4, C_2H_6, isoprene, HCHO, PAN, SO_2, SO_4, sea salt (fine and coarse, respectively) and dust (fine and coarse, respectively). These boundary data are only applied for the outer model domain (the mother domain, Figure 5.6). Boundary concentrations for the 2nd nest are provided by the EMEP model itself when running in nested mode.

At this stage in the project we have been focusing on the technical model aspects and model structure. Nevertheless, we are already performing daily EMEP-WRF air quality forecasts for Peoples Republic of China/Hubei, which eventually will be compared against measurements. Figure 5.7 shows an example of forecasted values of daily maximum ozone. The EMEP MSC-W model run was done 26 June 2013 and the map represents modelled ozone values the following day. The forecasted ozone concentrations in Peoples Republic of China ranged from 10 to 160 ppb this day.

5.5 EMEP-WRF application for Poland

The EMEP MSC-W model has been recently applied for the area of Poland with the 5 km × 5 km grid (EMEP4PL). The first test model run was performed for January 2011. For this period, high concentrations of SO_2, NO_x and PM_{10} were observed. These preliminary results are briefly described below.

Meteorological data for the EMEP model were provided by the Weather Research and Forecasting model (Skamarock and Klemp 2008). Three nested domains were defined for

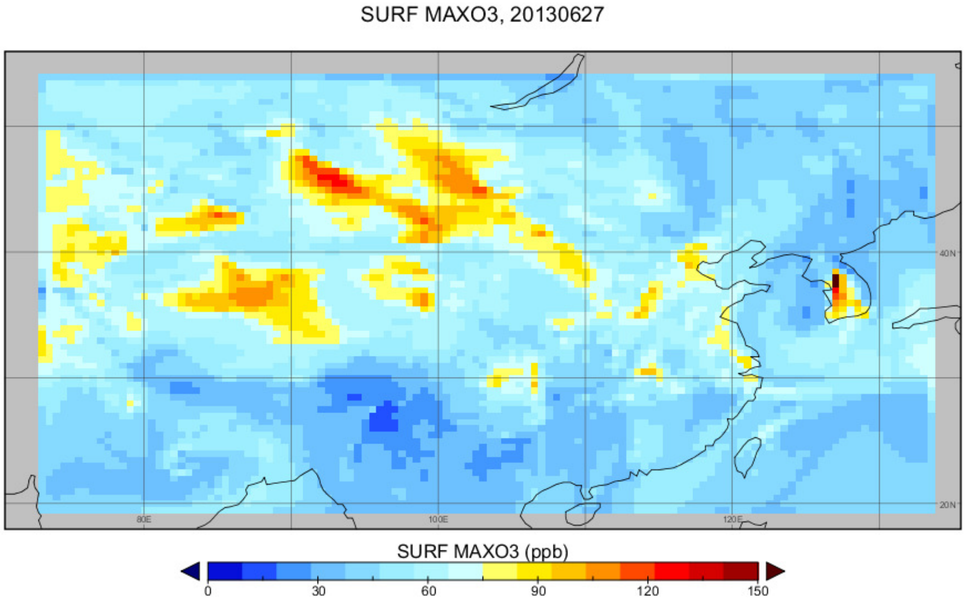

Figure 5.7: EMEP MSC-W mode forecast of maximum ozone 27 June 2013. The inner Hubei nest has a resolution of 0.1°whereas the outer domain has a resolution of 0.5°.

WRF model runs – d01 covering the EMEP domain with the 50 km × 50 km grid, d02 with 10 km × 10 km grid and the innermost domain (d03) covering the area of Poland with 5 km × 5 km grid. Vertically, the resolution matches the EMEP MSC-W model. The details on the WRF model configuration applied are provided by Kryza et al. (2012).

The EMEP4PL model is configured with two nested domains. The outermost domain is a regular EMEP MSC-W model domain and covers the area of Europe with 50 km × 50 km grid. For this domain, WRF derived d01 meteorology was used, together with the EMEP emission data for year 2010. The nested EMEP4PL domain covers the area of Poland with 5 km × 5 km grid. For this domain, WRF derived d03 meteorology was used, together with the TNO high resolution emission inventory for the year 2007 (Pouliot et al. 2012). The EMEP4PL emission inventory for the nested domain were prepared with GIS GRASS software.

The EMEP4PL modelled air concentrations of SO_2, SO_2 and PM_{10} for Jan 2011 were compared with the measurements gathered at 97 air quality measuring sites in Poland, for daily mean values. The factor of two (FAC2) statistics was calculated for all sites. The FAC2 is 0.55 for SO_2, 0.75 for NO_2 and 0.83 for PM_{10}. For NO_2, there is some overestimation if the model results are compared with the measurements (not shown here), but the majority of the high concentration peaks are properly resolved. An example of EMEP4PL model output for PM_{10} monthly average is shown in Figure 5.8 for the January 2011.

5.6 Summary and outlook

Three examples of non-standard usage of the EMEP MSC-W model have been presented. Whereas the EMEP MSC-W model is the main driver, it is built into a model hierarchy which includes the WRF model as meteorological processor and EMEP MSC-W or MACC-II/MOZART as provider of boundary chemical data. The main advantage of these configu-

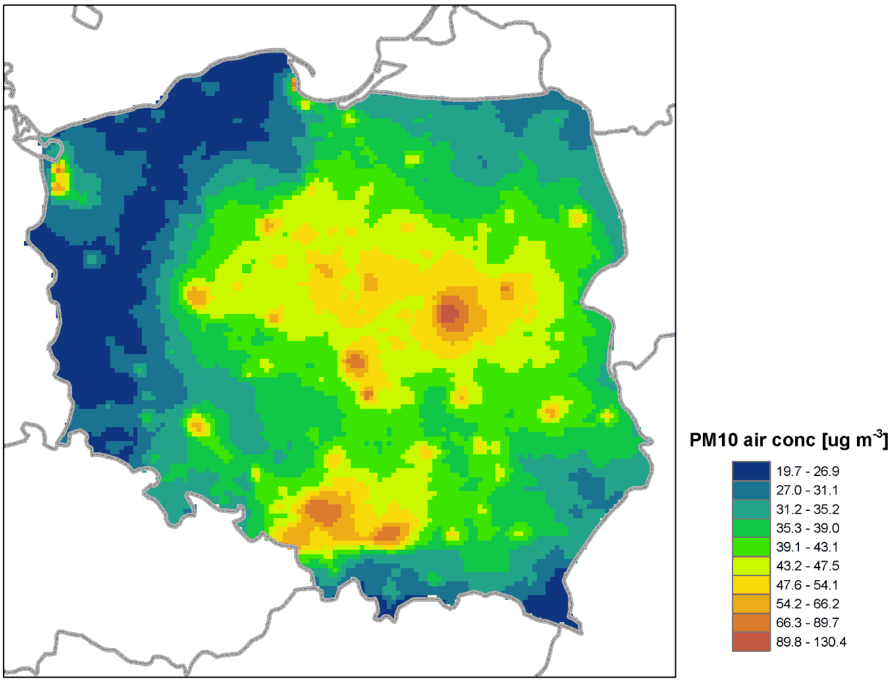

Figure 5.8: EMEP4PL January 2010 monthly average PM_{10}.

rations are the possibility of running the EMEP MSC-W model largely independent of scale and domain.

Substantial work remains before such model system as flexible as desirable. The choice of parameter settings and selection of processes in WRF needs testing and evaluation. Furthermore, input parameters like anthropogenic emission data, landuse categories, BVOC emissions all need to be evaluated with respect to measurement data.

The combination WRF and EMEP MSC-W model provides a framework for performing detailed analysis of air pollution for virtually any region of the world with consistent and appropriate boundary conditions. The open source nature of both codes allows virtually full flexibility, making it possible to do special adaptations for specific needs (output of special parameters or inclusion of non-standard processes).

Although the setup of the WRF/EMEP system is not yet put in a documented and tested standardized procedure, the main technical challenges left are essentially involving simple format transformations of publicly available data. The main limitation being often the availability and accuracy of the emissions source. A standard procedure for writing a WRF/EMEP is planed to be documented between the partners involved with the support of MSC-W (within budget limitations).

In the future the EMEP model will be further developed to allow for more flexibility, by providing more accurate default input values, valid for any grid. The model makes use of a large number of data, and normally only a small subset are of interest for a given project. A goal of such development is that the user can focus on the processes of interest and can rely on the default values for the rest.

Concretely we are currently developing flexible hybrid vertical coordinates, global default emission datasets as well as global landuse maps for parameterization of windblown dust. In the longer term a more user friendly interface between meteorological drivers and the EMEP model is planned. The aim being to be able to test different WRF resolutions and to use meteorological data from different sources directly as input to the model.

A further development of the EMEP model that would allow an easier regional application is the capability of the EMEP model to run in a telescopic nesting without the need to run each domain independently. The implication of the current setup is the need of large disk space which for small research team may be a restriction, as the 3D output necessary as boundary condition for each nested domain may be quite large.

A WRF/EMEP user group for exchange and mutual support has been proposed at the EMEP MSC-W model training course. Interested institutions are welcome to contact MSC-W about being included in email lists and associated joint development projects.

Acknowledgements

We are grateful for data provided by the MACC-II project, funded by the European Union under the 7th Framework Programme, the UK Department for the Environment, Food and Rural Affairs (Defra), the NERC Centre for Ecology and Hydrology (CEH), the EMEP programme under the UNECE LRTAP Convention, the Norwegian Meteorological Institute (MET Norway) and the European Union projects NitroEurope IP and CLAIRE.

References

ENTEC: Defra, UK ship emissions inventory, final report., http://uk-air.defra.gov.uk/reports/cat15/1012131459_21897_Final_Report_291110.pdf, Crown copyright, 2010.

Kryza, M., Werner, M., Dore, A. J., Vieno, M., Bla's, M., DrzenieckaOsiadacz, A., and Netzel, P.: Modelling meteorological conditions for the episode (December 2009) of measured high PM10 air concentrations in SW Poland - application of the WRF model, International Journal of Environment and Pollution, 50, 41 – 52, doi:10.1504/IJEP.2012.051179, 2012.

Pouliot, G., Pierce, T., van der Gon, H. D., Schaap, M., Moran, M., and Nopmongcol, U.: Comparing emission inventories and model-ready emission datasets between Europe and North America for the AQMEII project, Atmospheric Environment, 53, 4 – 14, doi:http://dx.doi.org/10.1016/j.atmosenv.2011.12.041, 2012.

Simpson, D., Benedictow, A., Berge, H., Bergström, R., Emberson, L. D., Fagerli, H., Hayman, G. D., Gauss, M., Jonson, J. E., Jenkin, M. E., Nyíri, A., Richter, C., Semeena, V. S., Tsyro, S., Tuovinen, J.-P., Valdebenito, A., and Wind, P.: The EMEP MSC-W chemical transport model – technical description, Atmos. Chem. Physics, 12, 7825–7865, doi:10.5194/acp-12-7825-2012, 2012.

Skamarock, W. C. and Klemp, J. B.: A time-split nonhydrostatic atmospheric model for weather research and forecasting applications, J. Comp. Phys., 227, 3465–3485, doi:10.1016/j.jcp.2007.01.037, 2008.

Slørdal, L., Walker, S., and Solberg, S.: The urban air dispersion model EPISODE applied in AirQUIS2003., Technical description. Norwegian Institute for Air Research (NILU), Kjeller, Norway, Report (NILU 12/2003), 2003.

Solberg, S. and Svendby, T.: Development of a nested WRF/EMEP model, in: MSC-W (EMEP status report 1/2012), edited by Fagerli, H., Gauss, M., Benedictow, A., Jonson, J., Nyiri, A., Schulz, M., Simpson, D., Steensen, B., Tsyro, S., Valdebenito, A., Wind, P., Shamsudheen, S., Aas, W., Hjelbrekke, A.-G., Mareckova, K., Wankmuller, R., Solberg, S., Svendby, T., Vieno, M., p. Thunis, Covelier, K., Koffi, B., and Bengtstrom, R., chap. 6, pp. 81–89, Norwegian Meteorological Institute, Oslo, 2012.

Vieno, M., Dore, A. J., Stevenson, D. S., Doherty, R., Heal, M. R., Reis, S., Hallsworth, S., Tarrason, L., Wind, P., Fowler, D., Simpson, D., and Sutton, M. A.: Modelling surface ozone during the 2003 heat wave in the UK, Atmos. Chem. Physics, 10, 7963–7978, doi:10.5194/acp-10-7963-2010, 2010.

Part III

Ongoing research

CHAPTER 6

Modelling and evaluation of trends in the EMEP framework

Michael Schulz, Anna Benedictow, Philipp Schneider, Jerzy Bartnicki, Álvaro Valdebenito, Michael Gauss, Jan Griesfeller

6.1 Observed and modelled trends in EMEP region

6.1.1 Introduction and method

A consistent atmospheric transport simulation over long time periods allows to inspect mean annual cycles, trends in atmospheric composition, and the stability of any model bias and its performance over time. The agreement between emission based modelling and independent measurements ultimately provides the most convincing argument for having achieved pollution abatement.

Trends of eutrophying and nutrifying substances have been simulated with this report's EMEP MSC-W model version for 1990 and the period 2000–2011, using consistent meteorology from one ECMWF cycle version and standard EMEP emissions for the old EMEP domain. An accompanying model simulation, just used in this chapter, has used reported emission data but repeatedly applied the same meteorological conditions from 2011 to all years (called m̈eteo2011" hereafter). Due to computational constraints the years 1991-1999 had to be omitted.

The resulting model data have been compared at all European measurement sites contained in the EMEP/EBAS database for gases, aerosol components and deposition. Using the full EBAS database means that a considerable extension in data amount is used. This comparison comprises for instance also weekly deposition data, not used in the standard EMEP model verification. The evaluation has been done with the AeroCom tools and more detailed results can be found via the AeroCom web interface[1].

[1] http://http://aerocom.met.no/cgi-bin/aerocom/surfobs_annualrs.pl?MODELLIST=EMEPReports&Run0=EMEP_rv4_2599_Rep2013trend

Here we report monthly means for selected components of the sulphur cycle, as well as oxidised and reduced nitrogen components (see Figure 6.1, Figure 6.2 and Figure 6.3). The observations and model data are only averaged at the time and place when measurements are available. For better visibility of the decadal trend, the corresponding annual mean value trends are plotted in addition as figure inlet.

6.1.2 Results

Sulphur trends in model and observation, depicted in Figure 6.1, show a consistent decrease in Europe over the years, in particular of course in the meteo2011 simulation. The meteo2011 simulation being compared to the trend run with actual meteorology shows also that the year 2011 led to relatively high surface concentrations of gases and aerosols. Monthly variation of the sulphate surface concentration is larger than that of deposition. Modelled winter SO_2 concentrations were too high in the beginning of the period. A small opposite seasonal bias appears for sulphate aerosol and deposition, with more pronounced summer sulfate aerosol concentration deficits in the model lately. Deposition on the other hand seems to be too high in winter. From 2000 to 2011 both SO_2 concentrations and sulphur deposition seem to decrease more in the EMEP model simulation than in the observations (modelled: SO_2: -59% vs. observed -33%; modelled S-deposition: -45% vs. observed -39%). The bias in aerosol sulfate concentrations stays almost constant. Observed year-to-year variability is well reproduced by the model while the meteo2011 shows less variation.

The trends in oxidised nitrogen compounds, depicted in Figure 6.2, are clearly smaller, respectively rather absent for NO_2 and total nitrate (HNO_3+NO_3^- surface air concentrations, in particular in the observations. For NO_2 and total nitrate (HNO_3+NO_3^-) the model bias decreases from +5% (NO_2), respectively +20% (total nitrate) in 2000 to being absent in recent years on annual average. Interestingly no significant trend in bias is found for deposition of oxidised nitrogen. For the oxidised N-parameters only deposition has decreased by -15% from 2000 to 2011, consistently in model and observations. Significant seasonal bias appears for all oxidised N-parameters, with too high NO_2 model concentrations in winter and a too large seasonal amplitude in oxidised N-deposition. This together could indicate an uncertainty in the chemical modelling of the oxidised nitrogen cycle.

Gaseous ammonia trends are currently impossible to evaluate due to considerable network fluctuations and changes in measurement quality. However, Figure 6.3 shows that the comparison and trend for aerosol ammonium and reduced N-deposition is rather robust. Reduced nitrogen in deposition has almost no significant trend in the same ten–year period, while ammonium aerosol concentration seem to decline by ca. 10%. The decrease is a little steeper in the model. Seasonal bias in reduced nitrogen deposition seems to be too low in summer in the model.

Finally the trend evaluation as presented in this chapter is consistent with the reported trend evaluation as discussed in chapter 3, where only the standard EMEP network data is used, which comprises about half of the sites. The consistency indicates indirectly that the standard EMEP network is largely well suited to monitor trends in atmospheric composition for major sulphur and nitrogen compounds. With the exceptions discussed below.

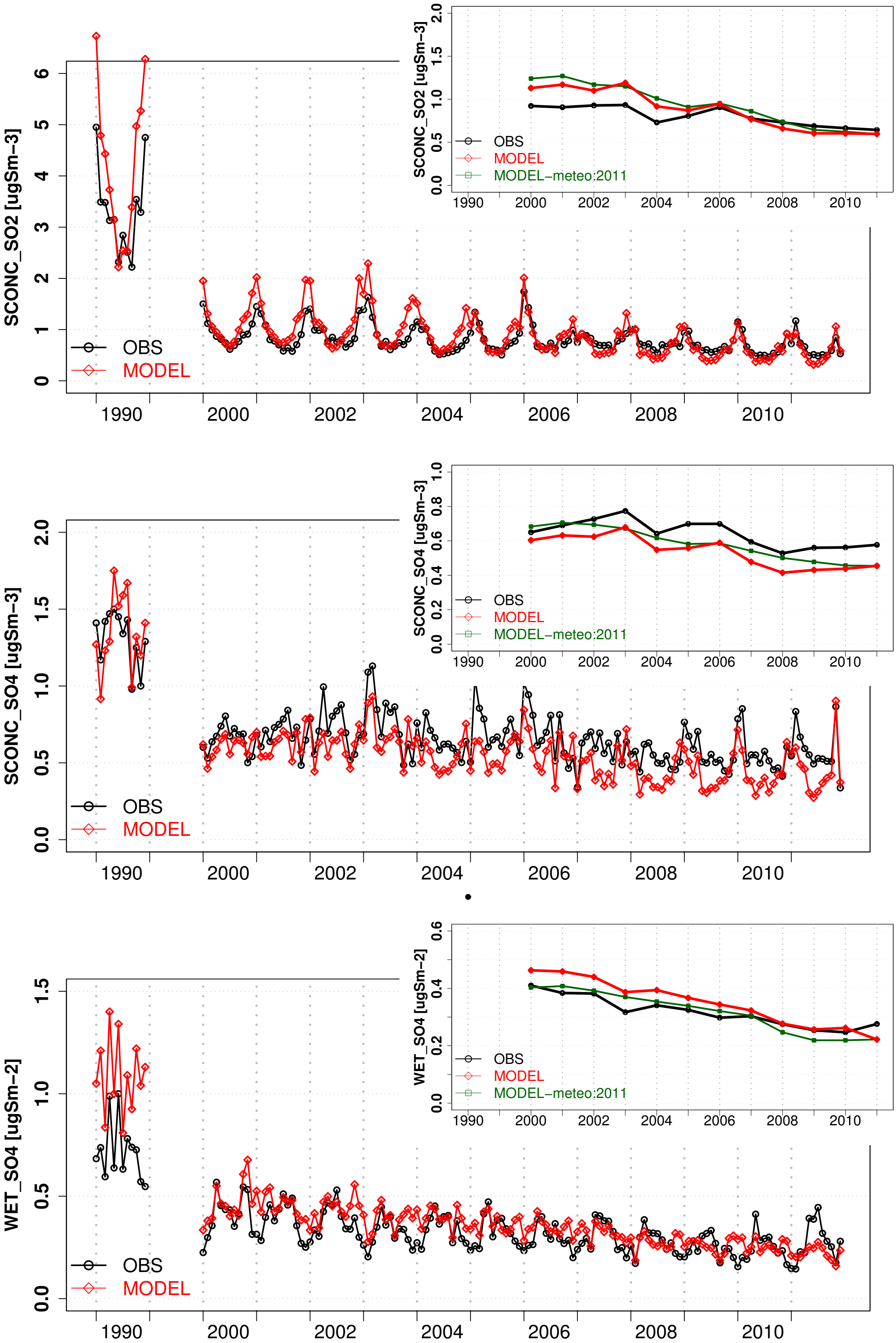

Figure 6.1: Trends of sulphur dioxide (upper panel), sulfate aerosol concentration (middle panel) and sulfate wet deposition (lower panel) observed at European background stations and simulated at these stations by the EMEP model for the period 1990-2011. Annual mean values are also shown for the model simulation using the same meteorology throughout (green line).

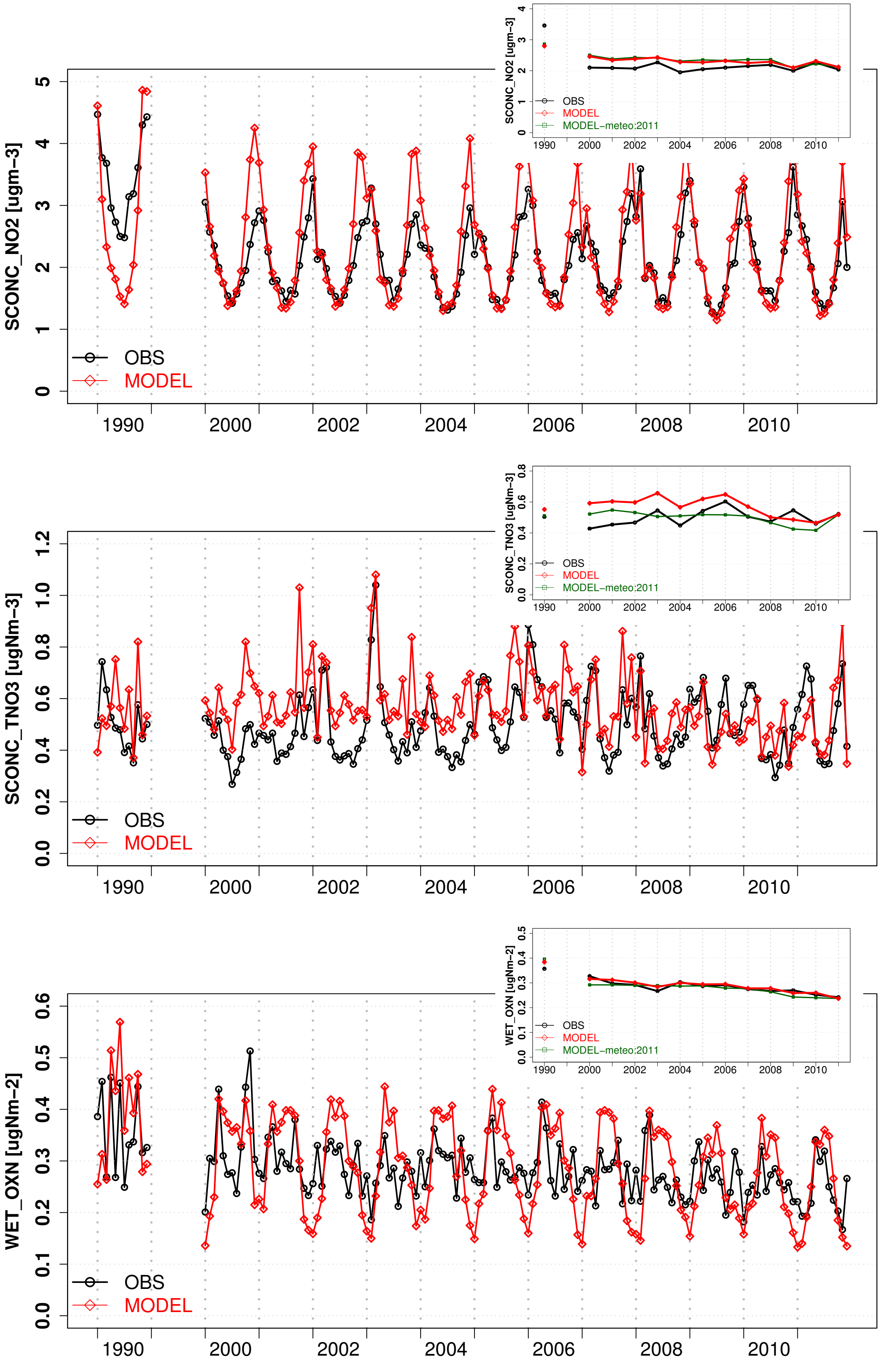

Figure 6.2: Trends of nitrogen dioxide (upper panel), total nitrate (nitric acid plus particulate nitrate) concentration (middle panel) and nitrate wet deposition (lower panel) observed at European background stations and simulated at these stations by the EMEP model for the period 1990-2011. Annual mean values are also shown for the model simulation using the same meteorology throughout (green line).

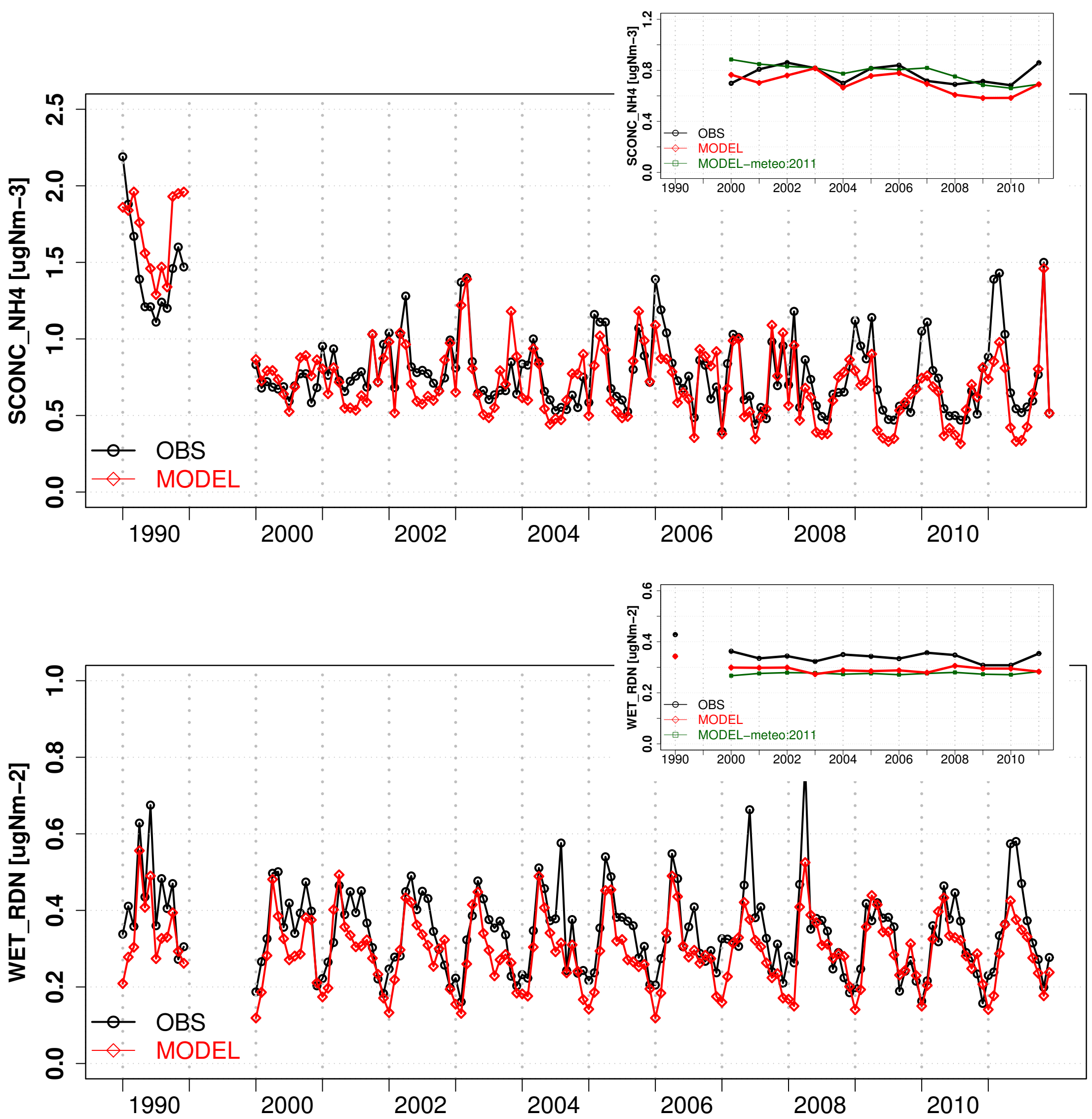

Figure 6.3: Trends of ammonium aerosol concentration (upper panel), and reduced nitrogen wet deposition (lower panel) observed at European background stations and simulated at these stations by the EMEP model for the period 1990-2011. Annual mean values are also shown for the model simulation using the same meteorology throughout (green line).

6.1.3 Discussion and perspective for EMEP trend work

The preliminary evaluation presented here, shows that there is considerable value in a joint exploration of gaseous precursors, aerosol components and deposition parameters. The trends, modelled and measured, are largely consistent showing the high quality of the joint EMEP programme. They confirm the lacking reduction of nitrogen emissions in Europe. This is of benefit both to the model development itself and to the better understanding of the temporal evolution of atmospheric pollution in the area of the LRTAP convention.

The trend evaluation is an interesting subject for future joint work in the framework of TFMM. Value would be added if other groups with experience in trend analysis could join. Also, the observational data from the EMEP network, which are of extraordinary value because of their long-term nature, require more attention. The usage of these data from different years requires extra attention because of changed instrumentation, protocols and personnel. Possibly, trends are also compared among multiple models.

Particular attention needs to be put on developing consistent observational data sets for the two recent decades, beginning in 1990. For diagnostic purposes, the model data could be used to identify extreme outlier data in the measurement time series. Inconsistency of instrumental records should be investigated for individual parameters, so that trends are not a result of changes in measurement method or quality. Also, measurement sites might have come under the influence of new local emission patterns. A final documentation of the data selection should be made through the EBAS database, so that subsequent work can make use of established, reproducible datasets. As these datasets might change again over time it would be good to attach version numbers to bundled datasets.

However, the small number of data retained for instance by Tørseth et al. (2012), who searched for consistent long-term trend data of high quality, shows that one will need to develop techniques to cope with a changing network structure. Gaseous ammonia and nitric acid are two examples, where the difficulty to measure the constituent led to a fluctuation of the data coverage, hampering trend analysis.

Model trends should be inspected with respect to such data selection. Reasonably sized subsets of the selected data should result in similar trends. Model bias trends evolving with time, or persistent seasonal bias should receive particular attention for a better understanding of trends and thus air quality policy achievements. Eventually also the reported emissions should be inspected for potential errors.

6.2 Atmospheric input of nitrogen to the Baltic Sea

6.2.1 Introduction

Nitrogen and phosphorus are the main nutrients which in high concentrations stimulate growth of algae which in turn leads to imbalanced functioning of the Baltic Sea system (HELCOM, 2009). The nitrogen input entering the Baltic Sea is both airborne and waterborne, whereas phosphorus input is mostly waterborne and only 1-4% is coming from the atmosphere (HELCOM 2009, 2011). Atmospheric deposition of nitrogen accounts typically for one quarter to one third of the total nitrogen load to the Baltic Sea (HELCOM, 2005).

The Helsinki Commission (HELCOM) was established to protect the marine environment of the Baltic Sea from all sources of pollution. This should be achieved through intergovernmental co-operation of the countries around the Baltic Sea: Denmark, Estonia, Finland, Germany, Latvia, Lithuania, Poland, Russia, Sweden and the European Union, in addition. Eutrophication of the Baltic Sea and its negative effects are the most important problem for HELCOM at present. The protection of the Baltic Sea from eutrophication is an important part of the Baltic Sea Action Plan and activities of MONAS and LOAD groups. Another important environmental problem for HELCOM is the pollution of the Baltic Sea by heavy metals and persistent organic pollutants.

EMEP has been conducting the work on air monitoring, modelling and compilation of emission inventories of all these pollutants for more than 30 years. Following the agreement between HELCOM and EMEP, three EMEP Centres (MSC-W, MSC-E and CCC) have been responsible for regular evaluation of the state of the atmosphere in the Baltic Sea region and have produced the annual joint summary reports with updated emissions of nitrogen compounds, heavy metals and POPs, modelled deposition fields, allocation budgets and measurement data since 1997. The first joint report of the three EMEP Centres with project results was published in 1997 Tarrasón et al. (1997), followed by 15 yearly reports, with the last one in 2012 (Bartnicki et al. 2012). This joint project with HELCOM, is performed by the three EMEP Centres as a long-term on-going project. It will be continued until 2018 and probably longer, according to the present agreement. The tasks of EMEP in this project are the following:

1. To compile and analyse measurements of selected pollutants at the HELCOM stations on annual and monthly basis.

2. To compute annual and monthly depositions of nitrogen compounds, HMs and POPs to the Baltic Sea and its sub-basins, based on latest available emission data.

3. To compute annual source-receptor matrices, with sub-basins of the Baltic Sea as receptors, for selected pollutants every year.

4. To prepare the joint summary report and specific indicator reports.

MSC-W of EMEP is responsible for coordination of the EMEP contribution to HELCOM and editing the joint summary report. A large part of the EMEP work for HELCOM, concerning nitrogen deposition in the period 1995-2006 was described in Bartnicki et al. (2011).

The assessment of nitrogen deposition and its trend to the Baltic Sea is especially important for HELCOM and therefore, some examples of the EMEP MSC-W model results concerning nitrogen deposition and source-receptor matrices will be presented here.

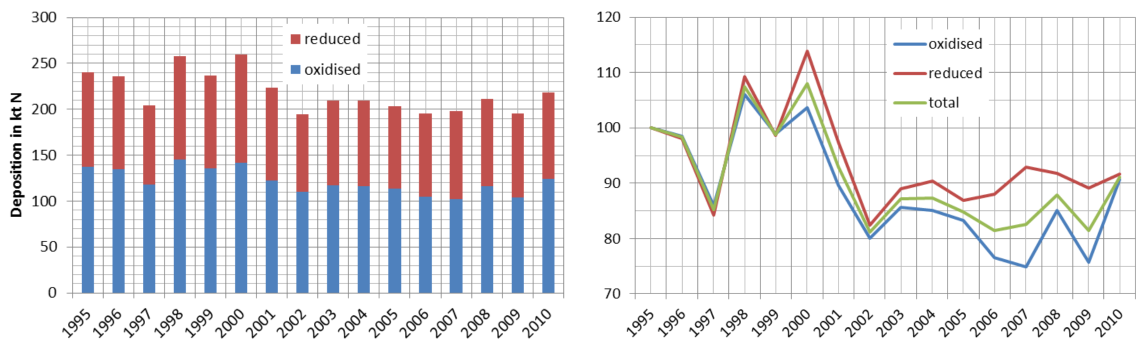

Figure 6.4: Left: Annual depositions to the Baltic Sea of oxidised, reduced and total (oxidised+reduced) nitrogen. Unit: kt N/year. Right: The relative annual depositions of the same components, in percent of their 1995 value.

6.2.2 Annual deposition of nitrogen

Time series of annual oxidised, reduced and total nitrogen deposition to the entire Baltic Sea basin, for the period 1995-2010 are shown in Figure 6.4, together with the relative annual depositions of the same components.

From this, no significant trends can be determined for atmospheric nitrogen loads entering the Baltic Sea in the considered period, however, annual depositions of all nitrogen compounds are approximately 10% lower in 2010 than in 1995. Maximum annual deposition of oxidised nitrogen (145 kt N) and reduced nitrogen (112 kt N) to the Baltic Sea takes place in the years 1998 and 2000, respectively. Minimum annual depositions can be noticed in the years 2007 and 2002 for oxidised nitrogen (103 kt N) and reduced nitrogen (85 kt N), respectively. Annual deposition of oxidised, reduced and total nitrogen in 2010 was respectively 9%, 8% and 9% lower than in 1995.

Calculated annual total nitrogen depositions to the six sub-basins of the Baltic Sea in the period 1995-2010 are presented in Figure 6.5. There is also no significant trend in nitrogen depositions to sub-basins of the Baltic Sea in 1995-2010, however annual depositions of oxidised and reduced nitrogen are lower in 2010 than in 1995 in all sub-basins and in the entire Baltic Sea basin.

Compared to 2009 deposition of oxidised nitrogen in 2010 is higher in all sub-basins (2-26%) and deposition of reduced nitrogen is higher in four out of six sub-basins (3-28%). Deposition of reduced and total nitrogen is lower in 2010, compared to 2009, in the sub-basins: BES and KAT, in the southwest of the Baltic Sea.

6.2.3 Source allocation budgets

Identification of main sources contribution to nitrogen deposition is also very important for HELCOM. As an example, the top twenty contributors to oxidised nitrogen deposition to the Baltic Sea are shown in Figure 6.6. Germany, Poland and ship traffic on the Baltic Sea are the three main contributors, accounting together for almost 40% of oxidised nitrogen deposition to the Baltic Sea. There is also a significant contribution of distant sources like for example, ship traffic on the North Sea and United Kingdom, being number five and six, respectively, in the contribution ranking.

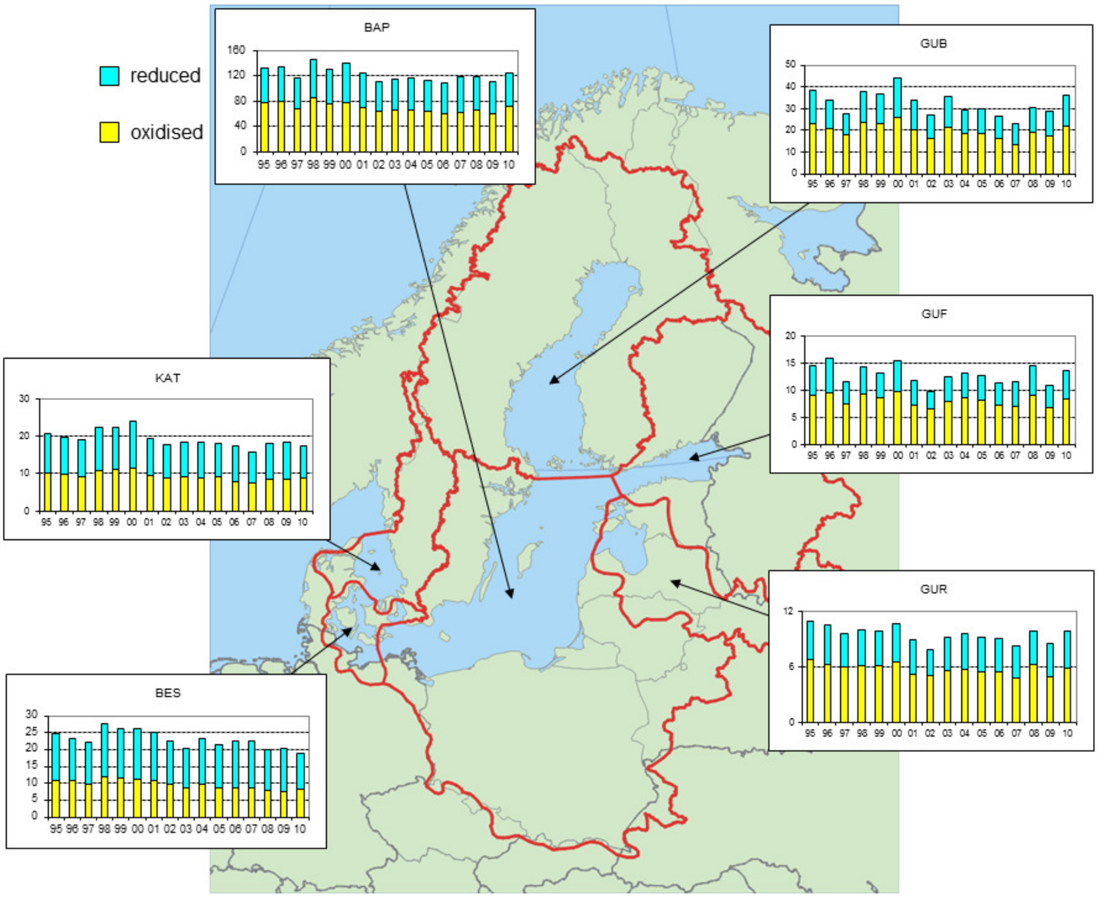

Figure 6.5: Annual atmospheric deposition of oxidised, reduced and total nitrogen to six sub-basins of the Baltic Sea for the period 1995-2010. Units: ktonnes N/year. Note: the scales for the sea regions are different!

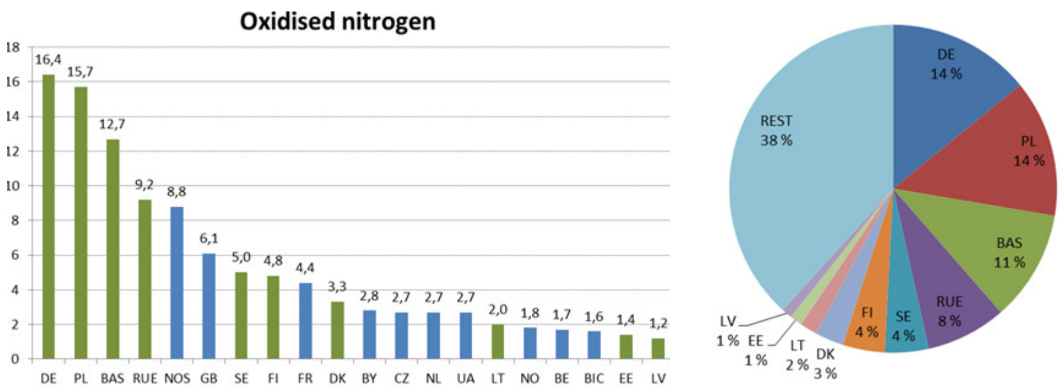

Figure 6.6: Left: Top twenty sources with highest contributions to annual deposition of oxidized nitrogen into the Baltic Sea basin in the year 2010. Unit: kt N/year. (BAS and NOS denote ship emissions from the Baltic Sea and from the North Sea, respectively. RUE denotes the contributions from emissions in the extended Russian territory.) Contributions from HELCOM countries and the Baltic Sea ship traffic are marked green. Right: Relative contributions to the Baltic Sea from HELCOM Contracting Parties, ship traffic and rest of source countries (REST), in percent of total oxidized nitrogen deposition.

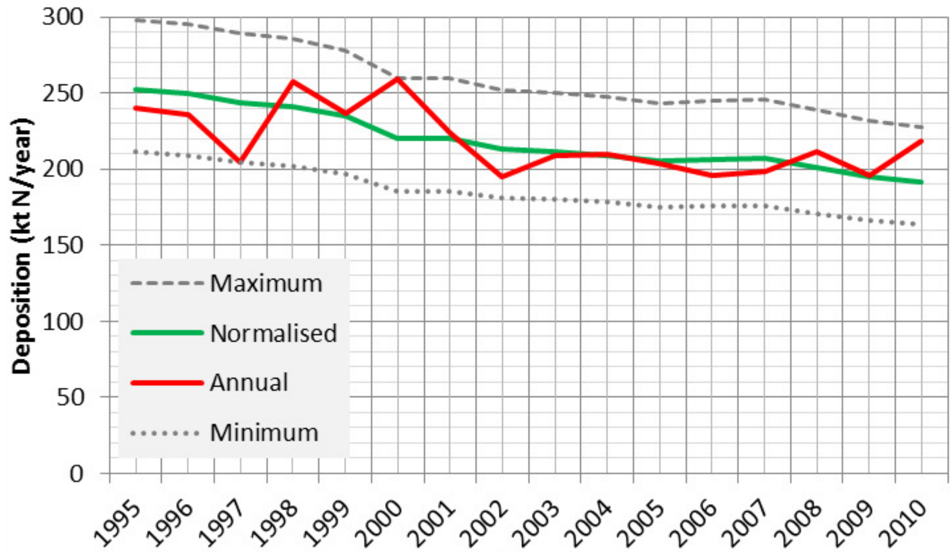

Figure 6.7: Normalised annual depositions of total (oxidized+reduced) nitrogen to the Baltic Sea in the period 1995-2010. The actual annual depositions, as well as minimum and maximum depositions are also shown. Unit: kt N/year.

6.2.4 Normalised depositions

The actual annual nitrogen depositions to the Baltic Sea basin are strongly influenced by the variable meteorological conditions. There are years when annual nitrogen emissions in the HELCOM Contracting Parties and in the entire EMEP domain has been reduced, but nitrogen deposition to the Baltic Sea increased anyway. In case of riverine input to the Baltic Sea, the influence of variable meteorology is limited by using the so called normalised flow and input. On the request from HELCOM, a similar approach was developed for atmospheric deposition. In this approach, all EMEP reported source receptor matrices are used multiple times for all years of the considered period. For any year of interest, emissions from this year are multiplied by every available source receptor matrix and 15 different depositions are calculated representing 15 meteorological years. A median value from these depositions is computed and defined as normalised deposition. The results for total (oxidised+reduced) nitrogen depositions are shown in Figure 6.7. In addition, the minimum and maximum potential depositions for each year are shown, representing the best and the worst meteorological conditions. The actual annual values, calculated with the real meteorological conditions of a given year, are oscillating between minimum and maximum values.

It should be stressed here that normalised depositions as well as the min/max depositions are not replacing the actual depositions, but that they are a part of an important additional information for decision makers.

The range between minimum and maximum potential deposition implies that meteorology may lead to $\pm$ 20 % variation in nitrogen depositions to the Baltic Sea.

During the MONAS meeting in Tallin in March 2013, HELCOM decided that both normalised depositions and normalised contributions to sub-basins should be routinely calculated every year as a part of the EMEP contribution.

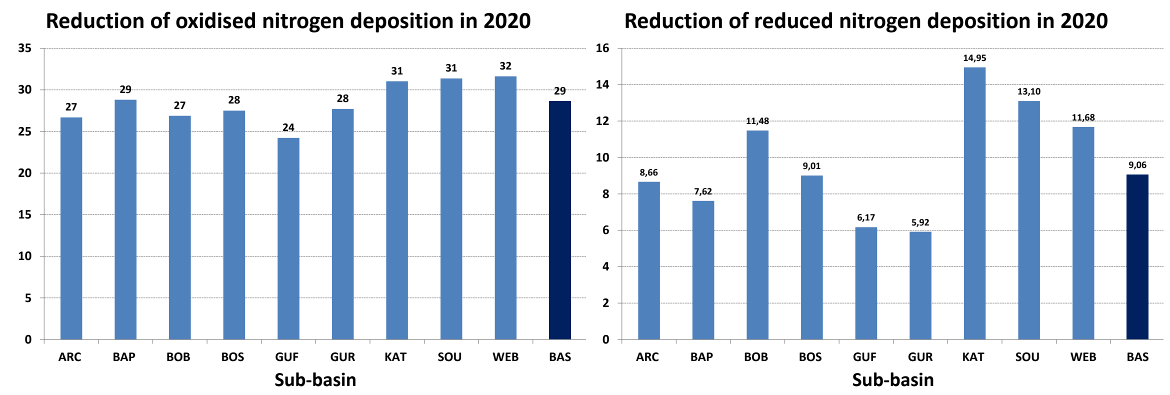

Figure 6.8: The reduction effects of revised Gothenburg Protocol emissions on oxidized and reduced nitrogen deposition to the Baltic Sea and its sub-basins in 2020. Here two sub-basins BES and GUB, from Fig 6.5, are further divided: BES=SOU+WEB and GUB=BOS+BOB+ARC. Reduction is expressed in percent of 2005 normalised annual deposition.

6.2.5 Effects of Gothenburg Protocol

Estimation of the effect of revised Gothenburg Protocol on nitrogen deposition to the Baltic Sea and its sub-basins was performed in the frame of additional project for HELCOM in 2013. All source receptor matrices for the Baltic Sea were used again in combination with expected 2020 emissions. An example of the results is presented in Figure 6.8. The reductions of the oxidised nitrogen deposition is relatively uniform among sub-basins and similar for the entire Baltic Sea basin, oscillating around 20%. For reduced nitrogen depositions, the reductions vary more among sub-basing being significantly lower, of the order of 10%. The reduction of total (oxidised+reduced) nitrogen deposition is around 20%.

6.3 NO_2 tropospheric column trends

One of the most prominent atmospheric pollutants is Nitrogen Dioxide (NO_2). It is emitted mostly by transportation, power plants, and industry. While NO_2 concentrations can be monitored quite well using ground-based air quality stations, such observations are only representative of the immediate station surroundings and are generally not available in many parts of the world. In contrast, satellite observations of atmospheric composition offer an unprecedented perspective and allow for spatially continuous mapping at regional, continental, and global scales. The SCIAMACHY (SCanning Imaging Absorption spectroMeter for Atmospheric CartograpHY) instrument onboard of the Envisat satellite platform has provided relatively high-resolution NO_2 data since 2002 (Gottwald et al. 2006). Previous studies have investigated tropospheric NO_2 trends from satellite data (Richter et al. 2005, van der A et al. 2006, 2008), however they primarily used data from the Global Ozone Monitoring Experiment (GOME) or a combination of this data with other sensors and thus were limited to the GOME relatively coarse spatial resolution of 320×40 km^2. In this study we report results from a recent global trend analysis of SCIAMACHY NO_2 data between August 2002 and March 2012 (Schneider and van der A 2012). As the trend analysis is limited to the data from this relatively high-resolution sensor, it was possible to be carried out at a previously unavailable spatial resolution of 0.25×0.25 degrees (roughly 30×30 km^2). The satellite-based trends are furthermore compared with corresponding trends in tropospheric NO_2 column derived from the EMEP MSC-W chemical transport model. The model results was sampled to most closely resemble the observations from the satellite instrument.

6.3.1 Data and Methodology

The satellite data used for this study was collected by the SCIAMACHY sensor onboard of the Envisat satellite. SCIAMACHY is a hyperspectral passive imaging grating spectrometer operating in the wavelength range of 214-2386 nm and has been providing data between 2002 and 2012. Datasets of monthly average tropospheric NO_2 column were acquired from the Tropospheric Emission Monitoring Internet Service (TEMIS) between August 2002 and March 2012. The retrieval algorithm is described in detail by (Boersma et al. 2004). Version 2.3 of the retrieval algorithm was used consistently for the entire data record.

For purposes of trend comparisons, the study also made use of model data on tropospheric NO_2 column, which were obtained from the EMEP MSC-W model version rv4.4. Model runs were performed with consistent ECMWF-IFS meteorology of the respective year and emissions for 2000-2010 derived from the 2012 official data submissions to UNECE CLRTAP as of June 2012 (Mareckova et al. 2012), whereas emissions for 2011 have been derived from the 2013 official data submissions to UNECE CLRTAP as of June 2013 (Mareckova et al. 2013).

A consistent EMEP MSC-W model run spanning the period from January 2000 to December 2011 was available. Monthly means were computed from the hourly model output using only the 10:00 UTC values in order to make the trend comparable to those obtained during the SCIAMACHY overpass time. Trends were computed for both the model data as well as the satellite data for the overlap period of August 2002 to December 2011.

In order to compute trends from the two datasets, a statistical model based on an trend analysis overview paper (Weatherhead et al. 1998) and later applied by other authors (van der A et al. 2006, 2008, Schneider and van der A 2012) was fitted to the 2002-2011 time series with monthly samples at each grid cell. The monthly average tropospheric NO_2 column at time t (in months) is thereby modelled as

$$C_t = \mu + \sum_{j=1}^{4}[\beta_{1,j}\sin(\tfrac{2\pi jt}{12}) + \beta_{2,j}\cos(\tfrac{2\pi jt}{12})] + \tfrac{1}{12}\omega t + R_t$$

where μ is a constant, ω is a linear trend, and R_t is the residual variability. The sum term represents the seasonal component, where $\beta_{1,1}$ through $\beta_{2,4}$ are coefficients of the fit. Figure 6.9 shows an example of the SCIAMACHY-derived time series over Eastern China and the fitted statistical model. The linear trend component of the model (not shown in the Figure 6.9) was then mapped on a global scale (Schneider and van der A 2012). The uncertainty of the trend σ_ω was computed as

$$\sigma_\omega = [\tfrac{\sigma_r}{n^{\frac{3}{2}}}\sqrt{\tfrac{1+\phi}{1-\phi}}]$$

where σ_r is the standard deviation of the de-trended residuals, n is the number of years with available data, and ϕ is the first-order autocorrelation. A trend ω is considered to be significant with a 95% confidence when $|\omega/\sigma_\omega| > t_\omega$ where t_ω is the value of the Student's t-distribution for a significance level of $\alpha = 0.05$ and the degrees of freedom given for the time series (Santer et al. 2000).

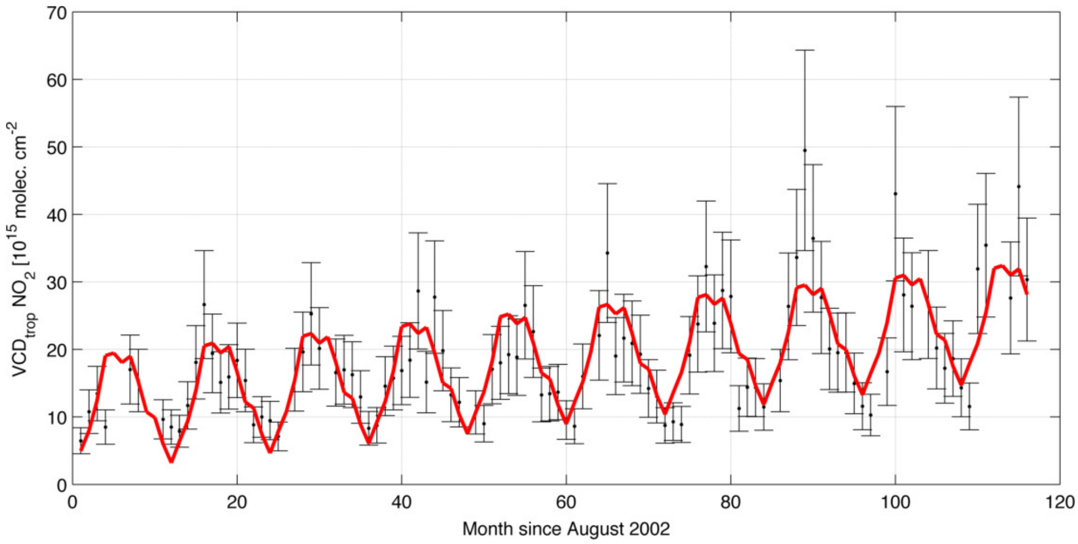

Figure 6.9: Typical time series of monthly SCIAMACHY tropospheric NO_2 data (black markers) over Eastern China and the fitted statistical model (red line) from which the linear trend was computed. The error bars for the monthly averages indicate an error of 30%.

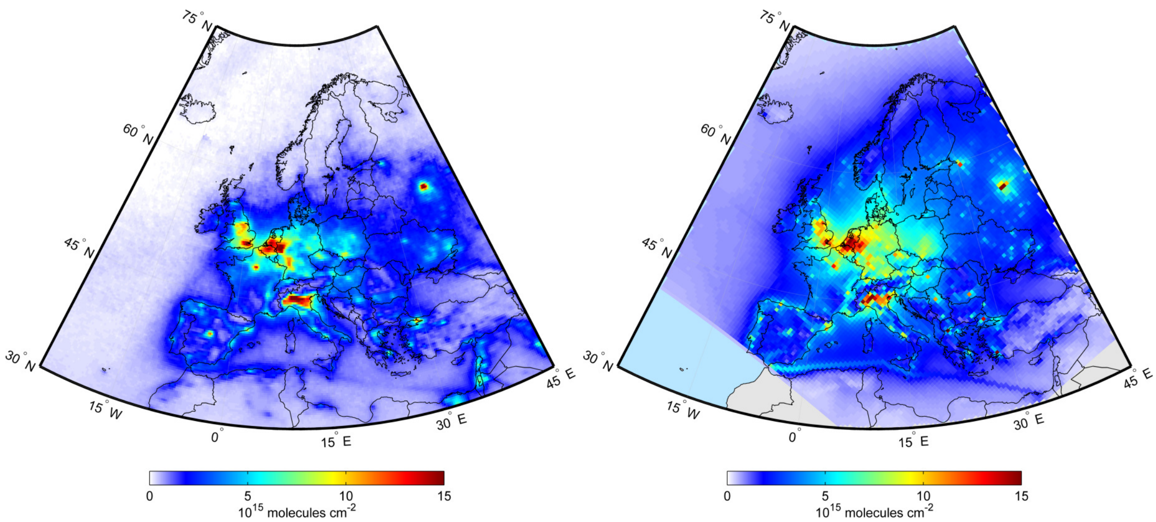

Figure 6.10: Comparison of the 2002-2011 average tropospheric NO_2 column from SCIAMACHY (left) and EMEP (right).

Figure 6.10 shows a comparison of the mean (August 2002 to December 2011) tropospheric NO_2 column as derived from SCIAMACHY data and the EMEP MSC-W model (sampled at 10:00 UTC). The primary spatial patterns such as the areas of very high concentrations over the Netherlands, and the Po valley area of Northern Italy can be clearly seen in both datasets. Many other minor features are also visible in both datasets, including main shipping lines in the Mediterranean. It can also be observed, however, that the average levels given by the model for central Europe (e.g. Germany and Poland) tend to be slightly higher than those observed by SCIAMACHY.

Figure 6.11 shows the difference map. Compared to the SCIAMACHY dataset, the EMEP MSC-W model output shows a fairly consistent bias of approximately 1-2 $10^{15} molecules/cm^2$ throughout most of Europe. In a few areas of very high pollution levels, such as in the Po

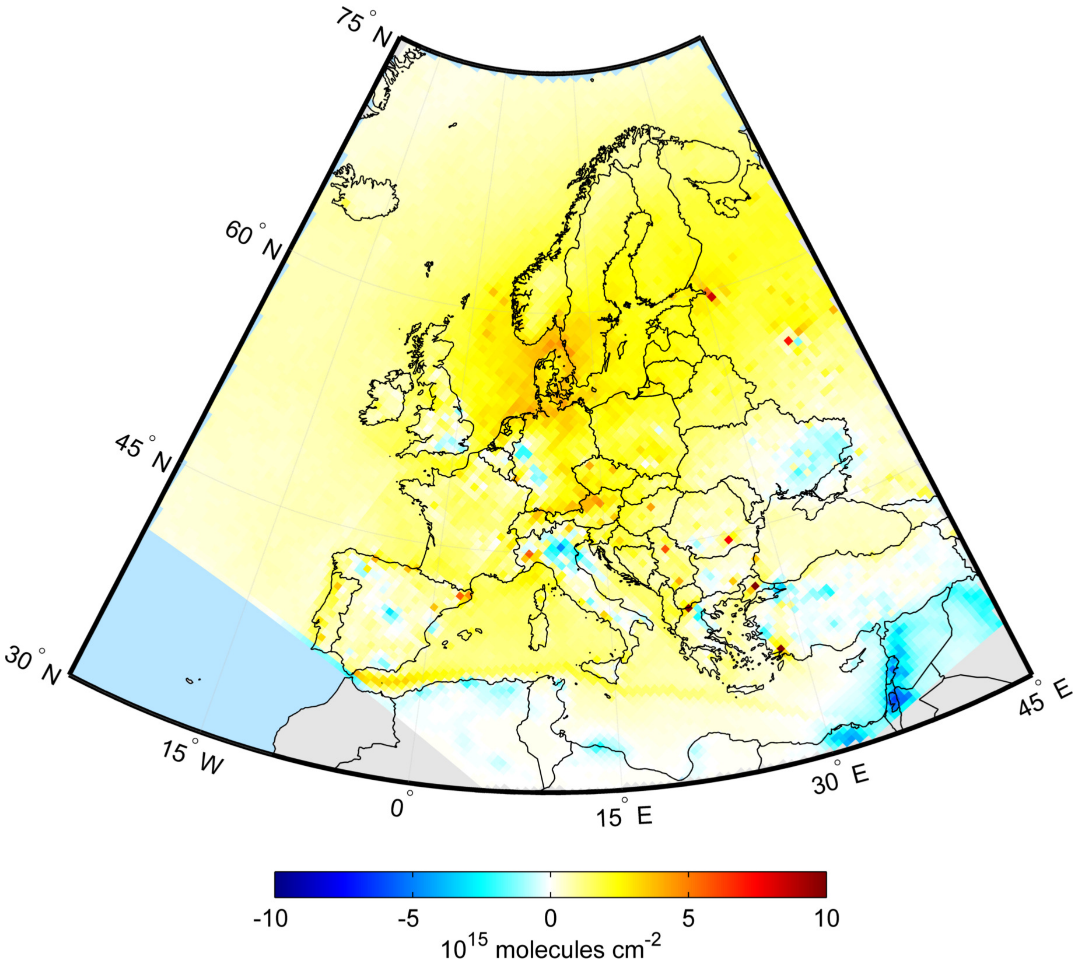

Figure 6.11: Difference image of the two maps shown in Figure 6.10. Note that this map is produced by resampling the SCIAMACHY dataset to the coarser resolution grid of EMEP. The difference was computed as EMEP - SCIAMACHY.

Valley region, the Rhein/Ruhr area of Germany, but for example also in some large urban areas such as London or Madrid, the model underestimates the tropospheric NO_2 columns compared to SCIAMACHY. This is also true in eastern Ukraine and parts of Turkey. In the Israel/Lebanon area no actual emissions are used.

Figure 6.12 shows the absolute trend values for both SCIAMACHY and EMEP MSC-W model, given for the available overlap period between the two datasets of August 2002 to December 2011. Overall the spatial patterns in trends match very well. The large areas of decreasing trends in most of western and central Europe are clearly visible in both datasets. In particular the major hotspots in the Netherlands and southern England show large reductions. Significant reductions are also found in the northwest of Spain, a pattern which has been recently explained by strong reductions of NO_x emissions at several power plants in the area (Schneider and van der A 2012). Slightly increasing NO_2 concentrations can be observed in many areas throughout eastern Europe. Overall, the EMEP trend map appear slightly more spatially consistent and less noisy than the SCIAMACHY trend map. Figure 6.12 shows the same trends as Figure 6.13, however it only displays grid cells for which the trends were statistically significant at the 95% level. The grid cells with significant trends can be mostly found over the most polluted regions in central and western Europe. The EMEP trend map ap-

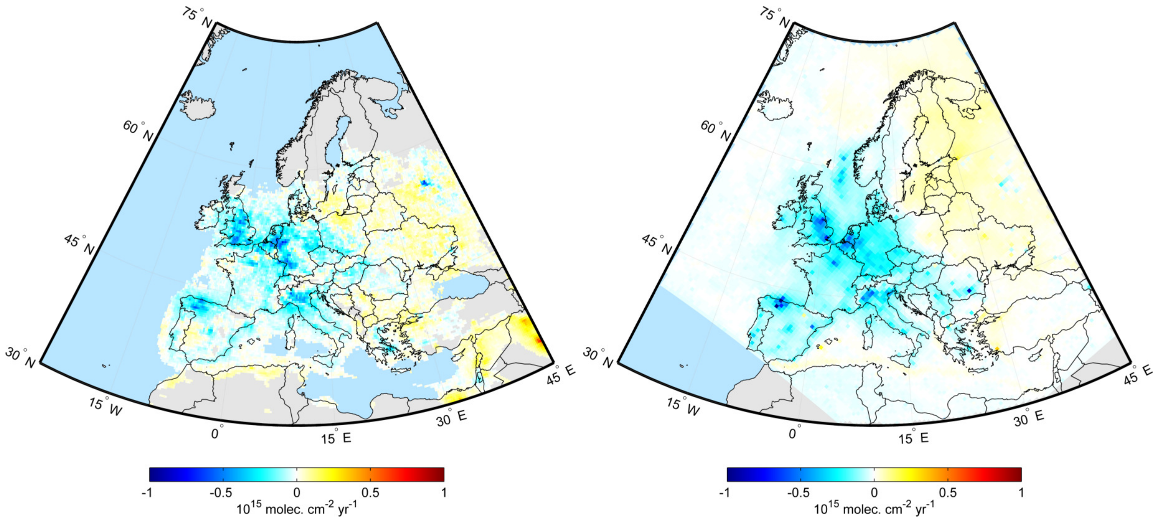

Figure 6.12: Comparison of the absolute change in tropospheric NO_2 column between August 2002 and December 2011 as computed from SCIAMACHY data (left) and EMEP MSC-W model output (right). Note that all grid cells are shown here, independent of the statistical significance of the derived trend. For the SCIAMACHY dataset trends were only computed for grid cells with a long-term average tropospheric NO2 column of greater than $1 \times 10^{15} molecules/cm^2$.

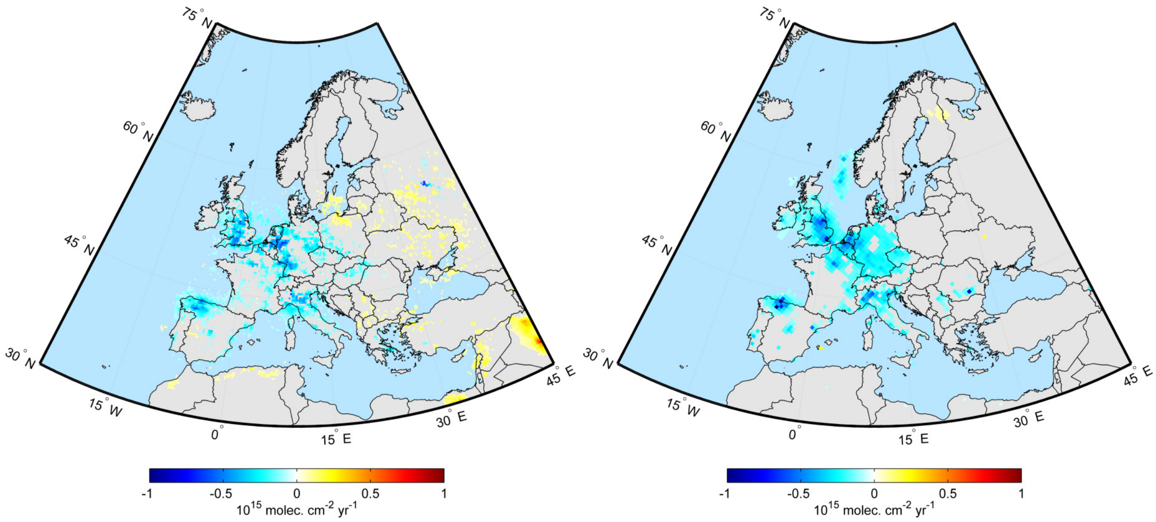

Figure 6.13: As Figure 6.12 but only showing grid cells for which the trend was found to be statistically significant at the 95% level.

pears slightly more homogeneous and thus has larger spatially contiguous areas of significant NO_2 decrease. While the SCIAMACHY dataset indicates some increasing trends in eastern Europe (albeit mostly with a scattered spatial appearance), the EMEP model does not indicate significantly increasing trends in eastern Europe except in one small area at the Finland/Russia border, which is unfortunately not covered by the SCIAMACHY dataset due to the exclusions of very low polluted areas.

In addition to trends in absolute levels of tropospheric columns, relative trends in % per year were also computed in order to better indicate comparatively rapid changes even in areas of low overall emissions. This has recently proven very valuable for example in China where some very remote regions were found to exhibit increases of 20-30 % per year

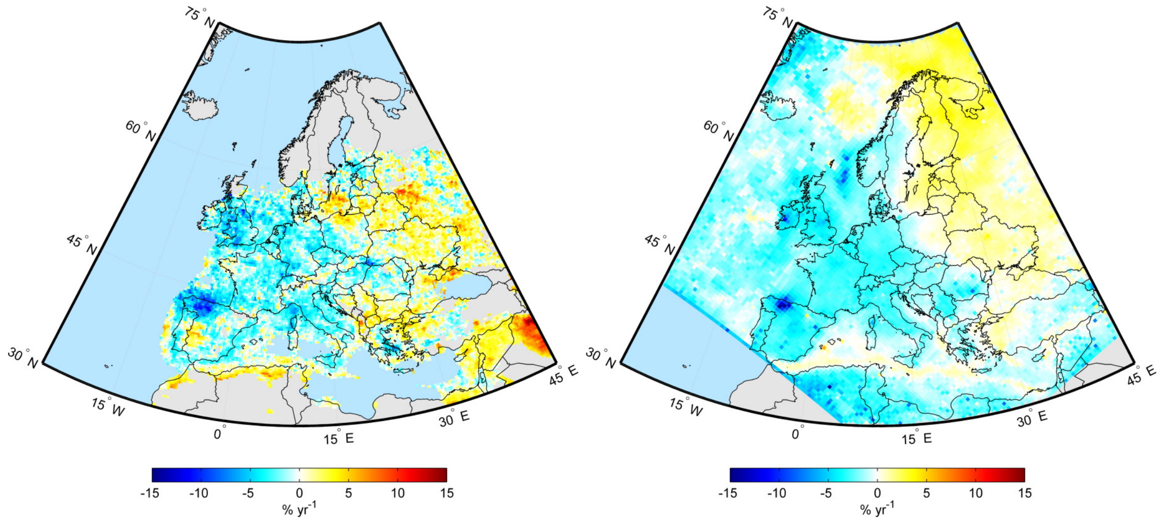

Figure 6.14: Comparison of the relative change in tropospheric NO_2 column between August 2002 and December 2011 as computed from SCIAMACHY data (left) and EMEP model output (right). Note that all grid cells are shown here, independent of the statistical significance of the derived trend. For the SCIAMACHY dataset trends were only computed for grid cells with a long-term average tropospheric NO2 column of greater than $1 \times 10^{15} molecules cm^2$

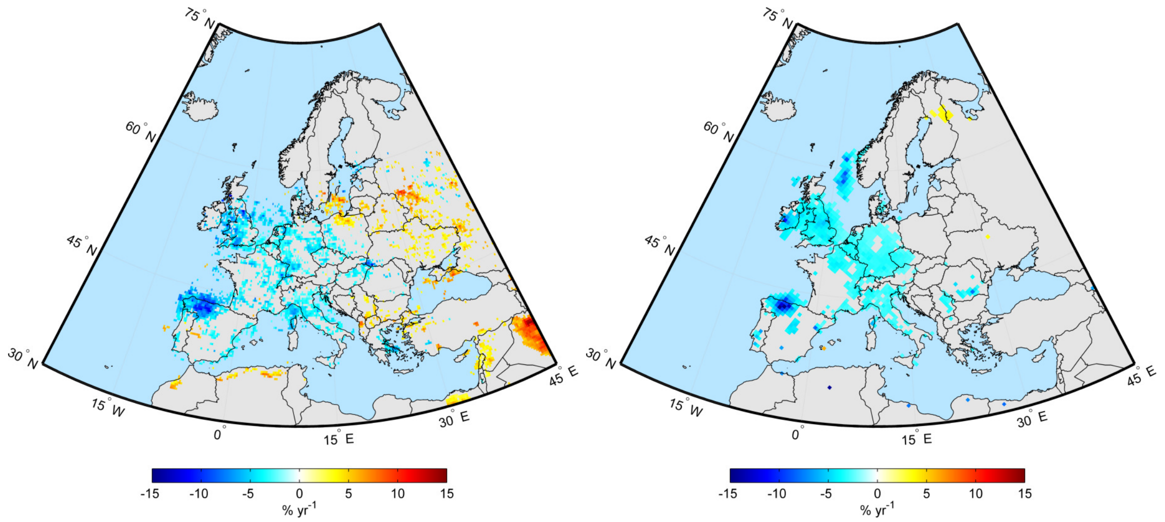

Figure 6.15: As Figure 6.14 but only showing grid cells for which the trend was found to be statistically significant at the 95% level.

(Schneider and van der A 2012). In Europe, the differences between relative and absolute trends are not quite as drastic. Figure 6.14 and Figure 6.15 show all trends and only the significant ones, respectively. Again, as for the absolute trend maps, it can be seen in the relative trend maps that in contrast to the relatively smooth and homogeneous spatial patterns exhibited by the EMEP model, the relative trends derived from the SCIAMACHY dataset appears much more scattered and noisy. This is likely due to cloud cover effects and other algorithm issues such as calculating the correct air mass factor, which influence the accuracy of the NO_2 tropospheric column dataset. Nonetheless, even quantitatively the trend maps from both data sources show comparable values such as an overall decrease of NO_2 concentration of approximately -4 % per year over large areas of central and western Europe.

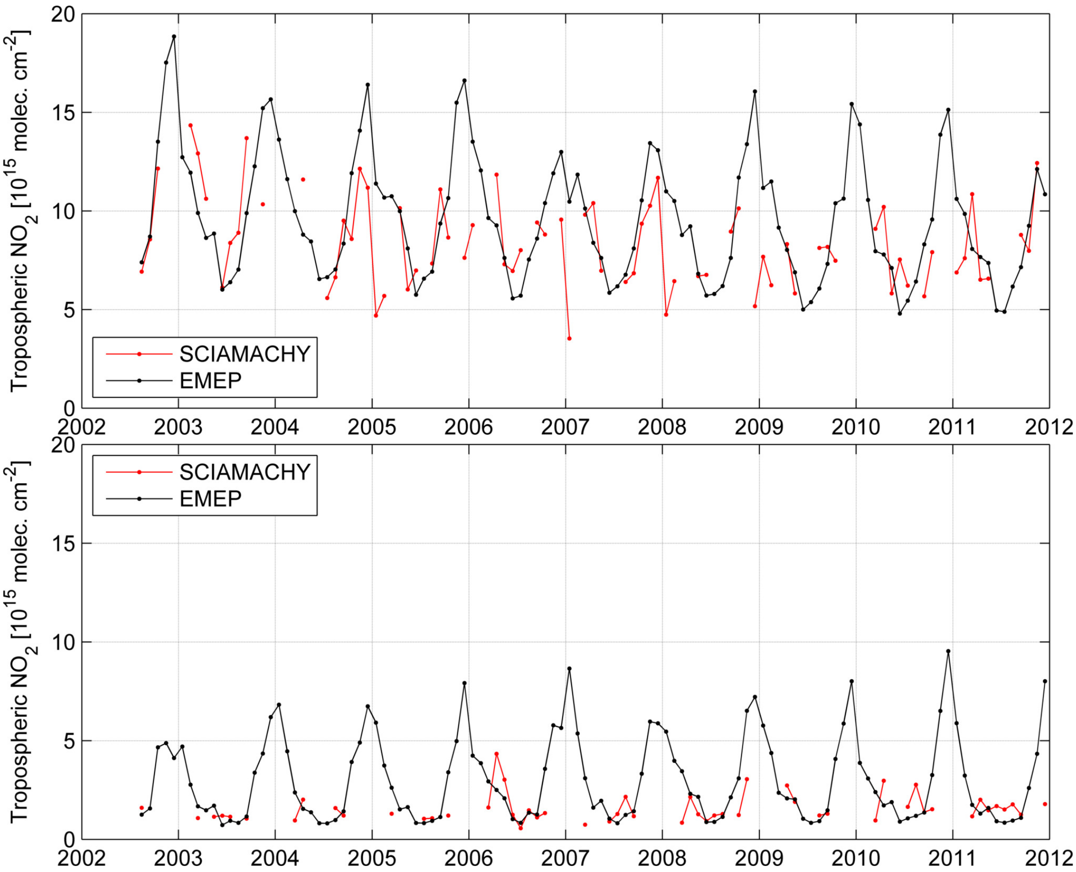

Figure 6.16: Time series in EMEP model and retrieved from SCIAMACHY in two representative areas of ca 500 km^2 of Western Europe, centered in Rhein-Ruhr (upper panel) and Eastern Europe, centered near Smolensk (lower panel).

Example time series of monthly mean tropospheric NO2 were extracted from both datasets for representative regions in western and in eastern Europe (Figure 6.16). While the model shows a continuous signal, the satellite-based time series has some gaps due to the low number of retrievals which prohibited the calculation of a monthly mean. Overall however, the time series from both datasets in western Europe are fairly similar in magnitude, although the satellite means tend to undererstimate the winter peaks as compared to the model output. The number of valid data points for the satellite datasets in eastern Europe is significantly reduced overall. This is particular obvious during the winter months, where persistent cloud cover does not allow the calculation of valid monthly means.

6.3.2 Conclusions

A comparison was carried out between SCIAMACHY NO_2 satellite data and NO_2 column output from the EMEP model in order to test the datasets' respective capabilities for estimating decadal trends in tropospheric NO_2 column over Europe. Following the methodology previously described in Schneider and van der A (2012), statistical models including a seasonal component and a linear trend were fitted to time series of monthly tropospheric NO_2 column data from the SCIAMACHY instrument as well as model output from the EMEP chemical transport model. The resulting trends were then mapped at the European scale. In order to make the two data sources as comparable as possible, the monthly averages for the

EMEP MSC-W model were computed over the 10:00 UTC values only, which is consistent with the local overpass time of the SCIAMACHY instrument. Doing so eliminates sampling issues due to the significant diurnal cycle exhibited by NO_2. Furthermore, the trends were computed only over the mutual overlap period between both datasets, namely August 2002 to December 2011.

In a first comparison, the long-term average tropospheric NO_2 column map from both data sources were computed. The EMEP model shows a relatively consistent positive bias of approximately 1-2 $10^{15} molecules/cm^2$ throughout most of Europe as compared against the SCIAMACHY NO_2 columns. Only in some of the most polluted areas the long-term averages from SCIAMACHY are slightly higher than the corresponding EMEP values.

Subsequently, various trend maps were produced from both data sources, both in absolute as well as relative terms. The results indicate that the main spatial patterns in trends are replicated quite consistently from both data sources, with regard to both negative as well as positive changes. All the major patterns of continuously decreasing NO_2 concentrations in the most polluted regions in Europe such as the Benelux states, the Rhein-Ruhr area in Germany and southern England are all visible. Strong decreases over northwestern Spain which are due to significant NO_x reductions at several power plants in the area are also well replicated by the model.

The largest differences can be seen in terms of the statistical significance of the trends where the EMEP model trend map shows a much smaller number of grid cells with significantly increasing trends in eastern Europe. On the other hand, the areas of significantly decreasing NO_2 concentrations of around -4 % per year in most of central and western Europe have a more homogeneous and spatially contiguous structure in the EMEP-based trend map than in the SCIAMACHY trend map.

Overall it is promising to see that two completely independent sources of information on tropospheric NO_2 data provide such similar results. While some small differences in terms of absolute concentrations were found between the satellite data and the model, these are likely consistent through time and thus do not have a significant impact on the resulting trend estimates. Mainly looking at the spatial patterns in trends at the European scale it can be concluded that both the SCIAMACHY NO_2 column dataset and the NO_2 data from the EMEP MSC-W model provide quite similar trend estimates, particularly given the associated trend uncertainties.

References

Bartnicki, J., Semeena, V. S., and Fagerli, H.: Atmospheric deposition of nitrogen to the Baltic Sea in the period 1995-2006, Atmos. Chem. Physics, 11, 10 057–10 069, doi:10.5194/acp-11-10057-2011, URL http://www.atmos-chem-phys.net/11/10057/2011/, 2011.

Bartnicki, J., Gusev, A., Aas, W., and Valiaveetil, S.: Atmospheric supply of nitrogen, lead, cadmium, mercury and dioxines/furanes to the Baltic Sea in 2010.EMEP Centres joint report for HELCOM., Eemep/msc-w technical report 2/2012, The Norwegian Meteorological Institute, Oslo, Norway, 2012.

Boersma, K., Eskes, H., and Brinksma, E.: Error analysis for tropospheric No_2 retrieval from space, J. Geophys. Res., 109, 1984–2012, 2004.

Gottwald, M., Bovensmann, H., Lichtenberg, G., Noël, S., von Bargen, A., Slijkhuis, S., Piters, A., Hoogeveen, R., von Savigny, C., Buchwitz, M., Kokhanovsky, A., Richter, A., Rozanov, A., Holzer-Popp, T., Bramstedt, K., Lambert, J.-C., Skupin, J., Wittrock, F., Schrijver, H., and Burrows, J.: SCIAMACHY - Monitoring the Changing Earths Atmosphere, DLR, Institute fuer Methodik der Fernerkundung (IMF), 2006.

Mareckova, K., Wankmüller, R., Whiting, R., and Pinterits, M.: Inventory Review 2012 stage 1 and 2 and review of gridded data, EMEP/CEIP Technical Report 1/2012, EEA/CEIP Vienna, 2012.

Mareckova, K., Wankmüller, R., Pinterits, M., and Moosman, L.: Inventory review 2013 stage 1 and 2 and review of gridded data, EMEP/CEIP Technical Report 1/2013, EEA/CEIP Vienna, 2013.

Richter, A., Burrows, J. P., Nüß, H., Granier, C., and Niemeier, U.: Increase in Tropospheric Nitrogen Dioxide Over China Observed from Space, Nature, 437, 129132, doi:10.1038/nature04092, 2005.

Santer, B., Wigley, T., J.Boyle, Gaffen, D., Hnilo, J., Nychka, D., Parker, D., and Taylor, K.: Statistical significance of trends and trend differences in layer-average atmospheric temperature time series, J. Geophys. Res., 105, 7337 – 7356, 2000.

Schneider, P. and van der A, R. J.: A global single-sensor analysis of 20022011 tropospheric nitrogen dioxide trends observed from space, J. Geophys. Res., 117, doi:10.1029/2012JD017571, 2012.

Tarrasón, L., Barrett, K., Erdman, L., and Gusev, A.: Atmospheric supply of nitrogen, lead and cadmium to the Baltic Sea., EMEP Summary Medellin Report for 1991-1995 for HELSINKI COMMISION Research report no.58, The Norwegian Meteorological Institute, Oslo, Norway, 1997.

Tørseth, K., Aas, W., Breivik, K., Fjæraa, A. M., Fiebig, M., Hjellbrekke, A. G., Lund Myhre, C., Solberg, S., and Yttri, K. E.: Introduction to the European Monitoring and Evaluation Programme (EMEP) and observed atmospheric composition change during 1972–2009, Atmospheric Chemistry and Physics, 12, 5447–5481, doi:10.5194/acp-12-5447-2012, URL http://www.atmos-chem-phys.net/12/5447/2012/, 2012.

van der A, R. J., Eskes, H. J., Boersma, K. F., van Noije, T. P., Roozendael, M. V., Smedt, I. D., Peters, D. H. M. U., and Meijer, E. W.: Trends, seasonal variability and dominant NO_x source derived from a ten year record of NO_2 measured from space, Journal of Geophysical Research, 113, D04 302, doi:oi:10.1029/2007JD009021, 2008.

van der A, R. J. M., Peters, D. H. M. U., Eskes, H., Boersma, K. F., M., V. R., De Smedt, I., and Kelder, H. M.: Detection of the trend and seasonal variation in tropospheric NO_2 over China, J. Geophys. Res., 111, D12 317, doi:10.1029/2005JD006594, 2006.

Weatherhead, E. C., Reinsel, G. C., Tiao, G. C., Meng, X.-L., Choi, D., Cheang, W.-K., Keller, T., DeLuisi, J., Wuebbles, D. J., Kerr, J. B., Miller, A. J., Oltmans, S. J., and Frederick, J. E.: Factors affecting the detection of trends: Statistical considerations and applications to environmental data, J. Geophys. Res., 103, 17 149 – 17 161, 1998.

CHAPTER 7

Global to regional model calculations

Jan Eiof Jonson, Valiyaveetil Shamsudheen Semeena and Michael Schulz

7.1 Introduction

The work presented here is ongoing, and may be seen as preliminary as test runs for the new set of global (and regional) source receptor runs to be made within the framework of the Task Force of Hemispheric Transport of Air Pollutants (TF HTAP) `http://www.htap.org/` later this year when the emission data for this project become available. With new sets of emissions the model runs will be repeated with calculations for more years. Additional sensitivity studies and source receptor calculations for more regions will also be performed. The emissions used in the global model calculations are from the ECLIPSE project (Evaluating the Climate and air quality Impacts of Short-lived pollutants). The ECLIPSE project aims to develop and assess effective emission abatement strategies for short-lived climate agents, see: `http://eclipse.nilu.no`.

The EMEP MSC-W model has been used, and will be used, in the future, for nesting global and regional model calculations, as was described in (Jonson et al. 2012). In that report it was shown that the regional model results were not very sensitive to the temporal frequency of the update at the lateral boundaries, and that monthly averaged lateral boundary concentrations would be sufficient. In order to comply with the requirements set by TF HTAP we have used here 3 hourly temporal resolution.

Furthermore, here we have also included model calculations comparing the effects on air pollution with future emission scenarios that are not planned for TF HTAP. The global model calculations have been made with a 1×1 degree model resolutions with emissions for 2010 and 2030 emission scenario from ECLIPSE. A set of regional model calculations have been made with nesting of the global model results. The regional model calculations have been made with an approximate 28 km resolution ($1/2 \times 1/4$ degrees) and the grid is called TNO28. The nested regional model calculations have been run with 2010 emissions in addition to three sets of 2025 TSAPHTAP emission scenarios exploring further European mitigation options in combination with the global 2030 emission scenario. All these set of simulations are performed for two meteorological years, 2008 and 2009. We have used abbreviations to represent the simulations and those are listed in the Table 7.1. Hereafter these abbreviations will be used in the text to represent each of the simulations. All model calculations for different scenarios are listed in Table 7.2.

Table 7.1: Abbreviations used to represent the model simulations

Abbreviations	Discription
GP	Global domain simulation for present emission scenario
GF	Global domain simulation for future emission scenario
RP	Regional domain calculation for present emission scenario
RPR	Regional domain calculation for present emission scenario with normal BC
RBC	Regional domain calculation for present emission scenario with BC from GP simulations
RCOB	Regional domain calculation with TSAPHTAP_COB emission scenario
Rb44	Regional domain calculation with TSAPHTAP_b44 emission scenario
RMFR	Regional domain calculation with TSAPHTAP_MFR emission scenario

Table 7.2: List of model simulations described in this chapter. BC refers to the boundary concentrations used in the nesting experiments. Reg. is the regular setup used as boundary concentrations as described in Simpson et al. (2012). Average of GP1 and GP2, RP1 and RP2 for 2008 and 2009 meteorological years are referred to in the text as GP and RP and so on.

Run	Grid Resolution	Met Year	Emission Scenarios	BC
GP1	1×1 degree	2008	ECLIPSE 2010	
GP2	1×1 degree	2009	ECLIPSE 2010	
GF1	1×1 degree	2008	ECLIPSE 2030	
GF2	1×1 degree	2009	ECLIPSE 2030	
RP1	TNO28	2008	TSAP_2010	GP1
RP2	TNO28	2009	TSAP_2010	GP2
RPR1	TNO28	2008	TSAP_2010	Reg
RPR2	TNO28	2009	TSAP_2010	Reg
RBC1	TNO28	2008	TSAP_2010	GP1
RBC2	TNO28	2009	TSAP_2010	GP2
RCOB1	TNO28	2008	TSAPHTAP_COB_2025	GF1
RCOB2	TNO28	2009	TSAPHTAP_COB_2025	GF2
Rb441	TNO28	2008	TSAPHTAP_b44_2025	GF1
Rb442	TNO28	2009	TSAPHTAP_b44_2025	GF2
RMFR1	TNO28	2008	TSAPHTAP_MFR_2025	GF1
RMFR2	TNO28	2009	TSAPHTAP_MFR_2025	GF2

In Jonson et al. (2012) it was shown that the global model calculations overpredicted surface ozone in the mid northern latitudes in the late winter and spring months, and that this overprediction was carried across to the nested regional model runs. In HTAP (2010), and in several peer reviewed papers using data from TF HTAP (Fiore et al. 2009, Shindell et al. 2008, Jonson et al. 2010) it was shown that the spread in surface ozone between individual global models is large, reflecting the large uncertainties in these calculations. In Jonson et al. (2012) it was also shown that using an ozone climatology constrained by monthly averaged clean sector measurements at Mace Head, Ireland as described in Simpson et al. (2012) resulted in a better match to ozone measurements in the regional model calculations. However, a clear advantage with the nested model runs is that air pollution originating outside the regional model domain can be attributed to its sources.

Below we attempt to extend the study of the import of air pollutants originating outside the regional model domain to other air pollutants as CO and $PM_{2.5}$.

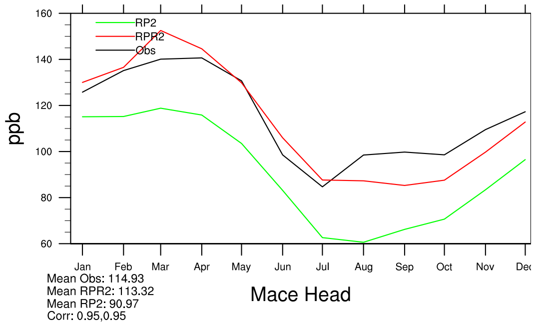

(a) Mace Head, Ireland

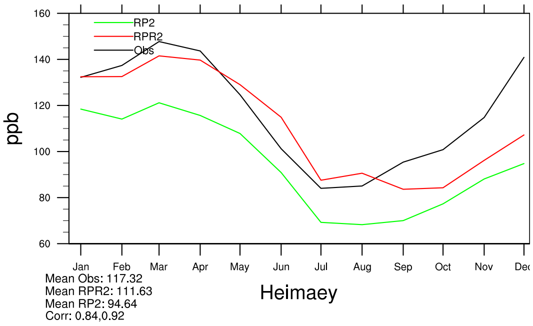

(b) Heimaey,Iceland

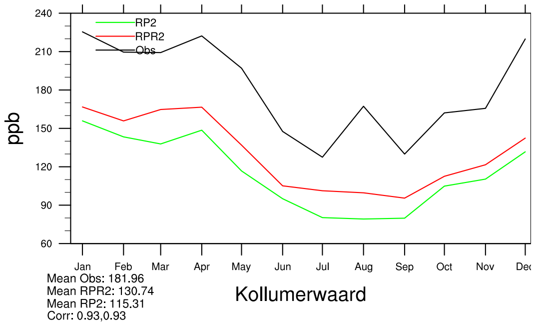

(c) Kollumerwaard, The Netherlands

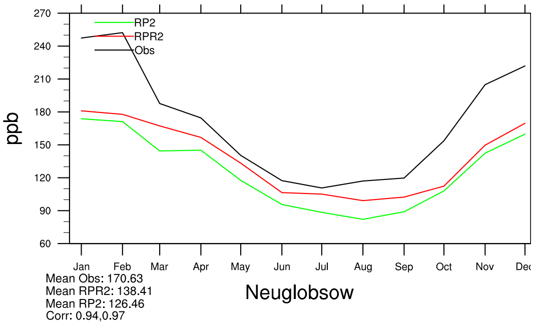

(d) Newglobsow, Germany

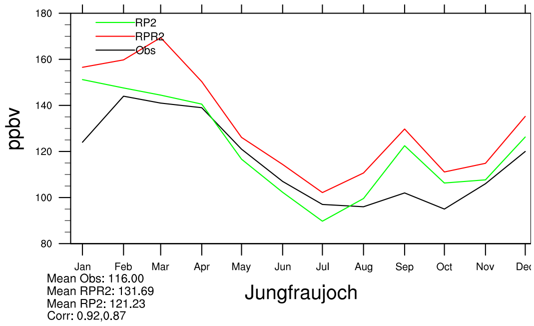

(e) Jungfraujoch, Switzerland

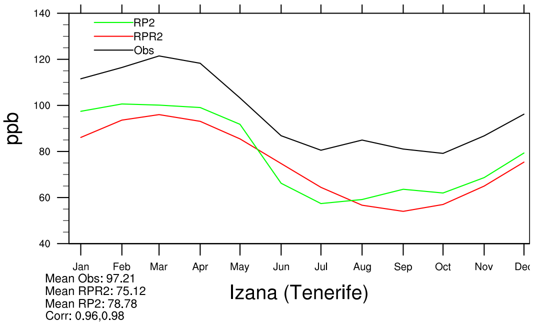

(f) Izana, Canary Islands

Figure 7.1: Measured and model calculated monthly averaged CO in ppb_v at selected sites for the year 2009.

CO has a long lifetime in the atmosphere, and can be advected between continents. The main sink is the reaction with OH. Main sources are emissions, and oxidation of methane and other NMVOC (Non Methane Volatile Organic Carbon). Over polluted continents as Europe the main source is emissions. Figure 7.1 shows the measured and model calculated CO levels at selected sites in 2009. Modelled CO levels are shown both for the nested model runs RP2 and the model run with regular boundary concentrations, RPR2. Both sets of model calculations reproduce the seasonal CO cycle with a winter/spring maximum and a summer minimum, but CO is underpredicted at most sites in both sets of model calculations. Both Mace Head in Ireland and Heimaey in Iceland are in the inflow region to Europe, measuring air masses most of the time unaffected by European sources. At both these sites CO from the nested model run RP2 is markedly lower than CO calculated with the regular boundary concentrations, RPR2. At Jungfraujoch, at more than 3500 m.a.s.l, there is actually a small overprediction of the measurements. It is however difficult to draw conclusions from this site, as the model topography is at a much lower altitude than the actual measurement. There is a tendency for the difference between the two sets of model calculations to decrease from west to east as airmasses pick up emissions. It is markedly smaller over continental Europe (Neuglobsow in Germany) compared to Mace Head and Heimaey, and has almost entirely disappeared at Izana on the Canary Islands, typically an outflow region in the regional model calculations. The reasons for the general underpredictions are currently unclear, but could be related both to an underestimation of the sources as well as an overprediction of global OH levels.

The typical residence time of $PM_{2.5}$ in the atmosphere is a few days only. We do therefore not expect marked signals of $PM_{2.5}$ in air masses advected over large distances such as across the Atlantic. There are however large sources of dust over Africa. Episodic dust events originating in Africa, occur in particular in the Mediterranean parts of Europe. Such African dust events originating in Northern Africa are observed at measurement sites and may serve as a test of the model parametrisation of boundary conditions. The model domain selected for the TNO28 regional calculations does however already include a large portion of Northern Africa. Running the model without nesting (RPR versus RP) results in only minor changes in $PM_{2.5}$ dust events at the measurement sites in Southern Europe, suggesting that the main source regions of African dust affecting Europe is included in the regional model domain. Figure 7.2 a and b shows the measured and model calculated $PM_{2.5}$ concentrations at Aiya Marina in Cyprus for both years. At both year the main dust episodes take place in winter and spring. Figure 7.2 c, d, e and f shows $PM_{2.5}$ concentrations for two sites in southern Spain (Viznar and Cabo de Creus). In particular at Viznar the African dust episodes can be identified with clear peak values. The model calculated $PM_{2.5}$ concentrations in the current TNO28 model domain are markedly higher for the African dust events than the regional EMEP MSC-W model calculations in other chapters of this report.

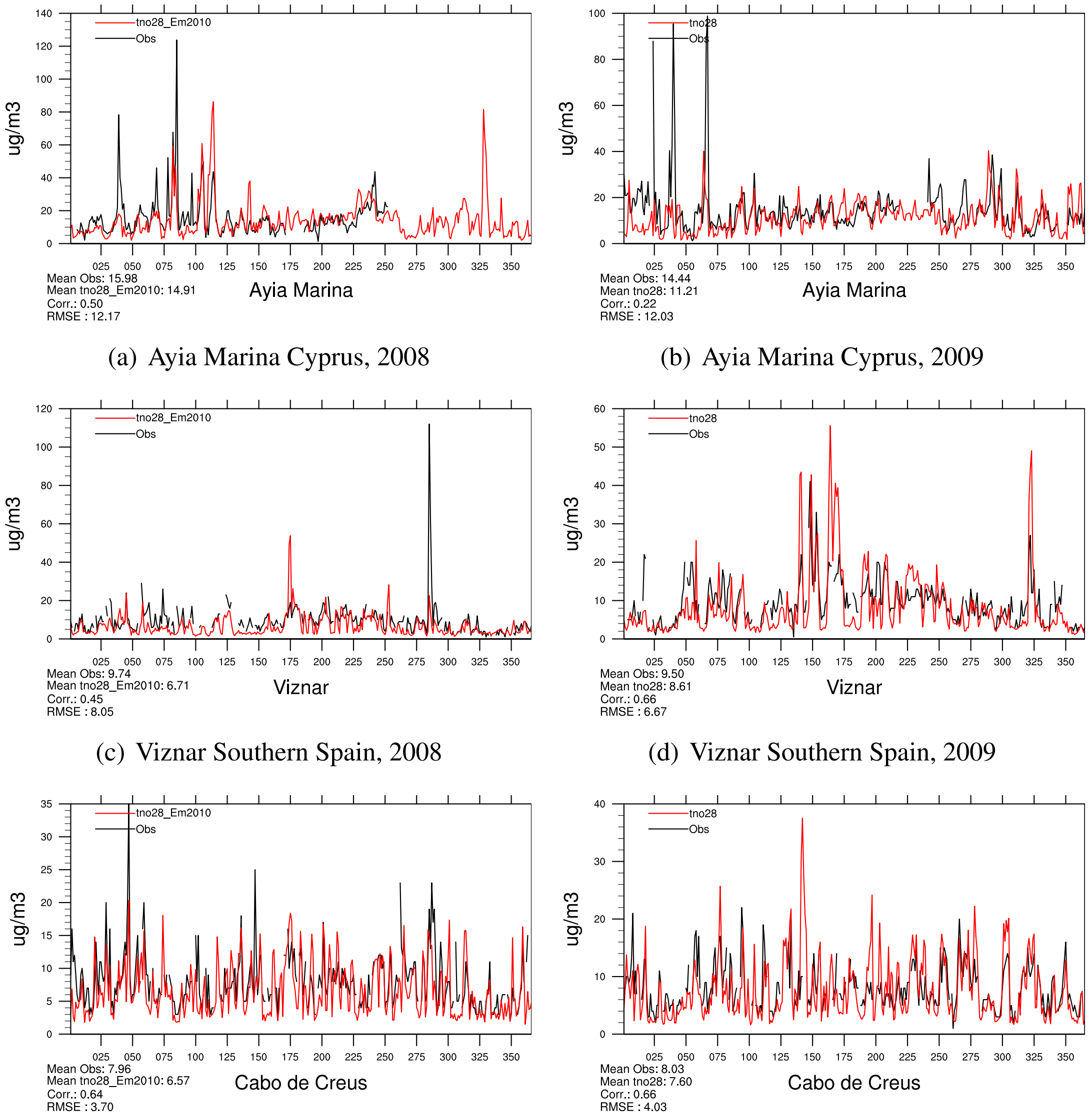

(a) Ayia Marina Cyprus, 2008

(b) Ayia Marina Cyprus, 2009

(c) Viznar Southern Spain, 2008

(d) Viznar Southern Spain, 2009

(e) Cabo de Creus Spain, 2008

(f) Cabo de Creus Spain, 2009

Figure 7.2: Measured and model calculated $PM_{2.5}$ (μgm^{-3}) at selected sites in Cyprus and Southern Spain for the year 2008 (left) and 2009 (right).

7.2 Transcontinental effects

Model calculations have been made based on the emissions for the years 2008 and 2009. The discussion below is limited to boundary layer ozone, focusing on Europe. For other pollutants, as particles, the trans continental contribution is likely to be much smaller.

Figure 7.3 (a) shows annually averaged ozone in ppb for the year 2008. High ozone levels are in particular seen over the Tibetan plateau. Ozone levels generally increase with height, and this is the cause of the high ozone levels here. High levels are also seen over North America, East Asia and around the Mediterranean sea, and here the elevated ozone levels are caused by regional emissions of ozone precursors. Figure 7.3 also shows the effects of 20% emission reductions (Base run - 20% perturbation) in EU27 including also Norway and Switzerland (b), Canada and USA combined (c) and China (d). Even though the largest calculated effects of emission reductions over N. America, EU and China are seen over the

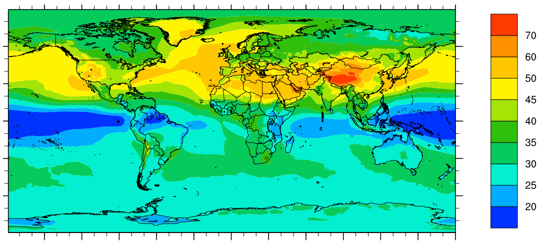

(a) Global ozone 2009, annual average

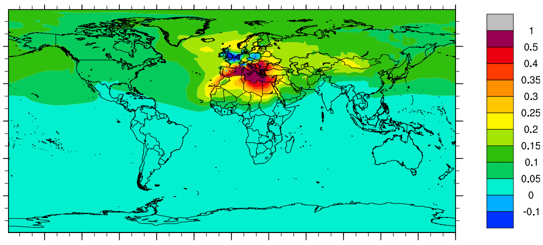

(b) 20% reduction in EU emissions

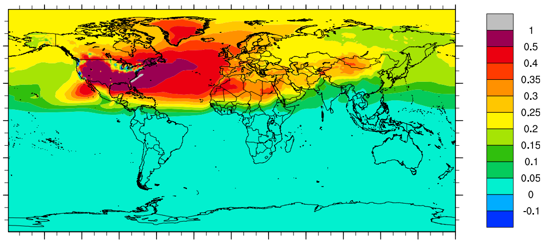

(c) 20% reduction in NA emissions

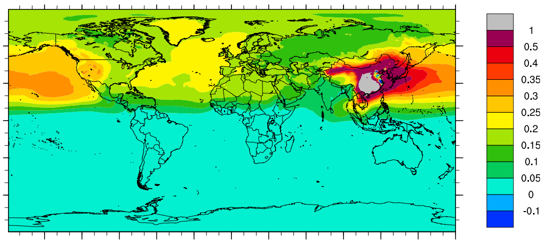

(d) 20% reduction in CH emissions

Figure 7.3: **a**: Annually averaged surface ozone. **b**: Effects of 20% reductions in all EU emissions (EU defined as EU27 + Norway and Switzerland). **c**: Effects of 20% reductions in all NA emissions (defined as Canada and USA). **d**: Effects of 20% reductions in all Chinese emissions.

source region and directly downwind, marked effects on ozone are also seen throughout the northern mid latitudes, with the largest transcontinental effects in the Spring months.

Zooming in on Europe, Figure 7.4 shows the effects of the 20% emissions reductions (Base run 20% reductions) in N. America (NA), Europe (EU) and China (CH) on European ozone levels split into seasons. In winter ozone production is low over the source continents, leaving only small amounts to be transported from other continents (North America and China) to Europe. In large parts of Europe there is widespread titration of ozone. As sunlight returns in spring, ozone production increases and the effects of intercontinental transport of ozone reach its annual maximum. In summer local/regional ozone production is at its maximum in Europe (as well as in other source regions). For transcontinental transport high local and regional net ozone production is counterbalanced by a shorter lifetime of ozone in the atmosphere in the summer. The transcontinental contribution to ozone in Europe again increase in the autumn.

7.3 Impacts of future emissions scenarios

In this section the model calculated effects of present (2010) and future (2025/2030) emission scenarios are compared. Furthermore the global model runs have been nested to a set of regional model runs with present and future emissions as defined in the Thematic Strategy on Air Pollution (TSAP) `http://ec.europa.eu/environment/air/review_air_policy.htm`. All model runs discussed below have been averaged over the two meteorological years 2008 and 2009. The model runs are listed in Table 7.2. Furthermore the model calculated averages for daily maximum ozone in winter and summer, and the annually averaged $PM_{2.5}$ levels are listed in Table 7.3 for the reference scenarios GP and RP along with the differences between scenario runs and the reference runs averaged over the 3 regions NW Europe, SW Europe and E Europe illustrated in Figure 7.5. In Table 7.3 there are marked differences between daily maximum ozone calculated with the global and the regionally nested

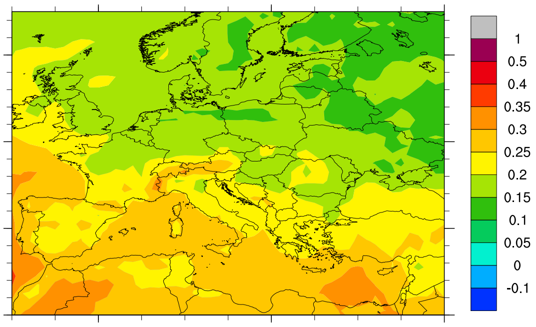

(a) NA effect on Europe, winter

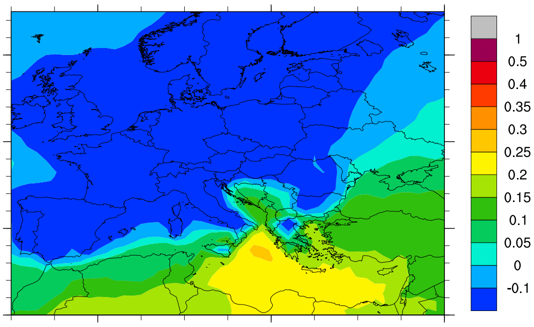

(b) EU effect on Europe, winter.

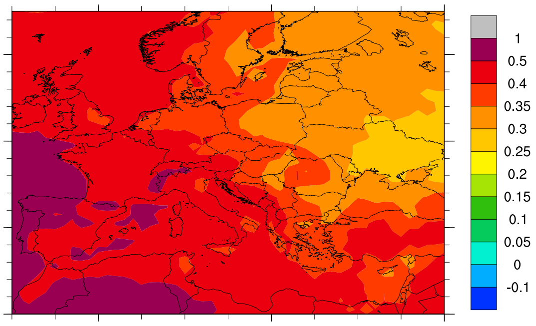

(c) NA effect on Europe, spring.

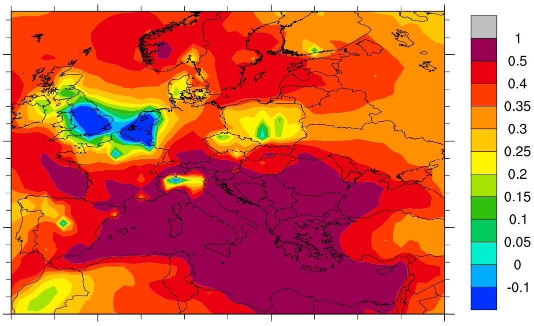

(d) EU effect on Europe, spring.

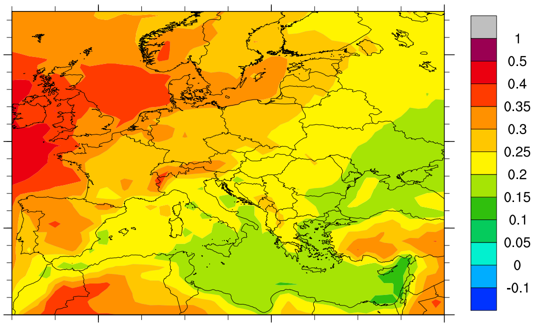

(e) NA effect on Europe, summer.

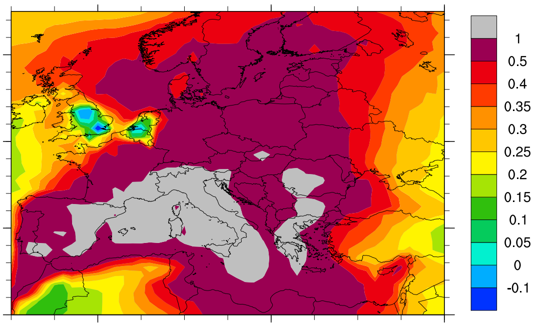

(f) EU effect on Europe, summer.

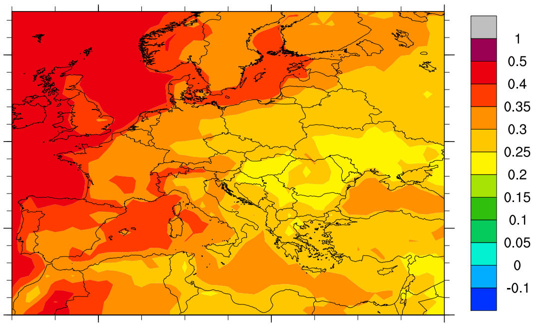

(g) NA effect on Europe, autumn.

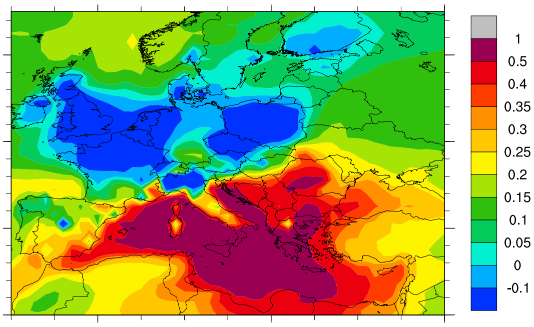

(h) EU effect on Europe, autumn.

Figure 7.4: Effects of 20% reductions of all antropogenic emissions in North America in **a**: winter, **c**: spring, **e**: summer and **g** autumn. Effects of 20% reductions of all antropogenic emissions in EU27 + Norway and Switzerland in **b**: winter, **d**: spring, **f**: summer and **h** autumn. Figure continues on next page.

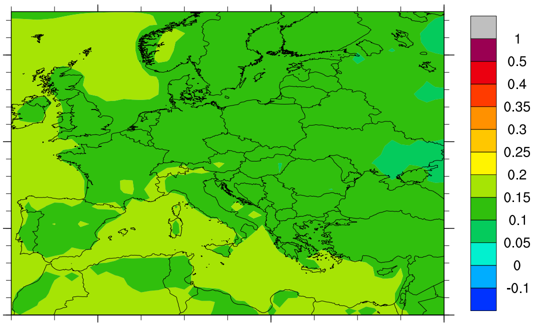

(a) CH effect on Europe, winter.

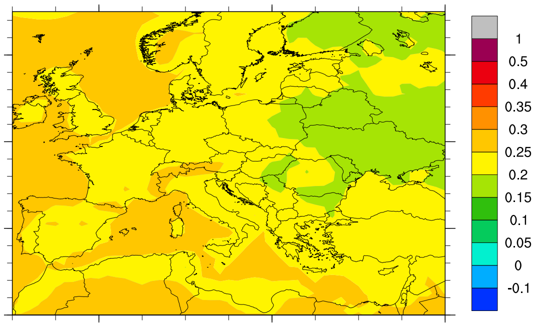

(b) CH effect on Europe, spring.

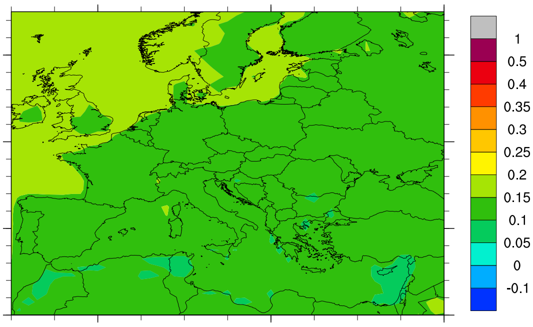

(c) CH effect on Europe, summer.

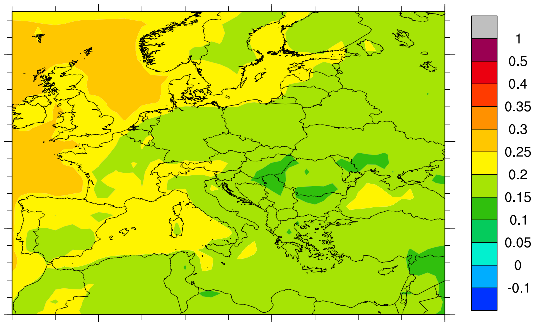

(d) CH effect on Europe, autumn.

Figure 7.4: continued. Effects of 20% reductions of all antropogenic emissions in China in **i**: winter, **j**: spring, **k**: summer and **l** autumn.

model versions for the same three areas, in particular in winter. In a similar modelling experiment such marked differences between global and regional nested runs were not seen (Jonson et al. 2012). The reason could be that contrary to the present study, emissions in the global and regional model calculations were (virtually) identical.

Table 7.3: Average daily maximum ozone (ppb) in winter (MAX ozone Wi) and summer (MAX ozone Su) and annual $PM_{2.5}$ in μgm^{-3}. Referring to the mask in Figure 7.5 NW is NW Europe, SW is SW Europe and E is Eastern Europe. Run refers to the model scenario notation introduced in Table 7.2. The Table lists the calculated levels for the global and regional reference runs and the difference between the scenario runs and the reference runs.

	MAX ozone Wi			Max ozone Su			PM2.5		
Run	NW	SW	E	NW	SW	E	NW	SW	E
GP	40	42	41	43	51	50			
GF - GP	0.6	-0.4	-0.2	-4.4	-6.8	-5.3			
RP	35	42	35	42	51	50	5.3	7.1	9.8
RCOB - RBC	-0.7	-1.0	-0.7	-0.7	-0.8	-0.7	-0.03	-0.03	-0.03
RCOB - RP	1.0	0.3	0.7	-4.5	-7.5	-6.8	-1.3	-2.0	-2.8
Rb44 - RP	1.1	0.1	0.4	-4.9	-8.4	-7.6	-1.7	-2.7	-4.0
RMFR - RP	1.1	-0.1	0.3	-5.5	-9.3	-8.5	-1.9	-3.0	-4.4

7.3.1 Global model calculations with future emissions scenarios

Figure 7.6 shows the difference in surface ozone calculated with 2030 and 2010 (GF - GP) emissions, split by season (see Table 7.2 for naming convention of the model runs). The left hand side of the figure, displaying the full global domain, shows substantial increases in daily maximum ozone levels from 2010 to 2030 over Africa - south of Sahara-, and large parts of Asia for all seasons. In particular large increases are calculated over the Indian subcontinent. Over parts of North America and Europe daily maximum ozone levels are projected to increase in winter as a result of less NOx titration and in general decrease in the rest of the year. Focusing on Europe (Figure 7.6, right hand side) shows an increas in calculated daily maximum ozone levels over the western European continent north of the Alps in winter. For the rest of the year calculated ozone levels decrease virtually everywhere except in the North Sea region in the autumn. Ozone reductions are particularly strong over Italy in summer. The strong reductions here are caused by a combination of high emissions of ozone precursors in 2010 and strong insolation. The average daily maximum ozone revels for NW Europe, SW Europe and E Europe and the differences between the model runs with 2030 versus 2010 emissions are listed in Table 7.3.

Figure 7.5: Regional mask for Europe. Brown: NW Europe (west of Baltic Sea). Light green: SW Europe (France follows provinces level at ca. 46 N). Dark red: Eastern Europe.

7.3.2 Regional nested model runs with TSAP emissions scenarios

Regional model calculations with present and future emission scenarios have been made by nesting the global model calculations described above (Table 7.2). Emission scenarios for year 2025 are from IIASA and have been produced for the revision of the TSAP [1] and the TFHTAP. The three scenarios considered here are the reference Cost-Optimal Baseline (COB), similar to CLE, the central case optimised scenario (b44) and the Maximum Feasible Reductions (MFR) scenario. In the b44 and MFR scenarios only the EU28 have their emissions reduced below the COB level.

COB: The baseline projections consider a detailed inventory of national emission control legislation (including the transposition of EU-wide legislation); EU and Member States have issued a wide body of legislation that limits emissions from specific sources, or have indirect impacts on emissions through affecting activity rates. The scenario assumes that these regulations will be fully complied with in all Member States according to the foreseen time schedule. For the non-EU countries, calculations assume the activity projections and current legislation control measures that have been used for the negotiations of the revised Gothenburg protocol.
b44 This scenario is an update of the A5 optimised scenario (described in the TSAP Report

[1] http://www.iiasa.ac.at/web/home/research/researchPrograms/MitigationofAirPollutionandGreenhousegases/TSAP-review.en.html

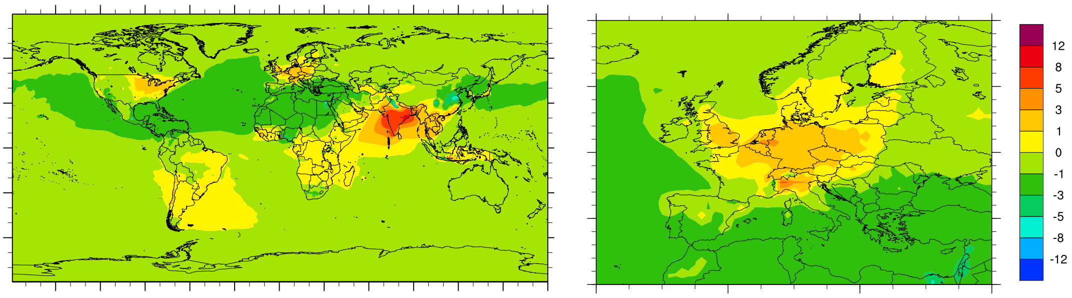

(a) NA effect on Europe, summer. (b) EU effect on Europe, summer.

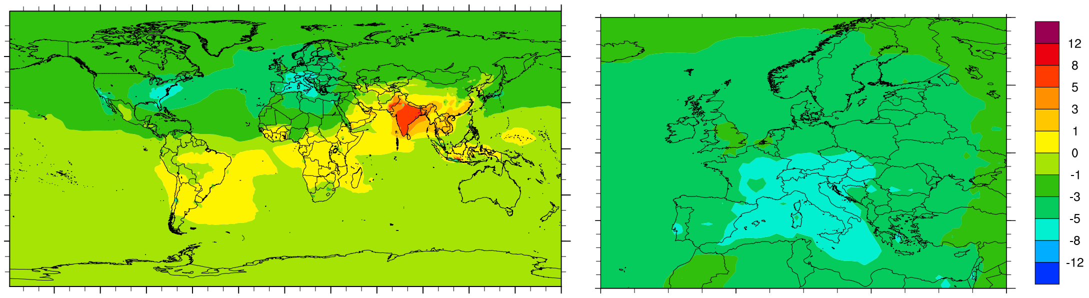

(c) NA spring, ozone 2030 - 2010. (d) EU spring, ozone 2030 - 2010.

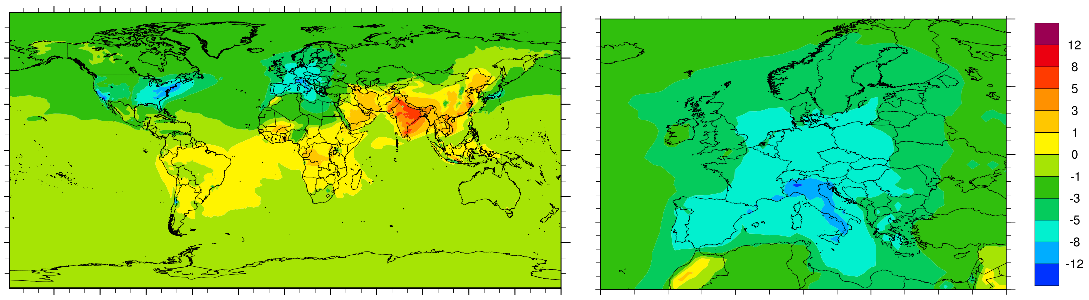

(e) NA summer, ozone 2030 - 2010. (f) EU summer, ozone 2030 - 2010.

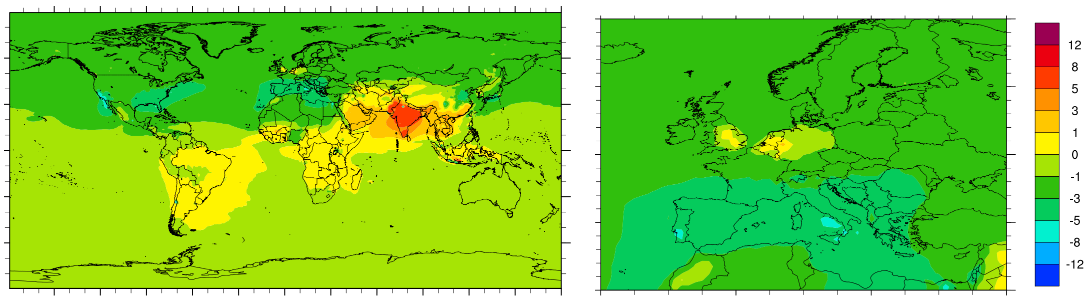

(g) NA autumn, ozone 2030 - 2010. (h) EU autumn, ozone 2030 - 2010.

Figure 7.6: Difference in global ozone levels calculated with 2030 versus 2010 emissions. Left hand figures shows the global domain. The right hand figures are from the same data set, but focusing on the European part of the model domain.

#10 [2] and is a result of the consultation between the Commission and IIASA. While the health targets (YOLL) remain in B44 as in A5 (European wide target of 75% gap closure), the B44,

[2] `http://www.iiasa.ac.at/web/home/research/researchPrograms/\MitigationofAirPollutionandGreenhousegases/TSAP-review.en.html`

also includes European wide targets for ozone and eutrophication, allowing for more stringent gap closure, i.e., 46% for ozone and 82.5% for eutrophication. Finally, the b44 allows also further (beyond COB) measures for non-road machinery.

MFR This scenario explores to what extent emissions of the various substances could be further reduced beyond what is required by current legislation, through full application of the available technical measures, without changes in the energy structures and without behavioural changes of consumers. However, the MFR scenario does not assume premature scrapping of existing capital stock; new and cleaner devices are only allowed to enter the market when old equipment is retired.

Regional COB emissions versus present emissions

Figure 7.7 shows the calculated differences, RCOB - RP split into season on the left hand side of the figure (see Table 7.2 for naming convention of the model runs) The right hand side of the figure shows the effects of changing only the lateral boundary concentrations (RCOB - RBC). Changing only the boundary concentrations, ozone levels decrease for all seasons over the whole regional model domain, with the exception of the southeast corner. The largest decrease was calculated for the spring months. This is also shown for winter and summer in Table 7.3 (RCOB - RBC) for the three European regions. In the table the effects on $PM_{2.5}$ levels from differences in lateral boundary concentrations are shown to be negligible. These changes in daily maximum ozone are relatively small compared to the calculated changes in ozone including regional emissions changes for year 2025 versus 2010 (RCOB - RP). Even though the absolute values differ, these differences are very similar to those calculated for present versus future emissions over Europe in the global model calculations discussed in section 7.3.1, with widespread ozone titration in winter in north and central Europe, and large ozone reductions, in particular in Italy, in the summer months. In order to derive the ozone changes caused purely by changes in regional emissions, the effects of the lateral boundaries (RCOB - RBC) should be subtracted from the effects of the other scenarios.

Effects of additional EU control measures in 2025

Regional model calculations have also been made with the b44 and MFR future scenarios with additional emission reductions in the EU28 countries. Figure 7.8 shows the effects of these additional emission control measures compared to COB for daily maximum ozone and PM2.5. The effects are also listed in Table 7.3 for NW Europe, SW Europe and E Europe. With additional emission control measures in the EU28 countries, ozone and PM2.5 levels are reduced throughout Europe (7.8 a for b44 and 7.8 c for MFR). The largest reductions are calculated for the Mediterranean region, and in particular for Northern Italy (region SE Europe). For $PM_{2.5}$ reductions are largest in E Europe and the Mediterranean region.

7.4 Final remarks

The model calculations in this section have been made in order to test the model setup to be used in the forthcoming TF HTAP modelling exercise, where global (and partially regional nested) model runs will be made for the years 2008 to 2010. Model sensitivity studies will be made with emphasis on year 2010 perturbing emissions by region and by emissions sector. A set of EMEP MSC-W model (hemispheric) calculations was also included in the previous

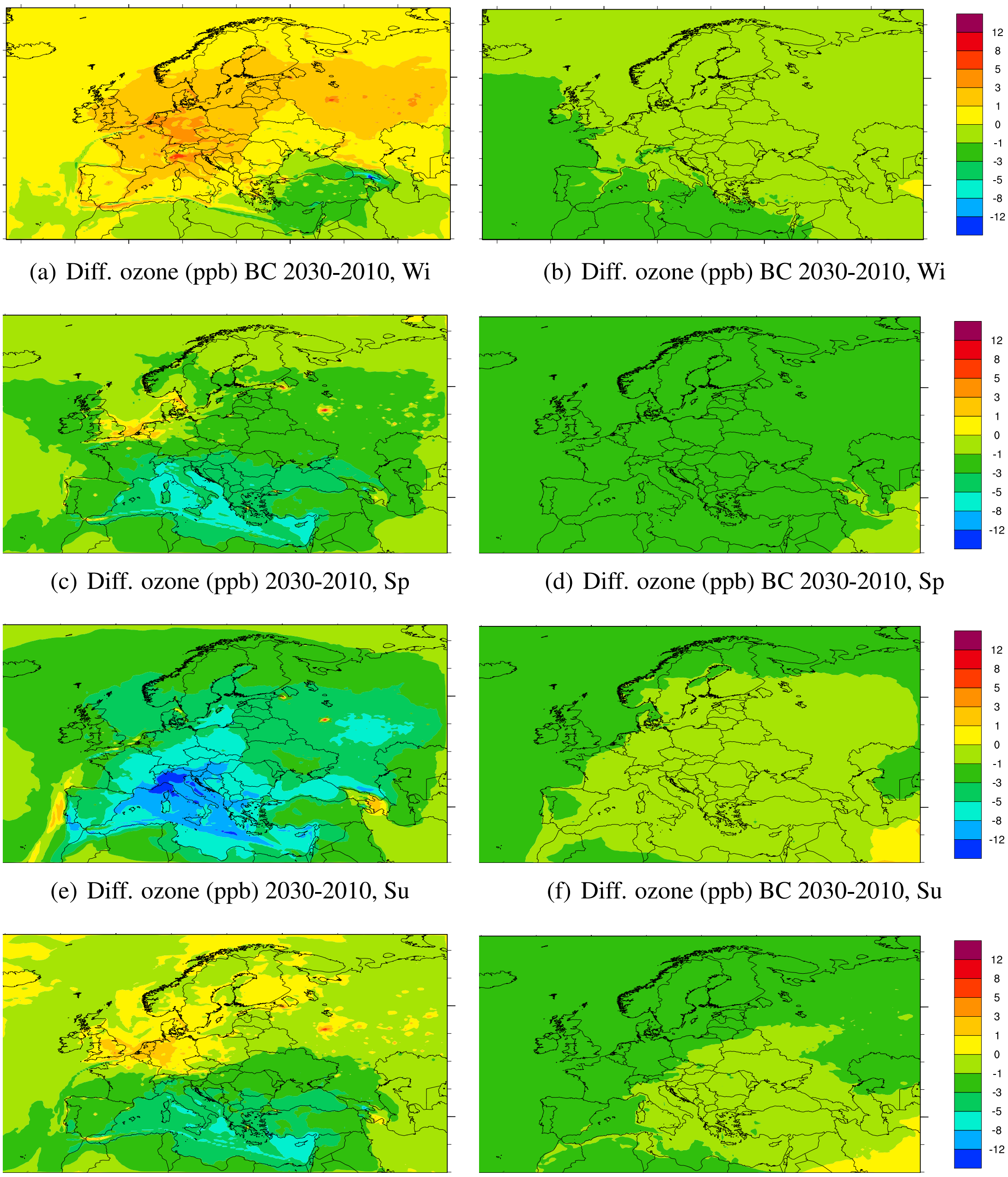

(a) Diff. ozone (ppb) BC 2030-2010, Wi

(b) Diff. ozone (ppb) BC 2030-2010, Wi

(c) Diff. ozone (ppb) 2030-2010, Sp

(d) Diff. ozone (ppb) BC 2030-2010, Sp

(e) Diff. ozone (ppb) 2030-2010, Su

(f) Diff. ozone (ppb) BC 2030-2010, Su

(g) Diff. ozone (ppb) 2030-2010, Au

(h) Diff. ozone (ppb) BC 2030-2010, Au

Figure 7.7: Difference in regional ozone levels calculated with 2025 COB versus 2010 emissions (RCOB - RP) and when changing only the lateral boundary concentrations (RBC - RP, left). Wi - winter, Sp - spring, Su - summer, Au - autumn.

TF HTAP modelling exercise (HTAP 2010). Model inter-comparisons showed that the EMEP MSC-W model was close to the median for most species and most of the sensitivity studies included in this report. Even though extensive model updates have been made since then, the model sensitivity to emission changes in other continents has remained relatively unchanged.

Previous model calculations, along with the calculations presented here, have shown that the global EMEP model over-predicts surface ozone in the late winter and spring months in the northern hemisphere. Furthermore CO levels are under-predicted in Europe and in many other sites in the northern hemisphere, but at the same time are CO from the same model

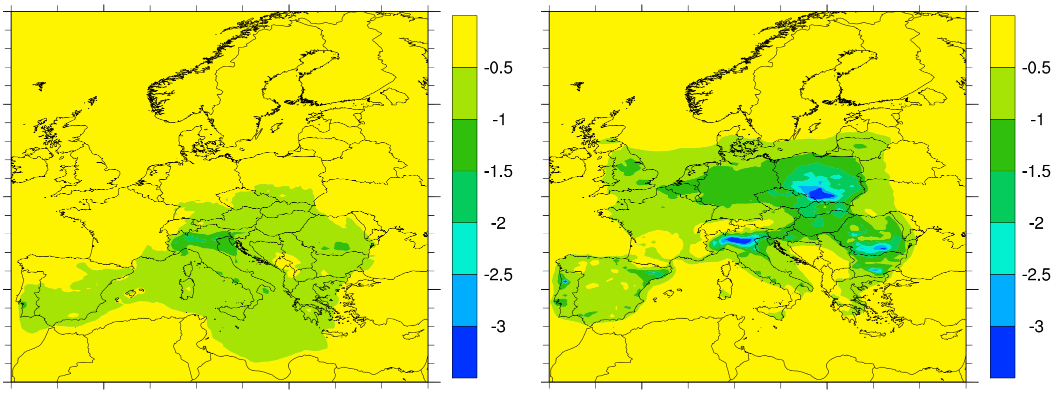

(a) Diff. ozone (ppb), b44 - COB (b) Diff. $PM_{2.5}$ (μgcm^{-3}), b44 - COB

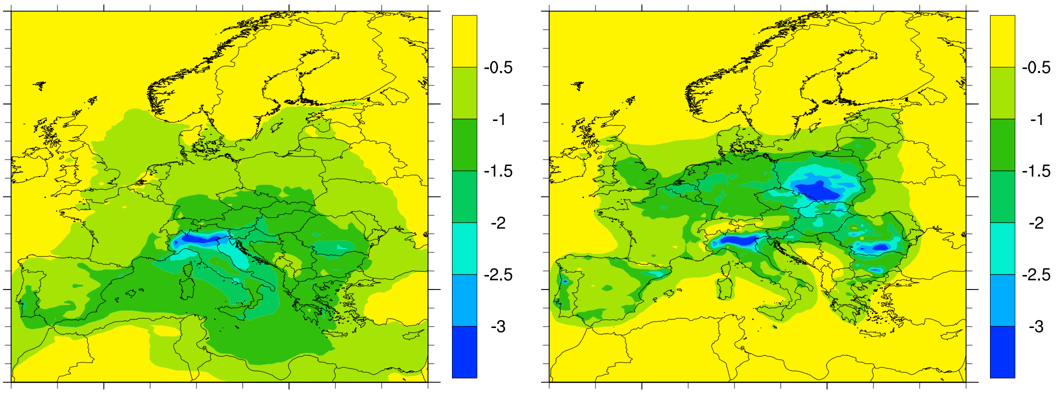

(c) Diff. ozone (ppb), MFR - COB (d) Diff. $PM_{2.5}$ (μgcm^{-3}), MFR - COB

Figure 7.8: Difference in regional ozone and $PM_{2.5}$ levels with b44 - COB, (a and b) and MFR - COB (c and d) emissions.

calculations overpredicted in the southern hemisphere (not shown in this report). The cause of these deviations from measurements has so far not been identified. The model calculations demonstrate that the modelling system is capable of attributing air pollution in Europe to sources outside the European continent. Compared to model calculations with present emission, the future emission scenarios result in marked improvements in European air quality. For boundary layer ozone the improvements are partially brought about by a decrease in future lateral boundary concentrations from the global model calculations as a result of future global emissions changes.

Acknowledgements

The CO measurements have been downloaded from the World Data Centre for Greenhouse Gases `http://ds.data.jma.go.jp/gmd/wdcgg/`. $PM_{2.5}$ data have been downloaded from the website of the EMEP Centre on Emission Inventories and Projections (CEIP) `http://www.ceip.at/webdab-emission-database/emissions-as-used-in-emep-models/`.

References

Fiore, A., Dentener, F., Wild, O., Cuvelier, C., Schultz, M., Textor, C., Schulz, M., Atherton, C., Bergmann, D., Bey, I., Carmichael, G., Doherty, R., Duncan, B., Faluvegi, G., Folberth, G., Garcia Vivanco, M., Gauss, M., Gong, S., Hauglustaine, D., Hess, P., Holloway, T., Horowitz, L., Isaksen, I., Jacob, D., Jonson, J., Kaminski, J., keating, T., Lupu, A., MacKenzie, I., Marmer, E., Montanaro, V., Park, R., Pringle, K., Pyle, J., Sanderson, M., Schroeder, S., Shindell, D., Stevenson, D., Szopa, S., Van Dingenen, R., Wind, P., Wojcik, G., Wu, S., Zeng, G., and Zuber, A.: Multi-model estimates of intercontinental source-receptor relationships for ozone pollution, J. Geophys. Res., 114, doi:10.1029/2008JD010816, doi:10.1029/2008JD010816, 2009.

HTAP, T.: Hemispheric transport of air pollution 2010. Edited by: Frank Dentener, Terry Keating and Hajime Akimoto, Tech. Rep. Air Pollution Studies No. 17, United Nations Economic Commission for Europe, Geneva, available at `www.htap.org`, 2010.

Jonson, J., Stohl, A., Fiore, A., Hess, P., Szopa, S., Wild, O., Zeng, G., Dentener, F., Lupu, A., Schultz, M., Duncan, B., Sudo, K., Wind, P., Schulz, M., Marmer, E., Cuvelier, C., Keating, T., Zuber, A., Valdebenito, A., Dorokhov, V., De Backer, H., Davies, J., Chen, G., Johnson, B., Tarasick, D., Stübi, R., Newchurch, M., von der Gathen, P., Steinbrecht, W., and Claude, H.: A multi-model analysis of vertical ozone profiles, Atmos. Chem. Physics, 10, 5759–5783, doi:10.5194/acp-10-5759-2010, 2010.

Jonson, J., Valiyaveetil, S., and Schulz, M.: Global and nested regional calculations: Comparing model results for Europe, In *Development of the EMEP global modeling framework: Progress report* EMEP/MSC-W Tech. Rep. 1/2012, URL: www.emep.int, The Norwegian Meteorological Institute, Oslo, Norway, 2012.

Shindell, D., Chin, M., Dentener, F., Doherty, R., Faluvegi, G., Fiore, A., Hess, P., Koch, M., MacKenzie, I., Sanderson, M., Schultz, M., Schulz, M., Stevenson, D., Teich, H., Textor, C., Wild, O., Bergmann, D., Bey, I., Bian1, H., Cuvelier, C., Duncan1, B., Folberth, G., Horowitz, L., Jonson, J., Kaminski1, J., Marmer, E., Park, R., Pringle, K., Schroeder, S., Szopa, S., Takemura, T., Zeng, G., Keating, T., and Zuber, A.: A multi-model assessment of pollution transport to the Arctic, Atmos. Chem. Physics, 8, 5.353–5.372, 2008.

Simpson, D., Benedictow, A., Berge, H., Bergström, R., Emberson, L. D., Fagerli, H., Hayman, G. D., Gauss, M., Jonson, J. E., Jenkin, M. E., Nyíri, A., Richter, C., Semeena, V. S., Tsyro, S., Tuovinen, J.-P., Valdebenito, A., and Wind, P.: The EMEP MSC-W chemical transport model – technical description, Atmos. Chem. Physics, 12, 7825–7865, doi:10.5194/acp-12-7825-2012, 2012.

CHAPTER 8

Interaction of short-lived climate forcers with air quality

Dirk Olivié, Michael Gauss, Alf Grini, Trond Iversen, Alf Kirkevåg, Øyvind Seland, and Michael Schulz

8.1 Introduction

There is a close connection between air quality and climate evolution. Important questions are: how will climate change over the next few decades? How will air quality be affected by future climate change? And, which measures can be taken to mitigate both air pollution and climate change? Certain species can affect both air quality and the radiative fluxes in the atmosphere. Examples of these are aerosols and ozone (O_3), and therefore changes in the emissions of aerosols, their precursors, and O_3 precursors might impact both air quality and climate. Disregarding water vapour, whose contribution to global warming has been debated (see e.g., Dessler et al. 2008), tropospheric O_3 is the third most important greenhouse gas (GHG) after carbon dioxide (CO_2) and methane (CH_4). Most particles, excluding black carbon (BC), cool the climate system, masking some of the warming from longer-lived GHGs.

The presence of BC (see also Petzold et al. (2013) for the definition of BC), being a strong absorber of solar radiation, can lead to a large variety of possible impacts including both warming and cooling processes, the net effect of which is not straightforward to assess:

- The absorption of solar radiation by BC in the atmosphere leads to upper-air heating, and even more so, where the underlying surface or atmospheric layer is highly reflective (e.g. desert surfaces, snow/ice, low clouds).
- Beneath atmospheric layers of increased absorption, solar radiation may be attenuated and the effect close to the surface may actually be a local cooling rather than a warming.
- A secondary effect of the upper air heating by BC is an enhanced long-wave radiation as temperatures increase at these heights.

- Furthermore, as a so-called semi-direct effect, the upper-air heating may increase the static stability, thus reducing the development of deep convection and subsequent precipitation, and also leading to selective evaporation of cloud droplets at the respective altitude.

- Coated BC may also exhibit considerable indirect effects on cloud reflectivity, leading to cooling.

- Finally, BC deposited on snow and ice may reduce the surface albedo, thus contributing to surface and global warming.

In addition to the impact of short-lived air pollutants on climate, future climate change will, in turn, also impact air pollution, e.g. by changes in flow patterns, humidity, temperature and precipitation. Such changes affect the transport, deposition, physical properties, and the chemical and physical transformation of air pollutants. In future mitigation policies, air quality and climate change should thus be considered together. The fact that both O_3 and BC are short-lived (compared to, e.g., CO_2) implies that not only air quality, but also climate benefits can be realized in the near-term.

Since last year BC is included in the amendments to the 1999 Gothenborg Protocol to abate acidification, eutrophication and ground-level ozone. The revision of the Gothenburg Protocol now explicitly states that, in taking steps to reduce emissions of particulate matter, each Party to the Convention should seek reductions from those source categories known to emit high amounts of black carbon, to the extent it considers appropriate.

Raes et al. (2011) have made an integrated assessment of BC and O_3 with focus on the identification of mitigation strategies for these short-lived climate forcers, giving a comprehensive analysis of the multiple benefits of practical measures to reduce emissions of BC and the precursors of O_3. Very recently, Bond et al. (2013) assessed the impact of BC on the climate system. They quantified the top-of-the-atmosphere direct and indirect radiative forcing (RF) of BC, and also took into account that BC is often co-emitted with other short-lived species.

Several global model experiments have recently been used to study the anthropogenic impact on atmospheric composition and climate (see Table 8.1). The CMIP5 exercise compares the behaviour of coupled climate models. These models describe the different climate-relevant components of the Earth, i.e., the atmosphere, the ocean, sea ice, and the land surface, and the interactions between them. ACCMIP focuses more on historical and future changes in the atmospheric composition (both gases and aerosols), and the impact on RF, while AeroCom focuses mostly on the detailed study and uncertainty in RF estimates of aerosols. The resolution of the global models utilised for these studies is often much coarser than that of air quality models, but with global coverage and with calculation on decennial to centennial time scales they can give crucial information on the presence and impact of short-lived climate forcers and air pollutants over time from the pre-industrial era to the end of the 21st century (or later).

In this chapter we will describe selected results from global chemistry-transport models (CTMs) and global climate models of potential interest for EMEP. As the interaction between climate and air pollution can be approached from different angles, and to narrow the scope of this chapter, we will focus on three questions:

1. What is the historical impact of short-lived climate forcers?

2. What are the sources of uncertainty in the BC climate impact?

3. How may source-receptor relationships change in the future?

Where appropriate, we will mention specifically results obtained with the Norwegian Earth System Model (see fact box) which is jointly developed by different institutes (mainly) in Norway. The model has participated in the CMIP5 exercise, as well as in the aerosol intercomparison exercise AeroCom, and is developed in close cooperation with MSC-W in the same research department at the Norwegian Meteorological Institute.

8.2 Historical impact of short-lived climate forcers

Global anthropogenic emissions affecting the presence of short-lived climate forcers and pollutants have, in general, strongly increased since 1850, although for some of them regional reductions have been achieved. Estimates of the emissions evolution between 1850 and 2000 from Lamarque et al. (2010) show increases in the anthropogenic emissions of carbon monoxide (CO), nitrogen oxides (NO_x), volatile organic compounds (VOCs), and sulphur dioxide (SO_2) by a factor of 10 or more, in BC and ammonia (NH_3) by a factor of 5, and in organic carbon (OC) by a factor of 2–3. Despite the strong increase in anthropogenic emissions, for certain species natural emissions are estimated to be still of the same order of magnitude as the current anthropogenic emissions (e.g., VOCs and CO), or to be even larger (e.g., OC). In addition to anthropogenic emissions changes, also natural emissions might have changed. For instance, there are indications of a reduction in global biomass burning emissions in the first half of the 20th century due to reduced forest clearing in the mid-latitude and boreal regions (Lamarque et al. 2010, Mieville et al. 2010). These changes in emissions directly impact the atmospheric burden, of which an illustration is given in Fig. 8.1.

Several recent studies have made estimates of the climate impact of short-lived climate forcers, mainly focusing on the impact of aerosols and O_3. These studies can differ in the use of their pre-industrial reference year (usually 1750 or 1850) and present-day reference year (2000, 2006, or 2010). For aerosols, some studies limit themselves to the direct RF (e.g, Myhre et al. 2013), while some also calculate the indirect radiative forcing (e.g., Kirkevåg et al. 2013), and recently (e.g., Shindell et al. 2013) total aerosol forcing is also calculated using the Effective Radiative Forcing (ERF) concept (see Table 8.2). Bond et al. (2013) focus on BC and estimated the RF from BC between 1750–2005 at 0.71 W m^{-2} with 90 % uncertainty bounds of 0.08 and 1.27 W m^{-2}. Myhre et al. (2013) estimate the direct aerosol effect to be -0.32 W m^{-2} for the 1850–2000 period (or -0.35 W m^{-2} for the 1750–2010 period). Kirkevåg et al. (2013), using the NorESM1-M model, estimate the direct RF of aerosols for the period 1850–2006 to be -0.08 W m^{-2} and the indirect RF to be -1.2 W m^{-2}. For the period 1850–2000 their corresponding estimates are -0.10 W m^{-2} and -0.91 W m^{-2}, and for the period 1750–2006 they are -0.04 W m^{-2} and -1.53 W m^{-2} for the direct and indirect effects, respectively. Shindell et al. (2013) estimate both the direct and total aerosol effect based on the results from ACCMIP. For the direct aerosol RF (1850–2000) they find a best estimate of -0.42 W m^{-2}, and for the aerosol ERF -1.17 W m^{-2}. They find that the global aerosol direct RF peaks in most models around 1980, declining thereafter, whereas the aerosol ERF, in contrast, becomes stronger (more negative) from 1980 to 2000.

Also tropospheric O_3 has a considerable impact on RF. The tropospheric O_3 burden has increased considerably since the beginning of the industrial era: Young et al. (2013) estimate an increase of 30 % since 1850. Stevenson et al. (2013) estimate the pre-industrial (1750) to present-day (2010) tropospheric O_3 RF to be 0.41 W m^{-2}, and attribute this tropospheric O_3

Fact sheet: The Norwegian Earth System Model, NorESM1

NorESM1 is the first version of the Norwegian Climate Center's numerical model for global climate and earth system studies (see GMD – Special Issue: http://www.geosci-model-dev.net/special_issue20.html) and has been run with medium spatial resolution (1.9° × 2.5° in the atmosphere, NorESM1-M: Bentsen et al. (2013), Iversen et al. (2013), Kirkevåg et al. (2013)) to provide results for CMIP5 and the upcoming IPCC report (IPCC AR5).

NorESM1-M includes online integration of aerosol life-cycling, and evolution of size distributed aerosol number concentrations and composition, as well as the link with prognostic cloud droplet number concentrations. Transported atmospheric chemical components of interest are sulphate (SO_4), black carbon (BC), particulate organic matter (POM), sea-salt (SS) and mineral dust (DU). Aerosols interact with radiation and cloud microphysics, and thus with the climate dynamics of the atmosphere, ocean, sea-ice, and land surface. The effect of darkening of snow by deposited BC and DU is included both in the land and sea-ice modules of NorESM1-M. In a research version, the atmosphere module is also coupled with the advanced MOZART chemistry scheme (Emmons et al. 2010).

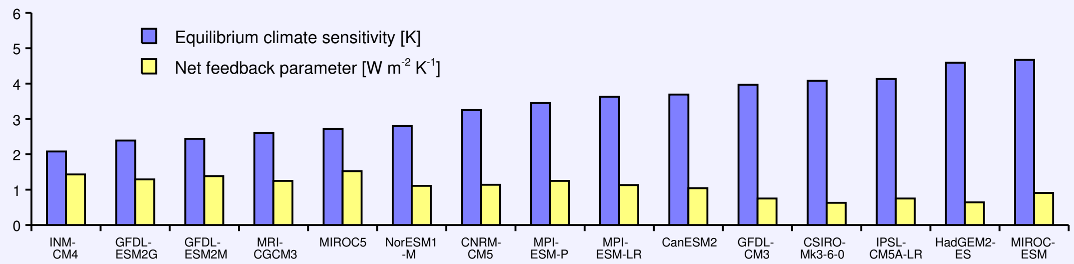

The equilibrium climate sensitivity, i.e. the change in global mean near-surface temperature at new equilibrium after abrupt doubling of CO_2, is estimated to be in the lower range of 15 climate and earth system models studied by Andrews et al. (2012).

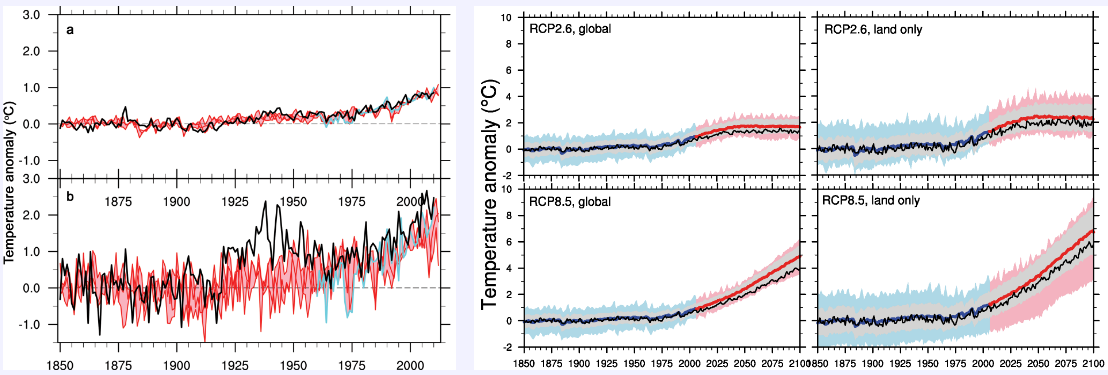

NorESM1-M calculated annual surface air temperature anomalies relative to the 1850–1899 average. Left (Bentsen et al. 2013): historical simulations (red and blue) and observations (black), globally (a) and north of 60°N (b). Right (Iversen et al. 2013): anomalies for RCP2.6 and RCP8.5 (see Table 8.2) averaged globally and over land areas. Black lines: NorESM1-M; blue and red lines: ensemble mean over 15 other models contributing to CMIP5; grey shading: one standard deviation on each side of the ensemble mean; blue and red shading: range defined by max and min values amongst the 15 models.

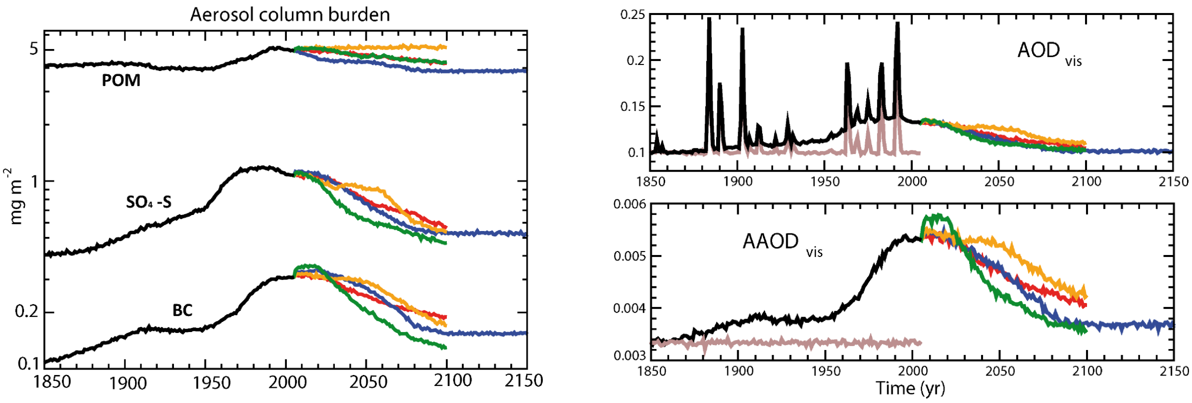

Figure 8.1: Globally and annually averaged aerosol column burdens for particulate organic matter (POM), SO_4 (as S), and black carbon (BC) (left panel), aerosol optical depth (AOD) (upper right panel), and aerosol optical depth for absorption (AAOD) (lower right panel) from 1850 onwards, calculated online in NorESM1-M. The black curves show the evolution over the period 1850 to 2005 (only one of three ensemble members is shown). Also shown is the evolution in different scenario projections: RCP2.6 for 2005–2100 (green), RCP4.5 for 2005–2300 with negligible variations after 2150 (blue), RCP6.0 for 2005–2100 (orange), and RCP8.5 for 2005–2100 (red). The brown curves are contributions to AOD and AAOD in the historical simulation by natural aerosols only, including prescribed stratospheric sulphate from explosive volcanoes. The figure is taken from Iversen et al. (2013).

RF to increased emissions of CH_4 (44 %), NO_x (31 %), CO (15 %), and non-methane VOCs (9 %). Apart from its role as GHG, tropospheric O_3 also affects the formation and atmospheric residence time of other short-lived climate forcers (e.g, as an oxidant in the formation of secondary aerosol).

Although O_3 and aerosols have a considerable impact on RF, the largest anthropogenic impact on RF is still assumed to come from long-lived and well-mixed GHGs (CO_2, CH_4, and N_2O). Shindell et al. (2013) indicate for year 2000 a RF of $2.30 \pm 0.23\,W\,m^{-2}$ from well-mixed GHGs, a RF of $0.43 \pm 0.20\,W\,m^{-2}$ from O_3, and an ERF of $-1.17 \pm 0.47\,W\,m^{-2}$ from aerosols (w.r.t. 1850). In addition to estimating the forcing, one also tries to attribute actual climate change and variability (in e.g. temperature and precipitation) since 1850 to possible causes. Therefore selected single forcing simulations were made as a part of the CMIP5 protocol, and here we present some results from the NorESM1-M model. Iversen et al. (2013) show results from three sensitivity experiments: in *GHG-forcing only*, all but the prescribed GHG concentrations are kept constant at the 1850-level; in *aerosol-forcing only* all but aerosol emissions are as in 1850, and in *natural forcing only*, only the natural contributions from solar activity and eruptive volcanoes are varied after 1850. Figure 8.2 shows results for surface air temperature and precipitation in these individual forcing experiments. For temperature it appears that the simulated warming since the 1970s cannot be reproduced with natural forcing only. Furthermore, GHGs alone lead to an exaggerated warming. When the effects of aerosols are taken into account together with GHG and natural forcing, however, the trend in the historical temperature record is well captured, globally. For global precipitation the picture is much less clear, although the increase since the 1970s seems to be reproducible by natural forcing only, at least globally. Even if the global trend in the annual precipitation is positive, there are considerable reductions in some continental regions (Iversen et al. 2013).

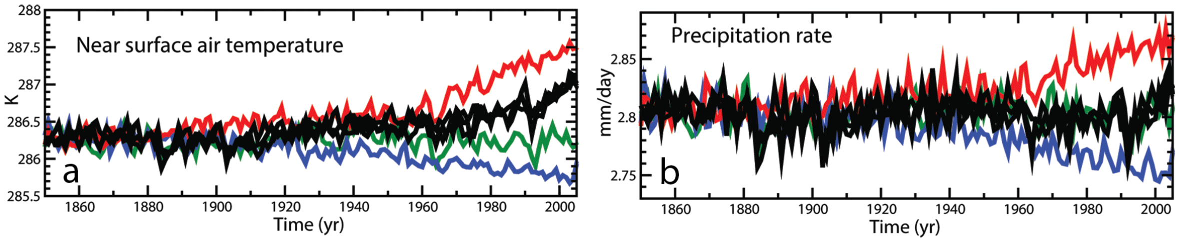

Figure 8.2: NorESM1-M single forcing simulations of the historical period 1850–2005. Response in annual mean surface air temperature (left panel) and average daily precipitation amounts (right panel): three historic simulations with full forcing (black), with natural forcing only (green), GHG-forcing only (red), and aerosol-forcing only (blue). The figure is taken from Iversen et al. (2013).

8.3 Sources of uncertainty in the BC climate impact

Several factors contribute to the uncertainty in the effect of BC on climate. Firstly, large uncertainties exist in the BC emission estimates. Bond et al. (2013) estimate the global BC emissions to be 7.5 Tg yr^{-1} in 2000, with an uncertainty range of 2 to 29 Tg yr^{-1}. In particular, there are possibly large emission uncertainties in regions where RF-efficiency is large and where an error in BC emissions would have a considerable impact on global and regional climate. Stohl et al. (2013) have investigated possible reasons for the underestimation by many models of BC in the Arctic. They point to the role of gas flaring and domestic combustion contributing to high concentrations of accumulation-mode aerosols in the Arctic in winter and early spring. They also show that a strong seasonal cycle in the domestic BC emissions can explain part of the observed seasonal cycle. Until recently, neither gas flaring nor the seasonal cycle of domestic BC emissions were well represented in emission data. One should also be aware that RF, especially regionally, can be impacted by the emission amounts assumed in the reference year (1850, 1750, or even earlier). Considerable uncertainties in the estimates of pre-industrial biomass burning emissions and its BC component therefore affect the net forcing of BC. Figure 8.3 shows European BC emission estimates (sum of anthropogenic and natural) for the years 1850 and 2000 (Lamarque et al. 2010). It shows a general increase in BC emissions over this period, but also regions with no changes or even a decrease in BC emissions (e.g. UK).

A second source of uncertainty is related to the fact that the atmospheric residence time of BC, its direct RF and its impact on clouds depend strongly on the interactions with other aerosol components (Bond et al. 2013). When calculating the climate effect of BC, one must be aware that it is often mixed with OC which is also produced during combustion. In contrast to BC, OC reflects much more sunlight than it absorbs. On the other hand, an internal mixture of BC with scattering aerosols can make the particle population more absorbing. This mixing can be caused by condensation of gaseous species on the surface of BC particles or by coagulation of BC with other aerosols.

Removal rates, and especially wet removal, affect most aspects of the RF of BC. They determine the lifetime of BC, its horizontal and vertical distribution, and its deposition rate over snow and ice. Samset et al. (2013) find that, based on a model inter-comparison exercise within the AeroCom framework, at least 20 % of the present uncertainty in modeled BC direct RF is due to differences in the vertical profile of BC. A considerable part of this uncertainty comes from variability at high altitudes, where BC to a large degree is located above clouds and therefore acts to reduce the planetary albedo more efficiently.

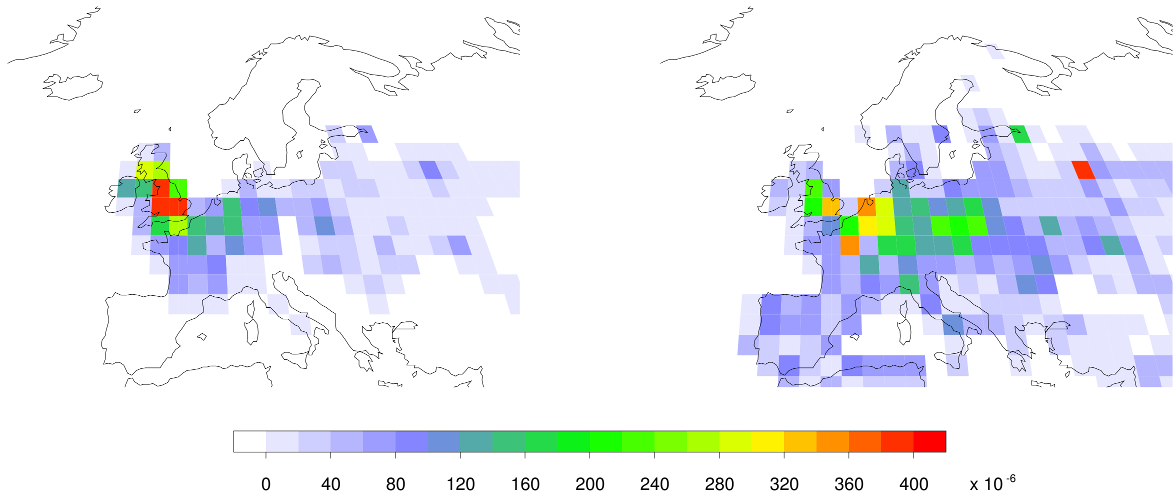

Figure 8.3: Annual BC emission estimates [kg m^{-2} yr^{-1}] in Europe in 1850 (left panel) and 2000 (right panel) from Lamarque et al. (2010).

Uncertainty in the impact of BC is also larger than that of GHGs, such as O_3, since BC can influence clouds, leading to impacts that are not fully understood (Bond et al. 2013). Models disagree on the sign and magnitude of liquid-cloud and semi-direct effects, and in addition, potentially large forcing terms and uncertainties come from the effects of BC on mixed-phase clouds, cloud-absorption and ice clouds. This implies that the uncertainties in the indirect RF of BC may be equal to or even larger than for the direct RF.

Finally, Bond et al. (2013) also mention that the lack of observational constraints hampers the ability to constrain the BC effect, since e.g., observations have difficulties in attributing atmospheric absorption to either BC, dust, or particulate matter (POM). Research within EMEP on BC monitoring would clearly help to study BC climate effects.

8.4 Source-receptor relationships changes in the future

Source-receptor relationships are expected to change in the future, and different factors might contribute to this.

Firstly, changes in emissions directly impact absolute-value source-receptor relationships. In all the RCP scenarios (see Table 8.2), aerosol-related anthropogenic and biomass burning emissions generally decrease in the 21st century, with global mean 2100 emissions roughly 80 % lower than today for SO_2, 50% for BC, and 10–40 % for POM (Shindell et al. 2013, van Vuuren et al. 2011). An illustration of this can be seen in the evolution of the aerosol burden in the NorESM1-M simulations for the 21st century in Fig. 8.1. For NH_3 however, emissions are estimated to increase by 10–80 % towards year 2100. Concerning O_3, reductions in its tropospheric burden are found for all RCP scenarios except RCP8.5 (Young et al. 2013). The changes in O_3 are the net result of the expected reduction in precursor emissions, doubled methane concentrations, and a net positive impact from climate change (see below).

Source-receptor relationships might also change due to changes in flow regimes and precipitation. The estimates of these changes are, however, considerably more uncertain than the estimates of temperature change. Iversen et al. (2013) find, using NorESM1-M, that precipitation is projected to increase in the tropics, decrease in the subtropics and in southern parts of the northern extra-tropics during summer, and otherwise increase in most of the extra-tropics.

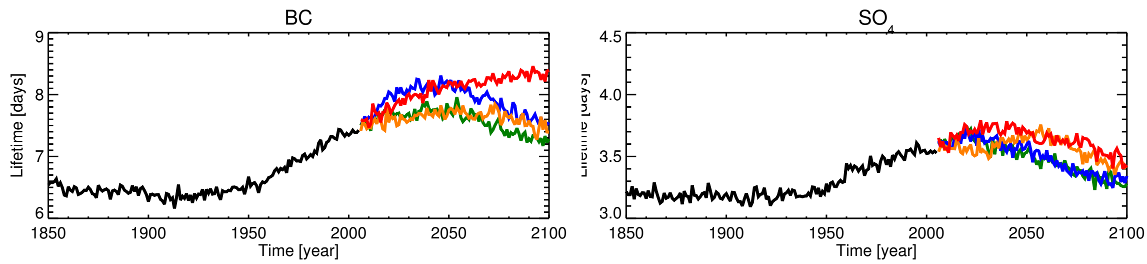

Figure 8.4: Global lifetime of BC (left panel) and SO_4 (right panel) as calculated in NorESM1-M, for the historical period (black line) and for four RCP scenarios: RCP2.6 (green), RCP4.5 (blue), RCP6.0 (orange), and RCP8.5 (red).

Precipitation events over continents will become more intense and dry spells more frequent. Extra-tropical storminess in the Northern hemisphere is projected to shift northwards – this has also been diagnosed in other climate model simulations as a response to anthropogenic GHG forcing (Yin 2005). There are indications of more frequent occurrences of spring and summer blocking in the Euro-Atlantic sector. However, these indications are uncertain because of biases in the models' representation of present-day conditions.

Stevenson et al. (2013) find some coherent response of O_3 to climate change in ACCMIP, with decreases of O_3 in the tropical lower troposphere (due to increases in water vapour), and increases in the sub-tropical to mid-latitude upper troposphere (due to increases in lightning and stratosphere-to-troposphere transport).

Source-receptor relationships might also change due to changes in the chemical state of the atmosphere. Modifications in the oxidizing capacity (mainly determined by OH and O_3) impact the lifetime of several species (e.g., CO, SO_2, ...). There are large uncertainties in the evolution of the OH distribution in the 21st century (Voulgarakis et al. 2013), however, similarly to inter-model diversity in the sign and magnitude of pre-industrial to present-day OH changes (Naik et al. 2013).

As an indicator of the fact that source-receptor relationships might change, we show in Fig. 8.4 the evolution of the global lifetime of BC and sulphate (SO_4) calculated with NorESM1-M, for the historical period, but also for four RCP scenarios. It indicates that the lifetime of BC peaks at the beginning of the 21st century, returning to a lower value at the end. For SO_4, the change in lifetime is less pronounced than for BC. As these lifetimes are global numbers, their change as function of time can also be caused by changes in emission patterns exposing emitted particles to a different meteorological regime, independent of changes in atmospheric conditions due to climate change. One should also take into account that the current NorESM1-M version uses fixed oxidants fields for the description of the oxidation in the sulphur cycle. Bell et al. (2005) have studied the impact of using online versus offline oxidant fields for the sulphur cycle, and found that the differences are small on annual and global scales, but that larger deviations occur on regional and seasonal scales. They also found that online coupling leads to increases of around 20 % in surface SO_4 over major SO_2 source regions in the Northern hemisphere.

Finally, in addition to changes in transport, transformation rates, and deposition due to a different climate or a modified oxidizing capacity of the atmosphere, climate change might also lead to considerably changed natural emissions, which can impact source-receptor relationships. Natural emissions from lightning, soil activity, sea-spray, ocean biochemistry, and biomass burning might all change in a changing climate.

8.5 Outlook

The Norwegian Meteorological Institute (MET Norway) is participating in a number of projects assessing the impact of climate change and the representation of certain atmospheric processes (see Table 8.3). Although NorESM1 has proven to be a valuable global climate model for research and for providing complementary results to the evaluation of possible anthropogenic climate change (e.g. Iversen et al. 2013, Bentsen et al. 2013), further improvements in the model are necessary.

Some of the planned improvements are to include nitrate aerosol in the aerosol scheme (a considerable number of climate models do not represent nitrate aerosol (Myhre et al. 2013)), a better description of secondary organic aerosol (SOA) formation, and a coupling of the interaction of aerosols with mixed-phase and ice clouds. Increased horizontal resolution in the atmospheric module of NorESM is expected to increase the model's ability to represent observed flow patterns. It is expected that these modifications will also improve the model's capability to quantify the interaction between air pollution and climate change.

Methane, a powerful GHG with a lifetime of around 8–12 years, is relatively long-lived compared to other major air pollutants, but much shorter-lived than well-mixed GHGs such as CO_2, N_2O, or SF_6. It has therefore become more and more common to consider it in the group of short-lived climate forcers. CH_4 is one of the few species for which one expects a further increase in emissions during the 21st century. The concentration of CH_4 in the atmosphere is mainly controlled by OH, and its increase since the pre-industrial era is responsible for a large part of the tropospheric O_3 increase during the same period (Stevenson et al. 2013). A new research project, funded by the Research Council of Norway, will support further development of the NorESM model to include CH_4 emissions and their effect on atmospheric chemistry and climate. For instance, large release of CH_4 can be expected due to climate change from thawing permafrost (Arctic Monitoring and Assessment Programme, http://www.amap.no/). Future versions of NorESM1 might be used to further investigate this.

In the future, links between the NorESM and EMEP model will be further strengthened. E.g., in the PEGASOS project, meteorological fields from NorESM will be used to drive the EMEP model. A consistent comparison of global models and the EMEP model is envisioned through the participation of EMEP in AeroCom and RF calculations within the EMEP model. It is also foreseen to contribute with both models to multi-model experiments, and to evaluate the coupled aerosol-gas chemistry in NorESM with EMEP data and EMEP model results. Both models will be used for joint exploration and analysis of future emission scenarios.

Table 8.1: Overview of climate and atmospheric pollution related model experiments

ACCMIP		Atmospheric Chemistry and Climate Model Inter-comparison Project
	Web	http://www.igacproject.org/ACCMIP
	Aim	Evaluation of the effect of short-lived species on climate, with focus on ozone and aerosols
	Period	1850–2005 (1850, 1930, 1980, 2000), different RCP scenarios for 2005–2100 (2030, 2050, 2100)
	Type	AGCMs and CTMs
	Result	O_3, aerosols, and RF
	Note	ACP/GMD Special Issue : http://www.atmos-chem-phys.net/special_issue296.html
AeroCom		Aerosol Comparisons between Observations and Models
	Web	http://aerocom.met.no/
	Aim	Understanding of the global aerosol and its impact on climate
	Period	Pre-industrial (1750 and 1850) and present-day (2000 and 2006)
	Type	AGCMs and CTMs
	Result	Aerosols, RF
HTAP		Task Force on Hemispheric Transport of Air Pollution
	Web	http://www.htap.org/
	Aim	Improve the understanding of the intercontinental transport of air pollution across the Northern hemisphere
CMIP5		Coupled Model Inter-comparison Project phase 5
	Web	http://cmip-pcmdi.llnl.gov/cmip5/
	Period	1850–2005, different RCP scenarios for 2005–2100
	Type	AOGCMs (Atmosphere Ocean General Circulation Models) and ESMs (Earth System Models)
	Result	Climate response: e.g. temperature, precipitation, circulation, climate variability (AO, NAO, El Niño, ...)

Table 8.2: Explanation of abbreviations

ERF	Effective Radiative Forcing: The top-of-the-atmosphere net energy flux change with ocean conditions held fixed but all other processes allowed to respond to aerosol changes. ERF thus includes the direct RF, aerosol indirect effects (affecting cloud albedo and lifetime), and responses of water vapor, lapse rate and clouds to aerosol thermodynamic impacts.
NorESM	Norwegian Earth System Model
RCP	Representative Concentration Pathways: RCP2.6, RCP4.5, RCP6.0, and RCP8.5. These scenarios are named by their nominal 2100 forcing relative to year 1750 (van Vuuren et al. 2011) and have been used for the upcoming IPCC AR5.
RF	Radiative Forcing: This term has been employed in the IPCC Assessments to denote an externally imposed perturbation in the radiative energy budget of the Earths climate system. Such a perturbation can be brought about by secular changes in the concentrations of radiatively active species. Typically, radiative forcing is quantified at the tropopause or at the top-of-the-atmosphere. A positive forcing generally warms the system, while negative forcing cools it.

Table 8.3: Overview of climate-related projects the Norwegian Meteorological Institute is involved in

ACCESS	Arctic Climate Change, Economy and Society http://www.access-eu.org/
CRAICC	CRyosphere-Atmosphere Interactions in a Changing Arctic Climate http://www.atm.helsinki.fi/craicc/
EarthClim	Integrated Earth System Approach to Explore Natural Variability and Climate Sensitivity http://www.uib.no/People/ngfhd/EarthClim/
ECLIPSE	Evaluating the CLimate and Air Quality ImPacts of Short-livEd Pollutants http://eclipse.nilu.no/
IS-ENES	Infrastructure for the European Network for Earth System Modelling https://is.enes.org/
PEGASOS	Pan-European Gas-AeroSOls-climate interaction Study http://pegasos.iceht.forth.gr/
IMPACT2C	Quantifying Projected Impacts under 2C warming http://www.hzg.de/mw/impact2c/
AMAP CH4-EG	The Expert Group on Methane under the Arctic Monitoring and Assessment Programme (AMAP) http://www.amap.no/
COST ES1004	European Framework for Online Integrated Air Quality and Meteorology Modelling http://eumetchem.info/

References

Andrews, T., Gregory, J. M., Webb, M. J., and Taylor, K. E.: Forcing, feedbacks and climate sensitivity in CMIP5 coupled atmosphere-ocean climate models, Geophys. Res. Lett., 39, L09 712, doi:10.1029/2012GL051607, 2012.

Bell, N., Koch, D., and Shindell, D. T.: Impacts of chemistry-aerosol coupling on tropospheric ozone and sulfate simulations in a general circulation model, J. Geophys. Res., 110, D14 305, doi:10.1029/2004JD00538, 2005.

Bentsen, M., Bethke, I., Debernard, J. B., Iversen, T., Kirkevåg, A., Seland, Ø., Drange, H., Roelandt, C., Seierstad, I. A., Hoose, C., and Kristjánsson, J. E.: The Norwegian Earth System Model, NorESM1-M Part 1: Description and basic evaluation of the physical climate, Geoscientific Model Dev., 6, 687–720, doi:10.5194/gmd-6-687-2013, 2013.

Bond, T. C., Doherty, S. J., Fahey, D. W., Forster, P. M., Berntsen, T., DeAngelo, B. J., Flanner, M. G., Ghan, S., Kärcher, B., Koch, D., Kinne, S., Kondo, Y., Quinn, P. K., Sarofim, M. C., Schultz, M. G., Schulz, M., Venkataraman, C., Zhang, H., Zhang, S., Bellouin, N., Guttikunda, S. K., Hopke, P. K., Jacobson, M. Z., Kaiser, J. W., Klimont, Z., Lohmann, U., Schwarz, J. P., Shindell, D., Storelvmo, T., Warren, S. G., and Zender, C. S.: Bounding the role of black carbon in the climate system: A scientific assessment, J. Geophys. Res., 118, 5380–5552, doi:10.1002/jgrd.50171, 2013.

Dessler, A. E., Zhang, Z., and Yang, P.: Water-vapor climate feedback inferred from climate fluctuations, 2003-2008, Geophys. Res. Lett., 35, L20 704, doi:10.1029/2008GL035333, 2008.

Emmons, L. K., Walters, S., Hess, P. G., Lamarque, J.-F., Pfister, G. G., Fillmore, D., Granier, C., Guenther, A., Kinnison, D., Laepple, T., Orlando, J., Tie, X., Tyndall, G., Wiedinmyer, C., Baughcum, S. L., and Kloster, S.: Description and evaluation of the Model for Ozone and Related chemical Tracers, version 4 (MOZART-4), Geoscientific Model Dev., 3, 43–67, doi:10.5194/gmd-3-43-2010, 2010.

Iversen, T., Bentsen, M., Bethke, I., Debernard, J. B., Kirkevåg, A., Seland, Ø., Drange, H., Kristjansson, J. E., Medhaug, I., Sand, M., and Seierstad, I. A.: The Norwegian Earth System Model, NorESM1-M Part 2: Climate response and scenario projections, Geoscientific Model Dev., 6, 389–415, doi:10.5194/gmd-6-389-2013, 2013.

Kirkevåg, A., Iversen, T., Seland, Ø., Hoose, C., Kristjánsson, J. E., Struthers, H., Ekman, A. M. L., Ghan, S., Griesfeller, J., Nilsson, E. D., and Schulz, M.: Aerosol-climate interactions in the Norwegian Earth System Model – NorESM1-M, Geoscientific Model Dev., 6, 207–244, doi:10.5194/gmd-6-207-2013, 2013.

Lamarque, J. F., Bond, T. C., Eyring, V., Granier, C., Heil, A., Klimont, Z., Lee, D., Liousse, C., Mieville, A., Owen, B., Schultz, M. G., Shindell, D., Smith, S. J., Stehfest, E., Van Aardenne, J., Cooper, O. R., Kainuma, M., Mahowald, N., McConnell, J. R., Naik, V., Riahi, K., and van Vuuren, D. P.: Historical (1850-2000) gridded anthropogenic and biomass burning emissions of reactive gases and aerosols: methodology and application, Atmos. Chem. Physics, 10, 7017–7039, doi:10.5194/acp-10-7017-2010, 2010.

Mieville, A., Granier, C., Liousse, C., Guillaume, B., Mouillot, F., Lamarque, J.-F., Grégoire, J.-M., and Pétron, G.: Emissions of gases and particles from biomass burning during the 20th century using satellite data and an historical reconstruction, Atmos. Environ., 44, 1469 – 1477, doi:10.1016/j.atmosenv.2010.01.011, 2010.

Myhre, G., Samset, B. H., Schulz, M., Balkanski, Y., Bauer, S., Berntsen, T. K., Bian, H., Bellouin, N., Chin, M., Diehl, T., Easter, R. C., Feichter, J., Ghan, S. J., Hauglustaine, D., Iversen, T., Kinne, S., Kirkevåg, A., Lamarque, J.-F., Lin, G., Liu, X., Lund, M. T., Luo, G., Ma, X., van Noije, T., Penner, J. E., Rasch, P. J., Ruiz, A., Seland, Ø., Skeie, R. B., Stier, P., Takemura, T., Tsigaridis, K., Wang, P., Wang, Z., Xu, L., Yu, H., Yu, F., Yoon, J.-H., Zhang, K., Zhang, H., and Zhou, C.: Radiative forcing of the direct aerosol effect from AeroCom Phase II simulations, Atmos. Chem. Physics, 13, 1853–1877, doi:10.5194/acp-13-1853-2013, 2013.

Naik, V., Voulgarakis, A., Fiore, A. M., Horowitz, L. W., Lamarque, J.-F., Lin, M., Prather, M. J., Young, P. J., Bergmann, D., Cameron-Smith, P. J., Cionni, I., Collins, W. J., Dalsøren, S. B., Doherty, R., Eyring, V., Faluvegi, G., Folberth, G. A., Josse, B., Lee, Y. H., MacKenzie, I. A., Nagashima, T., van Noije, T. P. C., Plummer, D. A., Righi, M., Rumbold, S. T., Skeie, R., Shindell, D. T., Stevenson, D. S., Strode, S., Sudo, K., Szopa, S., and Zeng, G.: Preindustrial to present-day changes in tropospheric hydroxyl radical and methane lifetime from the Atmospheric Chemistry and Climate Model Intercomparison Project (ACCMIP), Atmos. Chem. Physics, 13, 5277–5298, doi:10.5194/acp-13-5277-2013, 2013.

Petzold, A., Ogren, J. A., Fiebig, M., Laj, P., Li, S.-M., Baltensperger, U., Holzer-Popp, T., Kinne, S., Pappalardo, G., Sugimoto, N., Wehrli, C., Wiedensohler, A., and Zhang, X.-Y.: Recommendations for the interpretation of "black carbon" measurements, Atmos. Chem. Phys. Discuss., 13, 9485–9517, doi:10.5194/acpd-13-9485-2013, URL http://www.atmos-chem-phys-discuss.net/13/9485/2013/, 2013.

Raes, F., Streets, D., Fowler, D., Emberson, L., and Williams, M.: Integrated assessment report on black carbon and tropospheric ozone, 2011.

Samset, B. H., Myhre, G., Schulz, M., Balkanski, Y., Bauer, S., Berntsen, T. K., Bian, H., Bellouin, N., Diehl, T., Easter, R. C., Ghan, S. J., Iversen, T., Kinne, S., Kirkevåg, A., Lamarque, J.-F., Lin, G., Liu, X., Penner, J. E., Seland, Ø., Skeie, R. B., Stier, P., Takemura, T., Tsigaridis, K., and Zhang, K.: Black carbon vertical profiles strongly affect its radiative forcing uncertainty, Atmos. Chem. Physics, 13, 2423–2434, doi:10.5194/acp-13-2423-2013, 2013.

Shindell, D. T., Lamarque, J.-F., Schulz, M., Flanner, M., Jiao, C., Chin, M., Young, P. J., Lee, Y. H., Rotstayn, L., Mahowald, N., Milly, G., Faluvegi, G., Balkanski, Y., Collins, W. J., Conley, A. J., Dalsoren, S., Easter, R., Ghan, S., Horowitz, L., Liu, X., Myhre, G., Nagashima, T., Naik, V., Rumbold, S. T., Skeie, R., Sudo, K., Szopa, S., Takemura, T., Voulgarakis, A., Yoon, J.-H., and Lo, F.: Radiative forcing in the ACCMIP historical and future climate simulations, Atmos. Chem. Physics, 13, 2939–2974, doi:10.5194/acp-13-2939-2013, 2013.

Stevenson, D. S., Young, P. J., Naik, V., Lamarque, J.-F., Shindell, D. T., Voulgarakis, A., Skeie, R. B., Dalsoren, S. B., Myhre, G., Berntsen, T. K., Folberth, G. A., Rumbold,

S. T., Collins, W. J., MacKenzie, I. A., Doherty, R. M., Zeng, G., van Noije, T. P. C., Strunk, A., Bergmann, D., Cameron-Smith, P., Plummer, D. A., Strode, S. A., Horowitz, L., Lee, Y. H., Szopa, S., Sudo, K., Nagashima, T., Josse, B., Cionni, I., Righi, M., Eyring, V., Conley, A., Bowman, K. W., Wild, O., and Archibald, A.: Tropospheric ozone changes, radiative forcing and attribution to emissions in the Atmospheric Chemistry and Climate Model Intercomparison Project (ACCMIP), Atmos. Chem. Physics, 13, 3063–3085, doi:10.5194/acp-13-3063-2013, 2013.

Stohl, A., Klimont, Z., Eckhardt, S., and Kupiainen, K.: Why models struggle to capture Arctic Haze: the underestimated role of gas flaring and domestic combustion emissions, Atmos. Chem. Phys. Discuss., 13, 9567–9613, doi:10.5194/acpd-13-9567-2013, 2013.

van Vuuren, D. P., Edmonds, J., Kainuma, M., Riahi, K., Thomson, A., Hibbard, K., Hurtt, G. C., Kram, T., Krey, V., Lamarque, J.-F., Masui, T., Meinshausen, M., Nakicenovic, N., Smith, S. J., and Rose, S. K.: The representative concentration pathways: an overview, Climatic Change, 109, 5–31, doi:10.1007/s10584-011-0148-z, 2011.

Voulgarakis, A., Naik, V., Lamarque, J.-F., Shindell, D. T., Young, P. J., Prather, M. J., Wild, O., Field, R. D., Bergmann, D., Cameron-Smith, P., Cionni, I., Collins, W. J., Dalsøren, S. B., Doherty, R. M., Eyring, V., Faluvegi, G., Folberth, G. A., Horowitz, L. W., Josse, B., MacKenzie, I. A., Nagashima, T., Plummer, D. A., Righi, M., Rumbold, S. T., Stevenson, D. S., Strode, S. A., Sudo, K., Szopa, S., and Zeng, G.: Analysis of present day and future OH and methane lifetime in the ACCMIP simulations, Atmos. Chem. Physics, 13, 2563–2587, doi:10.5194/acp-13-2563-2013, 2013.

Yin, J. H.: A consistent poleward shift of the storm tracks in simulations of 21st century climate, Geophys. Res. Lett., 32, L18 701, doi:10.1029/2005GL023684, 2005.

Young, P. J., Archibald, A. T., Bowman, K. W., Lamarque, J.-F., Naik, V., Stevenson, D. S., Tilmes, S., Voulgarakis, A., Wild, O., Bergmann, D., Cameron-Smith, P., Cionni, I., Collins, W. J., Dalsøren, S. B., Doherty, R. M., Eyring, V., Faluvegi, G., Horowitz, L. W., Josse, B., Lee, Y. H., MacKenzie, I. A., Nagashima, T., Plummer, D. A., Righi, M., Rumbold, S. T., Skeie, R. B., Shindell, D. T., Strode, S. A., Sudo, K., Szopa, S., and Zeng, G.: Pre-industrial to end 21st century projections of tropospheric ozone from the Atmospheric Chemistry and Climate Model Intercomparison Project (ACCMIP), Atmos. Chem. Physics, 13, 2063–2090, doi:10.5194/acp-13-2063-2013, 2013.

Part IV

Appendices

APPENDIX A

National emissions for 2011 in the extended EMEP domain

This appendix contains the national emission data for 2011 used throughout this report for main pollutants and primary particle emissions in the extended EMEP domain. These are the emissions that are used as basis for the 2011 source-receptor calculations. Results of these source-receptor calculations are presented in Appendix C.

The emissions for 2011 have been derived from the 2013 official data submissions to UN-ECE CLRTAP (Mareckova et al. 2013).

Emissions from the eruption at Grímsvötn volcano in Iceland in May 2011 are not included in the table, as the eruption event has not been included in the model simulations. The reason for this is that the eruption plume reached heights up to 16 km, which is currently above the top layer of the EMEP MSC-W model, thus the plume and its transport can not be simulated by the current version of the model. As described in Chapter 3, extension of the model's vertical domain is currently under development.

Note that emissions in this appendix are given in different units than used elsewhere in this report in order to keep consistency with the reported data.

References

Mareckova, K., Wankmüller, R., Pinterits, M., and Moosman, L.: Inventory review 2013 stage 1 and 2 and review of gridded data, EMEP/CEIP Technical Report 1/2013, EEA/CEIP Vienna, 2013.

Table A:1: National total emissions for 2011 in the extended EMEP domain. Unit: Gg. (Emissions of SO_x and NO_x are given as Gg(SO_2) and Gg(NO_2), respectively.)

Area/Pollutant	SO_x	NO_x	NH_3	NMVOC	CO	$PM_{2.5}$	PM_{co}	PM_{10}
Albania	21	24	24	28	92	11	4	15
Armenia	29	21	16	41	131	0	0	1
Austria	19	183	62	128	609	19	16	35
Azerbaijan	94	98	68	305	564	5	1	6
Belarus	63	171	154	346	880	49	14	63
Belgium	56	210	67	101	387	17	7	24
Bosnia and Herzegovina	431	51	17	43	120	19	24	43
Bulgaria	515	136	48	91	285	29	15	45
Croatia	39	66	37	73	289	10	5	15
Cyprus	21	21	5	10	18	2	1	3
Czech Republic	169	226	66	140	382	17	16	32
Denmark	14	126	74	81	383	23	6	29
Estonia	73	36	10	33	148	26	15	42
Finland	61	153	37	107	455	37	13	51
France	255	1005	674	734	3584	173	88	260
Georgia	31	58	28	253	284	2	0	2
Germany	445	1293	563	1008	3314	111	98	209
Greece	270	296	62	187	492	54	32	85
Hungary	35	129	65	100	396	31	13	44
Iceland	81	21	5	5	18	0	0	1
Ireland	23	71	109	44	127	8	4	12
Italy	195	930	382	989	2464	128	28	156
Kazakhstan (KZT)	3309	465	852	245	1824	458	790	1248
Kyrgyzstan	29	67	32	35	445	12	11	23
Latvia	3	32	13	70	226	25	6	31
Lithuania	36	51	29	69	194	11	3	14
Luxembourg	2	48	5	9	39	2	1	3
Malta	8	8	2	3	12	1	1	1
Montenegro	28	9	3	8	23	4	3	7
Netherlands	34	259	119	144	529	14	15	29
Norway	19	178	26	138	309	37	7	44
Poland	910	851	270	652	2916	139	119	257
Portugal	47	176	47	176	372	44	19	63
Republic of Moldova	6	31	20	33	94	5	3	8
Romania	331	222	159	356	1014	109	15	124
Russian Federation (RUE)	2870	2961	1354	2762	14997	792	874	1666
Serbia	303	208	86	154	343	20	15	35
Serbia and Montenegro	0	0	0	0	0	0	0	0
Slovakia	68	85	24	68	227	29	4	32
Slovenia	11	45	17	32	148	15	3	19
Spain	489	915	381	596	1776	71	31	101
Sweden	30	145	52	177	570	29	12	40
Switzerland	10	74	63	86	231	10	10	20
Tajikistan	36	57	34	26	663	21	21	43
TFYR of Macedonia	101	40	10	25	72	7	4	11
Turkey	2652	1112	510	729	3036	247	93	340
Turkmenistan	160	65	44	34	368	45	54	99
Ukraine	1320	603	25	357	2949	41	93	133
United Kingdom	379	1033	290	752	2145	67	46	113
Uzbekistan	775	227	82	80	1223	155	236	390
North Africa	413	96	236	96	336	60	88	149
Asian areas (AST)	1470	430	881	665	3935	189	231	421
Baltic Sea	82	339	0	14	41	13	1	14
Black Sea	72	100	0	4	11	8	1	9
Mediterranean Sea	1365	1935	0	71	212	159	9	168
North Sea	192	798	0	30	88	31	2	33
Remaining N-E Atlantic Ocean	644	888	0	32	93	75	4	79
Natural marine emissions	743	0	0	0	0	0	0	0
Volcanic emissions	2500	0	0	0	0	0	0	0
TOTAL	24383	19878	8239	13576	56883	3717	3224	6941

APPENDIX B

National emission trends 1990-2011

This appendix contains trends of national emission data for main pollutants and primary particle emissions in the old EMEP domain for the years 1990, 2000 and 2005–2011.

The emissions for 1990, 2000 and 2005–2010 have been derived from the 2012 official data submissions to UNECE CLRTAP as of June 2012 (Mareckova et al. 2012), whereas emissions for 2011 have been derived from the 2013 official data submissions to UNECE CLRTAP as of June 2013 (Mareckova et al. 2013).

As these emissions are given for the old EMEP domain (132$\times$111 grid cells, see Chapter 1.3), the tables of this Appendix include a smaller part of the Russain Federation, Kazakhstan and Asian areas than does Appendix A. This means that, for instance, the 2011 emission numbers listed for the Russian Federation in the tables below are smaller than those listed in Appendix A.

These emissions listed in the tables below are used for the modelling of trends of depositions and air concentrations, which are presented in the country notes for 2011 (Appendix D) and in Chapter 3 and 6.

Emissions from the eruption at Grímsvötn volcano in Iceland in May 2011 are not included in the table, as the eruption event has not been included in the model simulation for 2011. The reason for this is that the eruption plume reached heights up to 16 km, which is above the layer of the EMEP MSC-W model, implying that the plume and its transport can not be simulated correctly by the current version of the model. As described in Chapter 3, an extension of the model's vertical domain is currently under development. On the other hand, the 2010 eruption of Eyjafjallajökull is included in the 2010 trend run, since it was possible to model this volcanic event because of the significantly lower eruption plume.

Note that emissions in this appendix are given in different units than used elsewhere in this report in order to keep consistency with the reported data.

References

Mareckova, K., Wankmüller, R., Whiting, R., and Pinterits, M.: Inventory Review 2012 stage 1 and 2 and review of gridded data, EMEP/CEIP Technical Report 1/2012, EEA/CEIP Vienna, 2012.

Mareckova, K., Wankmüller, R., Pinterits, M., and Moosman, L.: Inventory review 2013 stage 1 and 2 and review of gridded data, EMEP/CEIP Technical Report 1/2013, EEA/CEIP Vienna, 2013.

Table B:1: National total emission trends of sulphur, as used for trend modelling at the MSC-W (Gg of SO_2 per year).

Area/Year	1990	2000	2005	2006	2007	2008	2009	2010	2011
Albania	78	39	39	41	42	37	21	21	21
Armenia	85	11	8	6	26	26	26	26	29
Austria	74	32	27	28	25	22	17	19	19
Azerbaijan	615	162	129	105	99	91	85	85	94
Belarus	888	162	79	94	100	84	158	59	63
Belgium	362	172	145	135	125	97	77	67	56
Bosnia–Herzegovina	484	420	427	429	431	431	431	431	431
Bulgaria	1100	861	776	763	819	569	440	387	515
Croatia	174	62	63	60	68	58	59	41	39
Cyprus	31	48	38	32	30	23	18	22	21
Czech Republic	1876	264	219	211	216	174	173	170	169
Denmark	176	29	23	26	24	19	14	14	14
Estonia	274	97	76	70	88	69	55	83	73
Finland	263	79	69	84	83	70	59	67	61
France	1354	644	467	429	412	344	289	262	255
Georgia	42	6	13	22	18	22	23	26	31
Germany	5292	653	517	520	497	490	435	449	445
Greece	473	495	538	533	537	444	425	264	270
Hungary	1010	486	129	118	84	88	80	32	35
Iceland	21	35	38	44	58	74	69	72	81
Ireland	182	140	71	61	55	45	33	26	23
Italy	1794	749	403	381	338	283	232	210	195
Kazakhstan	651	506	425	398	381	381	381	381	381
Latvia	105	16	7	6	6	5	4	3	3
Lithuania	222	43	44	43	39	27	30	38	36
Luxembourg	15	3	3	2	2	2	2	2	2
Malta	29	24	11	11	12	11	8	8	8
Montenegro	0	14	13	14	12	15	8	8	28
Netherlands	192	73	65	64	61	51	37	34	34
Norway	52	27	24	21	20	20	15	19	19
Poland	3210	1511	1224	1222	1216	995	862	974	910
Portugal	295	281	177	155	149	108	74	67	47
Republic of Moldova	175	13	13	16	16	7	7	7	6
Romania	1311	759	643	697	577	566	460	372	331
Russian Federation	4671	1997	1847	1931	1624	1436	1340	1314	1302
Serbia Montenegro	593	0	0	0	0	0	0	0	0
Serbia	0	210	249	249	249	265	270	277	303
Slovakia	542	127	89	88	71	69	64	69	68
Slovenia	198	92	40	16	14	13	11	10	11
Spain	2097	1470	1282	1172	1157	513	463	434	489
Sweden	105	42	36	36	33	30	30	34	30
Switzerland	41	16	17	15	14	14	12	13	10
TFYR of Macedonia	110	90	101	87	100	114	113	83	101
Turkey	1519	2000	1417	1481	1490	1041	1557	1661	2652
Ukraine	3921	1599	1192	1446	1363	1386	1290	1216	1320
United Kingdom	3707	1228	706	665	586	491	397	406	379
North Africa	413	413	413	413	413	413	413	413	413
Asian areas	854	853	853	853	853	853	853	853	853
Baltic Sea	168	188	213	190	167	145	122	99	82
Black Sea	45	56	63	64	66	67	69	71	72
Mediterranean Sea	858	1068	1211	1234	1258	1282	1306	1329	1365
North Sea	361	443	501	448	394	341	288	234	192
N-E Atlantic Ocean	384	494	558	572	586	600	614	628	644
Nat. marine emissions	743	743	743	743	743	743	743	743	743
Volcanic emissions	8327	5746	2500	2500	2500	2500	2500	2627	2500
TOTAL	52562	27793	20973	21045	20347	18067	17560	17263	18271

Table B:2: National total emission trends of nitrogen oxides, as used for trend modelling at the MSC-W (Gg of NO_2 per year).

Area/Year	1990	2000	2005	2006	2007	2008	2009	2010	2011
Albania	22	21	29	28	27	29	24	24	24
Armenia	59	31	38	41	24	24	24	24	21
Austria	195	206	236	223	217	204	187	189	183
Azerbaijan	171	104	97	81	80	91	91	91	98
Belarus	379	208	171	187	181	189	189	170	171
Belgium	401	332	291	265	262	239	207	221	210
Bosnia–Herzegovina	73	53	52	52	51	51	51	51	51
Bulgaria	249	126	154	151	141	141	117	115	136
Croatia	95	74	81	82	87	85	76	71	66
Cyprus	17	22	21	21	22	20	20	18	21
Czech Republic	742	321	278	282	283	261	251	239	226
Denmark	275	199	181	182	168	150	132	129	126
Estonia	74	38	37	35	39	36	30	37	36
Finland	323	201	169	188	187	168	155	167	153
France	1865	1602	1430	1358	1289	1194	1106	1080	1005
Georgia	62	27	45	44	46	46	51	53	58
Germany	2882	1925	1578	1564	1491	1418	1321	1323	1293
Greece	329	362	419	415	416	394	382	322	296
Hungary	238	185	203	208	190	183	167	162	129
Iceland	27	27	25	25	26	24	24	22	21
Ireland	121	135	127	123	120	110	87	76	71
Italy	2014	1421	1212	1158	1127	1057	973	963	930
Kazakhstan	179	119	151	164	171	171	171	171	109
Latvia	65	36	37	37	38	34	32	34	32
Lithuania	158	47	58	61	69	55	54	58	51
Luxembourg	39	45	62	57	52	50	44	46	48
Malta	14	8	9	9	9	9	9	8	8
Montenegro	0	9	8	8	8	9	7	7	9
Netherlands	566	398	346	332	317	309	280	276	259
Norway	190	210	200	199	201	189	180	184	178
Poland	1280	838	866	921	860	832	822	867	851
Portugal	234	266	261	239	232	211	199	186	176
Republic of Moldova	131	27	31	25	25	32	29	29	31
Romania	546	296	309	309	326	287	252	272	222
Russian Federation	3600	2357	2795	3353	3407	3492	3426	2421	2369
Serbia Montenegro	165	0	0	0	0	0	0	0	0
Serbia	0	149	181	181	181	194	201	200	208
Slovakia	215	107	102	96	96	94	84	89	85
Slovenia	60	50	47	46	48	53	46	45	45
Spain	1224	1282	1305	1252	1246	1061	944	881	915
Sweden	269	205	174	173	168	158	153	161	145
Switzerland	145	110	94	90	86	83	80	79	74
TFYR of Macedonia	46	39	34	30	35	37	33	29	40
Turkey	691	1118	1080	1120	1200	860	1278	1090	1112
Ukraine	1753	871	513	488	732	825	528	603	603
United Kingdom	2885	1791	1580	1525	1461	1317	1143	1106	1033
North Africa	96	96	96	96	96	96	96	96	96
Asian areas	169	169	169	169	169	169	169	169	169
Baltic Sea	236	276	303	309	315	321	327	333	339
Black Sea	62	81	89	91	93	95	97	98	100
Mediterranean Sea	1234	1562	1725	1761	1796	1832	1868	1903	1935
North Sea	508	649	714	729	743	757	771	786	798
N-E Atlantic Ocean	565	723	796	811	827	842	858	874	887
Nat. marine emissions	0	0	0	0	0	0	0	0	0
Volcanic emissions	0	0	0	0	0	0	0	0	0
TOTAL	27940	21554	21011	21396	21484	20586	19846	18647	18252

Table B:3: National total emission trends of ammonia, as used for trend modelling at the MSC-W (Gg of NH_3 per year).

Area/Year	1990	2000	2005	2006	2007	2008	2009	2010	2011
Albania	29	29	27	26	24	24	24	24	24
Armenia	24	13	17	18	17	17	17	17	16
Austria	65	65	63	63	63	63	63	62	62
Azerbaijan	68	37	48	50	53	53	53	53	68
Belarus	215	142	135	134	144	147	150	151	154
Belgium	120	86	71	71	68	67	69	69	67
Bosnia–Herzegovina	21	17	17	17	17	17	17	17	17
Bulgaria	133	52	58	59	62	62	52	51	48
Croatia	51	39	40	40	40	38	37	37	37
Cyprus	5	6	6	6	5	5	5	5	5
Czech Republic	157	74	68	63	60	58	73	69	66
Denmark	114	91	83	79	80	78	75	75	74
Estonia	25	10	10	10	10	11	10	10	10
Finland	38	37	39	38	38	38	37	37	37
France	704	699	661	655	656	672	656	645	674
Georgia	36	34	35	30	26	26	26	27	28
Germany	692	602	573	569	567	568	576	548	563
Greece	85	71	68	66	68	65	62	64	62
Hungary	124	71	80	81	71	69	68	65	65
Iceland	3	3	3	3	3	3	3	3	5
Ireland	107	113	109	109	106	107	108	106	109
Italy	468	449	416	411	420	409	393	379	382
Kazakhstan	664	470	537	559	573	573	573	573	573
Latvia	48	13	16	16	16	16	17	17	13
Lithuania	84	25	39	35	36	29	28	30	29
Luxembourg	5	6	5	5	5	5	5	5	5
Malta	1	2	2	2	2	2	2	2	2
Montenegro	0	6	4	3	3	3	3	3	3
Netherlands	355	161	140	141	140	127	125	122	119
Norway	21	23	23	22	23	23	23	23	26
Poland	508	322	270	287	289	285	273	271	270
Portugal	63	61	50	48	49	47	47	48	47
Republic of Moldova	63	25	27	27	27	26	27	27	20
Romania	300	206	199	197	203	187	188	161	159
Russian Federation	1191	650	531	584	558	548	771	832	830
Serbia Montenegro	74	0	0	0	0	0	0	0	0
Serbia	0	82	77	77	77	89	84	82	86
Slovakia	66	32	29	27	27	25	25	24	24
Slovenia	20	19	18	18	19	18	18	17	17
Spain	316	378	365	376	386	354	355	368	381
Sweden	55	59	55	54	53	52	50	52	52
Switzerland	73	66	64	64	65	65	63	63	63
TFYR of Macedonia	15	14	7	7	7	7	7	10	10
Turkey	373	402	407	408	409	409	409	515	510
Ukraine	682	485	260	227	213	206	187	25	25
United Kingdom	360	328	307	307	296	283	283	284	290
North Africa	235	235	234	234	235	236	236	236	236
Asian areas	278	277	277	277	277	277	277	277	277
Baltic Sea	0	0	0	0	0	0	0	0	0
Black Sea	0	0	0	0	0	0	0	0	0
Mediterranean Sea	0	0	0	0	0	0	0	0	0
North Sea	0	0	0	0	0	0	0	0	0
N-E Atlantic Ocean	0	0	0	0	0	0	0	0	0
Nat. marine emissions	0	0	0	0	0	0	0	0	0
Volcanic emissions	0	0	0	0	0	0	0	0	0
TOTAL	9132	7083	6568	6598	6586	6488	6649	6580	6639

Table B:4: National total emission trends of non-methane volatile organic compounds, as used for trend modelling at the MSC-W (Gg of NMVOC per year).

Area/Year	1990	2000	2005	2006	2007	2008	2009	2010	2011
Albania	43	23	33	33	32	32	28	28	28
Armenia	95	47	49	50	41	41	41	41	41
Austria	276	178	162	172	159	150	121	133	128
Azerbaijan	376	233	210	234	238	238	238	238	305
Belarus	497	340	349	358	367	387	362	308	346
Belgium	315	206	143	148	127	118	105	105	101
Bosnia–Herzegovina	48	40	42	42	43	43	43	43	43
Bulgaria	620	87	86	90	84	84	91	91	91
Croatia	113	85	101	110	114	109	77	76	73
Cyprus	17	14	14	14	13	12	11	11	10
Czech Republic	374	227	183	180	174	166	151	151	140
Denmark	166	134	110	105	100	96	89	86	81
Estonia	70	46	41	40	41	38	37	38	33
Finland	239	168	136	131	129	118	111	116	107
France	2589	1712	1232	1123	1032	957	866	852	734
Georgia	108	77	214	220	235	231	228	215	253
Germany	3128	1391	1144	1132	1070	1017	931	1053	1008
Greece	268	264	220	230	219	228	212	184	187
Hungary	205	173	177	177	148	141	128	109	100
Iceland	12	7	6	6	6	6	5	5	5
Ireland	93	73	56	55	53	51	48	45	44
Italy	2015	1607	1317	1286	1261	1194	1131	1080	989
Kazakhstan	214	140	150	153	155	155	155	155	148
Latvia	102	65	73	75	83	74	61	65	70
Lithuania	108	61	84	78	74	66	66	69	69
Luxembourg	19	12	12	11	11	10	9	9	9
Malta	8	3	3	4	3	3	3	3	3
Montenegro	0	10	8	9	10	10	10	10	8
Netherlands	477	238	177	167	164	162	152	151	144
Norway	289	379	218	190	186	154	139	140	138
Poland	831	599	593	929	568	641	634	662	652
Portugal	295	254	210	203	198	192	180	175	176
Republic of Moldova	124	21	38	37	37	35	36	36	33
Romania	616	519	425	434	444	465	433	445	356
Russian Federation	3668	2450	2567	2222	2207	2323	2258	2242	2081
Serbia Montenegro	158	0	0	0	0	0	0	0	0
Serbia	0	122	135	135	135	133	127	138	154
Slovakia	122	66	73	70	67	67	64	62	68
Slovenia	55	44	37	36	35	33	34	35	32
Spain	1006	957	809	794	782	730	672	671	596
Sweden	359	223	197	194	197	196	197	197	177
Switzerland	289	144	103	99	95	93	91	89	86
TFYR of Macedonia	21	25	25	45	26	28	28	25	25
Turkey	636	794	1105	1289	1306	1000	1320	750	729
Ukraine	1053	641	324	295	408	311	275	357	357
United Kingdom	2762	1586	1088	1039	1002	922	822	789	752
North Africa	96	96	96	96	96	96	96	96	96
Asian areas	204	204	204	204	204	204	204	204	204
Baltic Sea	8	10	12	12	12	13	13	13	14
Black Sea	2	3	3	3	3	3	4	4	4
Mediterranean Sea	41	53	61	62	64	66	67	69	71
North Sea	18	23	26	26	27	28	29	29	30
N-E Atlantic Ocean	19	24	27	28	29	30	30	31	32
Nat. marine emissions	0	0	0	0	0	0	0	0	0
Volcanic emissions	0	0	0	0	0	0	0	0	0
TOTAL	25269	16898	14909	14876	14314	13697	13263	12730	12162

Table B:5: National total emission trends of carbon monoxide, as used for trend modelling at the MSC-W (Gg of CO per year).

Area/Year	1990	2000	2005	2006	2007	2008	2009	2010	2011
Albania	191	91	151	158	145	147	92	92	92
Armenia	450	167	186	193	126	125	125	125	131
Austria	1436	959	809	769	717	678	632	639	609
Azerbaijan	898	306	361	401	447	496	530	530	564
Belarus	759	725	969	1070	1033	1063	990	870	880
Belgium	1356	1028	717	704	618	614	381	461	387
Bosnia–Herzegovina	132	96	111	116	120	120	120	120	120
Bulgaria	731	370	350	361	308	285	254	275	285
Croatia	574	441	353	355	332	289	285	266	289
Cyprus	53	35	27	25	24	23	20	19	18
Czech Republic	1050	648	511	484	509	439	404	402	382
Denmark	722	470	449	442	453	433	407	399	383
Estonia	227	183	158	144	163	167	168	177	148
Finland	721	610	530	507	501	486	465	485	455
France	10920	6567	5311	4786	4520	4355	3666	3985	3584
Georgia	526	131	221	225	244	257	283	291	284
Germany	12372	4810	3659	3579	3482	3396	3011	3332	3314
Greece	1133	923	721	737	682	622	591	527	492
Hungary	997	633	587	569	507	512	313	480	396
Iceland	45	21	18	20	21	20	20	19	18
Ireland	418	253	192	183	172	159	152	139	127
Italy	7093	4802	3446	3234	3098	2964	2725	2711	2464
Kazakhstan	869	287	321	333	341	341	341	341	298
Latvia	455	288	282	277	265	249	267	258	226
Lithuania	519	282	190	200	208	177	169	211	194
Luxembourg	484	93	64	57	53	44	38	39	39
Malta	23	1	1	1	1	1	31	11	12
Montenegro	0	40	37	36	37	35	29	29	23
Netherlands	1124	756	659	649	629	632	580	577	529
Norway	744	510	385	362	351	336	320	332	309
Poland	7406	3463	3333	2804	2553	2717	2778	3076	2916
Portugal	832	722	569	542	520	521	486	387	372
Republic of Moldova	494	84	140	137	137	110	117	117	94
Romania	3186	1198	1257	1220	1459	1409	1349	1402	1014
Russian Federation	13329	10811	12277	10391	10729	11009	10474	10122	9979
Serbia Montenegro	431	0	0	0	0	0	0	0	0
Serbia	0	361	449	449	449	445	390	488	343
Slovakia	570	300	272	273	249	245	208	221	227
Slovenia	319	199	152	139	137	136	151	161	148
Spain	3596	2618	2077	2063	2049	1922	1687	1748	1776
Sweden	1278	823	661	626	617	607	612	639	570
Switzerland	775	415	323	300	280	270	257	250	231
TFYR of Macedonia	95	84	96	96	98	98	90	70	72
Turkey	3825	3956	3650	3690	3552	2004	3532	3532	3036
Ukraine	3725	2276	2923	2553	3182	2551	2425	2949	2949
United Kingdom	9087	5653	3510	3280	2982	2818	2317	2125	2145
North Africa	336	336	336	336	336	336	336	336	336
Asian areas	449	449	449	449	449	449	449	449	449
Baltic Sea	24	31	35	36	37	38	39	40	41
Black Sea	6	8	9	10	10	10	10	11	11
Mediterranean Sea	124	160	182	187	191	196	201	206	212
North Sea	52	67	75	77	79	81	83	85	88
N-E Atlantic Ocean	55	70	80	82	84	86	88	90	93
Nat. marine emissions	0	0	0	0	0	0	0	0	0
Volcanic emissions	0	0	0	0	0	0	0	0	0
TOTAL	97015	60608	54632	50715	50286	47522	45488	46644	44154

Table B:6: National total emission trends of fine Particulate Matter, as used for trend modelling at the MSC-W (Gg of $PM_{2.5}$ per year).

Area/Year	1990	2000	2005	2006	2007	2008	2009	2010	2011
Albania	7	9	14	14	13	14	11	11	11
Armenia	0	1	1	1	0	0	0	0	0
Austria	26	23	22	21	21	21	19	20	19
Azerbaijan	6	6	5	4	4	4	4	4	5
Belarus	40	40	46	52	51	53	52	45	49
Belgium	35	34	24	25	21	20	16	17	17
Bosnia–Herzegovina	20	20	19	19	19	19	19	19	19
Bulgaria	59	24	29	30	30	31	29	31	29
Croatia	20	10	13	12	11	11	10	10	10
Cyprus	1	4	3	3	3	3	2	2	2
Czech Republic	28	28	21	22	21	21	20	20	17
Denmark	23	22	25	26	30	28	25	26	23
Estonia	38	21	20	15	20	20	19	24	26
Finland	38	39	36	37	34	38	38	41	37
France	342	368	304	288	273	267	251	255	173
Georgia	3	3	2	2	2	2	2	2	2
Germany	115	143	121	119	114	110	106	111	111
Greece	49	49	54	55	56	63	63	63	54
Hungary	26	26	31	29	21	23	28	32	31
Iceland	1	1	1	1	0	0	0	0	0
Ireland	13	11	11	10	10	10	9	8	8
Italy	209	178	166	165	176	173	169	173	128
Kazakhstan	31	31	27	26	25	25	25	25	25
Latvia	11	23	27	27	26	26	28	27	25
Lithuania	17	17	9	9	10	9	9	10	11
Luxembourg	3	3	3	2	2	2	2	2	2
Malta	1	1	1	1	1	1	1	1	1
Montenegro	0	4	5	5	5	6	4	4	4
Netherlands	29	24	19	19	18	17	16	15	14
Norway	58	60	52	49	49	46	44	48	37
Poland	135	135	133	136	134	122	123	137	139
Portugal	95	74	65	61	61	59	57	49	44
Republic of Moldova	23	2	6	7	7	6	6	6	5
Romania	115	116	106	102	109	123	115	118	109
Russian Federation	694	694	350	409	348	316	312	418	367
Serbia Montenegro	45	0	0	0	0	0	0	0	0
Serbia	0	0	24	24	24	25	23	31	20
Slovakia	26	23	37	32	28	28	27	27	29
Slovenia	7	14	14	14	14	13	16	17	15
Spain	139	96	93	90	91	82	75	74	71
Sweden	46	28	29	29	29	28	28	32	29
Switzerland	9	12	11	10	10	10	10	10	10
TFYR of Macedonia	9	9	9	9	9	9	9	9	7
Turkey	305	305	268	255	247	247	247	247	247
Ukraine	289	289	278	274	272	276	276	77	41
United Kingdom	108	100	81	79	77	73	67	67	67
North Africa	0	60	60	60	60	60	60	60	60
Asian areas	0	114	114	114	114	114	114	114	114
Baltic Sea	22	22	25	23	21	19	17	15	13
Black Sea	6	6	7	7	8	8	8	8	8
Mediterranean Sea	123	124	141	144	147	150	152	155	159
North Sea	50	52	58	53	49	44	39	34	31
N-E Atlantic Ocean	57	57	65	67	68	70	71	73	75
Nat. marine emissions	0	0	0	0	0	0	0	0	0
Volcanic emissions	0	0	0	0	0	0	0	1673	0
TOTAL	3553	3559	3083	3088	2993	2945	2876	4496	2551

Table B:7: National total emission trends of Particulate Matter, as used for trend modelling at the MSC-W (Gg of PM_{10} per year).

Area/Year	1990	2000	2005	2006	2007	2008	2009	2010	2011
Albania	9	12	17	18	17	18	15	15	15
Armenia	1	1	1	1	1	1	1	1	1
Austria	44	39	38	37	36	37	35	35	35
Azerbaijan	7	7	5	5	4	4	4	4	6
Belarus	56	56	54	60	63	66	65	58	63
Belgium	66	46	34	34	30	28	23	24	24
Bosnia–Herzegovina	48	48	45	44	43	43	43	43	43
Bulgaria	94	42	51	53	57	59	49	51	45
Croatia	30	13	17	17	16	16	15	14	15
Cyprus	1	6	4	4	4	4	4	3	3
Czech Republic	44	44	34	35	35	35	36	37	32
Denmark	30	29	32	33	36	34	31	32	29
Estonia	51	37	27	20	29	25	23	32	42
Finland	54	54	50	52	48	52	52	55	51
France	549	502	428	410	393	385	364	367	260
Georgia	4	4	3	2	2	2	2	2	2
Germany	193	240	207	206	201	195	187	193	209
Greece	75	75	84	88	89	100	100	100	85
Hungary	60	47	52	48	36	38	48	46	44
Iceland	1	1	1	1	1	1	1	1	1
Ireland	20	17	17	16	16	15	13	13	12
Italy	273	209	197	197	207	204	198	202	156
Kazakhstan	56	56	45	41	39	39	39	39	39
Latvia	14	27	33	32	33	32	33	33	31
Lithuania	21	21	11	11	12	12	11	13	14
Luxembourg	4	4	4	3	3	3	3	3	3
Malta	1	1	2	2	2	2	2	1	1
Montenegro	0	8	8	9	8	10	7	7	7
Netherlands	48	39	33	33	32	32	30	29	29
Norway	64	66	59	56	56	53	50	54	44
Poland	279	282	284	285	269	247	249	279	257
Portugal	119	101	97	88	85	85	83	71	63
Republic of Moldova	41	5	8	8	8	10	10	10	8
Romania	171	172	126	123	137	144	136	143	124
Russian Federation	1161	1161	591	613	522	475	484	622	569
Serbia Montenegro	93	0	0	0	0	0	0	0	0
Serbia	0	0	40	40	40	40	38	46	35
Slovakia	45	45	42	37	32	31	31	30	32
Slovenia	9	19	19	18	18	17	19	20	19
Spain	208	140	135	131	133	117	108	107	101
Sweden	68	40	41	41	41	40	39	44	40
Switzerland	20	22	21	21	21	21	20	20	20
TFYR of Macedonia	21	21	19	19	18	18	18	18	11
Turkey	436	436	374	354	340	340	340	340	340
Ukraine	473	473	458	453	450	461	461	173	133
United Kingdom	180	171	135	133	131	126	114	114	113
North Africa	0	149	149	149	149	149	149	149	149
Asian areas	0	291	291	291	291	291	291	291	291
Baltic Sea	23	23	26	24	22	20	17	15	14
Black Sea	7	7	8	8	8	8	8	9	9
Mediterranean Sea	129	131	149	152	155	158	161	164	168
North Sea	52	54	62	56	51	46	41	36	33
N-E Atlantic Ocean	60	61	68	70	72	74	75	77	79
Nat. marine emissions	0	0	0	0	0	0	0	0	0
Volcanic emissions	0	0	0	0	0	0	0	5970	0
TOTAL	5519	5557	4734	4682	4542	4461	4376	10256	3949

APPENDIX C

Source-receptor tables for 2011

The source-receptor tables in this appendix are calculated for the meteorological and chemical conditions of 2011.

The tables are calculated for the extended EMEP domain and are based on model runs driven by ECMWF meteorology.

The source-receptor (SR) relationships give the change in air concentrations or depositions resulting from a change in emissions from each emitter country.

For each country, reductions in five different pollutants have been calculated separately, with an emission reduction of 15% for SO_x, NO_x, NH_3, NMVOC or PPM, respectively. Here reduction in PPM means that PPM_{fine} and PPM_{coarse} are reduced together in one simulation.

For year 2011, reductions in volcanic emissions are done only for passive SO_2 degassing of Italian volcanoes (Etna and Stromboli). Although there was an eruption episode at Grímsvötn volcano in Iceland in May 2011, this eruption event has not been included in the EMEP model simulations. The eruption plume reached heights up to 16 km, which is above the top layer of the EMEP MSC-W model. Therefore, the plume and its transport can not be simulated by the current version of the model. As described in chapter 3, extension of the model's vertical domain is currently under development.

The deposition tables show the contribution from one country to another. They have been calculated adding the differences obtained by a 15% reduction for all emissions in one country multiplied by a factor of 100/15, in order to arrive at total estimates.

For the concentrations and indicator tables, the differences obtained by the 15% emission reduction of the relevant pollutants are given directly. Thus, the tables should be interpreted as estimates of this reduction scenario from the chemical conditions in 2011.

The SR tables in the following aim to respond to two fundamental questions about transboundary air pollution:

1. Where do the pollutants emitted by a country or region end up?
2. Where do the pollutants in a given country or region come from?

Each column answers the first question. The numbers within a column give the change in the value of each pollutant (or indicator) for each receiver country caused by the emissions in the country given at the top of the column.

Each row answers the second question. The numbers given in each row show which emitter countries were responsible for the change in pollutants in the country given at the beginning of each row.

Note that more information on aerosol components and SR tables in electronic format can be found on the web.

The following SR tables are presented in this appendix, all in the extended EMEP domain, including new EECCA countries, and using 2011 ECMWF meteorology:

Acidification and eutrophication

- Deposition of OXS (oxidised sulphur). The contribution from SO_x, NO_x, NH_3, PPM and VOC emissions have been summed up and scaled to a 100% reduction.
- Deposition of OXN (oxidised nitrogen). The contribution from SO_x, NO_x, NH_3, PPM and VOC emissions have been summed up and scaled to a 100% reduction.
- Deposition of RDN (reduced nitrogen). The contribution from SO_x, NO_x, NH_3, PPM and VOC emissions have been summed up and scaled to a 100% reduction.

Ground Level Ozone

- $AOT40_f^{uc}$. Effect of a 15% reduction in NO_x emissions.
- $AOT40_f^{uc}$. Effect of a 15% reduction in VOC emissions.
- SOMO35. Effect of a 15% reduction in NO_x emissions.
- SOMO35. Effect of a 15% reduction in VOC emissions.

Particulate Matter

- $PM_{2.5}$. Effect of a 15% reduction in PPM emissions.
- $PM_{2.5}$. Effect of a 15% reduction in SO_x emissions.

- $PM_{2.5}$. Effect of a 15% reduction in NO_x emissions.
- $PM_{2.5}$. Effect of a 15% reduction in NH_3 emissions.
- $PM_{2.5}$. Effect of a 15% reduction in VOC emissions.
- $PM_{2.5}$. Effect of a 15% reduction in all emissions. The contribution from a 15% reduction in PPM, SO_x, NO_x, NH_3 and VOC emissions have been summed up.

Table C.1: 2011 country-to-country blame matrices for **oxidised sulphur** deposition.
Units: 100 Mg of S. **Emitters** →, **Receptors** ↓. (Based on ECMWF meteorology.)

	AL	AM	AT	AZ	BA	BE	BG	BY	CH	CY	CZ	DE	DK	EE	ES	FI	FR	GB	GE	GR	HR	HU	IE	IS	IT	KG	KZT	LT	LU	LV	MD	ME	
AL	37	0	0	0	10	0	11	0	0	0	1	1	0	0	1	0	0	0	0	27	1	0	0	0	4	-0	0	0	0	-0	0	3	AL
AM	0	62	-0	17	0	0	0	0	0	0	0	0	-0	0	0	0	0	0	4	0	0	0	0	0	0	0	3	0	0	0	0	0	AM
AT	0	0	29	0	18	1	4	0	3	0	18	45	0	0	6	0	7	3	0	1	4	3	0	0	11	0	0	0	0	-0	0	0	AT
AZ	0	13	0	153	0	0	0	0	0	0	0	0	0	0	0	0	0	0	15	0	0	0	0	0	0	0	23	0	0	0	0	0	AZ
BA	1	0	1	0	429	0	12	0	0	0	5	4	0	0	3	0	1	0	0	3	11	4	0	0	7	-0	0	0	0	0	0	11	BA
BE	0	0	0	-0	1	53	0	0	0	0	2	18	0	0	4	0	25	15	-0	0	0	0	0	0	0	0	0	0	1	-0	0	0	BE
BG	1	0	1	0	27	0	632	1	0	0	3	3	0	0	1	0	1	1	0	30	1	2	0	0	2	0	4	0	0	0	1	2	BG
BY	0	0	1	0	25	2	10	132	0	0	18	26	1	8	3	2	5	10	0	1	2	3	0	0	2	0	15	15	0	1	1	1	BY
CH	0	0	0	0	1	1	0	-0	18	0	1	7	0	0	6	0	12	2	-0	0	0	0	0	0	8	0	0	0	0	0	-0	0	CH
CY	0	0	0	0	0	0	1	0	0	3	0	0	0	0	0	0	0	0	0	1	0	0	0	0	0	0	0	0	0	-0	0	0	CY
CZ	0	0	5	0	20	2	5	0	1	0	172	55	0	0	4	0	7	4	-0	1	3	3	0	0	3	0	0	0	0	-0	0	1	CZ
DE	0	0	8	-0	13	47	3	0	9	0	83	924	2	1	32	1	107	70	-0	0	1	1	1	0	6	-0	0	1	2	-0	0	0	DE
DK	0	0	0	0	1	3	1	0	0	0	5	25	14	0	1	0	5	18	-0	0	0	0	0	0	0	-0	0	0	0	0	0	0	DK
EE	0	0	0	0	2	1	1	2	0	0	3	7	1	20	1	4	1	4	0	0	0	0	0	0	0	0	1	3	0	1	0	0	EE
ES	0	0	0	0	6	1	1	0	0	-0	4	9	0	0	848	0	18	4	0	0	1	0	0	0	7	-0	0	0	0	0	0	0	ES
FI	0	0	0	0	5	2	2	3	0	0	8	18	1	34	2	106	4	11	0	0	0	1	0	0	0	0	4	5	0	0	0	0	FI
FR	0	0	2	0	13	18	2	0	6	0	14	74	0	0	228	0	485	58	-0	1	2	1	2	0	25	-0	0	0	1	0	0	1	FR
GB	0	0	0	0	3	6	1	0	0	0	3	15	0	0	17	0	28	471	-0	0	0	0	14	1	1	0	0	0	0	0	0	0	GB
GE	0	10	0	27	1	0	2	0	0	0	0	0	-0	0	0	0	0	0	65	1	0	0	0	0	0	0	6	0	0	0	0	0	GE
GL	-0	0	0	0	0	0	0	0	0	-0	0	0	-0	0	0	0	0	0	0	0	0	0	0	2	0	0	0	0	0	-0	-0	0	GL
GR	4	0	0	0	18	0	209	0	0	0	2	2	0	0	2	0	1	1	0	269	1	1	0	0	5	0	2	0	0	0	0	2	GR
HR	1	0	2	0	121	0	9	0	0	0	6	5	0	0	6	0	2	1	0	4	42	5	0	0	13	-0	0	0	0	-0	0	3	HR
HU	1	0	4	0	101	1	23	0	0	0	15	12	0	0	7	0	3	2	0	3	14	63	0	0	8	-0	1	0	0	-0	0	3	HU
IE	0	0	0	0	0	0	0	0	0	0	0	1	0	0	3	0	2	16	0	0	0	0	34	0	0	0	0	0	0	0	-0	0	IE
IS	0	-0	0	0	0	0	0	0	0	-0	0	1	0	0	1	0	1	3	0	0	0	0	0	113	0	0	0	0	0	0	-0	0	IS
IT	3	0	4	0	105	1	29	0	3	0	8	11	0	0	42	0	30	2	0	19	17	3	0	0	337	0	1	0	0	-0	0	5	IT
KG	0	0	0	1	0	0	0	0	0	0	0	0	0	0	0	0	0	0	0	0	0	0	0	0	0	70	392	0	0	0	0	0	KG
KZT	0	14	0	40	7	0	11	5	0	0	4	5	0	4	1	2	1	2	8	3	0	1	0	0	0	36	6737	2	0	0	0	0	KZT
LT	0	0	0	0	5	1	1	7	0	0	8	14	1	2	1	1	3	5	0	0	0	1	0	0	0	0	1	51	0	1	0	0	LT
LU	0	-0	0	-0	0	1	0	-0	0	0	0	2	0	0	0	0	3	1	-0	0	0	0	0	0	0	-0	-0	0	1	0	-0	0	LU
LV	0	0	0	0	3	1	1	6	0	0	5	11	1	4	1	2	2	6	0	0	0	0	0	0	0	-0	2	16	0	7	0	0	LV
MD	0	0	0	0	3	0	10	1	0	0	1	1	0	0	0	0	0	0	0	1	0	0	0	0	0	0	2	0	0	0	8	0	MD
ME	3	0	0	0	13	0	4	0	0	0	1	0	0	0	1	0	0	0	0	2	0	0	0	0	2	0	0	0	0	-0	0	19	ME
MK	3	0	0	0	7	0	49	0	0	0	1	1	0	0	0	0	0	0	0	33	0	0	0	0	1	-0	0	0	0	0	0	1	MK
MT	0	-0	0	0	0	0	0	0	0	-0	0	0	-0	0	0	0	0	0	-0	0	0	0	0	-0	0	-0	0	0	0	-0	0	0	MT
NL	0	-0	0	0	1	25	0	0	0	-0	3	32	0	0	3	0	16	27	-0	0	0	0	1	0	0	-0	0	0	0	-0	0	0	NL
NO	0	0	0	0	4	4	1	1	0	0	5	24	2	2	6	3	8	38	0	0	0	0	1	3	0	0	1	1	0	0	-0	0	NO
PL	0	0	4	0	50	6	14	10	1	0	112	148	4	4	10	1	18	22	0	2	6	8	1	0	5	-0	2	6	0	0	1	1	PL
PT	0	0	0	0	0	0	0	0	0	-0	0	1	0	0	35	0	1	0	0	0	0	0	0	0	0	-0	0	0	0	0	0	0	PT
RO	2	0	2	0	88	1	152	2	0	0	14	15	0	1	5	0	4	3	0	14	4	11	0	0	6	0	8	1	0	0	4	7	RO
RS	4	0	1	0	104	0	69	0	0	0	6	4	0	0	3	0	1	1	0	13	5	8	0	0	5	0	1	0	0	-0	0	15	RS
RUE	2	18	4	72	112	8	119	90	1	1	70	106	4	196	19	83	21	44	23	25	6	9	1	2	9	5	5659	39	0	3	3	6	RUE
SE	0	0	1	0	8	6	2	2	0	0	17	52	8	9	5	17	12	37	0	0	1	1	1	1	1	-0	2	4	0	0	-0	0	SE
SI	0	0	2	0	14	0	2	0	0	0	2	2	0	0	3	0	1	0	0	1	8	1	0	0	10	-0	0	0	0	-0	0	0	SI
SK	0	0	2	0	31	1	9	0	0	0	17	9	0	0	4	0	2	1	0	1	4	13	0	0	4	0	0	0	0	-0	0	1	SK
TJ	0	0	0	0	0	0	0	0	0	0	0	0	0	0	0	0	0	0	0	0	0	0	0	0	0	2	54	0	0	0	0	0	TJ
TM	0	3	0	9	0	0	0	0	0	0	0	0	0	0	0	0	0	0	1	0	0	0	0	0	0	0	135	0	0	0	0	0	TM
TR	1	12	0	5	17	0	93	1	0	12	4	4	0	0	2	0	2	1	5	44	1	1	0	0	3	0	7	0	0	0	1	1	TR
UA	1	0	2	3	81	2	91	33	1	0	37	39	1	7	7	3	8	10	2	17	4	11	0	0	6	0	56	5	0	0	8	4	UA
UZ	0	2	0	6	0	0	0	0	0	0	0	0	0	0	0	0	0	0	1	0	0	0	-0	0	0	9	308	0	0	0	0	0	UZ
ATL	0	0	2	0	19	21	13	4	1	0	36	122	3	26	315	35	106	373	0	2	2	2	45	297	7	0	132	5	1	0	0	1	ATL
BAS	0	0	2	0	17	10	5	4	1	0	41	119	16	35	7	39	20	49	0	1	1	3	1	0	2	0	3	15	0	2	-0	1	BAS
BLS	1	3	1	6	26	1	153	4	0	1	14	12	0	2	2	1	2	3	20	28	1	3	0	0	3	0	25	2	0	0	4	1	BLS
MED	33	0	6	0	471	2	513	1	3	40	32	35	0	1	390	0	136	10	0	500	39	8	0	0	373	0	7	1	0	-0	1	33	MED
NOS	0	0	1	0	17	44	10	2	1	-0	35	167	9	2	37	1	116	542	0	1	1	1	10	4	3	0	1	2	1	0	0	1	NOS
AST	0	14	0	132	8	0	8	1	0	10	2	3	0	1	1	0	1	1	9	8	0	0	0	0	2	14	1199	0	0	0	0	0	AST
NOA	1	0	1	0	34	0	46	0	0	1	3	4	0	0	61	0	14	2	0	40	2	1	0	0	26	0	1	0	0	0	0	3	NOA
SUM	101	152	92	474	2060	274	2334	314	52	69	842	2200	69	361	2135	304	1242	1873	153	1098	188	175	116	425	912	137	14797	177	9	16	32	128	SUM
EXC	65	135	79	335	1468	195	1587	298	45	18	679	1738	41	295	1322	227	846	894	124	518	141	157	59	124	496	123	13430	152	7	14	27	89	EXC
EU	12	0	66	1	532	178	1094	34	25	3	517	1509	33	76	1263	133	784	781	0	344	67	114	56	4	435	0	29	89	6	9	6	26	EU
emis	105	145	93	468	2153	278	2573	316	51	105	845	2223	70	363	2446	305	1273	1894	153	1351	194	174	117	406	976	143	16544	178	9	16	32	139	emis
	AL	AM	AT	AZ	BA	BE	BG	BY	CH	CY	CZ	DE	DK	EE	ES	FI	FR	GB	GE	GR	HR	HU	IE	IS	IT	KG	KZT	LT	LU	LV	MD	ME	

Table C.1 Cont.: 2011 country-to-country blame matrices for **oxidised sulphur** deposition.
Units: 100 Mg of S. **Emitters →, Receptors ↓**. (Based on ECMWF meteorology.)

	MK	MT	NL	NO	PL	PT	RO	RS	RUE	SE	SI	SK	TJ	TM	TR	UA	UZ	ATL	BAS	BLS	MED	NOS	AST	NOA	BIC	DMS	VOL	SUM	EXC	EU	
AL	23	0	0	0	2	0	3	30	0	0	0	0	-0	0	4	3	0	0	0	0	18	0	0	2	6	1	54	246	164	53	AL
AM	0	0	0	0	0	-0	0	0	1	0	0	0	0	1	36	1	1	0	0	0	1	0	29	0	9	0	45	214	129	1	AM
AT	1	0	1	0	18	0	5	9	1	0	5	4	0	0	1	7	0	1	0	0	8	2	0	1	12	1	7	238	206	161	AT
AZ	0	0	0	0	2	-0	0	0	16	0	0	0	0	5	21	12	5	0	0	0	1	0	44	0	10	0	37	361	268	3	AZ
BA	3	0	0	0	18	0	9	50	1	0	0	5	-0	0	2	7	0	0	0	0	13	0	0	2	7	0	19	633	591	74	BA
BE	0	0	4	0	3	0	0	0	0	0	0	0	-0	0	0	1	0	3	0	0	1	13	-0	0	5	1	0	153	129	127	BE
BG	25	0	0	0	20	0	86	59	14	0	0	3	0	0	99	61	0	0	0	11	12	0	0	2	12	1	79	1200	1083	787	BG
BY	1	0	1	0	223	0	20	15	51	1	1	10	0	0	3	147	0	2	6	1	3	5	0	1	19	1	18	816	759	365	BY
CH	0	0	0	0	1	0	0	0	0	0	0	0	0	0	0	0	0	1	0	0	5	1	0	1	9	0	2	77	59	39	CH
CY	0	0	0	0	0	0	0	0	0	0	0	0	0	0	24	0	0	0	0	0	5	0	1	1	1	0	8	48	31	5	CY
CZ	1	0	1	0	67	0	8	15	2	0	1	14	0	0	0	12	0	1	1	0	3	2	0	0	9	1	4	428	407	353	CZ
DE	1	0	31	0	106	1	6	8	3	1	1	5	-0	0	0	20	0	17	18	0	11	62	0	1	49	8	6	1672	1499	1442	DE
DK	0	0	3	0	19	0	1	1	1	1	0	1	0	0	0	2	0	3	16	0	0	18	0	0	6	3	0	152	105	98	DK
EE	0	0	0	0	24	0	2	1	8	1	0	1	-0	0	0	6	0	1	8	0	0	2	0	0	4	1	1	113	95	74	EE
ES	0	0	1	0	8	21	2	3	0	0	0	1	-0	0	0	4	0	69	0	0	136	2	0	20	139	9	7	1325	942	927	ES
FI	0	0	2	2	63	0	5	3	56	13	0	3	0	0	1	20	0	3	21	0	1	8	0	0	28	4	3	445	376	280	FI
FR	1	0	5	0	23	5	3	5	1	0	1	3	-0	0	0	8	0	90	1	0	106	42	0	9	101	17	13	1367	988	951	FR
GB	0	0	4	0	7	1	1	1	1	0	0	1	0	0	0	4	0	83	1	0	3	44	0	0	49	22	2	786	583	572	GB
GE	0	0	0	0	3	0	2	1	8	0	0	0	0	2	59	14	1	0	0	4	1	0	17	0	12	0	55	291	200	8	GE
GL	0	-0	0	0	0	0	0	0	0	0	0	0	0	0	0	0	0	1	0	0	0	0	0	0	143	1	0	149	4	1	GL
GR	62	0	0	0	11	0	26	36	6	0	0	2	0	0	155	29	0	0	0	5	75	0	0	8	18	2	171	1130	849	532	GR
HR	2	0	0	0	19	0	10	39	1	0	2	5	0	0	2	8	0	0	0	0	25	0	0	2	7	1	13	359	309	89	HR
HU	5	0	0	0	55	0	42	81	3	0	2	27	-0	0	2	28	0	1	0	1	11	1	0	1	10	1	13	546	507	268	HU
IE	0	0	0	0	1	0	0	0	0	0	0	0	0	0	0	1	0	30	0	0	1	2	0	0	18	9	0	122	62	60	IE
IS	0	0	0	0	1	0	0	0	0	0	0	0	0	0	0	0	0	7	0	0	0	0	0	0	20	7	1	155	120	7	IS
IT	12	1	0	0	25	1	14	35	2	0	6	5	0	0	10	15	0	3	0	1	233	1	0	21	54	6	530	1596	746	538	IT
KG	0	0	0	0	0	0	0	0	4	0	0	0	30	6	3	2	699	0	0	0	0	0	40	0	47	0	70	1365	1207	0	KG
KZT	2	0	0	0	40	0	11	5	813	1	0	2	20	125	122	346	890	1	2	3	3	1	268	1	194	1	322	10061	9264	93	KZT
LT	0	0	1	0	93	0	4	3	11	1	0	3	0	0	0	20	0	1	5	0	1	3	0	0	7	1	2	262	242	193	LT
LU	0	0	0	0	0	0	0	0	0	0	0	0	0	-0	0	0	-0	0	0	0	0	0	-0	0	0	0	0	11	9	9	LU
LV	0	0	1	0	53	0	2	2	9	2	0	2	-0	0	0	12	0	1	7	0	0	3	0	0	6	1	1	172	151	117	LV
MD	1	0	0	0	11	0	20	3	5	0	0	1	0	0	9	42	0	0	0	2	1	0	0	0	2	0	13	140	121	47	MD
ME	2	0	0	0	2	0	1	16	0	0	0	0	0	0	1	1	0	0	0	0	7	0	0	1	3	0	14	96	72	14	ME
MK	73	0	0	0	3	0	5	27	1	0	0	1	-0	0	6	5	0	0	0	0	4	0	0	1	3	0	23	249	217	94	MK
MT	0	1	0	-0	0	0	0	0	0	0	0	0	-0	-0	0	0	-0	0	0	0	2	0	0	0	0	0	1	5	1	1	MT
NL	0	0	30	0	6	0	0	0	0	0	0	0	-0	0	0	2	0	4	1	0	1	41	0	0	6	2	0	203	148	144	NL
NO	0	0	3	29	27	0	2	3	7	5	0	1	0	0	0	5	0	20	8	0	1	31	0	0	51	14	2	314	186	133	NO
PL	3	0	5	0	1432	0	36	39	17	2	2	36	-0	0	1	107	0	5	14	1	6	12	0	1	30	4	14	2202	2116	1877	PL
PT	0	0	0	0	1	64	0	0	0	0	0	0	-0	0	0	0	0	44	0	0	8	0	0	2	37	2	1	198	104	103	PT
RO	18	0	0	0	79	0	569	96	25	0	1	15	0	0	51	178	0	1	1	10	12	2	0	2	24	1	76	1507	1377	892	RO
RS	25	0	0	-0	23	0	55	357	3	0	0	7	0	0	11	20	0	0	0	1	8	0	0	2	10	0	34	802	745	198	RS
RUE	21	0	5	4	608	1	128	70	10854	18	2	32	4	74	513	2183	263	21	46	32	27	28	175	4	1207	20	672	23771	21539	1554	RUE
SE	0	0	5	7	103	0	7	7	17	53	0	4	0	0	0	19	0	8	42	0	1	36	0	0	41	8	3	548	408	343	SE
SI	0	0	0	0	5	0	3	6	0	0	13	1	-0	0	1	2	0	0	0	0	9	0	0	1	3	0	3	94	78	46	SI
SK	2	0	0	0	62	0	17	25	2	0	1	57	0	0	0	17	0	0	0	0	5	1	0	1	6	0	5	302	284	201	SK
TJ	0	0	0	0	0	0	0	0	1	0	0	0	64	10	2	1	218	0	0	0	0	0	22	0	45	0	40	459	353	0	TJ
TM	0	0	0	0	1	0	0	0	18	0	0	0	4	146	15	12	173	0	0	0	1	0	149	0	69	0	52	792	521	3	TM
TR	10	0	0	0	22	0	32	21	32	0	0	2	0	1	4831	112	2	0	0	33	116	1	223	33	131	8	832	6661	5284	225	TR
UA	13	0	1	0	349	0	133	57	195	1	1	25	0	1	240	1712	3	3	4	25	17	5	3	3	52	4	125	3414	3174	760	UA
UZ	0	0	0	0	2	0	0	0	20	0	0	0	28	50	15	13	827	0	0	0	1	0	77	0	57	0	65	1483	1282	4	UZ
ATL	3	0	14	34	156	39	12	11	297	14	1	9	0	1	7	63	4	1930	18	0	40	88	2	8	4809	1194	47	10372	2236	1359	ATL
BAS	1	0	8	3	303	0	13	14	36	31	1	10	0	0	0	47	0	8	156	0	2	43	0	0	39	13	4	1127	861	732	BAS
BLS	10	0	0	0	104	0	125	33	156	0	1	9	0	1	990	682	3	1	2	168	32	2	22	5	42	15	164	2886	2433	467	BLS
MED	108	23	1	0	124	4	140	206	29	0	7	21	0	0	3060	187	1	18	2	35	4140	5	82	400	447	121	1855	13653	6548	2368	MED
NOS	2	0	36	13	137	2	8	11	5	3	1	6	0	0	1	22	0	102	22	0	8	441	0	1	137	92	5	2066	1258	1177	NOS
AST	2	0	0	0	15	0	4	3	157	0	0	1	22	139	375	147	334	1	1	3	52	1	2801	22	994	3	498	6990	2616	58	AST
NOA	9	3	0	0	11	2	15	17	3	0	0	2	0	0	148	18	0	8	0	2	342	1	4	306	395	14	121	1663	470	232	NOA
SUM	447	31	165	95	4491	145	1589	1425	12899	148	54	337	171	564	10825	6389	3426	2494	406	342	5521	955	3962	867	9654	1618	6154	108490			SUM
EXC	311	4	105	45	3642	97	1271	1130	12215	100	44	279	149	423	6243	5222	3084	426	205	133	905	375	1051	125	2790	167	3460		60095	14867	EXC
EU	132	3	93	11	2286	95	839	437	181	74	36	185	0	0	348	576	1	369	138	30	653	300	2	71	676	107	952		13526	11102	EU
emis	505	40	168	94	4550	233	1655	1515	14349	148	54	342	182	800	13258	6599	3876	3221	408	362	6826	961	7352	2065	0	3715	12500	121917	84507	22480	emis
	MK	MT	NL	NO	PL	PT	RO	RS	RUE	SE	SI	SK	TJ	TM	TR	UA	UZ	ATL	BAS	BLS	MED	NOS	AST	NOA	BIC	DMS	VOL	SUM	EXC	EU	

Table C.2: 2011 country-to-country blame matrices for **oxidised nitrogen** deposition.
Units: 100 Mg of N. **Emitters →, Receptors ↓**. (Based on ECMWF meteorology.)

	AL	AM	AT	AZ	BA	BE	BG	BY	CH	CY	CZ	DE	DK	EE	ES	FI	FR	GB	GE	GR	HR	HU	IE	IS	IT	KG	KZT	LT	LU	LV	MD	ME
AL	8	0	1	0	1	0	2	0	0	0	1	2	0	0	1	0	1	1	0	25	1	1	0	0	10	0	0	0	0	0	0	1
AM	0	13	0	11	-0	0	0	0	0	0	0	0	0	-0	0	0	0	0	3	0	0	0	0	0	0	0	0	0	0	0	0	0
AT	0	0	74	0	2	4	1	0	10	0	15	86	1	0	6	0	21	5	0	1	5	6	0	0	42	0	0	0	2	0	0	0
AZ	0	4	0	65	-0	0	0	0	0	0	0	1	0	0	0	0	0	0	13	0	0	0	0	0	0	0	3	0	0	0	0	0
BA	1	0	6	0	25	1	2	0	1	0	7	14	0	0	3	0	4	2	0	3	8	9	0	0	23	0	-0	0	0	0	0	2
BE	0	0	1	0	0	16	0	0	1	0	2	20	0	0	5	0	34	20	0	0	0	0	1	0	2	0	0	0	3	0	0	0
BG	2	0	4	0	2	1	78	2	1	0	5	13	1	0	2	0	4	3	0	25	2	7	0	0	7	0	0	0	0	0	3	0
BY	0	0	7	0	2	7	2	56	2	0	15	68	8	3	5	5	16	25	0	1	2	9	1	0	10	0	1	12	1	4	3	0
CH	0	0	3	0	0	2	0	0	30	-0	1	14	0	-0	5	0	30	4	0	0	0	0	0	0	29	-0	0	-0	1	-0	0	0
CY	0	0	0	0	0	0	0	0	0	2	0	0	0	-0	0	0	0	0	0	1	0	0	0	0	0	0	0	0	0	0	0	0
CZ	0	0	24	0	2	6	1	1	4	0	55	99	2	0	5	0	24	9	0	1	4	11	0	0	12	0	0	0	3	0	0	0
DE	0	0	44	0	2	77	1	3	29	0	56	605	11	1	37	2	235	125	0	1	3	7	5	0	33	0	0	1	27	1	0	0
DK	0	0	1	0	0	7	0	1	0	-0	4	36	4	0	2	0	14	31	0	0	0	1	1	0	1	0	0	0	1	0	0	0
EE	0	0	1	0	0	2	0	3	0	0	2	17	3	4	1	4	4	9	0	0	0	1	0	0	1	0	0	2	0	2	0	0
ES	0	0	4	-0	0	6	0	0	2	0	3	23	1	0	675	0	68	13	0	0	1	1	1	0	27	0	-0	0	2	0	0	0
FI	0	0	2	0	0	8	0	9	1	0	7	50	11	10	2	79	13	32	0	0	0	2	2	0	2	0	0	6	1	4	0	0
FR	0	0	17	0	1	42	0	1	22	0	14	137	3	0	246	0	644	106	0	1	3	4	6	0	106	0	0	0	13	0	0	0
GB	0	0	2	0	0	11	0	0	1	0	3	33	2	0	22	0	67	269	0	0	0	1	20	0	8	0	0	0	1	0	0	0
GE	0	4	0	15	-0	0	0	0	0	0	0	1	0	0	0	0	0	0	38	0	0	0	0	0	0	0	0	0	0	0	0	0
GL	-0	-0	0	-0	-0	0	-0	0	0	0	0	1	0	0	0	0	0	1	-0	0	-0	0	0	0	0	0	0	0	0	0	0	-0
GR	4	0	3	0	2	1	36	1	1	0	3	8	0	0	3	0	4	2	0	123	1	4	0	0	14	0	0	0	0	0	1	0
HR	1	0	12	0	11	1	2	0	1	0	8	17	0	0	7	0	6	2	0	3	17	9	0	0	43	0	0	0	0	0	0	1
HU	1	0	20	0	9	2	5	1	2	0	19	42	1	0	8	0	12	4	0	3	10	38	0	0	29	0	0	0	1	0	1	1
IE	0	0	0	0	0	2	0	0	0	0	0	3	0	0	4	0	7	20	0	0	0	0	10	0	1	0	0	0	0	0	0	0
IS	0	0	0	0	-0	1	-0	0	0	-0	0	3	0	0	1	0	2	5	0	0	0	0	0	5	0	0	-0	0	0	0	0	-0
IT	3	0	33	0	11	4	4	0	16	0	10	44	1	0	49	0	76	8	0	15	19	10	0	0	745	0	-0	0	1	0	0	1
KG	0	0	0	0	0	0	0	0	0	0	0	0	0	0	0	0	0	0	0	0	0	0	0	0	0	69	31	0	0	0	0	0
KZT	0	6	3	23	-0	4	1	11	1	0	5	29	5	1	3	8	10	21	7	2	1	2	1	1	5	56	570	2	1	2	2	0
LT	0	0	2	0	0	4	0	10	1	0	6	36	5	1	2	1	8	14	0	0	1	2	1	0	2	0	0	8	1	2	0	0
LU	0	0	0	0	0	1	0	0	0	0	0	2	0	0	1	0	4	1	0	0	0	0	0	0	0	0	0	0	2	0	0	0
LV	0	0	1	0	0	4	0	7	0	0	4	30	5	2	2	3	7	14	0	0	0	1	1	0	2	0	0	7	1	4	0	0
MD	0	0	1	0	0	0	2	2	0	0	2	5	0	0	0	0	1	1	0	1	0	1	0	0	1	0	0	0	0	0	3	0
ME	1	0	1	-0	2	0	1	0	0	0	1	2	0	0	1	0	1	0	0	2	1	1	0	0	6	-0	-0	0	0	0	0	3
MK	2	0	1	0	1	0	6	0	0	0	1	2	0	0	1	0	1	0	0	21	0	2	0	0	3	0	0	0	0	0	0	0
MT	0	0	0	0	0	0	0	0	0	0	0	0	0	0	0	0	0	0	0	0	0	0	0	0	0	0	0	0	0	0	0	0
NL	0	0	1	0	0	14	0	0	0	-0	2	26	1	0	4	0	25	32	0	0	0	0	1	0	2	0	0	0	1	0	0	0
NO	0	0	1	0	0	11	0	2	1	0	4	52	15	1	7	5	25	63	0	0	0	1	3	1	2	0	0	1	2	1	0	0
PL	0	0	25	0	4	26	3	16	5	-0	80	278	18	2	12	3	58	60	0	2	7	27	2	0	22	0	1	6	6	2	2	0
PT	0	0	0	-0	0	1	0	0	0	0	0	2	0	0	55	0	5	2	0	0	0	0	0	0	1	-0	-0	0	0	0	0	0
RO	2	0	13	0	7	3	29	5	3	0	17	49	3	0	7	1	13	9	0	11	5	27	0	0	24	0	1	1	1	0	9	1
RS	3	0	7	-0	9	1	14	1	1	0	9	19	1	0	3	0	5	3	0	14	4	16	0	0	16	0	0	0	0	0	1	3
RUE	1	7	33	39	5	43	18	168	9	0	63	340	56	53	27	143	93	177	21	18	7	29	8	3	47	8	476	46	10	29	13	1
SE	0	0	4	0	0	18	0	6	1	0	14	109	33	4	6	25	34	81	0	0	1	3	3	0	3	0	0	4	3	3	0	0
SI	0	0	11	0	1	0	0	0	1	0	3	9	0	0	3	0	3	1	0	0	6	2	0	0	24	0	0	0	0	0	0	0
SK	0	0	10	0	3	2	2	1	1	0	15	27	1	0	4	0	7	3	0	1	4	19	0	0	14	0	0	0	1	0	0	0
TJ	0	0	0	0	0	0	0	0	0	0	0	0	0	0	0	0	0	0	0	0	0	0	0	0	0	3	5	0	0	0	0	0
TM	0	1	0	8	-0	0	0	1	0	0	0	2	0	0	0	0	1	2	2	0	0	0	0	0	1	1	19	0	0	0	0	0
TR	1	5	4	4	1	2	20	3	1	7	4	16	1	0	4	1	7	5	5	25	1	4	0	0	13	0	1	1	0	0	3	0
UA	1	0	16	2	6	11	19	49	4	0	37	120	10	3	10	7	30	32	2	13	6	30	1	0	25	0	8	7	3	3	17	1
UZ	0	1	0	4	-0	0	0	1	0	0	0	3	0	0	0	1	1	2	1	0	0	0	0	0	1	11	39	0	0	0	0	0
ATL	0	0	20	-0	1	76	1	13	9	0	36	325	42	14	325	65	346	646	-0	2	2	8	70	34	33	0	11	7	14	5	1	0
BAS	0	0	9	0	1	28	1	12	3	0	26	190	32	8	10	30	57	102	0	1	2	7	4	0	7	0	0	10	5	6	1	0
BLS	1	2	10	4	2	4	31	11	2	0	13	44	4	1	3	3	13	14	17	18	2	11	1	0	11	0	3	2	1	1	12	0
MED	27	0	57	-0	41	18	85	5	22	22	35	141	5	0	452	2	352	57	1	331	47	34	4	0	922	0	0	1	6	0	6	8
NOS	0	0	11	0	2	66	2	5	7	0	25	241	32	1	49	3	207	559	0	2	2	6	26	1	22	0	0	2	9	1	0	0
AST	0	7	2	67	0	2	2	4	1	9	2	13	2	0	2	2	5	8	9	7	1	1	0	0	9	21	95	1	1	0	1	0
NOA	3	0	9	0	3	4	10	2	4	1	5	24	1	0	107	1	67	14	0	49	4	4	1	0	115	0	0	0	1	0	1	1
SUM	63	52	513	242	160	547	381	413	204	44	639	3474	320	109	2190	399	2672	2625	121	726	181	363	178	49	2479	168	1266	132	128	74	83	25
EXC	31	43	395	172	111	348	249	361	155	11	497	2495	204	86	1242	294	1627	1224	94	317	122	290	73	13	1359	147	1157	109	92	59	61	16
EU	12	0	297	1	49	262	161	67	103	2	338	1784	106	24	1163	122	1391	876	1	186	73	174	57	3	1124	0	3	39	72	20	19	5
emis	73	65	556	299	156	639	413	520	226	63	688	3935	382	109	2786	467	3060	3144	176	901	202	393	215	65	2830	204	1416	154	146	97	95	28

Table C.2 Cont.: 2011 country-to-country blame matrices for **oxidised nitrogen** deposition.
Units: 100 Mg of N. **Emitters →, Receptors ↓.** (Based on ECMWF meteorology.)

	MK	MT	NL	NO	PL	PT	RO	RS	RUE	SE	SI	SK	TJ	TM	TR	UA	UZ	ATL	BAS	BLS	MED	NOS	AST	NOA	BIC	DMS	VOL	SUM	EXC	EU	
AL	7	0	0	0	2	0	1	14	1	0	0	0	0	0	2	1	0	0	0	0	16	1	0	0	2	-0	0	107	87	51	AL
AM	0	0	0	0	0	0	0	0	1	0	0	0	0	0	14	0	0	0	0	0	1	0	3	0	2	-0	0	50	44	1	AM
AT	0	0	6	0	13	0	2	4	1	0	11	2	0	0	0	1	0	2	1	0	7	7	0	0	2	-0	0	345	325	299	AT
AZ	0	0	0	0	1	0	0	0	20	0	0	0	0	1	9	3	1	0	0	1	1	1	8	0	1	-0	0	135	124	4	AZ
BA	1	0	1	0	14	0	4	24	1	0	1	4	0	0	1	2	0	1	1	0	12	2	0	0	1	-0	0	182	165	99	BA
BE	0	0	6	0	2	1	0	0	0	0	0	0	0	0	0	0	0	5	1	0	1	14	0	0	4	0	0	142	116	114	BE
BG	6	0	1	1	16	0	39	27	17	1	1	3	0	0	32	23	0	1	2	9	12	4	0	0	-1	-0	0	357	329	211	BG
BY	0	0	11	3	120	1	9	6	62	6	2	8	0	0	1	48	0	5	21	1	4	27	0	-0	3	-0	-0	602	542	355	BY
CH	0	0	1	0	1	0	0	0	0	0	0	0	-0	0	0	0	0	1	0	0	4	3	0	0	3	-0	0	134	123	92	CH
CY	0	0	0	0	0	0	0	0	0	0	0	0	0	0	8	0	0	0	0	0	6	0	0	0	0	-0	0	20	13	4	CY
CZ	0	0	7	1	38	0	3	8	2	1	4	7	0	0	0	3	0	2	4	0	3	12	0	0	3	0	0	363	338	313	CZ
DE	0	0	77	5	67	3	3	4	6	4	3	5	0	0	0	6	0	30	24	0	11	125	0	0	31	1	0	1710	1488	1429	DE
DK	0	0	10	2	10	0	0	1	1	2	0	1	0	0	0	1	0	4	12	0	1	32	0	0	3	0	0	186	134	128	DK
EE	0	0	3	2	14	0	1	0	12	5	0	1	0	0	0	2	0	2	15	0	0	10	0	-0	1	0	-0	125	97	78	EE
ES	0	0	5	1	5	55	1	1	1	0	1	1	0	0	0	0	0	65	1	0	160	12	0	2	52	0	-0	1190	898	891	ES
FI	0	0	12	11	41	0	2	1	62	29	0	2	0	0	0	6	0	7	51	0	1	41	0	-0	6	0	0	515	408	317	FI
FR	0	0	28	2	15	15	2	2	2	1	3	2	0	0	0	2	0	89	4	0	104	97	0	1	39	0	0	1777	1442	1407	FR
GB	0	0	14	2	7	3	1	1	1	1	0	1	0	0	0	1	0	59	3	0	5	64	0	0	24	1	0	633	478	468	GB
GE	0	0	0	0	1	0	0	0	10	0	0	0	0	0	22	3	0	0	0	3	1	1	2	0	2	-0	0	108	99	6	GE
GL	0	-0	0	1	0	0	-0	0	1	0	0	0	0	-0	0	0	0	1	0	0	0	1	-0	-0	65	0	0	73	6	4	GL
GR	15	0	1	0	9	0	12	20	7	0	0	2	0	0	63	10	0	1	1	6	71	3	0	1	3	-0	0	435	349	224	GR
HR	1	0	1	0	14	0	4	17	1	0	5	4	0	0	1	2	0	1	1	0	22	3	0	0	2	-0	0	221	192	140	HR
HU	1	0	3	0	46	1	17	35	3	1	5	17	0	0	1	9	0	1	2	1	11	6	0	0	3	-0	0	376	351	277	HU
IE	0	0	2	0	1	1	0	0	0	0	0	0	0	0	0	0	0	16	1	0	1	6	0	0	7	0	0	82	52	51	IE
IS	0	0	1	0	1	0	-0	0	0	0	0	0	0	0	0	0	0	4	0	0	0	2	0	0	7	0	0	35	21	15	IS
IT	3	1	4	1	16	2	5	18	2	0	18	4	0	0	4	2	0	5	2	1	224	8	0	2	18	-0	1	1396	1135	1053	IT
KG	0	0	0	0	0	0	0	0	3	0	0	0	24	1	1	0	118	0	0	0	0	0	7	0	13	-0	0	272	251	2	KG
KZT	0	0	7	9	29	0	3	2	781	7	0	3	19	22	37	79	149	11	18	5	6	26	46	0	30	-1	1	2073	1932	158	KZT
LT	0	0	7	1	47	0	2	1	12	4	0	2	0	0	0	6	0	2	14	0	1	16	0	0	2	0	0	225	190	158	LT
LU	0	0	0	0	0	0	0	0	0	0	0	0	0	0	0	0	0	0	0	0	0	1	0	0	0	0	0	15	13	13	LU
LV	0	0	6	2	30	0	1	1	13	6	0	1	0	0	0	4	0	2	17	0	1	16	0	-0	1	0	-0	196	158	131	LV
MD	0	0	1	0	10	0	8	1	7	0	0	1	0	0	3	18	0	0	1	2	1	2	0	0	-1	-0	0	78	73	37	MD
ME	1	0	0	0	1	0	1	8	0	0	0	0	-0	0	0	0	0	0	0	0	5	0	0	0	1	-0	0	40	33	17	ME
MK	11	0	0	0	2	0	2	15	1	0	0	1	0	0	4	1	0	0	0	0	4	1	0	0	1	-0	0	85	79	44	MK
MT	0	0	0	0	0	0	0	0	0	0	0	0	0	0	0	0	0	0	0	0	1	0	0	0	0	0	0	2	1	1	MT
NL	0	0	17	1	3	1	0	0	0	0	0	0	0	0	0	0	0	7	2	0	1	27	0	0	6	0	0	176	133	130	NL
NO	0	0	16	47	16	1	0	1	7	17	0	1	0	0	0	1	0	15	27	0	1	74	0	0	14	0	0	437	306	246	NO
PL	1	0	36	5	413	1	16	15	21	8	6	26	0	0	1	38	0	12	44	1	7	70	0	0	14	0	0	1405	1257	1140	PL
PT	0	0	1	0	0	63	0	0	0	0	0	0	-0	-0	0	0	-0	38	0	0	11	1	0	0	17	0	-0	200	132	132	PT
RO	4	0	4	1	65	1	176	39	29	2	3	13	0	0	19	68	0	2	6	10	13	12	0	0	-3	-0	0	707	666	473	RO
RS	7	0	2	0	21	0	22	94	3	0	1	7	0	0	4	6	0	1	2	1	9	4	0	0	1	-0	0	317	300	163	RS
RUE	4	0	65	70	401	3	45	26	5505	83	5	27	4	12	140	518	34	67	208	31	45	226	28	-1	309	-2	5	9853	8935	1865	RUE
SE	0	0	28	27	68	1	2	2	22	62	1	3	0	0	0	5	0	14	85	0	1	107	0	0	13	0	0	799	579	512	SE
SI	0	0	1	0	4	0	1	3	0	0	12	1	0	0	0	1	0	0	0	0	8	1	0	0	1	-0	0	98	88	75	SI
SK	0	0	2	0	41	0	7	11	2	0	3	16	0	0	0	5	0	1	1	0	4	4	0	0	2	-0	0	218	205	176	SK
TJ	0	0	0	0	0	0	0	0	1	0	0	0	45	3	1	0	41	0	0	0	0	0	11	0	15	-0	0	127	101	1	TJ
TM	0	0	1	1	2	0	0	0	31	1	0	0	6	39	7	4	45	1	1	0	1	2	38	0	31	-0	0	252	177	12	TM
TR	2	0	2	1	16	0	15	9	47	1	1	2	0	0	984	42	0	3	3	37	112	6	18	4	21	-0	1	1470	1264	153	TR
UA	3	0	14	6	250	1	66	24	240	7	3	24	0	0	61	442	1	9	25	22	22	39	1	-0	-0	-0	0	1734	1617	743	UA
UZ	0	0	1	1	2	0	0	0	34	1	0	0	28	13	6	4	150	1	1	1	1	2	22	0	20	-0	0	355	307	13	UZ
ATL	1	0	101	118	121	71	1	5	263	48	2	8	0	0	2	19	0	817	92	1	50	379	0	0	2164	6	1	6378	2867	2388	ATL
BAS	0	0	41	14	130	1	5	4	37	38	1	6	0	0	0	11	0	17	113	0	3	114	0	0	14	1	0	1102	841	754	BAS
BLS	2	0	6	3	68	0	54	16	193	3	2	8	0	0	245	194	0	5	11	84	34	18	2	0	-22	-0	0	1166	1033	324	BLS
MED	29	14	18	5	75	19	50	104	39	3	22	17	0	0	705	54	0	53	12	43	2724	52	9	40	75	0	5	6848	3834	2742	MED
NOS	0	0	83	31	75	7	4	5	8	11	2	4	0	0	1	6	0	103	45	0	11	332	0	0	57	3	0	2072	1520	1450	NOS
AST	1	0	3	3	12	0	1	2	188	2	0	1	21	29	170	34	56	4	5	5	72	9	344	4	548	-0	1	1789	797	88	AST
NOA	4	3	4	1	12	6	9	11	9	1	3	2	0	0	69	8	0	13	2	5	578	10	1	38	282	-0	-0	1501	573	453	NOA
SUM	107	19	663	382	2365	264	598	585	7708	357	126	238	147	122	2620	1697	596	1504	887	272	4404	2032	541	94	3907	10	19	53286			SUM
EXC	70	2	407	206	1874	158	474	438	6972	251	94	192	126	93	1429	1369	539	491	606	135	933	1119	184	11	790	0	11		28151	14425	EXC
EU	32	1	282	65	970	150	292	196	215	127	74	110	0	0	131	195	0	369	294	29	665	697	0	7	249	3	3		11374	10203	EU
emis	122	24	790	541	2589	534	674	634	9010	443	136	259	174	198	3384	1836	691	2701	1031	304	5889	2430	1310	292	0	0	0	60498	46541	26426	emis
	MK	MT	NL	NO	PL	PT	RO	RS	RUE	SE	SI	SK	TJ	TM	TR	UA	UZ	ATL	BAS	BLS	MED	NOS	AST	NOA	BIC	DMS	VOL	SUM	EXC	EU	

Table C.3: 2011 country-to-country blame matrices for **reduced nitrogen** deposition.
Units: 100 Mg of N. **Emitters →, Receptors ↓**. (Based on ECMWF meteorology.)

	AL	AM	AT	AZ	BA	BE	BG	BY	CH	CY	CZ	DE	DK	EE	ES	FI	FR	GB	GE	GR	HR	HU	IE	IS	IT	KG	KZT	LT	LU	LV	MD	ME	
AL	69	0	1	0	0	0	0	0	0	0	0	1	0	0	1	0	1	0	0	10	1	1	0	0	7	0	0	0	0	0	0	1	AL
AM	0	60	0	42	0	0	0	0	0	0	0	0	0	0	0	-0	0	0	6	0	0	0	0	-0	0	0	2	0	0	0	0	0	AM
AT	0	0	179	0	1	2	0	0	24	0	19	122	1	0	6	0	22	2	0	0	6	10	0	0	59	0	0	0	0	0	0	0	AT
AZ	0	15	0	262	0	0	0	0	0	0	0	0	0	0	0	0	0	0	12	0	0	0	0	0	0	0	19	0	0	0	0	0	AZ
BA	2	0	5	0	51	0	1	1	1	0	4	9	0	0	3	0	2	0	0	2	26	12	0	0	20	0	0	0	0	0	0	1	BA
BE	0	0	2	0	-0	128	0	0	1	0	1	24	0	0	4	0	84	14	-0	0	0	0	2	0	1	-0	0	0	4	0	0	0	BE
BG	3	0	2	0	1	0	157	4	1	0	2	6	1	0	1	0	2	1	0	26	2	7	0	0	5	0	5	0	0	0	5	0	BG
BY	0	0	3	0	1	3	1	524	2	0	8	41	6	1	3	1	11	9	0	0	3	8	1	0	5	0	14	21	0	5	4	0	BY
CH	0	-0	3	0	0	1	0	0	248	0	0	22	0	0	5	0	44	2	0	0	0	0	0	0	36	0	0	0	0	0	0	0	CH
CY	0	0	0	0	0	0	0	0	0	6	0	0	0	0	0	0	0	0	0	0	0	0	0	0	0	-0	0	0	0	0	0	0	CY
CZ	0	0	34	0	1	3	1	1	6	0	186	121	2	0	4	0	23	3	0	0	6	14	0	0	10	0	0	0	0	0	0	0	CZ
DE	0	0	49	0	0	84	0	3	76	0	41	2112	18	0	28	0	317	58	-0	0	2	6	9	0	33	0	0	1	12	0	1	0	DE
DK	0	0	1	0	0	5	0	1	0	0	2	64	138	0	1	0	15	16	-0	0	0	1	2	-0	1	-0	0	0	0	0	0	0	DK
EE	0	0	0	0	0	1	0	7	0	0	1	12	3	27	0	2	3	3	0	0	0	1	0	0	0	0	1	4	0	5	0	0	EE
ES	0	0	2	0	1	3	0	0	2	-0	2	15	0	0	1457	0	93	6	0	0	1	1	2	0	21	-0	0	0	0	0	0	0	ES
FI	0	0	1	0	0	3	0	14	1	-0	3	32	8	6	2	159	10	10	0	0	0	2	2	0	1	0	2	6	0	4	0	0	FI
FR	0	0	14	0	1	41	0	1	49	0	7	116	3	0	233	0	2821	51	0	0	2	3	14	-0	96	0	0	0	4	0	0	0	FR
GB	0	0	1	0	0	12	0	0	1	-0	1	27	2	0	15	0	126	838	-0	0	0	1	107	0	4	-0	0	0	0	0	0	0	GB
GE	0	11	0	37	0	0	0	0	0	0	0	0	0	0	0	0	0	0	112	0	0	0	0	0	0	0	4	0	0	0	0	0	GE
GL	0	0	0	0	0	0	0	0	0	0	0	0	0	0	0	0	0	0	0	0	0	0	0	0	0	0	0	0	0	0	0	0	GL
GR	11	0	2	0	1	0	26	2	0	0	1	4	0	0	2	0	2	0	0	210	1	3	0	0	8	0	2	0	0	0	2	0	GR
HR	1	0	11	0	10	0	1	0	1	0	5	11	0	0	6	0	4	1	0	1	82	18	0	0	40	0	1	0	0	0	0	0	HR
HU	1	0	22	0	4	1	2	2	2	0	12	24	1	0	8	0	9	1	0	2	30	166	0	0	22	0	1	0	0	0	1	0	HU
IE	0	-0	0	0	0	1	0	0	0	-0	0	3	0	0	3	0	13	28	-0	0	0	0	334	-0	1	-0	0	0	0	0	0	0	IE
IS	0	0	0	0	0	0	0	0	0	0	0	2	0	0	1	0	2	3	0	0	0	0	1	14	0	0	0	0	0	0	0	0	IS
IT	5	0	20	0	3	1	3	1	25	0	5	27	0	0	37	0	46	2	0	7	13	8	0	0	1736	-0	1	0	0	0	0	1	IT
KG	0	0	0	1	0	0	0	0	0	0	0	0	0	0	0	0	0	0	0	0	0	0	0	0	0	138	63	0	-0	0	0	0	KG
KZT	0	10	1	42	0	0	1	16	0	0	1	7	1	1	1	1	2	2	11	2	0	1	0	0	2	61	3351	2	0	1	2	0	KZT
LT	0	0	1	0	0	2	0	38	1	0	4	27	5	1	1	1	7	5	0	0	1	2	1	0	1	0	1	78	0	5	1	0	LT
LU	0	-0	0	-0	-0	4	0	0	0	0	0	4	0	0	0	0	10	1	0	0	0	0	0	0	0	0	0	0	4	0	0	0	LU
LV	0	0	1	0	0	2	0	21	0	0	2	21	6	3	1	1	5	5	0	0	0	1	1	0	1	0	1	21	0	33	0	0	LV
MD	0	0	0	0	0	0	1	3	0	0	1	2	0	0	0	0	1	0	0	0	0	1	0	0	1	0	2	0	0	0	27	0	MD
ME	5	0	1	0	2	0	0	0	0	0	0	1	0	0	1	0	0	0	0	1	1	1	0	0	4	0	0	0	0	0	0	7	ME
MK	7	0	1	0	0	0	3	0	0	0	0	1	0	0	0	0	0	0	0	15	1	2	0	0	2	0	0	0	0	0	0	0	MK
MT	0	0	0	0	-0	0	0	0	0	-0	0	0	0	0	0	0	0	0	0	0	0	0	0	-0	0	-0	0	0	0	0	0	0	MT
NL	0	-0	1	-0	-0	44	0	0	1	-0	1	72	1	0	3	0	41	23	-0	-0	0	0	3	-0	1	-0	0	0	0	0	0	0	NL
NO	0	0	1	0	0	7	0	3	1	0	2	44	20	0	5	2	27	36	0	0	0	1	5	0	1	0	0	1	0	1	0	0	NO
PL	0	0	19	0	2	12	1	45	6	0	68	267	22	1	10	1	52	23	0	0	10	30	3	0	16	0	3	11	1	2	3	0	PL
PT	0	0	0	0	0	0	0	0	0	-0	0	2	0	0	79	0	6	1	0	0	0	0	0	0	1	-0	0	0	0	0	0	0	PT
RO	4	0	9	0	4	1	19	11	2	0	8	29	2	0	6	0	10	2	0	6	7	39	0	0	18	0	11	1	0	0	20	1	RO
RS	10	0	5	0	7	0	6	1	1	-0	5	10	1	0	3	0	3	1	0	5	15	25	0	0	13	0	1	0	0	0	1	2	RS
RUE	3	12	12	69	4	11	12	313	8	0	22	146	29	24	16	54	48	36	45	9	7	20	5	0	30	8	2359	44	1	26	16	0	RUE
SE	0	0	2	0	0	10	0	12	2	0	8	98	62	2	4	15	34	35	0	0	1	3	4	0	3	0	1	5	1	2	1	0	SE
SI	0	0	14	0	1	0	0	0	1	0	2	6	0	0	3	0	2	0	0	0	9	3	0	0	29	0	0	0	0	0	0	0	SI
SK	0	0	11	0	2	1	1	1	2	0	15	19	1	0	4	0	6	1	0	1	7	35	0	0	10	0	0	0	0	0	0	0	SK
TJ	0	0	0	0	0	0	0	0	0	0	0	0	0	0	-0	0	0	0	0	0	0	0	0	-0	0	4	9	0	-0	0	0	-0	TJ
TM	0	2	0	9	0	0	0	0	0	0	0	0	0	0	0	0	0	0	2	0	0	0	0	0	0	1	81	0	0	0	0	0	TM
TR	2	8	3	6	1	0	13	4	1	4	2	10	1	0	2	0	4	1	7	17	2	3	0	0	7	0	7	0	0	0	3	0	TR
UA	2	0	8	2	3	3	13	120	3	0	16	62	7	1	7	2	17	9	2	5	6	29	1	0	13	0	56	8	0	2	35	0	UA
UZ	0	2	0	7	0	0	0	0	0	0	0	0	0	0	0	0	0	0	1	0	0	0	0	0	0	16	109	0	0	0	0	0	UZ
ATL	0	0	12	0	1	35	1	16	11	0	14	201	31	3	299	20	625	486	0	1	2	5	307	30	30	0	21	5	2	2	1	0	ATL
BAS	0	0	5	0	1	16	0	24	4	0	15	247	125	12	7	34	54	37	0	0	2	7	5	-0	5	0	1	16	1	10	1	0	BAS
BLS	1	2	4	6	1	1	29	18	1	0	5	20	2	0	2	1	5	2	19	10	2	7	0	0	6	0	24	2	0	1	17	0	BLS
MED	47	0	28	0	20	4	55	8	19	15	15	55	2	0	310	0	253	9	1	120	33	27	3	0	655	0	6	1	0	0	7	5	MED
NOS	0	0	7	0	1	85	1	4	8	-0	10	325	96	0	31	1	448	531	0	0	2	4	66	0	12	-0	0	2	2	1	0	0	NOS
AST	1	9	1	81	1	0	1	4	1	4	1	4	0	0	1	0	2	0	10	4	1	1	0	0	7	22	515	0	0	0	0	0	AST
NOA	5	0	3	0	4	1	10	2	3	0	2	8	0	0	71	0	45	2	0	13	3	3	1	0	60	0	1	0	0	0	1	1	NOA
SUM	182	133	500	564	133	531	361	1229	516	31	520	4484	598	83	2690	297	5360	2298	228	469	289	513	882	46	3038	250	6678	233	37	104	153	21	SUM
EXC	127	121	440	477	104	390	264	1153	469	11	458	3624	342	68	1969	241	3928	1229	199	320	244	459	500	16	2263	227	6108	207	30	90	126	15	EXC
EU	26	0	386	1	22	362	211	164	203	6	390	3253	276	41	1913	180	3762	1129	1	252	100	336	485	0	2079	0	31	129	28	54	35	3	EU
emis	198	133	513	560	137	555	393	1270	518	42	541	4640	611	85	3135	305	5550	2389	227	507	303	534	895	44	3149	265	7016	241	38	107	163	23	emis
	AL	AM	AT	AZ	BA	BE	BG	BY	CH	CY	CZ	DE	DK	EE	ES	FI	FR	GB	GE	GR	HR	HU	IE	IS	IT	KG	KZT	LT	LU	LV	MD	ME	

Table C.3 Cont.: 2011 country-to-country blame matrices for **reduced nitrogen** deposition.
Units: 100 Mg of N. **Emitters →, Receptors ↓.** (Based on ECMWF meteorology.)

	MK	MT	NL	NO	PL	PT	RO	RS	RUE	SE	SI	SK	TJ	TM	TR	UA	UZ	ATL	BAS	BLS	MED	NOS	AST	NOA	BIC	DMS	VOL	SUM	EXC	EU	
AL	3	0	0	0	1	0	2	16	0	0	0	0	0	0	0	-0	0	0	0	-0	-0	0	0	2	5	-0	-0	125	119	28	AL
AM	0	0	0	-0	0	-0	0	0	1	0	0	0	0	0	57	0	0	-0	-0	0	0	-0	34	0	7	0	0	210	168	1	AM
AT	0	0	4	0	6	0	4	3	2	0	17	4	0	0	0	0	0	0	-0	0	0	-0	0	0	9	0	0	504	494	457	AT
AZ	0	0	0	-0	1	0	0	0	23	0	0	0	0	2	21	1	1	-0	0	0	0	0	24	0	8	0	0	390	358	2	AZ
BA	0	0	1	0	5	0	6	21	1	0	1	3	0	0	0	0	0	0	0	0	0	0	0	1	5	0	-0	188	181	76	BA
BE	0	0	25	0	1	0	0	0	0	0	0	0	-0	0	-0	0	0	-0	0	0	0	-1	0	0	4	0	-0	295	292	290	BE
BG	5	0	1	0	8	0	63	27	15	0	0	2	0	0	13	2	0	0	0	-0	0	0	0	1	9	0	0	379	369	284	BG
BY	0	0	6	1	109	0	15	4	54	4	1	4	0	0	1	5	0	0	-1	0	0	0	0	0	15	0	0	897	881	268	BY
CH	0	0	1	0	0	0	0	0	0	0	0	0	0	0	0	0	-0	0	-0	-0	0	-0	0	0	7	0	-0	371	364	116	CH
CY	0	0	0	0	0	0	0	0	0	0	0	0	-0	0	4	0	0	0	0	0	-0	0	1	1	1	-0	0	14	12	7	CY
CZ	0	0	5	0	28	0	6	6	2	0	4	12	0	0	0	1	0	0	0	0	0	0	0	0	7	0	0	489	481	458	CZ
DE	0	0	195	1	47	1	4	2	3	2	2	3	0	0	0	0	0	1	-1	-0	1	-7	0	0	36	0	-0	3143	3113	3025	DE
DK	0	0	13	1	7	0	0	0	0	3	0	0	0	-0	0	-0	-0	0	-1	-0	0	-2	0	0	4	-0	0	272	271	269	DK
EE	0	0	2	1	10	0	1	0	7	5	0	0	0	0	0	0	0	0	-0	0	0	0	0	0	3	0	0	101	97	82	EE
ES	0	0	2	0	3	44	1	1	0	0	1	1	-0	0	0	0	0	-2	0	0	-5	1	0	11	102	-0	-0	1767	1660	1654	ES
FI	0	0	6	3	25	0	3	1	27	20	0	1	0	0	0	1	0	1	0	0	0	1	0	0	22	0	0	379	355	304	FI
FR	0	0	20	0	8	8	2	1	1	0	2	2	0	0	0	0	-0	-8	0	0	-1	-6	0	3	76	-1	-0	3563	3501	3445	FR
GB	0	0	14	0	3	1	1	0	0	0	0	0	-0	0	0	1	-0	-6	-0	0	0	-3	-0	0	36	-1	0	1187	1161	1156	GB
GE	0	0	0	0	1	0	1	0	25	0	0	0	0	1	78	0	0	0	0	-0	0	0	10	0	10	0	0	292	271	3	GE
GL	0	0	0	0	0	0	0	0	0	0	0	0	0	0	0	0	0	0	0	0	0	0	0	0	111	0	0	113	2	1	GL
GR	7	0	0	0	3	0	14	16	6	0	0	1	0	0	19	1	0	0	0	-0	-1	0	0	7	14	-0	-0	366	346	278	GR
HR	0	0	1	0	5	0	6	16	1	0	10	3	-0	0	0	0	0	0	-0	0	0	0	0	1	6	0	0	245	238	124	HR
HU	1	0	2	0	14	0	34	38	4	0	7	18	0	0	0	0	0	0	0	-0	0	0	0	1	8	0	0	441	431	346	HU
IE	0	0	1	0	1	0	0	0	0	0	0	0	-0	-0	0	0	-0	-4	-0	0	0	-1	-0	0	13	-1	0	395	387	387	IE
IS	0	0	0	0	0	0	0	0	0	0	0	0	0	0	0	0	0	0	0	0	0	0	0	0	15	0	0	40	25	10	IS
IT	1	0	1	0	5	1	7	11	2	0	12	2	-0	0	2	0	0	0	-0	0	-7	0	0	12	41	-0	-1	2030	1985	1920	IT
KG	0	0	0	0	0	-0	0	0	2	0	0	0	36	2	2	0	105	0	0	0	0	0	25	0	37	0	0	414	351	0	KG
KZT	0	0	1	0	11	0	5	1	640	1	0	1	22	46	70	3	128	0	0	0	0	0	219	1	149	0	2	4822	4450	45	KZT
LT	0	0	4	0	53	0	3	1	12	4	0	1	0	0	0	0	0	0	-0	-0	0	1	0	0	5	0	0	267	261	206	LT
LU	0	0	0	0	0	0	0	0	0	0	0	0	0	0	0	-0	0	-0	0	-0	0	-0	-0	0	0	0	0	25	24	24	LU
LV	0	0	4	0	25	0	1	1	8	6	0	1	0	0	0	0	0	0	-0	-0	0	1	0	0	5	0	0	178	173	140	LV
MD	0	0	0	0	3	0	24	1	5	0	0	0	0	0	1	1	0	0	-0	-0	0	0	0	0	2	0	0	79	77	36	MD
ME	0	0	0	0	1	0	1	9	0	0	0	0	0	0	0	0	0	0	0	0	0	0	0	1	2	0	0	39	36	12	ME
MK	26	0	0	0	1	0	3	17	1	0	0	0	0	0	1	0	0	0	0	-0	0	0	0	1	3	0	0	87	83	30	MK
MT	0	1	0	0	0	0	0	0	0	0	0	0	-0	0	0	-0	0	-0	-0	-0	-0	0	0	0	0	-0	-0	1	1	1	MT
NL	0	-0	260	0	2	0	0	0	0	0	0	0	-0	0	-0	-0	-0	-0	-0	-0	0	-2	-0	0	4	-0	-0	455	453	452	NL
NO	0	0	13	102	12	0	1	1	2	15	0	0	0	0	0	0	0	1	0	0	0	1	0	0	38	0	0	346	305	196	NO
PL	0	0	26	1	1008	0	28	12	17	8	5	20	0	0	0	3	0	1	-0	0	1	1	0	0	24	0	0	1768	1741	1635	PL
PT	0	0	0	0	0	131	0	0	0	0	0	0	-0	-0	0	0	0	1	0	0	-0	0	0	1	28	0	0	250	220	220	PT
RO	2	0	2	0	26	0	592	43	27	1	2	7	0	0	6	2	0	0	0	-0	1	0	0	1	19	0	0	944	923	783	RO
RS	6	0	1	0	7	0	37	256	3	0	1	4	0	0	1	0	0	0	-0	-0	0	0	0	1	7	0	-0	440	431	125	RS
RUE	2	0	21	8	195	1	68	18	8802	36	3	10	4	26	177	54	32	2	2	0	2	5	140	2	1034	1	4	14043	12851	882	RUE
SE	0	0	22	18	52	0	4	2	10	184	0	2	0	0	0	2	0	1	-1	0	0	1	0	0	32	0	0	637	603	555	SE
SI	0	0	0	0	1	0	2	2	1	0	42	1	0	0	0	0	0	0	-0	0	0	-0	0	0	2	0	0	122	119	106	SI
SK	0	0	1	0	20	0	13	10	2	0	3	55	0	0	0	0	0	0	0	0	0	0	0	0	5	0	0	229	223	197	SK
TJ	0	-0	0	0	0	-0	0	0	1	0	0	0	126	4	1	0	34	-0	0	0	0	-0	37	0	32	0	-0	249	179	0	TJ
TM	0	0	0	0	0	0	0	0	19	0	0	0	6	109	12	1	39	0	0	0	0	0	50	0	49	0	0	380	281	2	TM
TR	1	0	1	0	7	0	18	7	33	0	0	1	0	1	2336	-1	0	0	0	-1	-0	0	128	30	100	0	-5	2768	2516	97	TR
UA	1	0	6	1	138	0	113	18	193	4	2	11	0	1	40	80	0	1	0	0	1	1	1	1	39	0	0	1090	1044	479	UA
UZ	0	0	0	0	0	0	0	0	20	0	0	0	41	23	10	0	228	0	0	0	0	0	34	0	39	0	0	534	460	2	UZ
ATL	0	0	54	48	53	61	6	2	98	21	2	3	0	0	1	5	0	-15	2	0	2	3	2	5	3763	-2	0	6277	2516	2278	ATL
BAS	0	0	38	6	120	0	7	3	20	83	1	3	0	0	0	0	0	1	-7	0	0	-5	0	0	28	-1	0	930	913	849	BAS
BLS	1	0	2	0	26	0	70	11	156	1	1	3	0	1	239	20	0	0	0	-2	1	0	10	3	30	-0	1	764	721	199	BLS
MED	12	8	4	0	25	7	66	70	28	1	13	7	0	0	284	9	0	1	0	0	-19	1	57	249	313	-1	1	2836	2233	1684	MED
NOS	0	0	183	22	37	3	4	3	2	13	1	2	0	0	0	0	-0	-3	-2	0	0	-12	0	0	97	-2	0	1988	1909	1865	NOS
AST	0	0	1	0	4	0	2	1	143	0	0	0	30	59	187	2	42	-0	0	0	-0	0	3392	15	856	0	-4	5404	1144	35	AST
NOA	2	1	1	0	5	3	11	9	4	0	1	1	0	0	28	2	0	1	0	0	5	0	2	447	342	0	1	1106	307	243	NOA
SUM	75	11	945	214	2123	266	1251	664	10424	416	138	191	267	274	3597	200	610	-23	-7	-2	-14	-20	4167	804	7657	-5	0	67668			SUM
EXC	59	2	663	138	1853	192	1084	563	9972	297	119	171	237	214	2857	162	567	-9	-1	-1	-3	-9	705	84	2228	0	1		45367	21213	EXC
EU	18	1	612	26	1357	189	783	178	145	235	100	132	0	0	46	15	0	-14	-3	-0	-8	-16	1	40	509	-1	-1		19696	18682	EU
emis	81	13	977	215	2227	385	1311	709	11148	426	142	199	283	363	4202	207	672	0	0	0	0	0	7258	1945	0	0	0	67852	58650	29911	emis
	MK	MT	NL	NO	PL	PT	RO	RS	RUE	SE	SI	SK	TJ	TM	TR	UA	UZ	ATL	BAS	BLS	MED	NOS	AST	NOA	BIC	DMS	VOL	SUM	EXC	EU	

Table C.4: 2011 country-to-country blame matrices for $\mathbf{AOT40}_f^{\mathbf{uc}}$.
Units: ppb.h per 15% emis. red. of NO_x. **Emitters →, Receptors ↓**. (Based on ECMWF meteorology.)

	AL	AM	AT	AZ	BA	BE	BG	BY	CH	CY	CZ	DE	DK	EE	ES	FI	FR	GB	GE	GR	HR	HU	IE	IS	IT	KG	KZT	LT	LU	LV	MD	
AL	446	0	37	1	62	3	86	10	7	0	32	63	3	1	57	4	68	16	1	99	53	50	2	1	262	0	5	2	1	1	5	AL
AM	1	414	3	569	1	1	3	6	1	4	3	12	1	1	9	2	9	5	206	6	1	3	1	0	9	0	30	1	0	1	2	AM
AT	1	0	238	1	11	-8	6	7	61	0	44	255	2	2	68	7	240	13	1	4	46	43	6	3	304	0	3	4	3	3	2	AT
AZ	0	38	2	943	1	1	3	11	1	1	4	14	3	1	9	5	9	10	175	3	1	3	1	1	5	0	87	2	0	1	2	AZ
BA	10	0	89	1	542	4	30	14	9	0	77	129	4	1	70	7	91	23	2	21	220	134	4	2	250	0	3	4	2	2	4	BA
BE	0	0	8	0	1	-379	1	5	7	0	6	-70	2	1	42	6	267	-46	0	0	2	5	10	4	11	0	0	3	-27	1	1	BE
BG	6	1	27	3	19	2	589	30	5	0	31	81	6	2	21	9	40	20	4	78	16	60	3	2	43	0	10	7	1	3	32	BG
BY	0	0	5	0	1	2	2	250	1	0	13	66	13	9	7	21	31	36	0	1	2	9	6	4	5	0	7	39	2	17	10	BY
CH	0	0	35	1	3	-3	3	2	301	0	2	49	1	1	102	3	600	16	1	2	8	9	7	2	487	0	1	1	1	1	1	CH
CY	3	1	6	4	4	1	21	13	2	342	6	20	2	1	16	3	18	8	7	103	3	8	1	1	46	0	5	3	0	1	4	CY
CZ	1	0	103	0	10	-5	6	13	18	0	15	263	4	3	43	14	198	25	0	3	30	62	8	4	44	0	2	7	3	4	2	CZ
DE	0	0	20	0	1	-46	1	8	24	0	7	-14	2	3	45	12	268	10	0	0	3	9	12	5	28	0	1	5	-7	3	2	DE
DK	0	0	2	0	0	-16	0	7	0	0	-1	-37	-68	2	7	19	39	81	0	0	0	2	27	7	1	0	1	10	-0	5	1	DK
EE	0	0	1	0	0	-1	0	46	0	0	4	42	23	49	3	38	23	48	0	0	0	1	10	5	1	0	4	22	1	32	1	EE
ES	0	0	6	0	2	4	1	2	4	0	2	22	1	0	1140	1	188	24	0	3	3	3	6	2	51	0	0	1	2	0	0	ES
FI	0	0	1	0	0	0	0	15	0	0	2	23	9	11	2	74	12	21	0	0	0	1	4	3	1	0	1	8	1	7	0	FI
FR	0	0	12	0	2	-9	2	4	16	0	5	33	1	1	170	3	795	22	0	2	5	6	12	3	101	0	0	2	-2	1	1	FR
GB	0	0	1	0	0	-13	0	2	1	0	1	-5	2	1	22	6	50	-191	0	0	0	1	29	6	6	0	0	1	-0	1	0	GB
GE	0	63	3	350	1	1	5	16	1	1	6	19	3	1	10	5	10	8	787	5	1	6	1	1	6	0	32	3	0	2	5	GE
GL	0	0	0	0	0	0	0	0	0	0	0	0	0	0	0	0	0	0	0	0	0	0	0	0	0	0	0	0	0	0	0	GL
GR	46	0	21	2	22	3	308	20	5	0	23	50	4	2	36	6	50	18	3	619	18	35	2	1	130	0	8	4	1	2	16	GR
HR	6	0	141	1	196	3	20	13	11	0	87	176	3	2	62	7	117	26	1	16	403	155	4	2	326	0	3	5	2	3	3	HR
HU	1	0	106	1	37	-1	32	28	10	0	87	171	5	3	47	10	99	28	0	6	86	329	5	3	88	0	4	8	2	5	7	HU
IE	0	0	1	0	0	-6	0	1	0	0	1	-6	1	1	14	6	23	-26	0	0	0	1	22	3	3	0	0	1	0	1	0	IE
IS	0	0	0	0	0	0	0	0	0	0	-0	2	1	0	3	2	4	20	0	0	0	0	2	15	1	0	0	0	0	0	0	IS
IT	5	0	85	1	32	3	15	7	35	0	20	85	1	1	111	4	308	20	1	23	63	32	5	2	1080	0	2	2	2	1	2	IT
KG	0	3	3	14	1	1	1	2	1	0	2	12	1	0	20	1	13	5	5	1	1	2	1	0	12	503	260	1	0	0	0	KG
KZT	0	1	2	8	1	2	2	9	1	0	2	15	3	2	13	10	13	15	3	1	1	2	2	1	8	16	345	3	0	2	1	KZT
LT	0	0	4	0	0	-1	1	135	1	0	12	65	24	10	6	25	32	51	0	0	1	8	9	5	3	0	4	118	1	30	5	LT
LU	0	0	10	0	1	-75	1	5	12	0	10	-54	1	1	54	6	340	-0	0	0	3	6	8	3	12	0	1	3	-676	2	1	LU
LV	0	0	3	0	0	0	1	87	1	0	7	55	26	20	5	32	28	50	0	0	1	3	10	5	2	0	5	66	1	71	2	LV
MD	0	0	13	2	3	2	23	73	3	0	24	59	7	3	13	13	34	22	2	3	4	33	3	2	14	0	12	11	1	4	169	MD
ME	69	0	49	1	178	3	64	12	9	0	48	82	4	1	60	5	74	18	1	51	84	79	3	1	239	0	4	3	2	2	5	ME
MK	85	0	33	2	36	2	237	14	7	0	37	69	4	1	47	6	60	17	2	49	24	68	2	1	124	0	5	4	1	2	9	MK
MT	9	0	23	0	20	5	22	6	6	0	10	41	1	1	110	3	237	26	0	55	22	14	5	2	438	0	2	1	1	1	2	MT
NL	0	0	4	0	0	-135	0	7	3	0	8	-89	1	2	19	10	74	-38	0	0	1	3	19	5	6	0	0	3	-6	2	1	NL
NO	0	0	1	0	0	-1	0	4	0	0	2	17	7	2	5	14	17	41	0	0	0	1	7	3	1	0	1	3	0	2	0	NO
PL	0	0	21	0	4	-6	7	42	4	0	33	124	14	5	18	16	80	42	0	2	10	41	10	4	13	0	2	18	3	8	6	PL
PT	0	0	4	0	1	3	0	1	2	0	2	18	1	0	594	1	85	22	0	1	1	1	6	1	23	0	0	0	2	0	0	PT
RO	1	0	32	1	13	2	79	42	5	0	38	88	7	3	23	11	45	20	1	8	16	86	3	2	33	0	9	8	1	3	40	RO
RS	19	0	51	2	79	2	134	19	8	0	63	109	4	2	44	7	69	22	2	35	48	140	3	2	98	0	5	4	1	2	11	RS
RUE	0	0	1	3	0	1	0	8	0	0	1	7	2	2	2	6	4	6	2	0	0	1	1	1	1	0	23	2	0	1	1	RUE
SE	0	0	2	0	1	-1	1	12	0	0	5	26	10	6	4	33	20	46	0	0	1	3	9	3	1	0	2	9	1	6	1	SE
SI	3	0	240	1	33	2	9	7	18	0	60	224	1	2	61	6	157	25	1	8	234	87	4	3	457	0	3	5	3	3	2	SI
SK	1	0	75	0	14	-2	24	31	9	0	103	151	6	3	37	11	98	30	0	5	40	247	6	3	55	0	3	11	3	6	5	SK
TJ	0	3	3	13	1	1	1	2	1	0	2	8	0	0	18	1	10	3	5	1	1	2	0	0	12	45	93	1	0	0	0	TJ
TM	0	7	3	43	1	2	2	9	2	1	3	18	3	2	18	7	15	14	11	2	1	2	2	1	11	4	224	3	1	2	1	TM
TR	2	17	7	28	3	1	25	21	2	9	9	26	3	1	15	5	16	9	36	29	3	10	1	1	20	0	11	4	0	2	11	TR
UA	0	1	9	3	3	1	10	88	2	0	19	53	8	5	11	16	28	27	3	3	4	21	4	3	10	0	21	13	1	6	26	UA
UZ	0	4	3	19	1	2	2	8	1	0	3	16	3	2	16	7	14	13	8	2	1	2	2	1	10	19	294	2	0	1	1	UZ
ATL	0	0	0	0	0	-0	0	0	0	0	0	0	0	0	1	0	2	0	0	0	0	0	0	0	0	0	0	0	0	0	0	ATL
BAS	0	0	1	0	0	-5	0	16	0	0	3	13	3	10	3	26	19	33	0	0	1	2	9	3	1	0	1	13	1	12	1	BAS
BLS	0	1	2	5	0	0	8	14	0	0	4	11	2	1	2	4	4	5	18	1	1	4	1	1	2	0	6	3	0	1	7	BLS
MED	3	0	9	1	8	1	21	4	2	2	5	14	1	0	39	1	56	6	1	35	13	7	1	0	79	0	1	1	0	0	2	MED
NOS	0	0	0	0	0	-8	0	1	0	0	0	-5	-0	0	4	2	11	-10	0	0	0	0	6	2	1	0	0	1	-0	0	0	NOS
AST	0	3	2	24	1	1	2	3	1	7	1	7	1	0	10	2	7	4	5	6	1	1	0	0	9	27	93	1	0	0	1	AST
NOA	2	0	4	0	3	1	8	2	2	0	2	8	0	0	57	1	41	4	0	25	3	3	1	0	56	0	1	0	0	0	1	NOA
EXC	1	2	7	10	4	-1	9	14	3	0	5	20	3	2	41	9	46	10	6	6	5	8	3	1	29	7	66	4	0	2	3	EXC
EU	2	0	26	0	7	-10	32	17	10	1	15	50	4	4	191	16	203	13	0	23	13	27	9	3	118	0	2	8	-0	5	5	EU
	AL	AM	AT	AZ	BA	BE	BG	BY	CH	CY	CZ	DE	DK	EE	ES	FI	FR	GB	GE	GR	HR	HU	IE	IS	IT	KG	KZT	LT	LU	LV	MD	

Table C.4 Cont.: 2011 country-to-country blame matrices for $\mathbf{AOT40}_f^{\mathbf{uc}}$.
Units: ppb.h per 15% emis. red. of NO_x. **Emitters →, Receptors ↓.** (Based on ECMWF meteorology.)

	ME	MK	MT	NL	NO	PL	PT	RO	RS	RUE	SE	SI	SK	TJ	TM	TR	UA	UZ	ATL	BAS	BLS	MED	NOS	AST	NOA	BIC	DMS	VOL	EXC	EU	
AL	49	112	1	4	7	73	4	79	399	63	6	8	21	0	0	37	44	0	27	8	10	231	14	1	3	167	0	0	2289	986	AL
AM	0	1	0	1	3	15	1	9	3	157	2	1	2	0	15	363	37	10	9	3	24	34	5	151	4	145	0	0	1923	103	AM
AT	1	1	0	-17	11	49	4	27	22	46	8	71	20	0	0	7	25	0	68	4	2	39	-3	0	1	171	0	0	1642	1395	AT
AZ	0	0	0	2	7	21	1	8	3	467	5	0	2	0	33	111	60	22	17	8	19	13	10	122	2	136	0	0	2082	118	AZ
BA	44	7	0	2	9	113	5	76	196	55	7	17	48	0	0	13	35	0	45	7	6	88	14	1	2	176	0	0	2378	1212	BA
BE	0	0	0	-124	13	21	6	5	1	16	5	1	5	0	0	0	12	0	100	0	0	6	-127	0	0	149	0	0	-175	-240	BE
BG	5	22	0	2	13	118	2	329	161	223	11	6	26	0	0	51	212	0	37	15	83	25	17	1	1	164	0	0	2332	1517	BG
BY	0	0	0	1	18	185	1	20	4	242	21	1	10	0	0	1	157	0	59	40	3	1	30	0	0	136	0	0	1222	521	BY
CH	0	1	0	-4	6	19	5	12	8	21	3	10	4	0	0	4	13	0	67	2	1	47	6	0	1	182	0	0	1736	1364	CH
CY	1	7	0	2	4	32	1	26	19	105	3	1	5	0	0	1046	72	0	13	5	45	882	6	7	9	152	0	0	1980	677	CY
CZ	1	1	0	-11	18	65	3	25	28	52	13	19	47	0	0	3	36	0	84	11	1	10	11	0	0	167	0	0	1182	962	CZ
DE	0	0	0	-66	22	37	4	9	3	33	12	3	8	0	0	1	21	0	102	-11	1	7	-53	0	0	165	0	0	490	366	DE
DK	0	0	0	-38	56	41	1	2	1	28	26	0	2	0	0	0	8	0	153	-148	0	1	-87	0	0	157	0	0	218	109	DK
EE	0	0	0	-3	31	60	0	3	1	180	51	0	1	0	0	0	18	0	75	77	0	0	44	0	0	123	0	0	696	410	EE
ES	0	1	0	2	3	6	165	4	4	4	1	2	1	0	0	2	4	0	166	1	0	132	14	0	4	240	0	0	1670	1638	ES
FI	0	0	0	-0	24	23	0	2	1	92	36	0	1	0	0	0	8	0	37	39	0	0	25	0	0	70	0	0	382	237	FI
FR	0	0	0	-12	9	16	9	8	5	14	4	4	3	0	0	1	9	0	124	1	0	67	-11	0	1	178	0	0	1258	1187	FR
GB	0	0	0	-18	20	6	3	1	0	7	9	0	1	0	0	0	4	0	140	-1	0	4	-70	0	0	126	0	0	-44	-85	GB
GE	0	1	0	2	7	30	1	16	4	352	5	1	4	0	13	257	95	9	15	8	111	15	9	51	3	139	0	0	2148	154	GE
GL	0	0	0	0	1	0	0	0	0	1	0	0	0	0	0	0	0	0	1	0	0	0	0	0	0	9	0	0	3	2	GL
GR	6	74	1	3	8	80	2	131	133	145	7	4	17	0	0	178	121	0	27	10	56	284	15	1	3	170	0	0	2366	1559	GR
HR	8	4	0	1	9	103	4	62	118	52	7	56	50	0	0	8	34	0	53	6	4	125	13	0	1	159	0	0	2312	1438	HR
HU	2	3	0	-0	13	194	3	166	124	81	9	22	129	0	0	4	86	0	60	11	6	21	16	0	0	158	0	0	2041	1550	HU
IE	0	0	0	-12	11	6	2	1	0	5	6	0	0	0	0	0	3	0	114	-1	0	2	-16	0	0	101	0	0	65	40	IE
IS	0	0	0	0	15	1	1	0	0	4	2	0	0	0	0	0	0	0	31	1	0	1	8	0	0	27	0	0	74	38	IS
IT	4	6	1	-0	6	33	5	29	37	28	3	38	12	0	0	12	18	0	56	4	3	298	10	0	4	167	0	0	2180	1920	IT
KG	0	0	0	2	2	7	2	3	3	83	1	1	1	217	27	33	8	575	7	2	1	6	3	111	1	229	0	0	1833	93	KG
KZT	0	0	0	2	12	15	1	5	2	549	9	1	1	5	8	16	31	33	24	10	2	4	13	20	0	194	0	0	1177	132	KZT
LT	0	0	0	-5	24	172	0	9	2	137	35	1	8	0	0	1	80	0	85	63	1	1	36	0	0	145	0	0	1015	621	LT
LU	0	0	0	-50	12	30	6	7	2	22	6	3	6	0	0	1	15	0	82	1	1	8	-30	0	0	150	0	0	-261	-341	LU
LV	0	0	0	-4	31	107	0	5	1	167	42	0	4	0	0	0	38	0	81	77	1	1	41	0	0	138	0	0	873	534	LV
MD	1	1	0	2	16	173	1	167	9	286	14	2	25	0	0	16	458	1	46	21	39	5	19	1	0	158	0	0	1726	668	MD
ME	343	22	1	3	9	104	4	83	431	61	8	9	35	0	0	20	40	0	36	8	7	164	14	1	3	178	0	0	2321	1031	ME
MK	15	395	0	3	8	95	3	124	474	94	8	6	28	0	0	57	70	0	31	10	20	77	14	1	2	179	0	0	2330	1030	MK
MT	4	6	-240	4	6	21	4	25	41	26	3	8	6	0	0	25	20	0	58	4	6	100	15	0	8	155	0	0	1022	827	MT
NL	0	0	0	-396	23	21	3	3	0	13	9	1	3	0	0	0	12	0	101	-10	0	3	-268	0	0	133	0	0	-409	-476	NL
NO	0	0	0	-1	75	23	1	2	1	21	29	0	1	0	0	0	5	0	55	10	0	0	16	0	0	69	0	0	286	175	NO
PL	0	1	0	-12	22	201	2	38	18	73	21	5	37	0	0	2	82	0	86	26	2	3	13	0	0	155	0	0	1012	741	PL
PT	0	0	0	1	2	4	581	2	1	3	1	1	1	0	0	1	3	0	263	1	0	50	11	0	2	224	0	0	1372	1354	PT
RO	2	3	0	1	14	162	2	655	58	189	13	5	43	0	0	11	252	0	42	18	40	10	16	1	0	161	0	0	2032	1371	RO
RS	30	28	0	2	10	131	3	221	432	98	9	9	56	0	0	16	76	0	43	9	15	34	15	1	1	166	0	0	2106	1222	RS
RUE	0	0	0	1	6	9	0	2	1	250	5	0	1	0	0	3	20	1	11	6	2	1	6	1	0	50	0	0	377	57	RUE
SE	0	0	0	-3	42	57	1	4	2	50	68	0	2	0	0	1	12	0	60	35	0	1	22	0	0	91	0	0	436	310	SE
SI	1	2	0	-5	8	60	3	37	44	44	6	227	32	0	0	6	24	0	56	4	3	111	7	0	1	153	0	0	2149	1714	SI
SK	1	2	0	-3	14	196	2	98	68	78	9	16	289	0	0	4	95	0	65	13	4	12	16	0	0	156	0	0	1846	1477	SK
TJ	0	0	0	1	1	6	1	3	3	56	1	1	1	636	53	32	7	477	4	1	1	6	2	215	1	246	0	0	1508	78	TJ
TM	0	0	0	3	8	18	2	5	3	334	7	1	2	13	196	46	30	221	20	9	4	8	11	115	1	250	0	0	1302	146	TM
TR	1	3	0	2	7	45	1	38	17	217	6	2	6	0	2	1128	136	2	17	9	90	108	9	42	6	202	0	0	1941	294	TR
UA	0	1	0	2	17	164	1	66	11	432	15	2	20	0	1	13	451	1	48	25	26	4	23	1	0	156	0	0	1595	516	UA
UZ	0	0	0	2	8	15	2	5	3	329	7	1	2	80	44	35	25	389	18	8	3	7	11	60	1	231	0	0	1400	132	UZ
ATL	0	0	0	-0	1	0	0	0	0	1	0	0	0	0	0	0	0	0	4	0	0	0	0	0	0	3	0	0	8	6	ATL
BAS	0	0	0	-11	24	49	0	2	1	51	28	0	2	0	0	0	11	0	63	-45	0	0	2	0	0	81	0	0	326	215	BAS
BLS	0	0	0	1	4	22	0	21	4	161	4	0	3	0	0	32	112	1	9	6	78	2	5	1	0	37	0	0	474	105	BLS
MED	1	3	1	1	2	14	2	16	13	29	1	3	3	0	0	63	23	0	16	2	13	163	4	1	3	46	0	0	490	321	MED
NOS	0	0	0	-14	14	4	1	0	0	4	4	0	0	0	0	0	1	0	42	-6	0	1	-69	0	0	37	0	0	20	-2	NOS
AST	0	1	0	1	2	7	1	3	2	99	2	0	1	26	26	141	14	61	6	2	4	50	3	341	2	184	0	0	609	77	AST
NOA	1	2	1	1	1	6	4	7	7	9	1	1	1	0	0	30	7	0	11	1	3	163	3	0	24	78	0	0	305	234	NOA
EXC	1	2	0	-2	10	28	7	19	9	233	8	2	5	8	7	48	42	24	31	8	7	18	6	11	1	106	0	0	779	271	EXC
EU	1	4	0	-14	17	60	35	62	22	57	18	8	16	0	0	11	42	0	94	12	7	61	-2	0	1	156	0	0	1134	921	EU
	ME	MK	MT	NL	NO	PL	PT	RO	RS	RUE	SE	SI	SK	TJ	TM	TR	UA	UZ	ATL	BAS	BLS	MED	NOS	AST	NOA	BIC	DMS	VOL	EXC	EU	

Table C.5: 2011 country-to-country blame matrices for **AOT40$_f^{\mathbf{uc}}$**.
Units: ppb.h per 15% emis. red. of VOC. **Emitters →, Receptors ↓.** (Based on ECMWF meteorology.)

	AL	AM	AT	AZ	BA	BE	BG	BY	CH	CY	CZ	DE	DK	EE	ES	FI	FR	GB	GE	GR	HR	HU	IE	IS	IT	KG	KZT	LT	LU	LV	MD	
AL	51	0	20	1	14	7	7	12	9	0	22	96	5	1	17	2	51	43	1	90	20	19	2	0	163	0	2	2	1	2	1	AL
AM	0	126	2	86	1	2	1	9	1	0	4	21	1	0	3	1	9	9	78	3	1	2	0	0	13	0	4	1	0	1	1	AM
AT	1	0	165	1	2	20	1	9	59	0	40	366	6	1	20	3	123	72	1	2	14	13	3	0	188	0	1	3	2	3	1	AT
AZ	0	9	2	264	0	2	1	17	1	0	5	30	3	1	3	3	11	18	94	2	1	2	1	0	9	0	10	2	0	2	1	AZ
BA	2	0	26	1	35	10	2	10	9	0	32	153	6	1	17	3	60	51	1	5	27	27	2	0	130	0	1	3	1	2	2	BA
BE	0	0	8	0	0	91	0	6	5	0	14	225	6	1	11	3	160	134	0	0	2	3	4	0	12	0	0	2	5	2	0	BE
BG	1	0	13	2	3	7	23	25	6	0	23	112	7	1	7	3	38	42	3	10	5	15	2	0	35	0	3	4	1	3	5	BG
BY	0	0	4	1	0	9	0	127	2	0	13	90	8	2	3	7	29	54	0	0	1	3	3	0	6	0	2	9	1	5	1	BY
CH	0	0	30	1	1	17	1	4	250	0	12	191	3	1	22	2	177	62	1	1	4	4	3	0	383	0	1	1	2	2	0	CH
CY	2	1	6	8	2	3	6	27	4	29	9	49	3	1	7	2	22	23	9	38	4	5	1	0	56	0	4	3	0	3	2	CY
CZ	0	0	52	1	2	24	1	15	22	0	145	349	8	1	13	4	112	88	0	1	7	14	3	0	41	0	1	4	2	3	1	CZ
DE	0	0	26	0	0	41	0	9	31	0	29	445	11	1	12	4	141	120	0	0	2	4	4	0	30	0	1	3	4	3	1	DE
DK	0	0	2	0	0	22	0	8	1	0	11	195	59	2	3	5	45	208	0	0	0	1	8	0	1	0	1	4	1	4	0	DK
EE	0	0	1	0	0	13	0	23	1	0	4	83	11	13	1	17	25	85	0	0	0	1	4	0	2	0	1	4	1	8	0	EE
ES	0	0	4	0	1	5	0	4	3	0	3	31	2	0	193	1	59	37	0	1	2	2	2	0	44	0	0	1	0	1	0	ES
FI	0	0	1	0	0	4	0	10	0	0	2	30	5	3	1	15	10	37	0	0	0	0	1	0	1	0	0	2	0	2	0	FI
FR	0	0	9	0	1	19	1	6	16	0	9	104	5	1	40	2	199	91	0	1	3	3	3	0	82	0	0	2	2	2	0	FR
GB	0	0	2	0	0	10	0	2	2	0	3	45	4	1	8	2	52	216	0	0	0	1	5	0	9	0	0	1	0	1	0	GB
GE	0	13	2	76	1	2	1	18	1	0	6	31	2	1	3	2	11	15	263	2	1	2	1	0	10	0	5	2	0	2	1	GE
GL	0	0	0	0	0	0	0	0	0	0	0	0	0	0	0	0	0	0	0	0	0	0	0	0	0	0	0	0	0	0	0	GL
GR	10	0	13	2	6	6	14	23	6	0	19	81	5	1	11	3	39	44	2	123	9	13	2	0	92	0	3	3	1	2	3	GR
HR	2	0	48	1	17	14	2	11	12	0	41	210	6	2	19	3	78	64	1	6	54	30	2	0	204	0	1	3	2	2	1	HR
HU	0	0	44	1	4	16	2	20	12	0	52	224	7	1	15	4	74	70	0	2	12	56	3	0	59	0	1	4	2	3	2	HU
IE	0	0	1	0	0	6	0	2	1	0	2	31	2	0	6	2	19	71	0	0	0	0	8	0	5	0	0	1	0	1	0	IE
IS	0	0	0	0	0	1	0	0	0	0	1	11	1	0	1	1	4	10	0	0	0	0	0	0	1	0	0	0	0	0	0	IS
IT	2	0	43	1	7	14	2	7	32	0	19	148	3	1	38	2	135	62	1	7	24	11	3	0	1057	0	1	2	1	2	1	IT
KG	0	1	1	7	0	1	0	4	1	0	2	12	1	0	4	1	7	6	3	1	1	1	0	0	9	43	10	1	0	1	0	KG
KZT	0	1	2	5	0	3	0	11	1	0	3	25	3	1	4	3	11	20	2	1	1	1	1	0	8	2	9	2	0	2	0	KZT
LT	0	0	4	0	0	13	0	59	2	0	13	116	14	3	2	6	35	94	0	0	1	3	4	0	3	0	1	24	1	9	1	LT
LU	0	0	12	0	0	50	0	6	9	0	15	265	6	1	14	3	179	98	0	0	2	3	3	0	14	0	1	2	19	2	0	LU
LV	0	0	3	1	0	13	0	40	1	0	8	104	13	5	2	8	31	92	0	0	0	2	4	0	3	0	2	10	1	20	1	LV
MD	0	0	8	2	1	8	2	36	3	0	20	98	8	1	5	4	32	46	2	1	2	8	2	0	14	0	3	4	1	2	15	MD
ME	10	0	19	1	18	7	4	12	8	0	23	109	6	1	15	2	51	43	1	11	18	21	2	0	126	0	1	3	1	2	2	ME
MK	9	0	16	1	6	6	10	14	7	0	22	91	5	1	12	3	42	38	2	97	8	19	2	0	71	0	2	3	1	2	2	MK
MT	5	0	16	1	8	9	4	10	8	0	10	77	3	1	49	2	111	57	1	21	14	10	3	0	448	0	1	2	1	2	1	MT
NL	0	0	4	0	0	57	0	6	2	0	12	221	12	1	6	3	89	169	0	0	1	2	6	0	7	0	0	2	2	2	0	NL
NO	0	0	1	0	0	5	0	4	0	0	2	37	9	1	1	2	14	44	0	0	0	1	2	0	1	0	0	1	0	1	0	NO
PL	0	0	15	0	1	21	1	29	6	0	43	236	14	1	6	4	66	109	0	1	3	10	4	0	13	0	1	6	2	4	1	PL
PT	0	0	3	0	0	4	0	3	2	0	3	27	2	0	99	1	36	36	0	0	1	1	2	0	23	0	0	1	0	1	0	PT
RO	0	0	13	1	2	9	4	24	6	0	26	120	8	1	7	3	41	46	1	2	4	15	2	0	28	0	2	3	1	2	5	RO
RS	2	0	22	1	10	9	6	17	8	0	35	143	8	1	12	3	52	49	1	7	12	34	2	0	62	0	1	4	1	3	3	RS
RUE	0	0	1	1	0	1	0	6	0	0	1	11	1	0	1	1	4	8	1	0	0	0	0	0	2	0	2	1	0	1	0	RUE
SE	0	0	1	0	0	7	0	10	1	0	4	53	12	2	1	7	17	63	0	0	0	1	3	0	2	0	1	3	0	3	0	SE
SI	2	0	101	1	5	17	1	9	21	0	37	269	5	1	21	3	99	66	1	4	47	23	2	0	309	0	1	3	2	3	1	SI
SK	0	0	33	0	2	16	2	25	11	0	61	211	7	2	12	4	69	73	0	2	7	33	3	0	42	0	1	6	2	4	1	SK
TJ	0	1	1	7	0	1	0	4	1	0	1	10	1	0	3	1	6	5	3	1	1	1	0	0	8	5	6	1	0	1	0	TJ
TM	0	3	3	24	0	3	0	15	2	0	4	31	3	1	5	4	14	21	9	1	1	2	1	0	13	1	12	3	0	2	1	TM
TR	1	5	5	12	1	3	4	21	3	1	8	44	3	1	5	2	16	18	16	9	2	4	1	0	23	0	3	3	0	2	2	TR
UA	0	0	6	3	1	8	1	45	2	0	16	88	7	2	4	5	27	47	2	1	2	6	2	0	11	0	3	5	1	3	3	UA
UZ	0	2	2	11	0	3	0	12	2	0	3	27	3	1	5	3	13	19	5	1	1	1	1	0	11	8	11	2	0	2	0	UZ
ATL	0	0	0	0	0	0	0	0	0	0	0	1	0	0	1	0	1	2	0	0	0	0	0	0	0	0	0	0	0	0	0	ATL
BAS	0	0	1	0	0	10	0	12	1	0	5	84	20	5	1	13	21	88	0	0	0	1	4	0	1	0	1	4	0	6	0	BAS
BLS	0	1	1	4	0	1	1	11	1	0	4	21	2	0	1	1	6	10	8	1	1	2	0	0	3	0	1	1	0	1	1	BLS
MED	2	0	5	1	2	2	2	6	3	0	5	26	1	0	14	1	26	15	1	15	5	3	1	0	82	0	1	1	0	1	1	MED
NOS	0	0	1	0	0	5	0	1	0	0	1	27	4	0	1	1	17	56	0	0	0	0	2	0	2	0	0	0	0	0	0	NOS
AST	0	1	1	11	0	1	1	5	1	1	2	12	1	0	3	1	6	7	4	3	1	1	0	0	10	2	4	1	0	1	0	AST
NOA	1	0	3	0	1	2	1	3	2	0	2	14	1	0	16	0	19	10	0	7	2	2	1	0	39	0	0	1	0	0	0	NOA
EXC	0	1	4	4	1	4	1	10	3	0	6	43	3	1	9	2	22	26	3	2	1	2	1	0	26	1	3	2	0	1	1	EXC
EU	1	0	16	1	1	15	2	12	11	0	18	137	7	1	37	4	81	81	0	5	5	7	3	0	109	0	1	3	1	3	1	EU
	AL	AM	AT	AZ	BA	BE	BG	BY	CH	CY	CZ	DE	DK	EE	ES	FI	FR	GB	GE	GR	HR	HU	IE	IS	IT	KG	KZT	LT	LU	LV	MD	

Table C.5 Cont.: 2011 country-to-country blame matrices for $\mathbf{AOT40}_f^{\mathbf{uc}}$.
Units: ppb.h per 15% emis. red. of VOC. **Emitters →, Receptors ↓.** (Based on ECMWF meteorology.)

	ME	MK	MT	NL	NO	PL	PT	RO	RS	RUE	SE	SI	SK	TJ	TM	TR	UA	UZ	ATL	BAS	BLS	MED	NOS	AST	NOA	BIC	DMS	VOL	EXC	EU	
AL	8	17	0	12	4	62	2	28	99	42	6	5	11	0	0	10	18	0	1	1	0	10	2	0	0	275	0	0	984	674	AL
AM	0	0	0	2	1	16	0	5	2	69	2	0	2	0	0	34	15	0	0	0	0	1	1	6	0	113	0	0	531	101	AM
AT	0	0	0	31	4	70	2	10	7	31	7	19	10	0	0	2	9	0	1	1	0	2	4	0	0	276	0	0	1322	1180	AT
AZ	0	0	0	4	3	26	1	5	2	169	5	0	2	0	1	20	27	1	0	1	0	1	1	15	0	220	0	0	761	140	AZ
BA	2	1	0	19	4	85	2	25	45	31	6	5	15	0	0	3	14	0	1	1	0	3	3	0	0	243	0	0	878	691	BA
BE	0	0	0	60	4	31	2	3	1	11	5	1	3	0	0	0	4	0	1	1	0	0	10	0	0	218	0	0	818	783	BE
BG	0	1	0	12	5	82	1	62	26	90	9	2	11	0	0	17	47	0	1	1	1	1	2	0	0	252	0	0	765	526	BG
BY	0	0	0	14	5	97	0	8	2	106	11	1	5	0	0	1	34	0	1	2	0	0	3	0	0	180	0	0	664	381	BY
CH	0	0	0	17	2	33	2	7	3	17	3	5	3	0	0	1	6	0	1	0	0	2	3	0	0	225	0	0	1275	983	CH
CY	0	2	0	5	3	43	1	24	10	98	5	1	5	0	0	374	40	0	0	1	1	16	1	1	2	354	0	0	941	351	CY
CZ	0	0	0	32	5	143	1	10	9	32	9	6	15	0	0	1	11	0	1	2	0	1	6	0	0	285	0	0	1190	1082	CZ
DE	0	0	0	57	5	69	2	5	2	21	10	1	4	0	0	1	8	0	1	2	0	1	9	0	0	270	0	0	1107	1027	DE
DK	0	0	0	50	15	46	1	2	1	21	26	0	2	0	0	0	5	0	2	8	0	0	15	0	0	228	0	0	747	696	DK
EE	0	0	0	22	6	32	0	2	1	102	19	0	1	0	0	0	6	0	1	4	0	0	5	0	0	164	0	0	491	348	EE
ES	0	0	0	6	1	11	28	4	2	6	2	1	1	0	0	1	3	0	3	0	0	9	2	0	1	223	0	0	465	440	ES
FI	0	0	0	8	4	12	0	1	0	50	10	0	0	0	0	0	3	0	0	2	0	0	2	0	0	75	0	0	215	147	FI
FR	0	0	0	23	3	27	4	6	3	12	4	2	3	0	0	0	5	0	1	1	0	3	6	0	0	207	0	0	691	641	FR
GB	0	0	0	14	3	12	1	1	0	5	5	0	1	0	0	0	2	0	1	1	0	0	6	0	0	101	0	0	410	394	GB
GE	0	0	0	4	2	27	0	7	2	122	4	0	3	0	0	27	30	0	0	0	1	1	1	4	0	147	0	0	705	141	GE
GL	0	0	0	0	0	0	0	0	0	0	0	0	0	0	0	0	0	0	0	0	0	0	0	0	0	-4	0	0	1	1	GL
GR	1	9	0	9	4	67	1	39	34	76	7	3	10	0	0	46	36	0	1	1	1	9	2	0	0	285	0	0	878	607	GR
HR	1	1	0	25	5	88	2	23	34	32	6	16	16	0	0	3	13	0	1	1	0	5	3	0	0	289	0	0	1103	913	HR
HU	0	0	0	24	5	156	2	35	28	41	7	6	29	0	0	2	23	0	1	1	0	1	4	0	0	274	0	0	1049	896	HU
IE	0	0	0	9	2	7	1	1	0	3	3	0	0	0	0	0	1	0	1	1	0	0	2	0	0	40	0	0	186	176	IE
IS	0	0	0	2	1	2	1	0	0	2	1	0	0	0	0	0	0	0	0	0	0	0	1	0	0	8	0	0	43	38	IS
IT	1	1	0	18	3	43	3	16	15	23	3	19	7	0	0	4	10	0	1	0	0	15	3	0	0	346	0	0	1794	1661	IT
KG	0	0	0	1	1	7	0	2	1	45	2	0	1	12	0	6	5	48	0	0	0	0	0	2	0	59	0	0	250	62	KG
KZT	0	0	0	4	3	17	1	3	1	131	5	0	1	1	0	4	11	3	0	1	0	0	1	1	0	141	0	0	310	121	KZT
LT	0	0	0	22	6	100	0	5	1	63	18	0	5	0	0	1	19	0	1	3	0	0	5	0	0	191	0	0	650	494	LT
LU	0	0	0	42	3	35	3	4	2	17	6	1	4	0	0	0	5	0	1	1	0	1	7	0	0	215	0	0	827	781	LU
LV	0	0	0	22	7	58	0	3	1	83	18	0	2	0	0	0	11	0	1	4	0	0	5	0	0	180	0	0	569	423	LV
MD	0	0	0	13	5	114	1	31	3	109	9	1	9	0	0	7	66	0	1	1	0	0	3	0	0	219	0	0	696	441	MD
ME	21	3	0	14	4	74	2	25	76	35	6	4	12	0	0	5	16	0	1	1	0	5	3	0	0	239	0	0	813	582	ME
MK	2	26	0	10	4	71	2	30	72	50	7	3	12	0	0	13	22	0	1	1	0	2	2	0	0	229	0	0	815	574	MK
MT	2	2	132	13	3	36	4	19	20	25	4	6	6	0	0	8	13	0	1	0	0	72	2	0	2	418	0	0	1166	1043	MT
NL	0	0	0	117	6	42	2	2	0	9	7	0	2	0	0	0	4	0	1	2	0	0	15	0	0	223	0	0	796	765	NL
NO	0	0	0	10	15	14	0	1	1	13	9	0	1	0	0	0	2	0	0	1	0	0	4	0	0	53	0	0	196	159	NO
PL	0	0	0	33	6	283	1	13	6	38	12	2	13	0	0	1	21	0	1	3	0	0	7	0	0	260	0	0	1027	913	PL
PT	0	0	0	5	1	10	176	3	1	4	2	1	1	0	0	0	2	0	8	0	0	2	1	0	0	195	0	0	453	436	PT
RO	0	0	0	14	5	106	1	90	12	72	8	2	12	0	0	6	46	0	1	1	0	1	3	0	0	227	0	0	751	563	RO
RS	2	3	0	15	5	113	2	47	125	46	7	3	20	0	0	4	24	0	1	1	0	1	3	0	0	253	0	0	924	659	RS
RUE	0	0	0	2	1	7	0	1	0	69	2	0	0	0	0	1	5	0	0	0	0	0	0	0	0	44	0	0	135	47	RUE
SE	0	0	0	13	6	30	0	3	1	30	22	0	1	0	0	0	5	0	1	3	0	0	4	0	0	96	0	0	304	248	SE
SI	0	1	0	29	4	76	2	15	15	30	6	79	12	0	0	2	10	0	1	1	0	5	4	0	0	302	0	0	1335	1185	SI
SK	0	0	0	24	5	246	1	24	16	42	7	4	42	0	0	2	22	0	1	2	0	1	4	0	0	261	0	0	1065	931	SK
TJ	0	0	0	1	1	6	0	2	1	37	1	0	1	25	1	6	4	25	0	0	0	0	0	5	0	39	0	0	181	53	TJ
TM	0	0	0	5	4	21	1	4	2	146	6	1	2	1	2	12	15	6	0	1	0	0	1	5	0	259	0	0	407	151	TM
TR	0	1	0	5	3	39	1	15	6	99	5	1	4	0	0	166	35	0	0	1	1	3	1	2	1	178	0	0	598	221	TR
UA	0	0	0	12	5	104	1	16	4	156	9	1	7	0	0	6	98	0	1	1	0	0	3	0	0	221	0	0	720	390	UA
UZ	0	0	0	4	3	18	1	4	1	124	6	0	1	8	1	9	12	30	0	1	0	0	1	3	0	212	0	0	374	132	UZ
ATL	0	0	0	0	0	0	1	0	0	0	0	0	0	0	0	0	0	0	0	0	0	0	0	0	0	2	0	0	7	7	ATL
BAS	0	0	0	20	6	38	0	2	1	45	24	0	1	0	0	0	4	0	1	6	0	0	5	0	0	138	0	0	420	350	BAS
BLS	0	0	0	2	2	19	0	8	2	59	3	0	2	0	0	16	27	0	0	0	1	0	1	0	0	73	0	0	225	91	BLS
MED	0	1	0	4	1	15	1	8	6	18	2	2	2	0	0	28	8	0	0	0	0	9	1	0	1	111	0	0	318	236	MED
NOS	0	0	0	10	4	6	0	0	0	3	3	0	0	0	0	0	1	0	0	1	0	0	4	0	0	44	0	0	148	138	NOS
AST	0	0	0	2	1	9	0	3	1	42	2	0	1	1	0	28	7	3	0	0	0	1	0	28	0	71	0	0	182	67	AST
NOA	0	1	0	2	1	8	2	5	4	9	1	1	1	0	0	10	4	0	0	0	0	5	0	0	1	93	0	0	176	137	NOA
EXC	0	0	0	7	3	25	2	5	3	70	4	1	2	1	0	8	11	2	0	1	0	1	1	1	0	105	0	0	326	201	EXC
EU	0	1	0	21	4	63	8	14	6	31	9	3	6	0	0	4	11	0	1	2	0	3	5	0	0	207	0	0	742	653	EU
	ME	MK	MT	NL	NO	PL	PT	RO	RS	RUE	SE	SI	SK	TJ	TM	TR	UA	UZ	ATL	BAS	BLS	MED	NOS	AST	NOA	BIC	DMS	VOL	EXC	EU	

Table C.6: 2011 country-to-country blame matrices for **SOMO35**.
Units: ppb.d per 15% emis. red. of NO_x. **Emitters →, Receptors ↓**. (Based on ECMWF meteorology.)

	AL	AM	AT	AZ	BA	BE	BG	BY	CH	CY	CZ	DE	DK	EE	ES	FI	FR	GB	GE	GR	HR	HU	IE	IS	IT	KG	KZT	LT	LU	LV	MD	
AL	37	0	3	0	5	0	8	1	1	0	2	3	0	0	6	0	5	2	0	-3	4	3	0	0	23	0	1	0	0	0	0	AL
AM	0	32	0	63	0	0	0	1	0	1	0	1	0	0	2	0	1	2	26	1	0	0	0	0	2	0	4	0	0	0	0	AM
AT	0	0	3	0	1	-1	1	0	3	0	0	7	-0	0	7	1	20	1	0	1	3	2	0	0	23	0	0	0	0	0	0	AT
AZ	0	5	0	114	0	0	0	1	0	0	0	2	0	0	1	1	1	2	28	1	0	0	0	0	1	0	11	0	0	0	0	AZ
BA	1	0	6	0	39	0	3	1	1	0	5	6	0	0	7	1	7	2	0	2	19	11	0	0	20	0	1	0	0	0	0	BA
BE	0	0	0	0	0	-60	0	0	0	0	-0	-21	0	0	5	0	17	-11	0	0	0	0	1	1	1	0	0	0	-4	0	0	BE
BG	1	0	2	1	2	0	48	3	0	0	2	5	0	0	3	1	3	2	1	7	1	4	0	0	5	0	2	1	0	0	3	BG
BY	0	0	1	0	0	-0	0	20	0	0	1	3	1	1	1	3	3	2	0	0	0	1	1	0	1	0	2	4	0	2	1	BY
CH	0	0	-1	0	0	-1	0	0	6	0	-1	-10	-0	0	11	0	47	1	0	1	1	0	1	0	23	0	0	0	-0	0	0	CH
CY	0	0	1	1	0	0	2	1	0	31	1	2	0	0	3	0	3	2	1	11	0	1	0	0	7	0	1	0	0	0	0	CY
CZ	0	0	6	0	1	-1	1	0	1	0	-11	3	-0	0	4	1	16	2	0	0	2	3	1	0	4	0	1	0	-0	0	0	CZ
DE	0	0	-0	0	0	-6	0	0	1	0	-2	-32	-0	0	5	1	22	-1	0	0	0	0	1	0	3	0	0	0	-2	0	0	DE
DK	0	0	0	0	0	-3	0	-0	0	0	-0	-8	-14	0	1	2	5	1	0	0	0	0	3	1	0	0	0	1	-0	0	0	DK
EE	0	0	0	0	0	-1	0	4	0	0	0	1	1	3	1	4	3	2	0	0	0	0	1	1	0	0	1	2	0	3	0	EE
ES	0	0	0	0	0	-0	0	0	0	0	-0	-1	0	0	104	0	14	1	0	1	0	0	1	0	7	0	0	0	0	0	0	ES
FI	0	0	0	0	0	-0	0	1	0	0	0	2	1	1	1	7	1	1	0	0	0	0	1	1	0	0	0	1	0	1	0	FI
FR	0	0	-0	0	0	-2	0	0	-0	0	-1	-8	0	0	16	0	59	-1	0	0	0	0	1	0	3	0	0	0	-1	0	0	FR
GB	0	0	0	0	0	-2	0	0	0	0	-0	-3	-0	0	3	0	4	-48	0	0	0	0	4	1	1	0	0	0	-0	0	0	GB
GE	0	7	0	41	0	0	1	1	0	0	0	2	0	0	2	1	1	2	103	1	0	0	0	0	2	0	4	0	0	0	1	GE
GL	0	0	-0	0	0	-0	0	0	-0	0	-0	-0	-0	0	0	0	-0	0	0	0	0	-0	0	0	0	0	0	0	-0	0	0	GL
GR	4	0	1	0	2	0	26	2	0	0	1	3	0	0	4	1	4	2	0	46	1	2	0	0	12	0	1	0	0	0	1	GR
HR	1	0	10	0	16	-0	2	1	1	0	5	8	0	0	6	1	9	2	0	2	33	13	0	0	20	0	1	0	0	0	0	HR
HU	0	0	8	0	3	-0	3	2	1	0	6	7	-0	0	5	1	9	2	0	1	8	25	0	0	7	0	1	1	-0	0	1	HU
IE	0	0	0	0	0	-1	0	0	0	0	0	-1	0	0	2	0	3	-10	0	0	0	0	-1	1	0	0	0	0	0	0	0	IE
IS	0	0	-0	0	0	-0	0	-0	-0	0	-0	-1	0	0	0	0	0	3	0	0	0	-0	1	2	0	0	0	-0	-0	-0	0	IS
IT	0	0	4	0	3	-0	2	0	2	0	0	3	-0	0	10	0	23	1	0	2	4	2	0	0	45	0	0	0	0	0	0	IT
KG	0	1	0	2	0	0	0	0	0	0	0	2	0	0	2	0	2	1	1	0	0	0	0	0	2	39	22	0	0	0	0	KG
KZT	0	0	0	2	0	0	0	1	0	0	0	2	1	0	2	1	2	3	1	0	0	0	0	0	1	2	42	0	0	0	0	KZT
LT	0	0	0	0	0	-1	0	9	0	0	1	1	1	1	1	2	3	1	0	0	0	1	1	1	1	0	1	8	0	3	0	LT
LU	0	0	0	0	0	-11	0	0	1	0	-0	-22	0	0	6	0	32	-4	0	0	0	0	1	0	2	0	0	0	-90	0	0	LU
LV	0	0	0	0	0	-0	0	7	0	0	0	1	1	2	1	3	3	1	0	0	0	0	1	1	0	0	1	5	0	5	0	LV
MD	0	0	1	0	0	0	2	7	0	0	1	3	1	0	2	1	3	2	0	1	0	3	0	0	1	0	2	1	0	0	16	MD
ME	7	0	3	0	15	0	5	1	1	0	3	4	0	0	6	0	6	2	0	4	7	5	0	0	21	0	1	0	0	0	0	ME
MK	7	0	2	0	3	0	20	1	1	0	2	3	0	0	5	0	5	2	0	-8	2	4	0	0	12	0	1	0	0	0	1	MK
MT	1	0	1	0	2	0	3	1	0	0	0	2	0	0	13	0	21	2	0	7	2	1	0	0	44	0	0	0	0	0	0	MT
NL	0	0	0	0	0	-20	0	0	0	0	0	-17	0	0	2	1	7	-12	0	0	0	0	2	1	1	0	0	0	-1	0	0	NL
NO	0	0	0	0	0	-0	0	0	0	0	0	1	1	0	1	2	2	2	0	0	0	0	1	1	0	0	0	0	-0	0	0	NO
PL	0	0	2	0	0	-2	1	2	0	0	1	-3	0	0	2	1	7	1	0	0	1	3	1	0	2	0	1	2	0	1	0	PL
PT	0	0	0	0	0	-0	0	0	0	0	-0	-0	0	0	69	0	6	2	0	0	0	0	1	0	3	0	0	0	0	0	0	PT
RO	0	0	2	0	1	0	7	4	0	0	2	4	0	0	3	1	4	2	0	1	1	7	0	0	3	0	2	1	0	0	4	RO
RS	2	0	3	0	6	0	12	1	1	0	4	5	0	0	5	1	6	2	0	2	4	11	0	0	10	0	1	0	0	0	1	RS
RUE	0	0	0	0	0	0	0	1	0	0	0	1	0	0	0	1	1	1	0	0	0	0	0	0	0	0	4	0	0	0	0	RUE
SE	0	0	0	0	0	-1	0	1	0	0	0	1	0	0	1	4	3	2	0	0	0	0	1	1	0	0	0	1	0	0	0	SE
SI	0	0	13	0	3	-0	1	0	1	0	1	9	-0	0	6	0	12	2	0	1	17	6	0	0	22	0	1	0	0	0	0	SI
SK	0	0	6	0	1	-1	2	2	1	0	6	2	-0	0	4	1	8	1	0	1	4	17	1	0	5	0	1	1	-0	0	1	SK
TJ	0	0	0	2	0	0	0	0	0	0	0	1	0	0	2	0	1	1	1	0	0	0	0	0	1	3	8	0	0	0	0	TJ
TM	0	1	0	8	0	0	0	1	0	0	1	3	1	0	2	1	2	4	3	0	0	0	0	0	2	1	26	0	0	0	0	TM
TR	0	2	1	3	0	0	2	2	0	1	1	2	0	0	3	0	2	2	4	4	0	1	0	0	3	0	1	0	0	0	1	TR
UA	0	0	1	1	0	-0	1	9	0	0	1	1	1	1	2	2	3	3	0	0	0	2	0	0	1	0	3	1	0	1	2	UA
UZ	0	1	0	4	0	0	0	1	0	0	0	3	0	0	2	1	2	3	2	0	0	0	0	0	1	1	36	0	0	0	0	UZ
ATL	0	0	0	0	0	-0	0	0	0	0	-0	-1	0	0	1	0	1	1	0	0	0	0	1	1	0	0	0	0	-0	0	0	ATL
BAS	0	0	0	0	0	-2	0	1	0	0	0	-4	-2	1	1	5	3	1	0	0	0	0	1	1	0	0	1	2	-0	2	0	BAS
BLS	0	1	0	3	0	0	3	6	-0	0	1	2	0	0	1	1	1	2	10	1	0	1	0	0	1	0	3	1	0	1	3	BLS
MED	1	0	1	0	2	0	5	1	0	1	1	1	0	0	12	0	20	2	0	12	3	2	0	0	27	0	1	0	0	0	1	MED
NOS	0	0	0	0	0	-4	0	-0	-0	0	-0	-7	-1	0	2	1	1	-16	0	0	0	-0	3	1	1	0	0	0	-0	0	0	NOS
AST	0	1	0	6	0	0	0	1	0	1	0	1	0	0	1	0	1	1	2	1	0	0	0	0	2	3	13	0	0	0	0	AST
NOA	1	0	1	0	1	0	3	0	1	0	1	2	0	0	15	0	10	2	0	11	1	1	0	0	18	0	0	0	0	0	0	NOA
EXC	0	0	0	1	0	-0	1	1	0	0	0	0	0	0	4	1	4	1	1	1	0	1	0	0	2	1	9	0	-0	0	0	EXC
EU	0	0	1	0	1	-2	3	1	0	0	0	-3	0	0	18	2	16	-2	0	2	1	2	1	0	6	0	0	1	-0	0	0	EU
	AL	AM	AT	AZ	BA	BE	BG	BY	CH	CY	CZ	DE	DK	EE	ES	FI	FR	GB	GE	GR	HR	HU	IE	IS	IT	KG	KZT	LT	LU	LV	MD	

Table C.6 Cont.: 2011 country-to-country blame matrices for **SOMO35**.
Units: ppb.d per 15% emis. red. of NO_x. **Emitters →, Receptors ↓.** (Based on ECMWF meteorology.)

	ME	MK	MT	NL	NO	PL	PT	RO	RS	RUE	SE	SI	SK	TJ	TM	TR	UA	UZ	ATL	BAS	BLS	MED	NOS	AST	NOA	BIC	DMS	VOL	EXC	EU	
AL	4	6	0	0	1	4	1	7	28	6	1	1	1	0	0	3	4	0	4	0	2	26	1	0	1	23	0	0	170	67	AL
AM	0	0	0	0	1	1	0	1	0	21	0	0	0	0	2	55	5	1	3	1	4	6	1	21	1	24	0	0	226	15	AM
AT	0	0	0	-2	1	-2	1	2	1	3	1	4	1	0	0	2	1	0	7	-0	0	7	-1	0	0	21	0	0	89	71	AT
AZ	0	0	0	0	1	2	0	1	0	54	1	0	0	0	5	18	8	3	3	1	3	2	2	17	0	20	0	0	265	16	AZ
BA	4	0	0	0	1	6	1	7	11	5	1	1	3	0	0	2	2	0	5	0	1	12	1	0	1	22	0	0	177	89	BA
BE	0	0	0	-17	1	0	1	0	0	1	0	0	0	0	0	0	1	0	14	-0	0	2	-21	0	0	21	0	0	-80	-85	BE
BG	0	2	0	0	1	9	0	32	12	20	1	0	2	0	0	3	17	0	5	1	8	5	1	0	0	21	0	0	194	127	BG
BY	0	0	0	-1	3	12	0	2	0	20	2	0	1	0	0	0	14	0	7	3	0	0	1	0	0	16	0	0	99	39	BY
CH	0	0	0	-1	1	0	1	1	1	2	0	0	0	0	0	1	1	0	8	0	0	8	-0	0	0	24	0	0	86	74	CH
CY	0	1	0	0	1	3	0	2	2	12	0	0	0	0	0	114	6	0	3	1	5	107	1	3	2	25	0	0	212	70	CY
CZ	0	0	0	-1	2	-4	0	2	1	3	1	1	2	0	0	1	2	0	10	-0	0	3	-1	0	0	20	0	0	46	30	CZ
DE	0	0	0	-9	2	-2	0	1	0	2	1	0	0	0	0	0	1	0	12	-2	0	2	-9	0	0	21	0	0	-8	-17	DE
DK	0	0	0	-6	6	-1	0	0	0	1	2	0	0	0	0	0	0	0	18	-19	0	0	-19	0	0	21	0	0	-7	-17	DK
EE	0	0	0	-1	5	5	0	0	0	16	5	0	0	0	0	0	2	0	9	1	0	0	1	0	0	16	0	0	60	31	EE
ES	0	0	0	-0	0	0	15	1	1	1	0	0	0	0	0	0	0	0	18	0	0	13	0	0	1	30	0	0	147	143	ES
FI	0	0	0	-0	4	2	0	0	0	10	4	0	0	0	0	0	1	0	7	3	0	0	1	0	0	13	0	0	39	22	FI
FR	0	0	0	-2	1	-0	1	1	0	1	0	-0	0	0	0	0	1	0	17	-0	0	8	-3	0	0	24	0	0	74	69	FR
GB	0	0	0	-3	2	-0	0	0	0	1	1	0	0	0	0	0	0	0	22	-0	0	1	-14	0	0	23	0	0	-38	-43	GB
GE	0	0	0	0	1	3	0	2	0	44	1	0	0	0	2	40	11	1	4	1	14	4	2	7	0	23	0	0	276	19	GE
GL	0	0	0	-0	0	-0	0	0	-0	0	0	-0	-0	0	0	0	-0	0	2	-0	0	0	0	0	0	8	0	0	1	0	GL
GR	1	6	0	0	1	5	0	12	9	13	1	0	1	0	0	13	10	0	4	1	6	32	1	0	1	22	0	0	189	124	GR
HR	1	0	0	-0	1	1	0	6	4	4	1	4	3	0	0	2	1	0	6	0	1	14	0	0	0	19	0	0	160	93	HR
HU	0	0	0	-1	1	7	0	16	9	6	1	2	9	0	0	1	4	0	6	0	1	4	-0	0	0	18	0	0	147	108	HU
IE	0	0	0	-1	1	0	0	0	0	1	0	-0	0	0	0	0	0	0	24	-0	0	0	-4	0	0	23	0	0	-4	-7	IE
IS	0	0	0	-0	3	-0	0	0	0	1	1	-0	-0	0	0	0	0	0	10	0	0	0	1	0	0	14	0	0	11	5	IS
IT	0	0	0	-0	1	-0	1	3	2	3	0	1	1	0	0	2	1	0	6	0	1	28	0	0	1	22	0	0	121	101	IT
KG	0	0	0	0	0	1	0	0	0	9	0	0	0	22	4	5	1	47	1	0	0	2	1	23	0	30	0	0	168	13	KG
KZT	0	0	0	0	2	2	0	1	0	61	1	0	0	1	2	3	4	5	4	1	1	1	2	5	0	25	0	0	147	19	KZT
LT	0	0	0	-2	3	11	0	1	0	11	3	0	1	0	0	0	6	0	10	2	0	0	-1	0	0	17	0	0	69	37	LT
LU	0	0	0	-6	1	0	1	1	0	2	0	0	0	0	0	0	1	0	11	-0	0	2	-5	0	0	20	0	0	-82	-89	LU
LV	0	0	0	-1	4	8	0	1	0	15	4	0	0	0	0	0	4	0	9	4	0	0	-1	0	0	16	0	0	68	36	LV
MD	0	0	-0	0	2	14	0	13	1	25	1	0	2	0	0	1	36	1	6	2	3	1	2	0	0	19	0	0	149	55	MD
ME	29	1	0	0	1	6	1	7	31	5	1	1	2	0	0	3	3	0	5	0	1	20	1	0	1	24	0	0	183	78	ME
MK	1	26	0	0	1	6	0	12	36	9	1	0	2	0	0	3	6	0	4	1	2	10	1	0	1	23	0	0	165	68	MK
MT	1	1	-42	0	1	1	1	4	5	3	0	1	0	0	0	3	2	0	8	0	1	19	1	0	2	26	0	0	82	59	MT
NL	0	0	0	-59	3	0	0	0	0	1	1	0	0	0	0	0	1	0	15	-1	0	1	-44	0	0	19	0	0	-87	-93	NL
NO	0	0	0	-1	10	1	0	0	0	2	4	0	0	0	0	0	0	0	11	1	0	0	-0	0	0	16	0	0	30	15	NO
PL	0	0	0	-3	3	-2	0	3	1	3	2	0	2	0	0	0	4	0	10	-0	0	1	-2	0	0	18	0	0	39	21	PL
PT	0	0	0	-0	0	-0	55	0	0	0	0	0	0	0	0	0	0	0	30	-0	0	7	0	0	0	31	0	0	139	137	PT
RO	0	0	0	-0	2	12	0	54	4	16	1	0	3	0	0	1	21	0	5	1	4	2	1	0	0	20	0	0	169	110	RO
RS	3	2	0	-0	1	8	0	19	25	8	1	1	4	0	0	1	5	0	5	0	2	6	1	0	0	20	0	0	157	94	RS
RUE	0	0	0	0	1	1	0	0	0	30	1	0	0	0	0	1	3	0	2	1	0	0	1	0	0	9	0	0	51	9	RUE
SE	0	0	0	-1	7	4	0	0	0	4	7	0	0	0	0	0	1	0	10	2	0	0	-1	0	0	16	0	0	40	25	SE
SI	0	0	0	-1	1	-4	0	3	0	4	0	7	2	0	0	2	1	0	6	-0	1	11	-0	0	0	18	0	0	114	83	SI
SK	0	0	0	-1	2	4	0	9	5	5	1	1	15	0	0	1	4	0	7	-0	1	3	-1	0	0	19	0	0	110	82	SK
TJ	0	0	0	0	0	1	0	0	0	6	0	0	0	57	7	4	1	40	1	0	0	1	1	33	0	31	0	0	139	9	TJ
TM	0	0	0	1	1	3	0	1	0	44	1	0	0	2	35	8	5	31	4	1	1	2	3	22	0	34	0	0	191	23	TM
TR	0	0	0	0	1	3	0	3	1	22	1	0	0	0	0	104	11	0	4	1	9	17	1	6	1	28	0	0	183	29	TR
UA	0	0	0	-0	2	10	0	6	1	38	2	0	2	0	0	2	36	0	6	2	3	1	2	0	0	18	0	0	135	39	UA
UZ	0	0	0	1	1	2	0	1	0	45	1	0	0	9	8	5	4	40	4	1	1	1	2	12	0	31	0	0	179	21	UZ
ATL	0	0	0	-0	2	-0	0	0	0	2	0	0	0	0	0	0	0	0	18	0	0	0	0	0	0	17	0	0	9	4	ATL
BAS	0	0	0	-4	6	4	0	0	0	7	3	0	0	0	0	0	1	0	13	-18	0	0	-6	0	0	19	0	0	31	13	BAS
BLS	0	0	0	0	2	5	0	8	1	66	1	0	1	0	0	6	44	1	6	2	47	2	2	1	0	21	0	0	179	33	BLS
MED	1	1	1	0	1	2	1	5	4	7	0	0	1	0	0	22	5	0	8	0	3	78	1	1	2	27	0	0	145	95	MED
NOS	0	0	0	-7	8	-2	0	0	0	1	1	0	-0	0	0	0	-0	0	30	-3	0	1	-45	0	0	29	0	0	-17	-28	NOS
AST	0	0	0	0	1	1	0	1	0	21	0	0	0	3	5	19	3	7	2	1	1	7	1	49	0	28	0	0	97	13	AST
NOA	0	1	1	0	0	2	1	3	3	3	0	0	0	0	0	10	2	0	5	0	1	60	1	0	10	41	0	0	96	72	NOA
EXC	0	0	0	-0	2	2	1	2	1	27	1	0	0	1	1	5	4	3	5	1	1	2	0	2	0	16	0	0	80	22	EXC
EU	0	0	0	-2	2	2	3	6	2	5	2	0	1	0	0	1	3	0	12	0	1	7	-3	0	0	21	0	0	74	56	EU
	ME	MK	MT	NL	NO	PL	PT	RO	RS	RUE	SE	SI	SK	TJ	TM	TR	UA	UZ	ATL	BAS	BLS	MED	NOS	AST	NOA	BIC	DMS	VOL	EXC	EU	

Table C.7: 2011 country-to-country blame matrices for **SOMO35**.
Units: ppb.d per 15% emis. red. of VOC. **Emitters →, Receptors ↓**. (Based on ECMWF meteorology.)

	AL	AM	AT	AZ	BA	BE	BG	BY	CH	CY	CZ	DE	DK	EE	ES	FI	FR	GB	GE	GR	HR	HU	IE	IS	IT	KG	KZT	LT	LU	LV	MD	
AL	9	0	3	0	2	1	3	2	1	0	3	11	1	0	2	0	6	4	0	16	2	3	0	0	24	0	0	0	0	0	0	AL
AM	0	29	0	14	0	0	0	2	0	0	1	3	0	0	1	0	2	1	21	0	0	0	0	0	2	0	1	0	0	0	0	AM
AT	0	0	21	0	1	2	0	2	8	0	5	41	1	0	2	0	15	7	0	1	3	2	0	0	31	0	0	0	0	0	0	AT
AZ	0	3	0	41	0	0	0	3	0	0	1	4	0	0	1	1	2	2	34	0	0	0	0	0	1	0	1	0	0	0	0	AZ
BA	1	0	4	0	8	1	2	3	1	0	4	17	1	0	3	0	7	5	0	3	4	5	0	0	24	0	0	0	0	0	1	BA
BE	0	0	2	0	0	12	0	1	1	0	2	29	1	0	2	0	25	19	0	0	0	0	1	0	7	0	0	0	1	0	0	BE
BG	0	0	2	0	1	1	8	4	1	0	3	13	1	0	1	1	5	5	0	3	1	3	0	0	6	0	0	1	0	0	1	BG
BY	0	0	1	0	0	1	0	17	0	0	1	11	1	0	0	1	4	7	0	0	0	1	0	0	1	0	0	2	0	1	0	BY
CH	0	0	7	0	0	2	0	1	36	0	2	27	0	0	4	0	25	6	0	1	1	1	0	0	70	0	0	0	0	0	0	CH
CY	0	0	1	1	1	1	1	4	1	4	1	7	0	0	2	0	4	3	1	4	1	1	0	0	10	0	0	0	0	0	0	CY
CZ	0	0	6	0	0	2	1	3	3	0	17	41	1	0	2	1	13	9	0	1	1	3	0	0	7	0	0	0	0	0	0	CZ
DE	0	0	4	0	0	4	0	2	4	0	4	53	1	0	2	0	18	13	0	0	0	1	1	0	6	0	0	0	0	0	0	DE
DK	0	0	0	0	0	3	0	2	0	0	2	23	7	0	1	1	7	23	0	0	0	0	1	0	1	0	0	1	0	1	0	DK
EE	0	0	0	0	0	1	0	4	0	0	1	11	2	2	0	3	4	11	0	0	0	0	0	0	1	0	0	1	0	2	0	EE
ES	0	0	1	0	0	1	0	1	1	0	1	6	0	0	29	0	9	4	0	0	1	1	0	0	10	0	0	0	0	0	0	ES
FI	0	0	0	0	0	1	0	2	0	0	0	5	1	0	0	3	2	5	0	0	0	0	0	0	0	0	0	0	0	1	0	FI
FR	0	0	3	0	0	2	0	1	3	0	2	17	0	0	8	0	32	11	0	0	1	1	0	0	25	0	0	0	0	0	0	FR
GB	0	0	0	0	0	1	0	0	0	0	1	7	0	0	2	0	9	32	0	0	0	0	1	0	3	0	0	0	0	0	0	GB
GE	0	4	1	11	0	0	0	3	0	0	1	5	0	0	1	1	2	2	93	0	0	1	0	0	2	0	1	0	0	0	0	GE
GL	0	0	0	0	0	0	0	0	0	0	0	0	0	0	0	0	0	0	0	0	0	0	0	-0	0	0	0	0	0	0	0	GL
GR	2	0	2	0	1	1	5	3	1	0	2	10	1	0	2	0	5	4	0	20	1	2	0	0	14	0	0	0	0	0	1	GR
HR	1	0	6	0	4	1	1	3	2	0	5	24	1	0	2	0	9	6	0	2	9	5	0	0	40	0	0	0	0	0	1	HR
HU	0	0	5	0	1	2	1	3	2	0	6	26	1	0	2	1	8	7	0	1	2	9	0	0	10	0	0	1	0	0	0	HU
IE	0	0	0	0	0	1	0	0	0	0	0	4	0	0	2	0	4	14	0	0	0	0	2	0	1	0	0	0	0	0	0	IE
IS	0	0	0	0	0	0	0	0	0	0	0	2	0	0	0	0	1	2	0	0	0	0	0	0	1	0	0	0	0	0	0	IS
IT	1	0	7	0	2	1	1	2	4	0	3	16	0	0	5	0	15	6	0	2	4	3	0	0	159	0	0	0	0	0	0	IT
KG	0	0	0	1	0	0	0	1	0	0	0	1	0	0	0	0	1	1	0	0	0	0	0	0	1	9	1	0	0	0	0	KG
KZT	0	0	0	1	0	0	0	2	0	0	0	3	0	0	0	1	1	2	0	0	0	0	0	0	1	1	1	0	0	0	0	KZT
LT	0	0	1	0	0	2	0	9	0	0	2	14	2	0	0	1	5	11	0	0	0	1	0	0	2	0	0	4	0	1	0	LT
LU	0	0	2	0	0	5	0	1	2	0	2	33	1	0	2	0	26	14	0	0	0	0	0	0	6	0	0	0	2	0	0	LU
LV	0	0	0	0	0	1	0	6	0	0	1	13	2	1	0	1	4	11	0	0	0	0	0	0	1	0	0	2	0	4	0	LV
MD	0	0	1	0	0	1	1	4	1	0	3	13	1	0	1	1	4	5	0	0	1	2	0	0	2	0	1	0	0	0	2	MD
ME	3	0	3	0	3	1	2	2	1	0	3	13	1	0	2	0	6	4	0	4	2	4	0	0	21	0	0	0	0	0	1	ME
MK	2	0	2	0	1	1	5	2	1	0	3	11	1	0	2	0	5	4	0	17	1	4	0	0	12	0	0	0	0	0	1	MK
MT	1	0	3	0	1	1	2	2	2	0	2	11	1	0	9	1	16	6	0	5	2	2	0	0	67	0	0	0	0	0	0	MT
NL	0	0	1	0	0	7	0	1	1	0	1	27	1	0	1	0	13	23	0	0	0	0	1	0	3	0	0	0	0	0	0	NL
NO	0	0	0	0	0	1	0	1	0	0	0	6	1	0	1	0	3	7	0	0	0	0	0	0	1	0	0	0	0	0	0	NO
PL	0	0	2	0	0	2	0	6	1	0	5	29	2	0	1	1	8	12	0	0	0	1	0	0	3	0	0	1	0	1	0	PL
PT	0	0	1	0	0	1	0	0	0	0	1	5	0	0	17	0	6	4	0	0	0	0	0	0	5	0	0	0	0	0	0	PT
RO	0	0	2	0	1	1	1	4	1	0	3	15	1	0	1	1	5	5	0	1	1	4	0	0	6	0	0	1	0	0	1	RO
RS	1	0	3	0	2	1	3	3	1	0	4	17	1	0	2	0	6	5	0	3	2	6	0	0	10	0	0	0	0	0	1	RS
RUE	0	0	0	0	0	0	0	1	0	0	0	2	0	0	0	0	1	1	0	0	0	0	0	0	0	0	0	0	0	0	0	RUE
SE	0	0	0	0	0	1	0	2	0	0	1	8	2	0	0	1	3	9	0	0	0	0	0	0	0	0	0	1	0	1	0	SE
SI	0	0	14	0	2	2	1	2	3	0	6	30	1	0	2	0	11	6	0	1	10	4	0	0	60	0	0	0	0	0	0	SI
SK	0	0	4	0	1	2	1	3	1	0	7	27	1	0	1	1	8	8	0	1	1	6	0	0	7	0	0	1	0	1	0	SK
TJ	0	0	0	1	0	0	0	0	0	0	0	1	0	0	0	0	1	0	0	0	0	0	0	0	1	1	1	0	0	0	0	TJ
TM	0	0	0	3	0	0	0	2	0	0	1	4	0	0	1	1	2	3	2	0	0	0	0	0	2	0	1	0	0	0	0	TM
TR	0	1	1	1	0	0	1	3	0	0	1	6	0	0	1	0	3	2	2	1	0	1	0	0	4	0	0	0	0	0	0	TR
UA	0	0	1	0	0	1	0	6	0	0	2	11	1	0	1	1	3	5	0	0	0	1	0	0	2	0	1	1	0	1	0	UA
UZ	0	0	0	1	0	0	0	2	0	0	0	4	0	0	1	1	2	2	1	0	0	0	0	0	1	2	2	0	0	0	0	UZ
ATL	0	0	0	0	0	0	0	0	0	0	0	2	0	0	1	0	2	3	0	0	0	0	0	0	1	0	0	0	0	0	0	ATL
BAS	0	0	0	0	0	2	0	4	0	0	1	19	4	1	0	3	6	17	0	0	0	0	1	0	1	0	0	1	0	2	0	BAS
BLS	0	0	1	2	0	1	2	7	1	0	2	12	1	0	1	1	4	5	9	1	1	2	0	0	3	0	1	1	0	1	1	BLS
MED	1	0	3	0	2	1	2	3	2	0	2	13	1	0	10	0	16	7	0	8	3	2	0	0	54	0	0	1	0	0	0	MED
NOS	0	0	1	0	0	2	0	1	0	0	1	15	2	0	1	0	10	31	0	0	0	0	1	0	3	0	0	0	0	0	0	NOS
AST	0	0	0	3	0	0	0	1	0	0	0	2	0	0	0	0	1	1	1	0	0	0	0	0	2	0	1	0	0	0	0	AST
NOA	1	0	1	0	1	1	1	2	1	0	1	6	0	0	6	0	7	3	0	4	1	1	0	0	17	0	0	0	0	0	0	NOA
EXC	0	0	1	1	0	1	0	2	0	0	1	6	0	0	1	0	3	3	1	0	0	0	0	0	5	0	0	0	0	0	0	EXC
EU	0	0	2	0	0	2	1	2	2	0	2	18	1	0	6	1	11	10	0	1	1	1	0	0	19	0	0	0	0	0	0	EU
	AL	AM	AT	AZ	BA	BE	BG	BY	CH	CY	CZ	DE	DK	EE	ES	FI	FR	GB	GE	GR	HR	HU	IE	IS	IT	KG	KZT	LT	LU	LV	MD	

Table C.7 Cont.: 2011 country-to-country blame matrices for **SOMO35**.
Units: ppb.d per 15% emis. red. of VOC. **Emitters →, Receptors ↓**. (Based on ECMWF meteorology.)

	ME	MK	MT	NL	NO	PL	PT	RO	RS	RUE	SE	SI	SK	TJ	TM	TR	UA	UZ	ATL	BAS	BLS	MED	NOS	AST	NOA	BIC	DMS	VOL	EXC	EU	
AL	1	4	0	1	1	9	0	8	15	8	1	1	2	0	0	4	4	0	0	0	0	1	0	0	0	39	0	0	155	99	AL
AM	0	0	0	0	0	3	0	2	0	14	1	0	0	0	0	11	3	0	0	0	0	0	0	1	0	17	0	0	115	19	AM
AT	0	0	0	3	0	10	0	3	2	6	1	3	1	0	0	1	3	0	0	0	0	0	0	0	0	34	0	0	178	152	AT
AZ	0	0	0	1	1	5	0	2	0	27	1	0	0	0	0	4	5	0	0	0	0	0	0	2	0	27	0	0	145	24	AZ
BA	1	1	0	2	1	13	0	9	9	9	1	1	2	0	0	1	6	0	0	0	0	1	0	0	0	35	0	0	150	105	BA
BE	0	0	0	7	0	5	0	1	0	2	0	0	0	0	0	0	1	0	0	0	0	0	1	0	0	30	0	0	121	115	BE
BG	0	1	0	1	1	10	0	15	4	14	1	0	1	0	0	5	8	0	0	0	0	0	0	0	0	32	0	0	122	81	BG
BY	0	0	0	2	1	12	0	1	0	18	2	0	1	0	0	0	4	0	0	0	0	0	0	0	0	21	0	0	92	49	BY
CH	0	0	0	2	0	5	0	2	1	3	0	1	1	0	0	0	1	0	0	0	0	1	0	0	0	31	0	0	200	156	CH
CY	0	0	0	1	0	7	0	5	2	15	1	0	1	0	0	58	6	0	0	0	0	2	0	1	0	52	0	0	148	57	CY
CZ	0	0	0	3	1	18	0	3	2	8	1	1	2	0	0	0	3	0	0	0	0	0	1	0	0	35	0	0	154	132	CZ
DE	0	0	0	6	1	9	0	1	0	4	1	0	1	0	0	0	2	0	0	0	0	0	1	0	0	33	0	0	140	127	DE
DK	0	0	0	6	2	8	0	0	0	6	3	0	0	0	0	0	2	0	0	1	0	0	2	0	0	28	0	0	99	86	DK
EE	0	0	0	2	1	5	0	0	0	16	4	0	0	0	0	0	1	0	0	1	0	0	1	0	0	22	0	0	76	52	EE
ES	0	0	0	1	0	2	4	1	1	1	0	0	0	0	0	0	1	0	0	0	0	1	0	0	0	31	0	0	77	71	ES
FI	0	0	0	1	1	2	0	0	0	8	2	0	0	0	0	0	0	0	0	0	0	0	0	0	0	10	0	0	36	24	FI
FR	0	0	0	3	0	5	1	2	1	2	0	1	1	0	0	0	1	0	0	0	0	1	1	0	0	31	0	0	124	114	FR
GB	0	0	0	2	0	2	0	0	0	1	0	0	0	0	0	0	0	0	0	0	0	0	1	0	0	16	0	0	66	63	GB
GE	0	0	0	1	1	5	0	2	1	23	1	0	0	0	0	8	6	0	0	0	0	0	0	1	0	21	0	0	178	27	GE
GL	0	0	0	0	0	0	0	0	0	0	0	0	0	0	0	0	0	0	0	0	0	0	0	0	0	-3	0	0	3	2	GL
GR	0	2	0	1	1	9	0	9	6	12	1	0	1	0	0	10	6	0	0	0	0	1	0	0	0	39	0	0	138	92	GR
HR	0	0	0	2	1	15	0	8	7	9	1	3	2	0	0	1	5	0	0	0	0	1	0	0	0	39	0	0	180	138	HR
HU	0	0	0	3	1	20	0	9	4	10	1	1	4	0	0	1	7	0	0	0	0	0	0	0	0	35	0	0	148	117	HU
IE	0	0	0	1	0	1	1	0	0	1	0	0	0	0	0	0	0	0	0	0	0	0	0	0	0	7	0	0	34	33	IE
IS	0	0	0	0	0	1	0	0	0	1	0	0	0	0	0	0	0	0	0	0	0	0	0	0	0	0	0	0	12	10	IS
IT	0	0	0	2	0	9	1	5	3	5	1	4	1	0	0	2	3	0	0	0	0	2	0	0	0	48	0	0	269	242	IT
KG	0	0	0	0	0	1	0	0	0	5	0	0	0	2	0	1	1	7	0	0	0	0	0	1	0	6	0	0	35	6	KG
KZT	0	0	0	0	0	2	0	1	0	21	1	0	0	0	0	1	2	1	0	0	0	0	0	0	0	14	0	0	45	16	KZT
LT	0	0	0	3	1	13	0	1	0	12	3	0	1	0	0	0	3	0	0	0	0	0	1	0	0	23	0	0	92	66	LT
LU	0	0	0	4	0	5	0	1	0	2	1	0	0	0	0	0	1	0	0	0	0	0	1	0	0	28	0	0	112	106	LU
LV	0	0	0	3	1	8	0	0	0	14	3	0	0	0	0	0	2	0	0	0	0	0	1	0	0	22	0	0	83	59	LV
MD	0	0	0	1	1	13	0	9	1	20	1	0	1	0	0	2	11	0	0	0	0	0	0	0	0	27	0	0	105	62	MD
ME	4	1	0	1	1	11	0	9	14	9	1	1	2	0	0	3	5	0	0	0	0	1	0	0	0	35	0	0	140	91	ME
MK	0	7	0	1	1	9	0	10	13	9	1	0	2	0	0	4	5	0	0	0	0	0	0	0	0	32	0	0	139	91	MK
MT	0	1	16	2	1	8	1	7	4	7	1	1	1	0	0	3	4	0	0	0	0	10	0	0	0	65	0	0	194	164	MT
NL	0	0	0	14	1	5	0	0	0	2	1	0	0	0	0	0	1	0	0	0	0	0	2	0	0	29	0	0	107	102	NL
NO	0	0	0	2	3	3	0	0	0	4	2	0	0	0	0	0	0	0	0	0	0	0	1	0	0	7	0	0	36	28	NO
PL	0	0	0	4	1	33	0	2	1	11	2	0	1	0	0	0	4	0	0	0	0	0	1	0	0	32	0	0	136	110	PL
PT	0	0	0	1	0	2	25	1	0	1	0	0	0	0	0	0	0	0	1	0	0	0	0	0	0	29	0	0	74	70	PT
RO	0	0	0	2	1	14	0	28	2	13	1	1	2	0	0	2	9	0	0	0	0	0	0	0	0	30	0	0	129	94	RO
RS	0	1	0	2	1	15	0	15	18	10	1	1	3	0	0	2	7	0	0	0	0	0	0	0	0	34	0	0	147	99	RS
RUE	0	0	0	0	0	1	0	0	0	14	0	0	0	0	0	0	1	0	0	0	0	0	0	0	0	5	0	0	25	8	RUE
SE	0	0	0	2	1	4	0	0	0	6	3	0	0	0	0	0	1	0	0	0	0	0	1	0	0	12	0	0	48	38	SE
SI	0	0	0	3	0	14	0	7	4	7	1	13	2	0	0	1	4	0	0	0	0	1	0	0	0	40	0	0	215	179	SI
SK	0	0	0	3	1	29	0	7	2	10	1	1	6	0	0	0	6	0	0	0	0	0	1	0	0	34	0	0	151	123	SK
TJ	0	0	0	0	0	1	0	0	0	4	0	0	0	5	0	1	0	3	0	0	0	0	0	1	0	2	0	0	21	5	TJ
TM	0	0	0	1	1	3	0	1	0	21	1	0	0	1	0	2	2	1	0	0	0	0	0	1	0	27	0	0	59	21	TM
TR	0	0	0	1	0	6	0	4	1	15	1	0	1	0	0	40	5	0	0	0	0	0	0	0	0	26	0	0	107	35	TR
UA	0	0	0	1	1	13	0	3	1	25	1	0	1	0	0	1	13	0	0	0	0	0	0	0	0	26	0	0	99	51	UA
UZ	0	0	0	1	0	3	0	1	0	19	1	0	0	2	0	1	2	5	0	0	0	0	0	1	0	24	0	0	56	18	UZ
ATL	0	0	0	0	0	1	1	0	0	1	0	0	0	0	0	0	0	0	0	0	0	0	0	0	0	1	0	0	16	14	ATL
BAS	0	0	0	4	2	10	0	0	0	12	6	0	0	0	0	0	2	0	0	1	0	0	1	0	0	30	0	0	102	81	BAS
BLS	0	0	0	1	1	12	0	10	2	40	2	0	1	0	0	16	16	0	0	0	0	0	0	0	0	41	0	0	162	66	BLS
MED	0	1	0	2	1	9	1	7	4	10	1	1	1	0	0	17	5	0	0	0	0	6	0	0	0	65	0	0	193	143	MED
NOS	0	0	0	5	2	5	0	1	0	3	2	0	0	0	0	0	1	0	0	0	0	0	2	0	0	24	0	0	90	81	NOS
AST	0	0	0	0	0	2	0	1	0	10	0	0	0	0	0	4	2	0	0	0	0	0	0	6	0	10	0	0	36	12	AST
NOA	0	0	0	1	0	5	1	4	2	5	1	0	1	0	0	6	3	0	0	0	0	2	0	0	0	39	0	0	83	61	NOA
EXC	0	0	0	1	0	4	0	1	0	13	1	0	0	0	0	2	2	0	0	0	0	0	0	0	0	13	0	0	52	30	EXC
EU	0	0	0	3	1	9	1	4	1	6	1	1	1	0	0	1	2	0	0	0	0	0	1	0	0	28	0	0	112	95	EU
	ME	MK	MT	NL	NO	PL	PT	RO	RS	RUE	SE	SI	SK	TJ	TM	TR	UA	UZ	ATL	BAS	BLS	MED	NOS	AST	NOA	BIC	DMS	VOL	EXC	EU	

Table C.8: 2011 country-to-country blame matrices for **PM2.5**.
Units: ng/m^3 per 15% emis. red. of PPM. **Emitters →, Receptors ↓**. (Based on ECMWF meteorology.)

	AL	AM	AT	AZ	BA	BE	BG	BY	CH	CY	CZ	DE	DK	EE	ES	FI	FR	GB	GE	GR	HR	HU	IE	IS	IT	KG	KZT	LT	LU	LV	MD	
AL	146	0	1	0	3	0	4	0	0	0	0	1	0	0	0	0	1	0	0	41	1	2	0	0	5	0	0	0	0	0	0	AL
AM	0	4	0	5	0	0	0	0	0	0	0	0	0	0	0	0	0	0	1	0	0	0	0	0	0	0	1	0	0	0	0	AM
AT	0	0	84	0	1	0	1	0	4	0	5	17	0	0	0	0	4	0	0	0	3	13	0	0	12	0	0	0	0	0	0	AT
AZ	0	0	0	24	0	0	0	0	0	0	0	0	0	0	0	0	0	0	2	0	0	0	0	0	0	0	3	0	0	0	0	AZ
BA	2	0	2	0	76	0	3	0	0	0	2	3	0	0	0	0	2	0	0	2	11	8	0	0	6	0	0	0	0	0	0	BA
BE	0	0	2	0	0	99	0	0	2	0	1	35	0	0	1	0	74	8	0	0	0	1	0	0	1	0	0	0	5	0	0	BE
BG	1	0	1	0	1	0	139	1	0	0	0	1	0	0	0	0	1	0	0	9	0	3	0	0	1	0	0	0	0	0	1	BG
BY	0	0	0	0	0	0	0	75	0	0	1	3	1	2	0	1	1	1	0	0	0	2	0	0	0	0	1	5	0	5	0	BY
CH	0	0	5	0	0	0	0	0	86	0	0	15	0	0	0	0	22	0	0	0	0	0	0	0	22	0	0	0	0	0	0	CH
CY	0	0	0	0	0	0	0	0	0	22	0	0	0	0	0	0	0	0	0	3	0	0	0	0	1	0	0	0	0	0	0	CY
CZ	0	0	13	0	1	1	1	1	1	0	61	28	1	0	0	0	7	1	0	0	2	16	0	0	2	0	0	0	0	0	0	CZ
DE	0	0	9	0	0	5	0	0	4	0	6	131	2	0	0	0	19	3	0	0	0	2	0	0	2	0	0	0	1	0	0	DE
DK	0	0	1	0	0	2	0	1	0	0	1	18	77	0	0	0	4	6	0	0	0	1	0	0	0	0	0	0	0	1	0	DK
EE	0	0	0	0	0	0	0	4	0	0	0	2	2	68	0	8	0	1	0	0	0	0	0	0	0	0	0	2	0	20	0	EE
ES	0	0	0	0	0	0	0	0	0	0	0	1	0	0	56	0	5	0	0	0	0	0	0	0	1	0	0	0	0	0	0	ES
FI	0	0	0	0	0	0	0	1	0	0	0	1	0	3	0	48	0	0	0	0	0	0	0	0	0	0	0	0	0	1	0	FI
FR	0	0	1	0	0	2	0	0	3	0	1	10	0	0	3	0	145	3	0	0	0	1	0	0	6	0	0	0	1	0	0	FR
GB	0	0	0	0	0	1	0	0	0	-0	0	4	0	0	0	0	11	65	0	0	0	0	2	0	1	0	0	0	0	0	0	GB
GE	0	0	0	2	0	0	0	0	0	0	0	0	0	0	0	0	0	0	14	0	0	0	0	0	0	0	1	0	0	0	0	GE
GL	-0	0	-0	0	0	-0	-0	0	-0	0	-0	0	0	0	0	0	-0	0	-0	-0	-0	-0	0	0	-0	0	0	0	0	-0	-0	GL
GR	4	0	0	0	1	0	14	0	0	0	0	1	0	0	0	0	1	0	0	112	0	1	0	0	3	0	0	0	0	0	0	GR
HR	1	0	6	0	24	0	3	0	0	0	2	5	0	0	0	0	2	0	0	1	63	22	0	0	15	0	0	0	0	0	0	HR
HU	0	0	10	0	5	0	2	1	1	0	4	8	0	0	0	0	3	1	0	1	11	176	0	0	4	0	0	0	0	0	0	HU
IE	0	0	0	0	0	0	0	0	0	0	0	1	0	0	0	0	3	8	0	0	0	0	17	0	0	0	0	0	0	0	0	IE
IS	0	0	0	0	0	0	0	0	0	0	0	0	0	0	0	0	0	0	0	0	0	0	0	0	0	0	0	0	0	0	0	IS
IT	1	0	3	0	2	0	0	0	2	0	1	2	0	0	1	0	6	0	0	1	2	2	0	0	225	0	0	0	0	0	0	IT
KG	0	0	0	0	0	0	0	0	0	0	0	0	0	0	0	0	0	0	0	0	0	0	0	0	0	28	21	0	0	0	0	KG
KZT	0	0	0	0	0	0	0	0	0	0	0	0	0	0	0	0	0	0	0	0	0	0	0	0	0	1	81	0	0	0	0	KZT
LT	0	0	0	0	0	0	0	16	0	0	1	4	2	3	0	1	1	1	0	0	0	1	0	0	0	0	0	41	0	18	0	LT
LU	0	0	3	0	0	16	0	0	2	0	2	59	0	0	1	0	89	4	0	0	0	1	0	0	1	0	0	0	82	0	0	LU
LV	0	0	0	0	0	0	0	8	0	0	0	3	2	9	0	3	1	1	0	0	0	1	0	0	0	0	0	11	0	92	0	LV
MD	0	0	1	0	0	0	5	3	0	0	1	2	0	0	0	0	1	0	0	1	0	4	0	0	0	0	1	0	0	0	40	MD
ME	18	0	1	0	9	0	2	0	0	0	1	1	0	0	0	0	1	0	0	4	2	3	0	0	4	0	0	0	0	0	0	ME
MK	13	0	1	0	2	0	16	0	0	0	1	1	0	0	0	0	1	0	0	61	1	3	0	0	2	0	0	0	0	0	0	MK
MT	1	0	0	0	1	0	1	0	0	0	0	1	0	0	1	0	5	0	0	2	0	1	0	0	24	0	0	0	0	0	0	MT
NL	0	0	1	0	0	31	0	0	1	0	1	57	1	0	0	0	26	11	0	0	0	1	0	0	1	0	0	0	1	0	0	NL
NO	0	0	0	0	0	0	0	0	0	0	0	1	1	0	0	1	1	1	0	0	0	0	0	0	0	0	0	0	0	0	0	NO
PL	0	0	2	0	0	1	0	5	0	0	7	15	2	1	0	0	3	2	0	0	1	6	0	0	1	0	0	1	0	1	0	PL
PT	0	0	0	0	0	0	0	0	0	0	0	0	0	0	21	0	2	0	0	0	0	0	0	0	0	0	0	0	0	0	0	PT
RO	0	0	1	0	1	0	11	1	0	0	1	2	0	0	0	0	1	0	0	1	1	10	0	0	1	0	0	0	0	0	2	RO
RS	4	0	2	0	9	0	10	0	0	0	2	3	0	0	0	0	2	0	0	4	3	17	0	0	2	0	0	0	0	0	0	RS
RUE	0	0	0	0	0	0	0	1	0	0	0	0	0	0	0	0	0	0	0	0	0	0	0	0	0	0	7	0	0	0	0	RUE
SE	0	0	0	0	0	0	0	0	0	-0	0	2	4	1	0	2	1	1	0	0	0	0	0	0	0	0	0	0	0	1	0	SE
SI	0	0	23	0	4	0	1	0	1	0	2	6	0	0	0	0	3	0	0	1	29	13	0	0	32	0	0	0	0	0	0	SI
SK	0	0	7	0	1	0	1	1	1	0	8	8	0	0	0	0	3	1	0	0	2	55	0	0	2	0	0	0	0	0	0	SK
TJ	0	0	0	0	0	0	0	0	0	0	0	0	0	0	0	0	0	0	0	0	0	0	0	0	0	1	7	0	0	0	0	TJ
TM	0	0	0	0	0	0	0	0	0	0	0	0	0	0	0	0	0	0	0	0	0	0	0	0	0	0	16	0	0	0	0	TM
TR	0	0	0	0	0	0	1	0	0	0	0	0	0	0	0	0	0	0	0	1	0	0	0	0	0	0	0	0	0	0	0	TR
UA	0	0	0	0	0	0	1	7	0	0	1	2	0	0	0	0	1	0	0	0	0	3	0	0	0	0	2	1	0	1	2	UA
UZ	0	0	0	0	0	0	0	0	0	0	0	0	0	0	0	0	0	0	0	0	0	0	0	0	0	3	42	0	0	0	0	UZ
ATL	0	0	0	0	0	0	0	0	0	0	0	0	0	0	1	0	1	1	0	0	0	0	0	0	0	0	0	0	0	0	0	ATL
BAS	0	0	0	0	0	1	0	2	0	0	1	8	11	7	0	10	2	2	0	0	0	1	0	0	0	0	0	2	0	8	0	BAS
BLS	0	0	0	0	0	0	4	1	0	0	0	1	0	0	0	0	0	0	1	1	0	1	0	0	0	0	1	0	0	0	1	BLS
MED	2	0	1	0	2	0	2	0	0	0	0	1	0	0	4	0	7	0	0	8	1	1	0	0	20	0	0	0	0	0	0	MED
NOS	0	0	0	0	0	3	0	0	0	-0	0	8	3	0	0	0	11	15	0	0	0	0	1	0	0	0	0	0	0	0	0	NOS
AST	0	0	0	0	0	0	0	0	0	0	0	0	0	0	0	0	0	0	0	0	0	0	0	0	0	0	6	0	0	0	0	AST
NOA	0	0	0	0	0	0	0	0	0	0	0	0	0	0	1	0	1	0	0	2	0	0	0	0	3	0	0	0	0	0	0	NOA
EXC	0	0	1	0	0	0	1	1	0	0	1	3	0	1	1	1	5	1	0	1	0	2	0	0	3	0	14	0	0	1	0	EXC
EU	0	0	4	0	1	2	5	1	1	0	3	16	2	1	8	4	24	5	0	4	1	7	0	0	18	0	0	1	0	2	0	EU
	AL	AM	AT	AZ	BA	BE	BG	BY	CH	CY	CZ	DE	DK	EE	ES	FI	FR	GB	GE	GR	HR	HU	IE	IS	IT	KG	KZT	LT	LU	LV	MD	

Table C.8 Cont.: 2011 country-to-country blame matrices for **PM2.5**.
Units: ng/m^3 per 15% emis. red. of PPM. **Emitters** →, **Receptors** ↓. (Based on ECMWF meteorology.)

	ME	MK	MT	NL	NO	PL	PT	RO	RS	RUE	SE	SI	SK	TJ	TM	TR	UA	UZ	ATL	BAS	BLS	MED	NOS	AST	NOA	BIC	DMS	VOL	EXC	EU	
AL	5	17	0	0	0	2	0	7	21	1	0	0	1	0	0	0	0	0	0	0	0	6	0	0	0	0	0	0	261	66	AL
AM	0	0	0	0	0	0	0	0	0	1	0	0	0	0	0	12	0	0	0	0	0	0	0	7	0	0	0	0	25	0	AM
AT	0	0	0	0	0	6	0	3	1	0	0	27	13	0	0	0	0	0	0	0	0	1	0	0	0	0	0	0	197	187	AT
AZ	0	0	0	0	0	0	0	0	0	5	0	0	0	0	2	2	0	1	0	0	0	0	0	12	0	0	0	0	39	0	AZ
BA	9	1	0	0	0	4	0	11	13	0	0	2	4	0	0	0	0	0	0	0	0	2	0	0	0	0	0	0	162	49	BA
BE	0	0	0	15	0	4	0	0	0	0	0	0	1	0	0	0	0	0	1	0	0	0	11	0	0	0	0	0	253	250	BE
BG	0	2	0	0	0	3	0	50	7	3	0	0	2	0	0	5	2	0	0	0	2	1	0	0	0	0	0	0	236	211	BG
BY	0	0	0	0	0	24	0	4	0	9	1	0	3	0	0	0	4	0	0	1	0	0	1	0	0	0	0	0	144	55	BY
CH	0	0	0	0	0	0	0	0	0	0	0	1	0	0	0	0	0	0	0	0	0	1	0	0	0	0	0	0	155	69	CH
CY	0	0	0	0	0	0	0	1	0	1	0	0	0	0	0	65	0	0	0	0	0	19	0	2	1	0	0	0	95	28	CY
CZ	0	0	0	1	0	30	0	6	2	1	0	4	29	0	0	0	0	0	0	0	0	0	1	0	0	0	0	0	210	201	CZ
DE	0	0	0	4	0	13	0	2	0	0	0	1	2	0	0	0	0	0	1	1	0	0	4	0	0	0	0	0	211	204	DE
DK	0	0	0	2	4	11	0	1	0	1	3	0	1	0	0	0	0	0	1	11	0	0	11	0	0	0	0	0	138	132	DK
EE	0	0	0	0	2	6	0	1	0	7	4	0	0	0	0	0	1	0	0	5	0	0	1	0	0	0	0	0	130	116	EE
ES	0	0	0	0	0	0	6	0	0	0	0	0	0	0	0	0	0	0	3	0	0	7	0	0	0	0	0	0	71	71	ES
FI	0	0	0	0	2	2	0	0	0	3	4	0	0	0	0	0	0	0	0	1	0	0	0	0	0	0	0	0	67	60	FI
FR	0	0	0	1	0	1	0	0	0	0	0	1	1	0	0	0	0	0	2	0	0	3	2	0	0	0	0	0	180	176	FR
GB	0	0	0	1	0	1	0	0	0	0	0	0	0	0	0	0	0	0	4	0	0	0	6	0	0	0	0	0	89	88	GB
GE	0	0	0	0	0	0	0	0	0	3	0	0	0	0	0	6	0	0	0	0	0	0	0	1	0	0	0	0	26	0	GE
GL	-0	-0	0	0	0	-0	-0	-0	-0	0	0	-0	-0	0	0	-0	0	0	0	0	-0	-0	0	0	0	0	0	0	0	0	GL
GR	0	7	0	0	0	2	0	10	4	2	0	0	1	0	0	7	1	0	0	0	1	11	0	0	0	0	0	0	173	146	GR
HR	1	1	0	0	0	7	0	13	13	1	0	26	7	0	0	0	1	0	0	0	0	5	0	0	0	0	0	0	217	113	HR
HU	0	0	0	0	0	18	0	48	11	1	0	12	44	0	0	0	2	0	0	0	0	1	0	0	0	0	0	0	366	333	HU
IE	0	0	0	0	0	0	0	0	0	0	0	0	0	0	0	0	0	0	5	0	0	0	1	0	0	0	0	0	30	30	IE
IS	0	0	0	0	0	0	0	0	0	0	0	0	0	0	0	0	0	0	1	0	0	0	0	0	0	0	0	0	1	1	IS
IT	0	0	0	0	0	2	0	2	1	0	0	9	1	0	0	0	0	0	0	0	0	15	0	0	0	0	0	0	263	255	IT
KG	0	0	0	0	0	0	0	0	0	0	0	0	0	5	0	0	0	50	0	0	0	0	0	1	0	0	0	0	105	0	KG
KZT	0	0	0	0	0	0	0	0	0	20	0	0	0	0	1	0	0	7	0	0	0	0	0	1	0	0	0	0	111	1	KZT
LT	0	0	0	1	1	27	0	2	0	9	2	0	2	0	0	0	2	0	0	2	0	0	1	0	0	0	0	0	137	109	LT
LU	0	0	0	2	0	3	0	1	0	0	0	1	1	0	0	0	0	0	1	0	0	0	2	0	0	0	0	0	270	267	LU
LV	0	0	0	0	1	11	0	1	0	6	3	0	1	0	0	0	1	0	0	3	0	0	1	0	0	0	0	0	158	140	LV
MD	0	0	0	0	0	13	0	108	1	7	0	0	4	0	0	2	13	0	0	0	1	0	0	0	0	0	0	0	211	142	MD
ME	89	2	0	0	0	2	0	7	20	0	0	0	2	0	0	0	0	0	0	0	0	3	0	0	0	0	0	0	169	28	ME
MK	1	102	0	0	0	2	0	10	23	1	0	0	2	0	0	1	1	0	0	0	0	1	0	0	0	0	0	0	245	101	MK
MT	0	0	55	0	0	1	0	2	1	0	0	0	0	0	0	0	0	0	0	0	0	92	0	0	2	0	0	0	99	94	MT
NL	0	0	0	78	1	6	0	1	0	0	0	0	1	0	0	0	0	0	1	1	0	0	26	0	0	0	0	0	223	220	NL
NO	0	0	0	0	30	1	0	0	0	0	2	0	0	0	0	0	0	0	0	0	0	0	1	0	0	0	0	0	37	7	NO
PL	0	0	0	1	1	173	0	6	1	2	1	1	13	0	0	0	2	0	0	1	0	0	1	0	0	0	0	0	252	240	PL
PT	0	0	0	0	0	0	136	0	0	0	0	0	0	0	0	0	0	0	13	0	0	2	0	0	0	0	0	0	160	160	PT
RO	0	1	0	0	0	8	0	308	5	3	0	1	5	0	0	1	4	0	0	0	1	0	0	0	0	0	0	0	372	352	RO
RS	6	7	0	0	0	6	0	46	95	1	0	1	7	0	0	0	1	0	0	0	0	1	0	0	0	0	0	0	231	103	RS
RUE	0	0	0	0	0	1	0	0	0	42	0	0	0	0	0	0	0	0	0	0	0	0	0	0	0	0	0	0	53	3	RUE
SE	0	0	0	0	8	3	0	1	0	1	19	0	0	0	0	0	0	0	0	2	0	0	2	0	0	0	0	0	46	36	SE
SI	0	0	0	0	0	6	0	8	3	0	0	323	4	0	0	0	0	0	0	0	0	4	0	0	0	0	0	0	461	422	SI
SK	0	0	0	0	0	41	0	20	2	1	0	4	200	0	0	0	2	0	0	0	0	0	0	0	0	0	0	0	363	352	SK
TJ	0	0	0	0	0	0	0	0	0	0	0	0	0	64	1	0	0	39	0	0	0	0	0	10	0	0	0	0	113	0	TJ
TM	0	0	0	0	0	0	0	0	0	4	0	0	0	2	40	0	0	32	0	0	0	0	0	11	0	0	0	0	96	0	TM
TR	0	0	0	0	0	1	0	2	0	2	0	0	0	0	0	135	1	0	0	0	1	2	0	2	0	0	0	0	144	6	TR
UA	0	0	0	0	0	15	0	17	0	17	0	0	3	0	0	1	25	0	0	0	1	0	0	0	0	0	0	0	104	48	UA
UZ	0	0	0	0	0	0	0	0	0	5	0	0	0	9	6	0	0	135	0	0	0	0	0	4	0	0	0	0	201	0	UZ
ATL	0	0	0	0	0	0	1	0	0	0	0	0	0	0	0	0	0	0	2	0	0	0	0	0	0	0	0	0	5	4	ATL
BAS	0	0	0	1	3	14	0	1	0	3	11	0	1	0	0	0	0	0	0	12	0	0	3	0	0	0	0	0	91	81	BAS
BLS	0	0	0	0	0	3	0	16	0	14	0	0	1	0	0	26	7	0	0	0	11	1	0	0	0	0	0	0	81	29	BLS
MED	0	0	0	0	0	1	0	3	1	1	0	1	1	0	0	17	0	0	0	0	0	49	0	1	2	0	0	0	74	49	MED
NOS	0	0	0	3	4	3	0	0	0	0	1	0	0	0	0	0	0	0	2	1	0	0	16	0	0	0	0	0	56	50	NOS
AST	0	0	0	0	0	0	0	0	0	2	0	0	0	1	2	8	0	3	0	0	0	1	0	24	0	0	0	0	23	1	AST
NOA	0	0	0	0	0	0	0	1	0	0	0	0	0	0	0	3	0	0	0	0	0	9	0	0	7	0	0	0	14	9	NOA
EXC	0	0	0	0	1	4	1	5	1	24	1	1	1	1	1	5	1	5	0	0	0	1	0	1	0	0	0	0	90	35	EXC
EU	0	0	0	1	1	17	4	21	1	1	3	3	6	0	0	1	1	0	1	1	0	3	2	0	0	0	0	0	169	160	EU
	ME	MK	MT	NL	NO	PL	PT	RO	RS	RUE	SE	SI	SK	TJ	TM	TR	UA	UZ	ATL	BAS	BLS	MED	NOS	AST	NOA	BIC	DMS	VOL	EXC	EU	

Table C.9: 2011 country-to-country blame matrices for **PM2.5**.
Units: ng/m^3 per 15% emis. red. of SO_x. **Emitters →, Receptors ↓**. (Based on ECMWF meteorology.)

	AL	AM	AT	AZ	BA	BE	BG	BY	CH	CY	CZ	DE	DK	EE	ES	FI	FR	GB	GE	GR	HR	HU	IE	IS	IT	KG	KZT	LT	LU	LV	MD	
AL	73	0	1	0	78	0	67	0	0	0	6	6	0	0	4	0	3	2	0	76	4	3	0	0	13	0	1	0	0	0	0	AL
AM	0	108	0	74	0	-0	0	0	-0	0	0	0	0	-0	0	-0	-0	-0	16	0	0	0	-0	-0	0	0	15	-0	-0	-0	0	AM
AT	0	0	25	0	21	1	7	0	5	0	21	62	0	0	4	0	11	4	0	1	8	6	0	0	19	0	1	0	0	0	0	AT
AZ	0	11	0	224	0	0	0	0	-0	0	0	0	0	0	0	-0	-0	0	24	0	0	0	-0	-0	0	0	57	0	-0	0	0	AZ
BA	2	0	2	0	499	1	26	1	0	0	13	17	0	0	5	0	4	3	0	6	14	6	0	0	10	0	1	0	0	0	0	BA
BE	0	0	2	0	5	100	2	0	3	-0	11	84	0	0	9	0	94	48	-0	0	1	1	2	0	3	0	1	0	2	0	0	BE
BG	1	0	1	0	21	0	361	2	0	0	6	8	0	1	1	0	2	2	0	14	1	3	0	0	1	0	5	1	0	0	1	BG
BY	0	0	0	0	4	1	1	46	0	0	5	13	1	7	1	3	2	6	0	0	0	1	0	0	0	0	10	13	0	1	0	BY
CH	0	0	5	0	3	1	1	0	54	-0	6	47	0	0	7	0	29	5	0	0	1	1	0	0	25	0	0	0	0	0	0	CH
CY	0	0	0	0	8	0	27	1	0	22	1	2	0	0	1	0	1	0	0	30	0	0	0	0	3	0	3	0	0	0	0	CY
CZ	0	0	8	0	21	3	9	1	2	0	113	96	0	1	4	0	17	10	0	1	4	8	0	0	4	0	1	1	0	0	0	CZ
DE	0	0	6	0	8	13	4	1	4	0	27	203	1	1	6	1	35	25	0	1	1	2	1	0	4	0	1	1	1	0	0	DE
DK	0	0	0	0	4	7	2	1	0	-0	11	51	19	1	1	1	11	39	0	0	0	0	1	1	0	0	1	1	0	0	0	DK
EE	0	0	0	0	0	1	0	5	0	0	2	7	1	27	0	11	1	8	0	0	0	0	0	0	0	0	4	5	0	2	0	EE
ES	0	0	0	0	4	1	1	0	0	-0	1	3	0	0	202	0	10	3	0	0	1	0	0	0	4	0	0	0	0	0	0	ES
FI	0	0	0	0	0	0	0	1	0	0	1	3	0	7	0	34	1	2	0	0	0	0	0	0	0	0	1	1	0	0	0	FI
FR	0	0	1	0	5	6	1	0	3	-0	5	28	0	0	32	0	89	18	0	0	1	1	1	0	10	0	0	0	0	0	0	FR
GB	0	0	0	0	1	2	1	0	0	-0	2	11	0	0	5	0	14	128	0	0	0	0	8	1	1	0	0	0	0	0	0	GB
GE	0	12	0	46	0	0	1	0	0	0	0	0	0	0	0	-0	0	0	90	0	0	0	-0	-0	0	0	12	0	0	0	0	GE
GL	0	0	0	0	0	0	0	0	0	-0	0	0	0	0	0	0	0	0	0	0	0	0	0	0	0	0	0	0	0	0	0	GL
GR	6	0	1	0	29	0	201	1	0	0	4	5	0	0	2	0	2	1	0	138	2	2	0	0	8	0	3	0	0	0	0	GR
HR	2	0	5	0	251	1	24	1	1	0	20	29	0	1	6	0	7	4	0	5	49	11	0	0	22	0	1	0	0	0	0	HR
HU	1	0	6	0	61	2	21	2	1	0	28	39	0	1	4	0	8	6	0	2	13	48	0	0	7	0	2	1	0	0	0	HU
IE	0	0	0	0	0	1	0	0	0	-0	0	2	0	0	3	0	3	41	0	0	0	0	38	1	1	0	0	0	0	0	0	IE
IS	0	-0	0	-0	0	0	0	0	0	0	0	0	0	0	0	0	0	1	-0	0	0	0	0	95	0	0	0	0	0	0	0	IS
IT	1	0	3	0	53	1	9	0	2	0	8	11	0	0	16	0	18	2	0	5	11	2	0	0	144	0	0	0	0	0	0	IT
KG	0	0	-0	0	0	-0	0	0	-0	0	-0	-0	-0	0	-0	-0	-0	-0	0	0	0	-0	-0	-0	-0	35	141	0	-0	0	0	KG
KZT	0	0	0	1	0	-0	0	0	-0	0	0	0	0	0	0	0	-0	-0	0	0	0	0	-0	0	0	1	330	0	-0	0	0	KZT
LT	0	0	0	0	3	1	1	11	0	0	4	16	2	7	1	3	2	10	0	0	0	1	0	0	1	0	5	45	0	2	0	LT
LU	0	0	3	0	6	28	2	0	3	0	12	110	0	0	11	0	99	30	0	0	1	1	1	0	3	0	1	0	18	0	0	LU
LV	0	0	0	0	1	1	0	9	0	0	3	12	2	13	1	5	2	9	0	0	0	0	0	0	0	0	5	17	0	5	0	LV
MD	0	0	1	0	7	1	16	6	0	0	10	11	0	2	1	1	2	3	0	1	1	3	0	0	1	0	9	2	0	0	9	MD
ME	12	0	1	0	129	0	32	0	0	0	7	8	0	0	3	0	3	2	0	12	5	3	0	0	8	0	1	0	0	0	0	ME
MK	13	0	1	0	41	0	155	1	0	0	7	7	0	0	2	0	2	2	0	62	2	3	0	0	4	0	1	0	0	0	0	MK
MT	2	0	1	0	39	0	21	0	0	0	3	4	0	0	24	0	14	3	0	17	3	1	0	0	66	0	1	0	0	0	0	MT
NL	0	0	2	0	5	54	3	1	2	-0	12	120	1	0	5	0	53	64	-0	0	1	1	3	1	2	0	1	1	1	0	0	NL
NO	0	0	0	0	0	0	0	0	0	0	1	4	0	1	1	2	1	5	0	0	0	0	0	1	0	0	1	0	0	0	0	NO
PL	0	0	1	0	8	3	5	4	0	0	25	50	1	3	2	1	7	14	0	1	1	4	0	0	2	0	3	3	0	0	0	PL
PT	0	0	0	0	2	1	0	0	0	0	1	3	0	0	98	0	4	3	0	0	0	0	0	0	1	0	0	0	0	0	0	PT
RO	1	0	1	0	22	1	34	3	0	0	10	13	0	1	2	0	3	3	0	3	2	7	0	0	2	0	5	1	0	0	2	RO
RS	5	0	2	0	89	1	67	1	0	0	15	18	0	0	3	0	4	3	0	9	5	12	0	0	4	0	2	0	0	0	1	RS
RUE	0	0	0	1	0	0	0	1	0	0	0	1	0	1	0	1	0	0	0	0	0	0	0	0	0	0	53	0	0	0	0	RUE
SE	0	0	0	0	1	1	0	1	0	0	2	8	2	3	1	5	2	8	0	0	0	0	0	0	0	0	1	1	0	0	0	SE
SI	0	0	12	0	75	2	15	1	1	0	19	37	0	0	6	0	8	3	0	2	41	7	0	0	45	0	1	0	0	0	0	SI
SK	0	0	4	0	23	2	12	2	1	0	37	36	0	1	3	0	7	6	0	1	5	23	0	0	3	0	2	1	0	0	0	SK
TJ	0	0	-0	0	0	-0	0	0	-0	0	0	0	0	0	-0	0	-0	-0	0	0	0	0	-0	-0	-0	3	76	0	-0	0	0	TJ
TM	0	1	0	5	0	0	0	0	-0	0	0	0	0	0	0	0	-0	-0	1	0	0	0	-0	0	0	1	160	0	-0	0	0	TM
TR	0	2	0	1	3	0	14	1	0	1	1	1	0	0	0	0	0	0	1	5	0	0	0	0	0	0	3	0	0	0	0	TR
UA	0	0	0	0	5	1	6	9	0	0	7	10	0	3	1	1	2	3	0	1	0	2	0	0	0	0	17	2	0	0	1	UA
UZ	0	0	0	2	0	0	0	0	-0	0	0	0	0	0	0	0	-0	-0	0	0	0	0	-0	0	0	4	267	0	-0	0	0	UZ
ATL	0	0	0	0	0	0	0	0	0	0	0	1	0	0	3	0	1	3	0	0	0	0	0	2	0	0	2	0	0	0	0	ATL
BAS	0	0	0	0	1	2	1	2	0	0	4	20	4	7	1	11	4	16	0	0	0	0	1	0	0	0	1	3	0	1	0	BAS
BLS	0	1	0	2	4	0	21	3	0	0	4	5	0	1	0	0	1	1	5	3	0	1	0	0	0	0	13	1	0	0	1	BLS
MED	3	0	1	0	50	1	50	1	0	2	4	5	0	0	32	0	14	2	0	41	5	1	0	0	40	0	1	0	0	0	0	MED
NOS	0	0	0	0	2	4	1	0	0	-0	3	19	1	0	3	0	13	49	0	0	0	0	2	1	1	0	0	0	0	0	0	NOS
AST	0	1	0	5	0	0	1	0	0	1	0	0	0	0	0	0	0	0	0	1	0	0	0	0	0	1	63	0	0	0	0	AST
NOA	1	0	0	0	16	0	27	0	0	0	1	1	0	0	14	0	4	1	0	25	1	0	0	0	11	0	0	0	0	0	0	NOA
EXC	0	0	0	2	5	1	5	1	0	0	3	8	0	1	6	1	4	4	1	1	1	1	0	0	3	1	75	1	0	0	0	EXC
EU	0	0	2	0	12	4	20	1	1	0	11	35	1	2	33	4	21	17	0	5	2	3	1	0	14	0	1	2	0	0	0	EU
	AL	AM	AT	AZ	BA	BE	BG	BY	CH	CY	CZ	DE	DK	EE	ES	FI	FR	GB	GE	GR	HR	HU	IE	IS	IT	KG	KZT	LT	LU	LV	MD	

Table C.9 Cont.: 2011 country-to-country blame matrices for **PM2.5**.
Units: ng/m^3 per 15% emis. red. of SO$_x$. **Emitters →, Receptors ↓.** (Based on ECMWF meteorology.)

	ME	MK	MT	NL	NO	PL	PT	RO	RS	RUE	SE	SI	SK	TJ	TM	TR	UA	UZ	ATL	BAS	BLS	MED	NOS	AST	NOA	BIC	DMS	VOL	EXC	EU	
AL	19	73	1	0	0	26	0	29	180	4	0	0	6	0	0	9	24	0	0	0	1	60	1	0	2	11	2	17	710	243	AL
AM	0	0	0	-0	-0	1	-0	1	0	6	-0	0	0	0	4	75	5	4	0	0	1	1	-0	51	0	9	0	14	311	3	AM
AT	0	1	0	1	0	34	0	8	17	2	0	8	6	0	0	1	10	0	2	1	0	8	2	0	0	12	1	4	286	219	AT
AZ	0	0	0	0	-0	2	-0	1	0	31	-0	0	0	0	13	21	22	11	0	0	1	0	0	42	0	6	0	7	418	4	AZ
BA	16	8	0	1	0	40	0	23	115	3	0	1	10	0	0	2	20	0	1	1	1	18	2	0	1	11	1	6	852	170	BA
BE	0	0	0	11	0	21	0	2	2	1	0	0	2	0	0	0	6	0	20	1	0	3	45	0	0	15	8	3	415	394	BE
BG	1	10	0	0	0	33	0	93	58	21	0	0	5	0	0	26	96	0	0	1	12	6	1	0	0	10	1	3	778	534	BG
BY	0	0	0	1	0	81	0	4	3	43	1	0	3	0	0	0	55	0	1	5	0	1	4	0	0	7	1	0	310	147	BY
CH	0	0	0	1	0	7	0	2	2	0	0	1	1	0	0	0	3	0	3	0	0	7	2	0	0	15	1	4	203	139	CH
CY	1	4	0	0	0	9	0	12	10	9	0	0	1	0	0	1433	34	0	0	0	8	160	0	12	5	13	13	29	1614	110	CY
CZ	0	1	0	2	0	84	0	12	22	4	0	2	14	0	0	1	21	0	3	2	0	3	6	0	0	11	2	2	469	389	CZ
DE	0	1	0	8	0	43	0	4	6	2	0	1	3	0	0	0	11	0	8	6	0	3	24	0	0	12	4	2	425	388	DE
DK	0	1	0	6	2	34	0	3	3	3	2	0	1	0	0	0	7	0	9	28	0	1	50	0	0	9	11	0	219	195	DK
EE	0	0	0	1	1	19	0	1	0	30	4	0	1	0	0	0	10	0	2	17	0	0	6	0	0	5	3	0	143	92	EE
ES	0	0	0	0	0	3	9	1	2	0	0	0	1	0	0	0	1	0	26	0	0	59	1	0	4	21	5	3	248	239	ES
FI	0	0	0	0	1	7	0	0	0	20	6	0	0	0	0	0	3	0	2	6	0	0	2	0	0	5	2	0	91	64	FI
FR	0	0	0	2	0	9	1	2	2	0	0	1	1	0	0	0	4	0	27	0	0	23	12	0	1	15	7	3	224	207	FR
GB	0	0	0	2	0	4	0	1	1	0	0	0	0	0	0	0	2	0	37	1	0	2	18	0	0	10	12	1	186	181	GB
GE	0	0	0	0	-0	2	0	1	0	14	0	0	0	0	3	48	15	3	0	0	5	0	0	11	0	7	0	8	250	5	GE
GL	0	0	0	0	0	0	0	0	0	0	0	0	0	0	0	0	0	0	0	0	0	0	0	0	0	28	0	0	0	0	GL
GR	3	40	1	0	0	23	0	45	51	12	0	0	4	0	0	79	56	0	0	0	7	87	1	0	2	10	3	15	720	438	GR
HR	5	6	0	1	0	53	0	28	97	4	0	4	12	0	0	2	26	0	1	1	1	32	2	0	1	10	1	5	681	234	HR
HU	2	3	0	1	0	99	0	67	74	8	0	3	29	0	0	2	57	0	2	1	1	7	3	0	1	11	1	3	600	374	HU
IE	0	0	0	0	0	2	0	0	0	0	0	0	0	0	-0	0	1	0	44	0	0	1	3	0	0	11	15	0	94	92	IE
IS	0	0	0	0	0	0	0	0	0	0	0	0	0	0	0	0	0	0	4	0	0	0	0	0	0	7	6	0	99	3	IS
IT	2	4	1	0	0	21	0	9	18	1	0	5	4	-0	0	2	8	0	2	0	0	117	1	0	4	12	3	25	364	262	IT
KG	0	0	0	-0	-0	0	-0	0	0	2	-0	-0	-0	10	1	1	1	267	-0	-0	0	0	-0	15	0	11	0	18	459	-0	KG
KZT	0	0	0	0	0	2	-0	0	0	88	0	0	0	1	3	1	17	28	0	0	0	0	0	8	0	10	0	4	474	3	KZT
LT	0	0	0	1	1	67	0	2	2	27	2	0	2	0	0	0	31	0	2	11	0	0	7	0	0	6	3	0	252	172	LT
LU	0	0	0	5	0	20	0	2	2	1	0	0	3	0	0	0	7	0	14	1	0	4	17	0	0	15	4	3	372	350	LU
LV	0	0	0	1	1	33	0	1	1	27	3	0	1	0	0	0	17	0	2	12	0	0	7	0	0	5	3	0	171	110	LV
MD	0	1	0	0	0	74	0	54	9	42	0	0	6	0	0	8	209	1	1	1	6	1	2	0	0	9	1	1	494	190	MD
ME	84	18	0	0	0	27	0	22	160	3	0	0	6	0	0	3	15	0	1	0	1	26	1	0	1	10	1	11	566	136	ME
MK	5	104	0	0	0	27	0	39	152	6	0	0	6	0	0	10	31	0	0	0	2	14	1	0	1	11	1	8	684	319	MK
MT	3	6	32	0	0	10	0	11	22	2	0	1	2	0	0	12	9	0	3	0	1	432	1	0	18	12	13	51	308	210	MT
NL	0	1	0	29	0	33	0	2	3	1	0	0	2	0	0	0	8	0	18	2	0	2	87	0	0	13	10	2	411	389	NL
NO	0	0	0	0	7	5	0	0	0	3	2	0	0	0	0	0	1	0	5	1	0	0	5	0	0	6	4	0	38	24	NO
PL	0	1	0	3	0	228	0	13	8	11	1	1	9	0	0	0	44	0	3	7	0	2	9	0	0	8	2	1	460	377	PL
PT	0	0	0	0	0	2	45	1	1	0	0	0	0	0	0	0	1	0	78	0	0	16	1	0	3	21	7	2	164	160	PT
RO	1	3	0	0	0	59	0	191	32	21	0	0	9	0	0	6	114	0	1	1	5	2	1	0	0	10	1	2	553	340	RO
RS	11	17	0	1	0	53	0	81	277	8	0	1	14	0	0	3	46	0	1	1	2	8	2	0	1	11	1	5	754	289	RS
RUE	0	0	0	0	0	4	0	0	0	107	0	0	0	0	0	1	14	1	0	0	0	0	0	1	0	9	0	1	189	9	RUE
SE	0	0	0	1	4	14	0	1	1	5	11	0	0	0	0	0	3	0	4	9	0	0	9	0	0	5	3	0	75	60	SE
SI	1	3	0	1	0	43	0	16	40	3	0	36	8	0	0	1	15	0	1	1	0	29	2	0	1	10	1	4	444	261	SI
SK	1	2	0	1	0	130	0	36	29	7	0	2	51	0	0	1	49	0	2	1	1	4	3	0	0	9	1	2	478	356	SK
TJ	0	0	0	0	-0	0	-0	0	0	3	0	-0	0	40	7	1	1	203	-0	0	0	0	0	15	0	15	0	25	335	0	TJ
TM	0	0	0	0	0	1	0	0	0	30	0	0	0	3	45	5	14	103	0	0	0	0	0	27	0	12	0	12	369	2	TM
TR	0	1	0	0	0	8	0	9	4	12	0	0	1	0	0	584	42	1	0	0	9	16	0	15	1	12	2	21	701	43	TR
UA	0	1	0	0	0	66	0	16	5	68	0	0	4	0	0	10	255	1	1	2	5	1	2	0	0	8	1	1	499	126	UA
UZ	0	0	0	0	0	1	-0	0	0	38	0	0	0	10	13	4	14	275	-0	0	0	0	0	12	0	12	0	15	631	2	UZ
ATL	0	0	0	0	0	1	0	0	0	5	0	0	0	0	0	0	0	0	15	0	0	0	1	0	0	16	12	0	22	11	ATL
BAS	0	0	0	2	2	31	0	3	1	13	8	0	1	0	0	0	9	0	4	28	0	0	15	0	0	6	5	0	150	120	BAS
BLS	0	1	0	0	0	31	0	27	7	67	0	0	2	0	1	113	223	1	0	1	49	5	1	1	0	8	6	3	544	101	BLS
MED	4	8	3	0	0	16	1	19	27	7	0	1	3	0	0	288	31	0	3	0	5	339	1	3	15	14	13	37	661	237	MED
NOS	0	0	0	3	1	11	0	1	1	1	1	0	1	0	0	0	2	0	19	2	0	1	31	0	0	9	15	1	123	113	NOS
AST	0	0	0	0	0	1	0	1	0	14	0	0	0	1	7	56	10	22	0	0	0	7	0	102	1	19	1	15	187	7	AST
NOA	1	5	1	0	0	5	0	9	11	2	0	0	1	-0	0	79	10	0	1	0	1	105	0	1	35	24	5	35	228	102	NOA
EXC	0	1	0	0	0	13	0	5	4	67	1	0	1	1	2	23	22	15	3	1	1	5	2	3	0	11	1	3	281	60	EXC
EU	1	2	0	2	1	39	2	19	11	7	2	1	4	0	0	6	20	0	13	3	1	23	9	0	1	11	4	4	309	243	EU
	ME	MK	MT	NL	NO	PL	PT	RO	RS	RUE	SE	SI	SK	TJ	TM	TR	UA	UZ	ATL	BAS	BLS	MED	NOS	AST	NOA	BIC	DMS	VOL	EXC	EU	

Table C.10: 2011 country-to-country blame matrices for **PM2.5**.
Units: ng/m^3 per 15% emis. red. of NO_x. **Emitters →, Receptors ↓.** (Based on ECMWF meteorology.)

	AL	AM	AT	AZ	BA	BE	BG	BY	CH	CY	CZ	DE	DK	EE	ES	FI	FR	GB	GE	GR	HR	HU	IE	IS	IT	KG	KZT	LT	LU	LV	MD	
AL	34	0	1	0	5	0	6	0	0	0	1	2	0	0	1	0	1	1	0	13	3	3	0	0	8	0	0	0	0	0	0	AL
AM	0	36	0	40	0	0	0	0	0	0	0	1	0	0	0	0	0	0	13	0	0	0	0	0	0	0	0	0	0	0	0	AM
AT	0	0	46	0	1	1	0	0	11	0	10	52	0	0	1	0	14	2	0	0	5	8	0	0	42	0	0	0	1	0	0	AT
AZ	0	7	0	104	0	0	0	0	0	0	0	1	0	0	0	0	0	1	33	0	0	0	0	0	0	0	3	0	0	0	0	AZ
BA	1	0	4	0	47	0	2	0	0	0	3	5	0	0	1	0	2	1	0	1	13	8	0	0	8	0	0	0	0	0	0	BA
BE	0	0	4	0	0	-10	0	0	6	0	4	60	1	0	5	0	93	25	0	0	0	0	2	0	7	0	0	0	3	0	0	BE
BG	0	0	1	0	1	0	40	1	0	0	1	1	0	0	0	-0	0	0	0	4	0	2	0	0	1	0	0	0	0	0	1	BG
BY	0	0	1	0	0	1	0	25	0	0	1	9	2	1	0	1	2	5	0	0	0	1	0	0	1	0	0	5	0	2	1	BY
CH	0	0	18	0	0	2	0	0	107	0	3	72	0	0	3	0	54	4	0	0	0	1	0	0	96	0	0	0	1	0	0	CH
CY	0	0	0	0	0	0	1	-0	0	14	0	1	0	0	0	0	0	0	0	7	0	0	0	0	1	0	0	0	0	0	0	CY
CZ	0	0	22	0	1	2	1	-0	2	0	19	51	0	0	1	0	14	4	0	0	3	13	0	0	6	0	0	0	1	0	0	CZ
DE	0	0	14	0	0	8	0	0	8	0	9	78	2	0	3	0	36	13	0	0	0	1	1	0	9	0	0	0	2	0	0	DE
DK	0	0	1	0	0	8	0	0	0	0	3	49	5	0	1	1	13	25	0	0	0	1	1	0	1	0	0	1	1	0	0	DK
EE	0	0	0	0	0	1	0	5	0	0	0	4	1	5	0	2	1	3	0	0	0	0	0	0	0	0	0	2	0	3	0	EE
ES	0	0	0	0	0	1	0	0	0	0	0	2	0	0	65	-0	9	1	0	0	0	0	0	0	3	0	-0	0	0	0	0	ES
FI	0	0	0	0	0	0	0	1	0	0	0	2	0	0	0	7	0	1	0	0	0	0	0	0	0	0	0	0	0	0	0	FI
FR	0	0	4	0	0	7	0	0	9	0	2	35	0	0	11	0	110	12	0	0	0	0	1	0	17	0	0	0	2	0	0	FR
GB	0	0	0	0	0	3	0	0	1	0	1	10	1	0	3	0	30	37	0	0	0	0	5	0	2	0	0	0	1	0	0	GB
GE	0	8	0	19	0	0	0	0	0	0	0	1	0	0	0	0	0	0	54	0	0	0	0	0	0	0	0	0	0	0	0	GE
GL	-0	-0	0	-0	-0	0	-0	0	0	-0	0	0	0	0	0	-0	0	0	-0	-0	-0	0	0	0	0	0	0	0	0	0	-0	GL
GR	2	0	0	0	1	0	26	0	0	0	0	0	0	0	1	0	0	0	0	38	0	1	0	0	4	0	0	0	0	0	1	GR
HR	0	0	12	0	24	1	3	0	1	0	6	13	0	0	1	0	4	2	0	1	28	17	0	0	27	0	0	0	0	0	0	HR
HU	0	0	16	0	6	1	4	1	2	0	10	21	0	0	1	0	7	3	0	1	13	45	0	0	14	0	0	0	0	0	0	HU
IE	0	0	0	0	0	3	0	0	0	0	0	4	0	0	1	0	10	57	0	0	0	0	18	0	1	0	0	0	0	0	0	IE
IS	0	0	0	0	0	0	0	-0	0	0	-0	0	0	-0	0	0	0	1	0	0	0	-0	0	3	0	0	0	-0	0	-0	0	IS
IT	0	0	11	0	2	1	0	0	3	0	3	10	0	0	3	0	9	1	0	1	6	2	0	0	200	0	0	0	0	0	0	IT
KG	0	0	0	0	0	0	0	0	0	0	0	0	0	0	0	0	0	0	0	0	0	0	0	0	0	16	7	0	0	0	0	KG
KZT	0	0	0	0	0	0	0	0	0	0	0	1	0	0	0	0	0	1	0	0	0	0	0	0	0	1	32	0	0	0	0	KZT
LT	-0	0	1	0	0	2	0	12	0	0	1	11	3	1	0	1	3	6	0	0	0	1	0	0	2	0	0	9	0	3	1	LT
LU	0	0	7	0	0	14	0	-0	5	0	6	68	1	0	7	0	81	15	0	0	0	0	1	0	7	0	0	0	-18	0	0	LU
LV	-0	0	0	0	0	1	0	8	0	0	1	7	2	1	0	1	1	4	0	0	0	0	0	0	1	0	0	5	0	5	0	LV
MD	0	0	1	0	0	0	2	3	0	0	2	4	0	0	0	0	2	2	0	0	0	2	0	0	1	0	0	0	0	0	13	MD
ME	5	0	1	0	13	0	3	0	0	0	1	1	0	0	1	-0	1	1	0	3	4	3	0	0	5	0	0	0	0	0	0	ME
MK	6	0	1	0	2	0	18	0	0	0	1	2	0	0	1	0	1	1	0	10	1	4	0	0	3	0	0	0	0	0	0	MK
MT	0	0	1	0	1	0	1	0	0	0	0	1	0	0	3	-0	6	1	0	3	1	0	0	0	24	0	0	0	0	0	0	MT
NL	0	0	3	0	0	15	0	0	1	0	4	61	2	0	4	0	58	37	0	0	0	0	3	0	4	0	0	0	3	0	0	NL
NO	0	0	0	0	0	0	0	0	0	0	0	3	1	0	0	0	1	2	0	0	0	0	0	0	0	0	0	0	0	0	0	NO
PL	0	0	3	0	0	2	0	4	1	0	6	25	2	0	1	1	5	6	0	0	1	4	0	0	3	0	0	2	0	1	0	PL
PT	0	0	0	0	0	0	-0	0	0	0	0	1	0	-0	34	-0	2	1	0	0	0	0	0	0	1	0	-0	0	0	-0	0	PT
RO	0	0	3	0	1	0	6	1	1	0	3	6	0	0	0	0	2	1	0	1	1	8	0	0	2	0	0	0	0	0	3	RO
RS	2	0	6	0	8	1	13	1	1	0	6	12	0	0	1	0	4	2	0	6	5	19	0	0	4	0	0	0	0	0	1	RS
RUE	0	0	0	0	0	0	0	1	0	0	0	1	0	0	0	0	0	1	0	0	0	0	0	0	0	0	3	0	0	0	0	RUE
SE	0	0	0	0	0	1	0	0	0	0	0	5	1	0	0	1	1	3	0	0	0	0	0	0	0	0	0	0	0	0	0	SE
SI	0	0	32	0	5	1	1	0	2	0	7	21	0	0	1	0	5	2	0	1	31	12	0	0	81	0	0	0	0	0	0	SI
SK	0	0	7	0	2	0	2	0	1	0	9	13	-0	0	1	0	5	2	0	0	4	27	0	0	5	0	0	0	0	0	0	SK
TJ	0	0	0	0	-0	0	0	-0	0	0	0	0	0	-0	0	-0	0	0	0	0	-0	0	0	0	0	1	4	-0	0	-0	0	TJ
TM	0	0	0	1	0	0	0	0	0	0	0	1	0	0	0	0	0	1	0	0	0	0	0	0	0	0	14	0	0	0	0	TM
TR	0	1	0	1	0	0	1	0	0	0	0	1	0	0	0	0	0	1	1	1	0	0	0	0	1	0	0	0	0	0	0	TR
UA	0	0	0	0	0	0	0	4	0	0	-0	-0	0	0	0	0	1	1	0	0	0	1	0	0	0	0	1	0	0	0	2	UA
UZ	0	0	0	1	0	0	0	0	0	0	0	1	0	0	0	0	0	1	0	0	0	0	0	0	0	2	24	0	0	0	0	UZ
ATL	0	0	0	0	0	0	0	0	0	0	0	1	0	0	0	0	3	2	0	0	0	0	0	0	0	0	0	0	0	0	0	ATL
BAS	0	0	0	0	0	2	0	1	0	0	1	12	3	1	0	2	4	7	0	0	0	0	0	0	0	0	0	1	0	1	0	BAS
BLS	0	0	-0	0	-0	0	1	1	0	0	-0	-0	0	-0	0	-0	0	0	3	0	-0	0	0	0	0	0	1	0	0	0	1	BLS
MED	0	0	1	0	2	0	4	0	0	0	0	1	0	-0	3	-0	5	1	0	5	2	1	0	0	17	0	0	0	0	-0	0	MED
NOS	0	0	0	0	0	3	0	0	1	0	1	17	1	0	2	0	24	18	0	0	0	0	2	0	2	0	0	0	1	0	0	NOS
AST	0	0	0	2	0	0	0	0	0	0	0	0	0	0	0	0	0	0	0	0	0	0	0	0	0	1	5	0	0	0	0	AST
NOA	0	0	0	0	0	0	1	0	0	0	0	1	0	-0	3	-0	2	0	0	4	0	0	0	0	4	0	-0	0	0	-0	0	NOA
EXC	0	0	1	1	0	1	1	1	1	0	1	5	0	0	2	0	5	2	0	0	0	1	0	0	4	0	6	0	0	0	0	EXC
EU	0	0	5	0	1	2	2	1	3	0	3	20	1	0	11	1	24	8	0	1	1	3	1	0	20	0	0	0	1	0	0	EU
	AL	AM	AT	AZ	BA	BE	BG	BY	CH	CY	CZ	DE	DK	EE	ES	FI	FR	GB	GE	GR	HR	HU	IE	IS	IT	KG	KZT	LT	LU	LV	MD	

Table C.10 Cont.: 2011 country-to-country blame matrices for **PM2.5**.
Units: ng/m^3 per 15% emis. red. of NO$_x$. **Emitters →, Receptors ↓.** (Based on ECMWF meteorology.)

	ME	MK	MT	NL	NO	PL	PT	RO	RS	RUE	SE	SI	SK	TJ	TM	TR	UA	UZ	ATL	BAS	BLS	MED	NOS	AST	NOA	BIC	DMS	VOL	EXC	EU	
AL	4	10	0	0	0	2	0	5	43	1	0	0	1	0	0	1	2	0	1	0	1	13	0	0	0	7	0	0	152	47	AL
AM	0	0	0	0	0	1	0	0	0	3	0	0	0	0	0	30	1	0	0	0	1	1	0	8	0	4	0	0	131	5	AM
AT	0	0	0	2	0	6	0	1	2	0	0	10	3	0	0	0	1	0	2	1	0	4	3	0	0	7	0	0	223	202	AT
AZ	0	0	0	0	0	1	0	0	0	14	0	0	0	0	2	7	3	1	1	0	1	0	1	7	0	4	0	0	180	6	AZ
BA	3	0	0	1	0	3	0	4	9	1	-0	1	2	0	0	0	1	0	1	0	0	3	1	0	0	6	0	0	121	46	BA
BE	0	0	0	8	1	2	1	0	-0	0	0	0	0	0	0	0	0	0	14	1	0	4	18	0	0	16	0	0	215	206	BE
BG	0	1	0	-0	0	1	0	19	8	5	0	0	1	0	0	-4	8	0	1	0	5	1	0	0	0	6	0	0	90	70	BG
BY	0	0	0	2	1	19	0	1	1	18	2	0	1	0	0	0	12	0	2	5	0	0	6	0	0	4	0	0	115	56	BY
CH	0	0	0	2	0	2	0	0	-0	0	0	1	0	0	0	0	0	0	2	0	0	5	4	0	0	8	0	0	371	263	CH
CY	0	0	0	0	0	1	0	1	1	2	0	0	0	0	0	50	2	0	1	0	2	67	0	1	0	9	0	0	84	29	CY
CZ	0	0	0	3	0	12	0	3	4	0	0	3	7	0	0	0	1	0	3	1	0	2	4	0	0	8	0	0	175	162	CZ
DE	0	0	0	12	1	9	0	1	-1	0	1	0	1	0	0	0	1	0	7	3	0	3	17	0	0	12	0	0	213	202	DE
DK	0	0	0	14	4	10	0	1	0	1	3	-0	1	0	0	0	1	0	7	9	0	1	38	0	0	9	0	0	145	138	DK
EE	0	0	0	1	1	4	0	0	0	7	3	0	0	0	0	0	2	0	1	6	0	0	4	0	0	3	0	0	46	31	EE
ES	0	0	0	1	0	0	5	0	0	-0	0	0	0	0	0	0	0	0	6	0	0	4	1	0	0	6	0	0	90	89	ES
FI	0	0	0	0	1	1	0	0	0	3	2	0	0	0	0	0	0	0	1	2	0	0	2	0	0	2	0	0	21	16	FI
FR	0	0	0	5	0	1	1	0	0	0	0	0	0	0	0	0	0	0	10	1	0	6	14	0	0	8	0	0	222	211	FR
GB	0	0	0	4	1	1	0	0	0	0	0	0	0	0	0	0	0	0	12	1	0	1	17	0	0	7	0	0	100	98	GB
GE	0	0	0	0	0	1	0	0	0	6	0	0	0	0	0	13	1	0	0	0	2	0	0	1	0	2	0	0	107	3	GE
GL	-0	-0	-0	0	0	0	0	-0	0	0	-0	0	0	0	-0	0	0	0	0	0	-0	-0	0	-0	-0	3	0	0	0	0	GL
GR	0	6	0	-0	0	1	0	7	6	2	0	0	0	0	0	3	4	0	1	0	2	14	0	0	0	6	0	0	105	78	GR
HR	1	0	0	1	0	6	0	7	22	1	0	4	4	0	0	0	2	0	1	0	0	7	2	0	0	7	0	0	191	111	HR
HU	0	1	0	1	0	13	0	27	27	1	0	5	13	0	0	0	5	0	2	0	1	3	2	0	0	8	0	0	240	183	HU
IE	0	0	0	3	0	0	0	0	0	0	0	0	0	0	0	0	0	0	16	1	0	1	11	0	0	4	0	0	101	100	IE
IS	0	0	0	0	0	-0	0	0	-0	-0	0	0	-0	0	0	0	0	0	1	0	0	0	0	0	0	2	0	0	4	1	IS
IT	0	0	0	1	0	2	0	1	1	0	0	7	1	0	0	0	0	0	2	0	0	23	1	0	0	9	0	0	268	254	IT
KG	0	0	0	0	0	0	0	0	0	0	0	0	0	4	0	0	0	17	0	0	0	0	0	2	0	4	0	0	46	1	KG
KZT	0	0	0	0	0	1	0	0	0	32	0	0	0	0	1	0	1	2	1	0	0	0	1	2	0	6	0	0	76	5	KZT
LT	0	0	0	3	1	21	0	1	0	10	3	0	1	0	0	0	7	0	2	9	0	0	8	0	0	4	0	0	104	71	LT
LU	0	0	0	8	1	3	1	0	-0	0	0	-0	1	0	0	0	0	0	8	1	0	5	13	0	0	12	0	0	208	201	LU
LV	0	0	0	2	1	8	0	0	0	8	2	0	0	0	0	0	4	0	1	7	0	0	5	0	0	3	0	0	67	44	LV
MD	0	0	0	0	0	11	0	32	2	10	0	0	2	0	0	0	32	0	1	1	3	0	1	0	0	6	0	0	125	62	MD
ME	19	1	0	0	0	2	0	4	31	1	-0	0	1	0	0	0	1	0	1	0	0	6	0	0	0	5	0	0	103	26	ME
MK	1	22	0	0	0	3	0	8	41	2	0	0	1	0	0	3	3	0	1	0	1	5	0	0	0	6	0	0	134	54	MK
MT	0	0	-6	0	0	0	0	1	2	0	-0	0	0	0	0	1	1	0	1	0	0	-4	0	0	1	6	0	0	42	36	MT
NL	0	0	0	-4	2	7	0	0	-0	0	1	-0	0	0	0	0	1	0	16	4	0	3	27	0	0	18	0	0	205	199	NL
NO	0	0	0	1	3	0	0	0	0	0	1	0	0	0	0	0	0	0	1	1	0	0	2	0	0	1	0	0	14	10	NO
PL	0	0	0	4	1	35	0	4	1	3	1	1	4	0	0	0	6	0	3	5	0	1	7	0	0	7	0	0	127	109	PL
PT	0	-0	0	0	0	0	19	0	0	-0	-0	0	0	0	0	0	0	0	7	0	0	2	1	0	0	6	0	0	59	59	PT
RO	0	1	0	0	0	8	0	71	8	5	0	1	3	0	0	-0	13	0	1	0	2	1	1	0	0	6	0	0	151	116	RO
RS	3	6	0	1	0	10	0	27	68	2	0	1	6	0	0	0	4	0	2	0	1	3	2	0	0	8	0	0	222	120	RS
RUE	0	0	0	0	0	1	0	0	0	28	0	0	0	0	0	0	1	0	0	1	0	0	1	0	0	3	0	0	38	4	RUE
SE	0	0	0	1	2	2	0	0	0	1	5	0	0	0	0	0	0	0	1	3	0	0	4	0	0	2	0	0	27	23	SE
SI	0	0	0	1	0	6	0	3	6	1	0	35	3	0	0	0	1	0	2	1	0	10	2	0	0	7	0	0	259	213	SI
SK	0	0	0	0	0	7	0	11	6	1	-0	2	20	0	0	0	3	0	2	-0	0	1	1	0	0	6	0	0	131	112	SK
TJ	0	0	0	0	0	0	0	0	0	-0	-0	0	0	23	1	0	0	19	0	0	0	0	0	6	0	4	0	0	49	0	TJ
TM	0	0	0	0	0	1	0	0	0	8	0	0	0	1	14	1	1	18	0	0	0	0	1	5	0	6	0	0	62	4	TM
TR	0	0	0	0	0	1	0	1	0	4	0	0	0	0	0	48	4	0	1	0	3	4	0	2	0	6	0	0	68	8	TR
UA	0	0	0	0	0	2	0	5	0	11	0	0	0	0	0	-0	14	0	1	1	1	0	1	0	0	4	0	0	44	12	UA
UZ	0	0	0	0	0	1	0	0	0	10	0	0	0	5	3	1	1	30	1	0	0	0	1	3	0	7	0	0	83	4	UZ
ATL	0	0	0	0	0	0	0	0	0	1	0	0	0	0	0	0	0	0	3	0	0	0	1	0	0	2	0	0	9	8	ATL
BAS	0	0	0	4	1	8	0	1	0	2	3	0	0	0	0	0	1	0	3	4	0	0	9	0	0	4	0	0	58	52	BAS
BLS	0	0	0	-0	0	0	0	4	0	13	-0	-0	-0	0	0	-7	14	0	1	0	14	-0	0	0	0	4	0	0	31	6	BLS
MED	0	0	0	0	0	0	0	2	1	1	-0	0	0	0	0	3	2	0	1	0	1	16	0	0	1	7	0	0	53	41	MED
NOS	0	0	0	4	2	2	0	0	0	0	1	0	0	0	0	0	0	0	7	2	0	1	7	0	0	6	0	0	81	78	NOS
AST	0	0	0	0	0	0	0	0	0	3	0	0	0	1	1	7	1	3	0	0	0	2	0	23	0	6	0	0	26	2	AST
NOA	0	0	0	0	0	0	0	1	1	0	-0	0	0	0	0	3	1	0	1	0	0	18	0	0	2	7	0	0	22	16	NOA
EXC	0	0	0	1	0	2	0	2	1	18	0	0	0	0	0	2	2	2	1	1	0	1	2	1	0	4	0	0	65	28	EXC
EU	0	0	0	3	1	6	1	6	2	1	1	1	1	0	0	0	2	0	5	2	0	4	7	0	0	7	0	0	135	123	EU
	ME	MK	MT	NL	NO	PL	PT	RO	RS	RUE	SE	SI	SK	TJ	TM	TR	UA	UZ	ATL	BAS	BLS	MED	NOS	AST	NOA	BIC	DMS	VOL	EXC	EU	

Table C.11: 2011 country-to-country blame matrices for **PM2.5**.
Units: ng/m^3 per 15% emis. red. of NH_3. **Emitters →, Receptors ↓**. (Based on ECMWF meteorology.)

	AL	AM	AT	AZ	BA	BE	BG	BY	CH	CY	CZ	DE	DK	EE	ES	FI	FR	GB	GE	GR	HR	HU	IE	IS	IT	KG	KZT	LT	LU	LV	MD	
AL	161	0	2	0	1	0	4	0	0	-0	1	5	0	0	0	0	1	0	0	26	2	4	0	-0	6	-0	0	0	0	0	0	AL
AM	0	70	-0	23	-0	-0	-0	-0	0	0	-0	-0	-0	-0	-0	-0	-0	-0	4	0	-0	-0	-0	-0	0	-0	-0	-0	-0	-0	-0	AM
AT	0	0	110	0	1	1	1	1	10	0	18	72	1	0	1	0	11	1	0	0	13	19	0	0	35	0	0	0	0	0	0	AT
AZ	-0	4	-0	89	-0	-0	-0	-0	-0	-0	-0	-0	-0	-0	-0	-0	-0	-0	8	-0	-0	-0	-0	-0	0	0	5	-0	-0	-0	-0	AZ
BA	2	0	5	0	85	1	2	1	1	0	6	14	0	0	0	0	3	1	0	1	38	14	0	0	10	0	0	0	0	0	1	BA
BE	0	0	6	0	0	155	0	0	6	0	6	108	1	0	2	0	103	36	0	0	0	1	3	0	5	0	0	0	7	0	0	BE
BG	1	0	1	0	1	0	93	2	1	0	2	5	0	0	0	0	2	0	0	12	2	5	0	-0	2	0	2	0	0	0	4	BG
BY	0	0	1	0	0	2	0	118	1	0	5	21	3	0	0	0	4	4	0	0	1	4	1	0	1	-0	3	8	0	2	1	BY
CH	-0	0	6	0	0	1	-0	0	122	-0	1	46	0	-0	1	0	26	1	0	-0	0	1	0	-0	60	0	0	0	0	0	0	CH
CY	-0	0	-0	-0	-0	-0	-2	-1	-0	-38	-0	-1	-0	-0	-0	-0	-0	-0	-0	-3	-0	-1	-0	-0	-1	0	-1	-0	-0	-0	-0	CY
CZ	0	0	34	0	2	4	1	2	3	0	186	111	1	0	1	0	19	4	0	0	10	33	1	0	8	0	1	0	1	0	0	CZ
DE	0	0	15	0	0	17	0	2	8	0	22	298	3	0	2	0	40	14	0	0	2	5	2	0	6	0	0	0	1	0	0	DE
DK	0	0	2	0	0	11	0	3	1	0	8	123	135	0	0	0	22	34	0	0	1	2	3	0	1	-0	1	1	0	0	0	DK
EE	0	0	0	0	0	1	0	12	0	-0	1	13	5	33	0	4	2	5	0	0	0	0	1	0	0	-0	1	7	0	9	0	EE
ES	-0	0	0	0	0	1	-0	0	0	-0	0	3	0	0	119	0	14	0	0	-0	0	0	0	-0	2	0	0	0	0	0	0	ES
FI	0	0	0	0	0	0	0	3	0	0	1	5	1	1	0	25	1	1	0	0	0	0	0	-0	0	-0	0	1	0	1	0	FI
FR	-0	0	3	0	0	10	-0	0	8	-0	3	40	1	0	9	0	164	11	0	-0	0	1	1	0	15	0	0	0	1	0	0	FR
GB	0	0	1	0	0	10	0	0	1	-0	1	28	2	0	2	0	43	177	0	0	0	0	8	0	2	-0	0	0	0	0	0	GB
GE	0	5	-0	23	-0	-0	-0	-0	0	-0	-0	-0	-0	-0	-0	-0	-0	-0	55	0	-0	-0	-0	-0	0	0	-0	-0	-0	-0	-0	GE
GL	-0	0	-0	0	-0	-0	-0	0	-0	-0	-0	-0	0	-0	-0	-0	-0	-0	0	0	-0	-0	-0	-0	-0	-0	-0	-0	-0	-0	-0	GL
GR	3	0	1	0	0	0	18	1	0	-0	1	2	0	-0	-0	0	1	0	0	87	1	2	0	-0	1	0	0	0	0	0	1	GR
HR	0	0	13	0	20	1	2	1	2	-0	10	22	1	0	0	0	4	1	0	0	135	29	0	0	43	0	0	0	0	0	1	HR
HU	0	0	18	0	4	1	3	2	3	0	18	39	1	0	0	0	7	2	0	0	37	204	0	-0	14	0	1	0	0	0	1	HU
IE	0	0	0	0	0	3	0	0	0	0	0	5	0	0	1	0	17	55	0	0	0	0	51	0	1	0	0	0	0	0	0	IE
IS	0	-0	0	-0	0	0	0	0	0	0	0	0	0	0	0	0	0	1	-0	0	0	0	0	4	0	-0	-0	0	0	0	0	IS
IT	1	0	7	0	1	0	0	0	4	0	2	7	0	0	1	0	4	-0	0	0	5	3	0	-0	297	0	0	0	0	0	0	IT
KG	-0	0	-0	0	-0	-0	-0	-0	-0	-0	-0	-0	-0	-0	-0	-0	-0	-0	0	0	-0	-0	-0	-0	0	30	7	-0	-0	-0	-0	KG
KZT	-0	0	-0	0	-0	-0	-0	0	-0	-0	-0	-0	-0	0	-0	0	-0	-0	0	-0	-0	-0	-0	-0	-0	1	72	0	-0	0	0	KZT
LT	0	0	1	0	0	3	0	33	0	0	5	34	8	1	1	1	6	8	0	0	1	2	1	0	2	-0	2	84	0	7	1	LT
LU	0	0	9	0	0	55	0	0	6	0	10	163	1	0	3	0	97	16	0	0	1	2	2	0	5	0	0	0	40	0	0	LU
LV	0	0	1	0	0	2	0	21	0	0	2	23	6	3	0	1	4	6	0	0	0	1	1	0	1	-0	2	30	0	36	0	LV
MD	0	0	2	0	0	1	10	6	1	0	5	13	1	0	0	0	4	1	0	1	1	7	0	-0	2	0	8	0	0	0	99	MD
ME	27	0	3	0	9	0	2	0	1	0	3	8	0	0	0	0	2	0	0	3	5	7	0	0	5	0	0	0	0	0	0	ME
MK	17	0	2	0	1	0	9	1	1	0	2	6	0	0	0	0	2	0	0	48	3	7	0	-0	3	0	0	0	0	0	1	MK
MT	0	-0	1	-0	1	0	0	0	0	0	0	1	0	0	1	0	5	0	-0	-0	1	1	0	0	26	0	-0	0	0	0	0	MT
NL	0	0	5	0	0	49	0	1	3	0	7	131	4	0	1	0	61	58	0	0	0	2	6	0	3	0	0	0	1	0	0	NL
NO	0	-0	0	-0	0	1	0	0	0	0	0	8	3	0	0	-0	3	3	0	0	0	0	0	-0	0	-0	-0	0	0	0	0	NO
PL	0	0	5	0	1	5	1	11	2	-0	34	88	7	0	1	0	12	8	0	0	3	14	1	0	5	0	2	3	0	1	1	PL
PT	-0	0	0	0	-0	0	-0	0	0	-0	0	1	0	0	38	0	5	0	0	-0	-0	-0	0	-0	0	0	0	0	0	0	-0	PT
RO	1	0	3	0	1	0	10	2	2	0	3	11	1	0	0	0	3	1	0	1	3	19	0	-0	4	0	3	0	0	0	7	RO
RS	5	0	5	0	8	1	8	1	2	0	7	18	0	0	0	0	4	1	0	4	17	31	0	-0	4	0	1	0	0	0	2	RS
RUE	0	0	0	0	0	0	0	2	0	-0	0	1	0	0	0	0	0	0	0	0	0	0	0	-0	0	0	13	0	0	0	0	RUE
SE	0	0	0	0	0	2	0	2	0	-0	1	19	12	0	0	1	4	5	0	0	0	1	1	-0	0	-0	0	0	0	0	0	SE
SI	0	0	37	0	4	1	1	1	3	0	9	25	1	0	0	0	4	0	0	0	61	20	0	0	103	0	0	0	0	0	1	SI
SK	0	0	13	0	1	2	2	2	3	0	34	44	1	0	1	0	9	2	0	0	9	89	0	0	7	0	1	1	0	0	0	SK
TJ	-0	0	-0	0	-0	-0	-0	-0	-0	-0	-0	-0	-0	-0	-0	-0	-0	-0	0	-0	-0	-0	-0	-0	-0	1	0	-0	-0	-0	-0	TJ
TM	-0	0	-0	1	-0	-0	-0	0	-0	-0	-0	-0	-0	-0	-0	-0	-0	-0	0	-0	-0	0	-0	-0	-0	0	10	0	-0	0	0	TM
TR	-0	0	0	0	-0	0	2	-0	0	-0	0	0	0	-0	-0	-0	0	-0	0	0	0	0	0	-0	0	0	-0	0	0	-0	0	TR
UA	0	0	1	0	0	1	2	15	1	0	4	13	1	0	0	0	3	1	0	0	1	6	0	0	1	0	9	1	0	0	8	UA
UZ	-0	0	-0	0	-0	-0	-0	0	-0	-0	-0	-0	-0	-0	-0	-0	-0	-0	0	-0	-0	-0	-0	-0	-0	3	16	0	-0	0	-0	UZ
ATL	0	-0	0	-0	0	0	0	0	0	-0	0	2	0	-0	2	-0	5	4	-0	0	0	0	1	-0	0	-0	-0	0	0	0	0	ATL
BAS	0	0	1	0	0	4	0	7	1	-0	4	65	31	2	0	6	9	12	0	0	0	2	1	0	1	-0	1	5	0	2	0	BAS
BLS	0	0	1	0	0	0	6	0	0	0	1	2	0	-0	0	-0	1	0	2	1	0	1	0	-0	0	0	2	-0	0	0	2	BLS
MED	-1	-0	1	-0	-1	0	-3	-1	0	-1	-0	1	-0	-0	0	-0	1	-0	-0	-4	-0	-1	-0	-0	10	-0	-1	-0	0	-0	-0	MED
NOS	0	0	2	0	0	17	0	1	1	-0	3	63	13	0	2	0	50	73	0	0	0	1	5	-0	2	0	0	0	0	0	0	NOS
AST	-0	0	0	1	-0	-0	-0	0	0	-0	-0	-0	0	-0	-0	-0	-0	-0	0	-0	-0	-0	-0	-0	-0	0	6	0	-0	-0	-0	AST
NOA	-1	-0	-0	-0	-0	-0	-2	-0	-0	-0	-0	-0	-0	-0	-1	-0	-0	-0	-0	-2	-0	-0	-0	-0	-4	-0	-0	-0	-0	-0	-0	NOA
EXC	0	0	1	1	0	1	1	3	1	-0	2	11	1	0	3	1	7	3	0	1	1	2	0	0	5	0	15	1	0	0	1	EXC
EU	0	0	7	0	0	6	4	3	3	-0	10	51	4	1	16	2	33	16	0	3	3	10	2	0	26	0	1	2	0	1	1	EU
	AL	AM	AT	AZ	BA	BE	BG	BY	CH	CY	CZ	DE	DK	EE	ES	FI	FR	GB	GE	GR	HR	HU	IE	IS	IT	KG	KZT	LT	LU	LV	MD	

Table C.11 Cont.: 2011 country-to-country blame matrices for **PM2.5**.
Units: ng/m^3 per 15% emis. red. of NH_3. **Emitters →, Receptors ↓**. (Based on ECMWF meteorology.)

	ME	MK	MT	NL	NO	PL	PT	RO	RS	RUE	SE	SI	SK	TJ	TM	TR	UA	UZ	ATL	BAS	BLS	MED	NOS	AST	NOA	BIC	DMS	VOL	EXC	EU	
AL	3	18	0	0	0	1	-0	9	59	0	0	0	1	-0	0	0	0	0	0	0	0	0	0	0	0	2	0	0	307	61	AL
AM	-0	-0	-0	-0	-0	-0	-0	-0	-0	-0	-0	-0	-0	-0	-0	25	-0	-0	0	0	0	0	0	11	0	1	0	0	120	-1	AM
AT	0	0	0	2	0	11	0	5	7	0	0	20	5	0	0	0	0	0	0	0	0	0	0	0	0	2	0	0	346	313	AT
AZ	-0	-0	-0	-0	-0	-0	-0	-0	-0	4	-0	-0	-0	0	1	5	-0	0	0	0	0	0	0	5	0	1	0	0	117	-1	AZ
BA	3	1	0	1	0	5	-0	14	58	1	0	1	2	0	0	0	0	0	0	0	0	0	0	0	0	2	0	0	272	80	BA
BE	0	0	-0	49	0	8	0	0	0	0	0	0	1	-0	0	-0	0	0	0	0	0	0	0	0	-0	2	0	0	500	492	BE
BG	0	2	0	0	0	2	-0	54	33	2	0	0	1	0	0	9	1	0	0	0	0	0	0	0	0	2	0	0	239	181	BG
BY	0	0	0	3	0	67	0	5	1	14	2	0	2	-0	0	0	2	0	0	0	0	0	0	0	0	1	0	0	280	137	BY
CH	-0	-0	-0	1	0	0	0	0	0	-0	0	1	0	-0	0	-0	0	0	0	0	0	0	0	0	-0	2	0	0	270	147	CH
CY	-0	-0	-0	-0	-0	-2	-0	-3	-2	-3	-0	-0	-0	-0	-0	-62	-0	-0	0	0	0	0	0	3	-0	-1	0	0	-121	-50	CY
CZ	0	0	0	6	0	48	0	8	11	1	1	5	17	0	0	0	0	0	0	0	0	0	0	0	0	2	0	0	517	487	CZ
DE	0	0	-0	27	0	26	0	2	2	1	1	2	2	-0	0	0	0	0	0	0	0	0	0	0	0	2	0	0	504	488	DE
DK	0	0	-0	28	1	33	0	3	1	1	9	0	1	-0	0	0	0	0	0	0	0	0	0	0	0	2	0	0	430	418	DK
EE	0	0	-0	3	1	17	0	1	0	10	7	0	0	-0	0	0	0	0	0	0	0	0	0	-0	-0	1	0	0	135	110	EE
ES	-0	-0	0	1	0	0	2	-0	-0	-0	0	0	0	-0	0	-0	-0	0	0	0	0	0	0	0	0	2	0	0	142	142	ES
FI	0	0	-0	1	0	4	0	0	0	3	4	0	0	-0	-0	0	0	-0	0	0	0	0	0	-0	-0	0	0	0	53	46	FI
FR	0	-0	-0	8	0	2	0	0	0	0	0	1	0	-0	0	0	0	0	0	0	0	0	0	0	0	2	0	0	281	272	FR
GB	0	0	-0	16	0	3	0	0	0	0	1	0	0	-0	0	0	0	0	0	0	0	0	0	0	-0	2	0	0	298	296	GB
GE	-0	0	-0	-0	-0	-0	-0	0	-0	3	-0	-0	-0	0	0	13	-0	-0	0	0	0	0	0	2	0	1	0	0	98	-0	GE
GL	-0	-0	0	-0	0	-0	-0	-0	-0	-0	-0	-0	-0	-0	-0	-0	-0	-0	0	0	0	0	0	-0	0	12	0	0	-0	-0	GL
GR	0	5	-0	0	0	0	-0	9	11	0	0	0	0	0	0	-0	0	0	0	0	0	0	0	-0	-0	1	0	0	143	122	GR
HR	0	0	0	1	0	11	-0	16	47	1	0	15	4	0	0	-0	0	0	0	0	0	0	0	0	0	2	0	0	381	173	HR
HU	0	0	0	2	0	28	-0	38	43	1	0	8	21	0	0	0	0	0	0	0	0	0	0	0	0	2	0	0	499	406	HU
IE	0	0	0	3	0	1	0	0	0	0	0	0	0	0	-0	-0	0	0	0	0	0	0	0	-0	0	1	0	0	139	139	IE
IS	0	0	0	0	0	0	0	0	0	-0	0	0	0	-0	-0	-0	0	-0	0	0	0	0	0	-0	0	1	0	0	7	3	IS
IT	0	0	0	0	0	2	-0	2	3	-0	0	6	1	-0	0	-0	0	0	0	0	0	0	0	0	0	2	0	0	350	335	IT
KG	-0	-0	-0	-0	-0	-0	-0	-0	-0	-0	-0	-0	-0	1	-0	-0	-0	-0	0	0	0	0	0	4	-0	1	0	0	38	-0	KG
KZT	-0	-0	-0	-0	0	-0	-0	0	-0	25	0	-0	-0	0	0	-0	0	1	0	0	0	0	0	5	-0	1	0	0	100	-0	KZT
LT	0	0	0	8	0	85	0	3	1	16	6	0	1	-0	0	0	1	0	0	0	0	0	0	0	0	1	0	0	322	266	LT
LU	0	0	-0	17	0	6	0	1	1	0	0	1	1	-0	0	-0	0	0	0	0	0	0	0	0	0	2	0	0	435	427	LU
LV	0	0	0	6	0	35	0	2	0	11	7	0	1	-0	0	0	1	0	0	0	0	0	0	0	0	1	0	0	204	168	LV
MD	0	0	0	1	0	20	0	97	5	13	0	0	3	0	0	3	6	0	0	0	0	0	0	0	0	2	0	0	310	167	MD
ME	53	2	0	1	0	3	0	9	91	1	0	0	1	0	0	0	0	0	0	0	0	0	0	0	0	2	0	0	238	48	ME
MK	0	103	0	0	0	2	-0	14	78	1	0	0	1	0	0	1	0	0	0	0	0	0	0	0	0	2	0	0	305	96	MK
MT	0	0	112	0	0	0	-0	1	2	-0	0	0	0	0	0	-0	0	0	0	0	0	0	0	-0	1	1	0	0	154	150	MT
NL	0	0	0	196	0	15	0	1	1	0	1	0	1	-0	0	0	0	0	0	0	0	0	0	0	0	3	0	0	550	544	NL
NO	0	0	-0	2	9	1	0	0	0	-0	2	0	0	-0	-0	-0	0	-0	0	0	0	0	0	-0	0	0	0	0	34	25	NO
PL	0	0	0	10	0	289	0	9	4	4	2	1	10	0	0	0	1	0	0	0	0	0	0	0	0	2	0	0	534	506	PL
PT	-0	-0	-0	0	0	0	58	-0	-0	-0	0	-0	0	0	0	-0	-0	0	0	0	0	0	0	0	0	3	0	0	103	103	PT
RO	0	1	0	1	0	9	0	191	23	4	0	1	2	0	0	1	1	0	0	0	0	0	0	0	0	2	0	0	308	260	RO
RS	2	7	0	1	0	6	0	48	248	2	0	1	3	0	0	0	1	0	0	0	0	0	0	0	0	2	0	0	438	143	RS
RUE	0	0	-0	0	0	1	0	0	0	58	0	0	0	0	0	0	0	0	0	0	0	0	0	0	-0	1	0	0	78	4	RUE
SE	0	0	-0	4	2	8	0	1	0	0	24	0	0	-0	0	0	0	0	0	0	0	0	0	-0	0	1	0	0	88	83	SE
SI	0	0	0	1	0	11	-0	12	17	0	0	146	3	0	0	0	0	0	0	0	0	0	0	0	0	2	0	0	464	375	SI
SK	0	0	0	3	0	57	0	23	13	1	1	4	122	0	0	0	0	0	0	0	0	0	0	0	0	3	0	0	447	415	SK
TJ	-0	-0	-0	-0	-0	-0	-0	-0	-0	-0	-0	-0	-0	24	0	-0	-0	7	0	0	0	0	0	4	-0	1	0	0	32	-0	TJ
TM	-0	-0	0	-0	-0	-0	-0	-0	-0	0	-0	-0	0	1	21	0	0	7	0	0	0	0	0	4	0	1	0	0	40	-0	TM
TR	-0	-0	-0	0	0	-0	-0	2	0	0	-0	0	-0	0	-0	120	0	-0	0	0	0	0	0	2	0	1	0	0	125	4	TR
UA	0	0	0	1	0	28	0	20	2	26	0	0	2	0	0	1	10	0	0	0	0	0	0	0	0	1	0	0	158	86	UA
UZ	-0	-0	-0	-0	-0	-0	-0	-0	-0	-0	-0	-0	-0	4	3	-0	0	31	0	0	0	0	0	2	0	0	0	0	57	-0	UZ
ATL	0	0	0	1	0	0	0	0	-0	-1	0	0	0	-0	-0	-0	0	-0	0	0	0	0	0	-0	0	1	0	0	16	16	ATL
BAS	0	0	-0	12	1	42	0	3	1	5	22	0	1	-0	0	0	0	0	0	0	0	0	0	0	0	1	0	0	241	225	BAS
BLS	0	0	-0	0	0	1	-0	14	2	6	0	0	0	-0	0	13	-3	0	0	0	0	0	0	0	-0	1	0	0	53	28	BLS
MED	-0	-0	-1	0	0	-1	-0	-3	-2	-3	-0	1	-0	-0	-0	-22	-0	-0	0	0	0	0	0	-0	-3	-1	0	0	-32	0	MED
NOS	0	0	0	35	2	9	0	1	0	0	2	0	0	0	0	0	0	0	0	0	0	0	0	0	0	1	0	0	284	279	NOS
AST	-0	-0	-0	-0	-0	-0	-0	-0	-0	1	-0	-0	-0	0	1	1	-0	-0	0	0	0	0	0	17	0	2	0	0	10	-0	AST
NOA	-0	-0	-0	-0	-0	-1	-0	-2	-2	-1	-0	-0	-0	-0	-0	-5	-0	-0	0	0	0	0	0	0	-1	-0	0	0	-23	-13	NOA
EXC	0	0	0	2	0	8	0	4	2	32	1	0	1	0	1	4	0	1	0	0	0	0	0	1	0	2	0	0	120	56	EXC
EU	0	0	0	8	0	30	1	15	5	1	3	2	3	0	0	0	0	0	0	0	0	0	0	0	0	2	0	0	276	259	EU
	ME	MK	MT	NL	NO	PL	PT	RO	RS	RUE	SE	SI	SK	TJ	TM	TR	UA	UZ	ATL	BAS	BLS	MED	NOS	AST	NOA	BIC	DMS	VOL	EXC	EU	

Table C.12: 2011 country-to-country blame matrices for **PM2.5**.
Units: ng/m^3 per 15% emis. red. of VOC. **Emitters** →, **Receptors** ↓. (Based on ECMWF meteorology.)

	AL	AM	AT	AZ	BA	BE	BG	BY	CH	CY	CZ	DE	DK	EE	ES	FI	FR	GB	GE	GR	HR	HU	IE	IS	IT	KG	KZT	LT	LU	LV	MD	
AL	4	0	1	0	1	0	2	1	1	0	1	5	0	0	1	0	3	1	0	8	1	2	0	0	11	0	0	0	0	0	0	AL
AM	0	8	-0	-0	0	0	-0	0	-0	0	0	0	0	0	0	0	-0	0	5	0	-0	-0	0	0	0	0	0	0	0	0	0	AM
AT	0	0	12	0	1	0	0	1	3	0	2	12	0	0	1	0	4	1	0	0	3	4	0	0	15	0	0	0	0	0	0	AT
AZ	0	1	0	-1	0	0	0	1	0	0	0	0	0	0	0	0	0	0	8	0	0	0	0	0	0	0	0	0	0	0	0	AZ
BA	0	0	2	0	5	0	2	1	1	0	2	7	0	0	1	0	3	2	0	1	1	2	0	0	11	0	0	0	0	0	0	BA
BE	0	0	5	0	0	10	0	2	6	0	3	32	0	0	2	0	19	16	0	1	1	1	1	0	14	0	0	0	0	0	0	BE
BG	0	0	1	0	1	0	10	3	1	0	2	7	0	0	1	0	3	2	0	3	1	2	0	0	3	0	0	0	0	0	1	BG
BY	0	0	1	0	0	0	0	7	0	0	1	5	0	0	0	0	2	2	0	0	0	1	0	0	1	0	0	1	0	0	0	BY
CH	0	0	6	0	0	0	0	0	15	0	1	12	0	0	2	0	8	1	0	0	1	1	0	0	18	0	0	0	0	0	0	CH
CY	0	0	0	0	0	0	0	2	0	0	1	3	0	0	1	0	1	1	1	1	0	0	0	0	4	0	0	0	0	0	0	CY
CZ	0	0	6	0	1	1	1	2	2	0	8	19	0	0	1	0	7	3	0	0	2	5	0	0	6	0	0	0	0	0	0	CZ
DE	0	0	9	0	1	3	0	2	6	0	6	36	1	0	2	0	12	7	0	1	2	2	0	0	12	0	0	0	0	0	0	DE
DK	0	0	2	0	0	2	0	2	1	0	5	27	4	0	1	0	7	7	0	0	1	1	0	0	4	0	0	0	0	0	0	DK
EE	0	0	0	0	0	0	0	2	0	0	0	3	0	1	0	1	1	2	0	0	0	0	0	0	0	0	0	0	0	1	0	EE
ES	0	0	0	0	0	0	0	0	0	0	0	1	0	0	12	0	4	1	0	0	0	0	0	0	4	0	0	0	0	0	0	ES
FI	0	0	0	0	0	0	0	1	0	0	0	1	0	0	0	1	0	1	0	0	0	0	0	0	0	0	0	0	0	0	0	FI
FR	0	0	2	0	0	1	0	1	3	0	1	10	0	0	4	0	15	3	0	0	1	1	0	0	12	0	0	0	0	0	0	FR
GB	0	0	1	0	0	1	0	0	1	0	1	7	0	0	1	0	7	15	0	0	0	0	1	0	5	0	0	0	0	0	0	GB
GE	0	1	0	-0	0	0	0	0	0	0	0	0	0	0	0	0	0	0	18	0	0	0	0	0	0	0	0	0	0	0	0	GE
GL	0	0	0	0	0	0	0	0	0	0	0	0	0	0	0	0	0	0	0	0	0	0	0	0	0	0	0	0	0	0	0	GL
GR	1	0	1	0	1	0	2	2	1	0	1	5	0	0	1	0	3	2	0	7	1	1	0	0	7	0	0	0	0	0	0	GR
HR	0	0	3	0	4	1	1	2	1	0	3	10	0	0	1	0	5	2	0	1	5	5	0	0	22	0	0	0	0	0	0	HR
HU	0	0	5	0	2	1	1	3	1	0	3	13	0	0	1	0	5	3	0	1	4	13	0	0	8	0	0	0	0	0	0	HU
IE	0	0	0	0	0	-0	0	0	0	0	0	0	0	0	0	0	1	4	0	0	0	0	1	0	1	0	0	0	0	0	0	IE
IS	0	0	0	0	0	0	0	0	0	0	0	0	0	0	0	0	0	0	0	0	0	0	0	0	0	0	0	0	0	0	0	IS
IT	0	0	6	0	1	0	0	1	4	0	2	7	0	0	3	0	10	2	0	1	3	2	0	0	179	0	0	0	0	0	0	IT
KG	0	0	0	0	0	0	0	0	0	0	0	0	0	0	0	0	0	0	0	0	0	0	0	0	0	4	0	0	0	0	0	KG
KZT	0	0	0	0	0	0	0	1	0	0	0	0	0	0	0	0	0	0	0	0	0	0	0	0	0	0	0	0	0	0	0	KZT
LT	0	0	0	0	0	0	0	5	0	0	1	5	1	0	0	0	2	2	0	0	0	0	0	0	1	0	0	1	0	1	0	LT
LU	0	0	6	0	1	4	0	1	6	0	4	32	0	0	2	0	17	8	0	1	1	2	0	0	14	0	0	0	1	0	0	LU
LV	0	0	0	0	0	0	0	3	0	0	0	4	1	0	0	1	1	2	0	0	0	0	0	0	1	0	0	1	0	1	0	LV
MD	0	0	1	0	0	0	1	4	0	0	2	6	0	0	0	0	2	2	0	0	0	2	0	0	2	0	0	0	0	0	1	MD
ME	1	0	1	0	1	0	1	1	0	0	1	5	0	0	1	0	2	1	0	2	1	1	0	0	8	0	0	0	0	0	0	ME
MK	1	0	1	0	1	0	3	1	1	0	1	5	0	0	1	0	2	1	0	9	1	2	0	0	5	0	0	0	0	0	0	MK
MT	0	0	1	0	1	0	0	1	1	0	1	4	0	0	5	0	8	2	0	1	1	1	0	0	37	0	0	0	0	0	0	MT
NL	0	0	5	0	0	10	1	2	5	0	5	44	1	0	2	0	20	23	0	1	1	2	1	0	12	0	0	0	0	0	0	NL
NO	0	0	0	0	0	0	0	0	0	0	0	1	0	0	0	0	1	1	0	0	0	0	0	0	0	0	0	0	0	0	0	NO
PL	0	0	2	0	0	1	0	4	1	0	4	15	1	0	1	0	5	4	0	0	1	3	0	0	4	0	0	1	0	0	0	PL
PT	0	0	0	0	0	0	0	0	0	0	0	1	0	0	7	0	2	1	0	0	0	0	0	0	2	0	0	0	0	0	0	PT
RO	0	0	1	0	1	0	1	2	1	0	2	7	0	0	1	0	3	2	0	1	1	3	0	0	3	0	0	0	0	0	0	RO
RS	1	0	3	0	3	0	2	2	1	0	3	9	0	0	1	0	4	2	0	2	2	6	0	0	7	0	0	0	0	0	0	RS
RUE	0	0	0	0	0	0	0	1	0	0	0	1	0	0	0	0	0	0	0	0	0	0	0	0	0	0	0	0	0	0	0	RUE
SE	0	0	0	0	0	0	0	1	0	0	0	3	1	0	0	0	1	2	0	0	0	0	0	0	0	0	0	0	0	0	0	SE
SI	0	0	7	0	3	1	1	2	1	0	2	11	0	0	1	0	5	2	0	1	8	4	0	0	36	0	0	0	0	0	0	SI
SK	0	0	4	0	1	1	0	2	1	0	4	12	0	0	1	0	4	3	0	0	2	9	0	0	5	0	0	0	0	0	0	SK
TJ	0	0	0	0	0	0	0	0	0	0	0	0	0	0	0	0	0	0	0	0	0	0	0	0	0	1	0	0	0	0	0	TJ
TM	0	0	0	0	0	0	0	1	0	0	0	1	0	0	0	0	0	0	1	0	0	0	0	0	0	0	0	0	0	0	0	TM
TR	0	0	0	0	0	0	0	1	0	0	0	2	0	0	0	0	1	1	1	0	0	0	0	0	1	0	0	0	0	0	0	TR
UA	0	0	1	0	0	0	0	4	0	0	1	5	0	0	0	1	2	2	0	0	0	1	0	0	1	0	0	0	0	0	0	UA
UZ	0	0	0	0	0	0	0	1	0	0	0	1	0	0	0	0	0	0	1	0	0	0	0	0	0	2	1	0	0	0	0	UZ
ATL	0	0	0	0	0	0	0	0	0	0	0	0	0	0	0	0	0	0	0	0	0	0	0	0	0	0	0	0	0	0	0	ATL
BAS	0	0	1	0	0	1	0	2	0	0	1	9	1	0	0	1	2	4	0	0	0	0	0	0	1	0	0	0	0	1	0	BAS
BLS	0	0	1	0	0	0	1	4	0	0	1	5	0	0	0	0	1	1	3	1	0	1	0	0	1	0	0	0	0	0	0	BLS
MED	1	0	1	0	1	0	1	1	1	0	1	4	0	0	4	0	7	2	0	2	1	1	0	0	24	0	0	0	0	0	0	MED
NOS	0	0	1	0	0	2	0	1	1	0	1	12	1	0	1	0	6	8	0	0	0	0	0	0	3	0	0	0	0	0	0	NOS
AST	0	0	0	-0	0	0	0	0	0	0	0	0	0	0	0	0	0	0	0	0	0	0	0	0	0	0	0	0	0	0	0	AST
NOA	0	0	0	0	0	0	0	1	0	0	0	2	0	0	2	0	2	1	0	1	0	0	0	0	8	0	0	0	0	0	0	NOA
EXC	0	0	1	0	0	0	0	1	0	0	0	3	0	0	1	0	1	1	0	0	0	0	0	0	4	0	0	0	0	0	0	EXC
EU	0	0	3	0	0	1	1	1	2	0	2	10	0	0	3	0	6	4	0	1	1	2	0	0	18	0	0	0	0	0	0	EU
	AL	AM	AT	AZ	BA	BE	BG	BY	CH	CY	CZ	DE	DK	EE	ES	FI	FR	GB	GE	GR	HR	HU	IE	IS	IT	KG	KZT	LT	LU	LV	MD	

Table C.12 Cont.: 2011 country-to-country blame matrices for **PM2.5**.
Units: ng/m^3 per 15% emis. red. of VOC. **Emitters** →, **Receptors** ↓. (Based on ECMWF meteorology.)

	ME	MK	MT	NL	NO	PL	PT	RO	RS	RUE	SE	SI	SK	TJ	TM	TR	UA	UZ	ATL	BAS	BLS	MED	NOS	AST	NOA	BIC	DMS	VOL	EXC	EU	
AL	0	3	0	1	0	4	0	3	6	3	0	0	1	0	0	1	2	0	0	0	0	1	0	0	0	-3	0	0	67	45	AL
AM	0	0	0	0	0	0	-0	-0	-0	2	0	-0	0	0	0	3	0	0	0	0	0	0	0	1	0	-9	0	0	18	0	AM
AT	0	0	0	1	0	5	0	2	2	2	0	4	1	0	0	0	1	0	0	0	0	0	0	0	0	-0	0	0	81	66	AT
AZ	0	0	0	0	0	1	0	0	0	9	0	-0	0	0	0	1	1	0	0	0	0	0	0	1	0	-7	0	0	23	2	AZ
BA	0	0	0	1	0	6	0	6	8	3	0	0	1	0	0	0	3	0	0	0	0	0	0	0	0	-2	0	0	73	49	BA
BE	0	0	0	9	0	9	1	2	1	3	0	1	1	0	0	0	2	0	0	0	0	0	1	0	0	16	0	0	144	128	BE
BG	0	1	0	1	0	7	0	10	3	9	1	0	1	0	0	6	5	0	0	0	0	0	0	0	0	-2	0	0	82	53	BG
BY	0	0	0	1	0	7	0	1	0	8	1	0	0	0	0	0	2	0	0	0	0	0	0	0	0	-4	0	0	44	25	BY
CH	0	0	0	0	0	1	0	1	1	1	0	1	0	0	0	0	0	0	0	0	0	0	0	0	0	-1	0	0	72	54	CH
CY	0	0	0	0	0	3	0	2	1	7	0	0	0	0	0	24	3	0	0	0	0	1	0	0	0	-12	0	0	58	19	CY
CZ	0	0	0	1	0	12	0	3	2	4	1	1	2	0	0	0	2	0	0	0	0	0	0	0	0	4	0	0	96	79	CZ
DE	0	0	0	4	0	10	0	2	2	3	1	1	1	0	0	0	2	0	0	0	0	0	1	0	0	11	0	0	132	113	DE
DK	0	0	0	4	1	7	0	1	1	3	2	0	0	0	0	0	1	0	0	1	0	0	1	0	0	9	0	0	85	75	DK
EE	0	0	0	0	0	3	0	0	0	6	1	0	0	0	0	0	1	0	0	0	0	0	0	0	0	-2	0	0	26	16	EE
ES	0	0	0	0	0	1	1	0	0	0	0	0	0	0	0	0	0	0	0	0	0	1	0	0	0	-1	0	0	27	26	ES
FI	0	0	0	0	0	1	0	0	0	4	1	0	0	0	0	0	0	0	0	0	0	0	0	0	0	-1	0	0	13	7	FI
FR	0	0	0	1	0	3	0	1	1	1	0	0	0	0	0	0	1	0	0	0	0	0	0	0	0	1	0	0	65	57	FR
GB	0	0	0	2	0	2	0	1	0	1	0	0	0	0	0	0	0	0	0	0	0	0	1	0	0	5	0	0	48	45	GB
GE	0	0	0	0	0	0	0	0	0	4	0	0	0	0	0	2	1	0	0	0	0	0	0	0	0	-5	0	0	29	2	GE
GL	0	0	0	0	0	0	0	0	0	0	0	0	0	0	0	0	0	0	0	0	0	0	0	0	0	0	0	0	0	0	GL
GR	0	1	0	0	0	5	0	4	3	6	0	0	1	0	0	5	3	0	0	0	0	1	0	0	0	-4	0	0	66	42	GR
HR	0	0	0	1	0	8	0	7	8	4	0	2	1	0	0	0	3	0	0	0	0	0	0	0	0	-0	0	0	103	75	HR
HU	0	0	0	1	0	13	0	7	5	5	1	2	3	0	0	0	4	0	0	0	0	0	0	0	0	1	0	0	108	82	HU
IE	0	0	0	0	0	0	0	0	0	0	0	0	0	0	0	0	0	0	0	0	0	0	0	0	0	-2	0	0	9	8	IE
IS	0	0	0	0	0	0	0	0	0	0	0	0	0	0	0	0	0	0	0	0	0	0	0	0	0	-1	0	0	2	1	IS
IT	0	0	0	1	0	4	0	3	2	2	0	5	1	0	0	0	1	0	0	0	0	1	0	0	0	7	0	0	245	229	IT
KG	0	0	0	0	0	0	0	0	0	1	0	0	0	1	0	0	0	1	0	0	0	0	0	1	0	-4	0	0	8	1	KG
KZT	0	0	0	0	0	0	0	0	0	8	0	0	0	0	0	0	1	0	0	0	0	0	0	1	0	-10	0	0	14	3	KZT
LT	0	0	0	1	0	7	0	1	0	5	1	0	0	0	0	0	2	0	0	0	0	0	0	0	0	-2	0	0	39	26	LT
LU	0	0	0	3	0	6	0	2	1	2	0	1	1	0	0	0	1	0	0	0	0	0	0	0	0	9	0	0	121	106	LU
LV	0	0	0	1	0	4	0	0	0	6	1	0	0	0	0	0	1	0	0	0	0	0	0	0	0	-2	0	0	31	20	LV
MD	0	0	0	1	0	8	0	11	1	13	1	0	1	0	0	1	6	0	0	0	0	0	0	0	0	-6	0	0	70	42	MD
ME	1	1	0	0	0	4	0	2	3	2	0	0	1	0	0	1	1	0	0	0	0	0	0	0	0	-4	0	0	44	32	ME
MK	0	4	0	0	0	4	0	3	4	3	0	0	1	0	0	1	2	0	0	0	0	0	0	0	0	-4	0	0	60	41	MK
MT	0	0	4	1	0	2	0	2	1	2	0	0	0	0	0	1	1	0	0	0	0	5	0	0	0	-0	0	0	79	70	MT
NL	0	0	0	16	1	11	1	2	1	3	1	1	1	0	0	0	2	0	0	0	0	0	2	0	0	22	0	0	178	161	NL
NO	0	0	0	0	1	1	0	0	0	1	0	0	0	0	0	0	0	0	0	0	0	0	0	0	0	0	0	0	7	5	NO
PL	0	0	0	2	0	19	0	3	1	5	1	1	2	0	0	0	3	0	0	0	0	0	0	0	0	3	0	0	87	70	PL
PT	0	0	0	0	0	0	7	0	0	0	0	0	0	0	0	0	0	0	0	0	0	0	0	0	0	-1	0	0	23	22	PT
RO	0	0	0	1	0	7	0	18	2	7	1	0	1	0	0	1	4	0	0	0	0	0	0	0	0	-5	0	0	73	52	RO
RS	0	2	0	1	0	8	0	7	12	4	1	1	2	0	0	1	3	0	0	0	0	0	0	0	0	-1	0	0	87	57	RS
RUE	0	0	0	0	0	1	0	0	0	7	0	0	0	0	0	0	0	0	0	0	0	0	0	0	0	-2	0	0	12	3	RUE
SE	0	0	0	0	1	2	0	0	0	2	1	0	0	0	0	0	0	0	0	0	0	0	0	0	0	0	0	0	16	13	SE
SI	0	0	0	1	0	6	0	5	6	3	0	12	1	0	0	0	2	0	0	0	0	0	0	0	0	1	0	0	123	97	SI
SK	0	0	0	1	0	13	0	5	2	4	1	1	4	0	0	0	4	0	0	0	0	0	0	0	0	1	0	0	87	70	SK
TJ	0	0	0	0	0	0	0	0	0	1	0	0	0	2	0	0	0	1	0	0	0	0	0	1	0	-4	0	0	6	1	TJ
TM	0	0	0	0	0	1	0	0	0	7	0	0	0	0	0	1	1	0	0	0	0	0	0	1	0	-8	0	0	16	4	TM
TR	0	0	0	0	0	2	0	1	0	5	0	0	0	0	0	21	2	0	0	0	0	0	0	0	0	-7	0	0	43	11	TR
UA	0	0	0	1	0	7	0	3	0	16	1	0	1	0	0	1	6	0	0	0	0	0	0	0	0	-3	0	0	58	28	UA
UZ	0	0	0	0	0	1	0	0	0	7	0	0	0	1	0	0	1	2	0	0	0	0	0	1	0	-8	0	0	19	4	UZ
ATL	0	0	0	0	0	0	0	0	0	0	0	0	0	0	0	0	0	0	0	0	0	0	0	0	0	-0	0	0	3	2	ATL
BAS	0	0	0	1	1	5	0	1	0	4	2	0	0	0	0	0	1	0	0	0	0	0	0	0	0	2	0	0	41	33	BAS
BLS	0	0	0	0	0	6	0	4	1	19	1	0	1	0	0	12	7	0	0	0	0	0	0	0	0	-2	0	0	76	27	BLS
MED	0	0	0	0	0	3	0	2	1	4	0	1	0	0	0	7	2	0	0	0	0	3	0	0	0	-3	0	0	75	56	MED
NOS	0	0	0	3	0	3	0	0	0	1	1	0	0	0	0	0	0	0	0	0	0	0	1	0	0	5	0	0	46	42	NOS
AST	0	0	0	0	0	0	0	0	0	4	0	0	0	0	0	2	1	0	0	0	0	0	0	1	0	-6	0	0	10	2	AST
NOA	0	0	0	0	0	1	0	1	1	1	0	0	0	0	0	2	1	0	0	0	0	1	0	0	0	-2	0	0	28	21	NOA
EXC	0	0	0	0	0	2	0	1	0	6	0	0	0	0	0	1	1	0	0	0	0	0	0	0	0	-3	0	0	26	16	EXC
EU	0	0	0	1	0	5	0	3	1	3	1	1	1	0	0	1	1	0	0	0	0	0	0	0	0	2	0	0	72	61	EU
	ME	MK	MT	NL	NO	PL	PT	RO	RS	RUE	SE	SI	SK	TJ	TM	TR	UA	UZ	ATL	BAS	BLS	MED	NOS	AST	NOA	BIC	DMS	VOL	EXC	EU	

Table C.13: 2011 country-to-country blame matrices for **PM2.5**.
Units: ng/m^3 per 15% emis. red. of PPM, SO_x, NO_x, NH_3 and VOC. **Emitters →, Receptors ↓**. (Based on ECMWF meteorology.)

	AL	AM	AT	AZ	BA	BE	BG	BY	CH	CY	CZ	DE	DK	EE	ES	FI	FR	GB	GE	GR	HR	HU	IE	IS	IT	KG	KZT	LT	LU	LV	MD	
AL	417	0	6	0	88	1	83	2	1	0	10	19	1	0	6	0	9	4	0	164	12	14	0	0	42	0	1	0	0	0	1	AL
AM	0	227	0	143	0	0	1	0	0	0	0	1	0	0	0	0	0	0	39	0	0	0	0	0	0	0	16	0	0	0	0	AM
AT	1	0	277	0	26	5	9	2	33	0	56	215	2	1	8	0	45	9	0	2	32	49	0	0	124	0	1	1	1	0	0	AT
AZ	0	24	0	440	0	0	0	1	0	0	0	2	0	0	0	0	0	1	75	0	0	0	0	0	0	0	67	0	0	0	0	AZ
BA	8	0	15	0	712	2	35	3	3	0	26	46	1	0	8	0	14	6	0	11	77	39	0	0	45	0	2	0	0	0	2	BA
BE	0	0	18	0	6	354	2	3	22	0	26	319	3	1	20	1	384	133	0	1	2	5	8	1	30	0	1	1	17	1	0	BE
BG	3	0	5	0	23	1	642	8	2	0	10	22	1	1	2	1	7	5	0	40	5	15	0	0	7	0	8	1	0	1	8	BG
BY	0	0	3	0	5	4	2	271	1	0	13	51	7	10	2	6	11	17	0	0	2	9	1	0	4	0	14	31	0	10	3	BY
CH	0	0	41	0	3	5	1	0	384	0	12	193	1	0	14	0	140	10	0	1	2	3	0	0	222	0	0	0	1	0	0	CH
CY	0	0	1	0	9	0	28	2	0	20	2	4	0	0	2	0	2	2	1	38	1	1	0	0	8	0	2	0	0	0	0	CY
CZ	1	0	81	0	26	11	13	5	11	0	386	304	3	1	7	1	63	22	0	3	21	74	1	0	26	0	2	1	2	1	1	CZ
DE	0	0	53	0	10	46	5	5	31	0	70	745	9	1	13	1	142	63	0	2	6	13	5	1	33	0	2	2	6	1	0	DE
DK	0	0	5	0	5	28	3	7	3	0	28	269	239	1	4	3	57	112	0	1	2	4	6	1	6	0	2	4	2	2	0	DK
EE	0	0	1	0	0	3	0	27	0	0	4	29	9	134	1	27	5	19	0	0	0	1	1	0	1	0	5	17	0	35	1	EE
ES	0	0	1	0	4	2	1	0	1	0	2	10	0	0	452	0	42	6	0	0	1	1	1	0	13	0	0	0	0	0	0	ES
FI	0	0	0	0	0	1	0	7	0	0	2	12	3	12	0	115	2	6	0	0	0	0	0	0	0	0	2	3	0	2	0	FI
FR	0	0	12	0	5	26	1	1	26	0	12	124	1	0	59	0	523	47	0	1	2	3	3	0	60	0	1	0	4	0	0	FR
GB	0	0	3	0	1	18	1	1	3	0	4	59	3	0	11	1	105	423	0	0	1	1	23	1	11	0	0	0	1	0	0	GB
GE	0	27	0	91	0	0	1	1	0	0	0	1	0	0	0	0	0	0	230	1	0	0	0	0	0	0	13	0	0	0	0	GE
GL	0	0	0	0	0	0	0	0	0	-0	0	0	0	0	0	0	0	0	0	0	0	0	0	0	0	0	0	0	0	0	0	GL
GR	16	0	3	0	32	1	261	4	1	0	7	13	1	1	4	0	6	4	0	382	4	7	0	0	23	0	3	1	0	0	2	GR
HR	4	0	40	0	323	4	33	4	5	0	41	79	2	1	9	1	21	9	0	9	280	85	0	0	129	0	2	1	1	0	2	HR
HU	2	0	55	0	79	5	31	8	8	0	64	120	2	1	7	1	30	14	0	5	77	486	1	0	48	0	3	2	1	1	2	HU
IE	0	0	0	0	0	7	0	0	1	0	1	12	1	0	6	0	34	163	0	0	0	0	126	1	4	0	0	0	0	0	0	IE
IS	0	0	0	0	0	0	0	0	0	0	0	1	0	0	0	0	1	3	0	0	0	0	0	103	0	0	0	0	0	0	0	IS
IT	3	0	31	0	60	2	11	2	15	0	15	37	1	0	24	0	48	6	0	8	27	12	0	0	1046	0	0	0	0	0	0	IT
KG	0	0	0	0	0	0	0	0	0	0	0	0	0	0	0	0	0	0	0	0	0	0	0	0	0	113	177	0	0	0	0	KG
KZT	0	0	0	1	0	0	0	2	0	0	0	1	0	1	0	1	0	1	0	0	0	0	0	0	0	5	515	0	0	0	0	KZT
LT	0	0	3	0	3	7	1	77	1	0	12	71	15	12	2	8	14	28	0	0	2	5	2	0	6	0	8	180	0	30	2	LT
LU	0	0	27	0	7	117	2	2	23	0	34	432	2	0	24	1	382	72	0	2	3	6	4	0	30	0	1	1	123	0	0	LU
LV	0	0	1	0	1	5	1	49	1	0	7	48	12	26	1	12	9	23	0	0	1	3	2	0	3	0	7	63	0	138	1	LV
MD	1	0	6	0	8	2	34	22	2	0	19	36	2	3	2	2	11	7	0	4	3	18	0	0	5	0	19	3	0	1	162	MD
ME	62	0	7	0	162	1	40	2	2	0	12	23	1	0	5	0	9	4	0	22	17	17	0	0	30	0	1	0	0	0	1	ME
MK	50	0	6	0	47	1	201	3	2	0	12	21	1	1	4	0	8	4	0	189	7	19	0	0	16	0	2	0	0	0	2	MK
MT	3	0	4	0	43	1	23	1	1	0	4	10	0	0	34	0	39	5	0	23	6	4	0	0	176	0	1	0	0	0	0	MT
NL	1	0	16	0	6	158	4	4	11	0	29	414	8	1	13	2	219	194	0	2	2	6	13	1	21	0	1	2	6	1	0	NL
NO	0	0	0	0	0	2	0	1	0	0	2	16	5	1	2	3	6	11	0	0	0	0	1	1	0	0	1	1	0	0	0	NO
PL	0	0	13	0	10	11	7	29	3	0	77	194	14	4	4	3	32	33	0	1	6	31	3	0	14	0	6	10	1	3	2	PL
PT	0	0	0	0	2	1	0	0	0	0	1	6	0	0	197	0	16	6	0	0	0	0	1	0	4	0	0	0	0	0	0	PT
RO	2	0	11	0	25	2	62	10	4	0	19	38	1	1	3	1	12	7	0	6	8	47	0	0	12	0	9	2	0	1	14	RO
RS	17	0	18	0	116	2	99	5	4	0	32	60	1	1	5	1	17	9	0	26	32	84	0	0	22	0	3	1	0	0	4	RS
RUE	0	0	0	1	0	0	0	5	0	0	1	3	1	2	0	2	1	1	0	0	0	0	0	0	0	0	76	1	0	1	0	RUE
SE	0	0	1	0	1	4	1	4	0	0	4	36	19	4	1	9	9	18	0	0	0	1	1	1	1	0	1	2	0	1	0	SE
SI	1	0	112	0	92	4	19	4	7	0	39	99	2	1	9	1	24	8	0	5	170	55	0	0	297	0	2	1	1	0	1	SI
SK	1	0	34	0	29	4	17	7	6	0	91	113	2	1	5	1	28	14	0	3	22	204	1	0	22	0	3	2	1	1	1	SK
TJ	0	0	0	1	0	0	0	0	0	0	0	0	0	0	0	0	0	0	0	0	0	0	0	0	0	7	87	0	0	0	0	TJ
TM	0	2	0	7	0	0	0	1	0	0	0	1	0	0	0	0	1	1	2	0	0	0	0	0	0	1	200	0	0	0	0	TM
TR	0	4	1	2	3	0	18	2	0	2	2	4	0	0	1	0	2	1	4	8	0	1	0	0	2	0	3	0	0	0	1	TR
UA	0	0	3	1	6	2	10	38	1	0	12	30	2	4	2	2	8	7	1	2	2	12	1	0	3	0	28	4	0	2	13	UA
UZ	0	1	0	3	0	0	0	1	0	0	0	1	0	0	0	0	1	1	1	0	0	0	0	0	0	14	350	0	0	0	0	UZ
ATL	0	0	0	0	0	1	0	0	0	0	0	4	0	0	6	1	11	10	0	0	0	0	2	2	1	0	2	0	0	0	0	ATL
BAS	0	0	2	0	2	10	1	13	1	0	11	114	51	18	2	30	21	41	0	0	1	3	3	0	3	0	3	11	1	12	1	BAS
BLS	0	1	2	3	4	1	33	9	1	0	6	12	1	1	1	1	3	3	14	6	1	4	0	0	2	0	16	2	0	1	5	BLS
MED	4	0	4	0	53	1	54	2	2	2	5	12	0	0	44	0	35	5	0	51	9	3	0	0	110	0	1	0	0	0	0	MED
NOS	0	0	4	0	2	28	1	2	3	0	9	119	18	0	8	1	105	162	0	1	1	2	10	1	7	0	0	1	2	1	0	NOS
AST	0	1	0	8	0	0	1	1	0	2	0	1	0	0	0	0	0	0	1	2	0	0	0	0	1	1	79	0	0	0	0	AST
NOA	1	0	1	0	16	0	27	1	0	0	2	4	0	0	19	0	9	2	0	30	1	1	0	0	22	0	0	0	0	0	0	NOA
EXC	1	1	4	3	6	3	8	8	3	0	7	29	2	2	13	3	21	11	1	4	3	6	1	1	19	2	111	2	0	1	1	EXC
EU	1	0	20	0	14	15	31	7	9	0	28	132	8	4	70	11	107	50	0	14	8	24	5	0	96	0	2	6	2	4	1	EU
	AL	AM	AT	AZ	BA	BE	BG	BY	CH	CY	CZ	DE	DK	EE	ES	FI	FR	GB	GE	GR	HR	HU	IE	IS	IT	KG	KZT	LT	LU	LV	MD	

Table C.13 Cont.: 2011 country-to-country blame matrices for **PM2.5**.
Units: ng/m^3 per 15% emis. red. of PPM, SO_x, NO_x, NH_3 and VOC. **Emitters →, Receptors ↓**. (Based on ECMWF meteorology.)

	ME	MK	MT	NL	NO	PL	PT	RO	RS	RUE	SE	SI	SK	TJ	TM	TR	UA	UZ	ATL	BAS	BLS	MED	NOS	AST	NOA	BIC	DMS	VOL	EXC	EU	
AL	32	121	1	2	0	35	0	53	309	9	1	2	9	0	0	12	28	0	2	1	2	80	2	0	3	17	2	17	1497	463	AL
AM	0	0	0	0	0	2	0	1	0	11	0	0	0	0	5	145	7	4	0	0	1	2	0	78	0	4	0	14	605	7	AM
AT	1	1	0	5	1	61	1	19	29	5	1	69	28	0	0	1	13	0	3	1	0	12	6	0	1	20	1	4	1133	987	AT
AZ	0	0	0	0	0	4	0	1	0	63	0	0	0	0	17	36	26	13	1	0	1	1	1	68	0	4	0	7	777	12	AZ
BA	31	10	0	3	1	59	0	57	204	8	1	5	19	0	0	3	24	0	2	1	1	23	3	0	2	16	1	6	1481	394	BA
BE	0	1	0	92	2	44	2	5	4	4	1	2	4	0	0	0	8	0	36	2	0	8	75	0	0	49	8	3	1526	1470	BE
BG	2	16	0	1	1	47	0	226	108	40	1	1	9	0	0	42	112	0	1	1	19	8	1	0	1	15	1	3	1426	1048	BG
BY	0	0	0	7	2	198	0	15	5	92	6	1	9	0	0	1	77	0	3	11	1	1	10	0	0	8	1	0	893	420	BY
CH	0	0	0	4	0	11	1	3	3	1	0	5	2	0	0	0	4	0	5	1	0	13	6	0	1	24	1	4	1071	672	CH
CY	1	4	0	0	0	11	0	13	9	15	0	0	1	0	0	1509	39	0	1	0	11	247	1	18	5	9	13	29	1730	136	CY
CZ	1	2	0	12	1	186	1	32	41	10	2	15	68	0	0	1	25	0	6	3	1	6	12	0	0	25	2	2	1467	1318	CZ
DE	0	1	0	55	3	101	1	10	10	7	3	5	9	0	0	1	14	0	15	11	0	7	45	0	0	37	4	2	1485	1395	DE
DK	0	1	0	53	12	96	1	9	6	9	18	1	5	0	0	0	10	0	17	48	0	2	100	0	0	29	11	0	1017	958	DK
EE	0	0	0	6	5	49	0	3	1	60	19	0	2	0	0	0	14	0	3	28	0	0	11	0	0	7	3	0	479	365	EE
ES	0	0	0	2	0	4	23	2	3	0	0	1	1	0	0	0	1	0	34	0	0	72	3	0	5	28	5	3	578	566	ES
FI	0	0	0	2	5	14	0	1	0	32	16	0	0	0	0	0	4	0	3	9	0	0	4	0	0	6	2	0	244	193	FI
FR	0	0	0	16	1	17	2	4	3	2	0	3	3	0	0	0	4	0	39	1	0	32	29	0	1	26	7	3	971	924	FR
GB	0	0	0	25	1	11	1	2	1	1	2	1	1	0	0	0	2	0	54	2	0	3	42	0	0	24	12	1	721	708	GB
GE	0	0	0	0	0	3	0	1	0	30	0	0	0	0	4	81	18	3	0	0	7	1	0	16	0	5	0	8	510	10	GE
GL	0	0	0	0	0	0	0	0	0	0	0	0	0	0	0	0	0	0	0	0	0	0	0	0	0	43	0	0	0	0	GL
GR	4	59	1	1	0	31	0	75	75	21	1	1	6	0	0	93	65	0	1	1	10	113	1	0	3	13	3	15	1208	826	GR
HR	7	8	0	5	1	85	1	71	186	10	1	51	28	0	0	3	32	0	3	1	1	45	4	0	2	19	1	5	1573	707	HR
HU	3	5	0	6	1	170	1	188	159	16	2	30	109	0	0	2	68	0	4	2	2	11	6	0	1	21	1	3	1813	1378	HU
IE	0	0	0	6	1	4	0	0	0	1	1	0	0	0	0	0	1	0	66	1	0	1	15	0	0	15	15	0	373	368	IE
IS	0	0	0	0	1	0	0	0	0	0	0	0	0	0	0	0	0	0	6	0	0	0	1	0	0	8	6	0	113	9	IS
IT	3	4	1	2	0	32	1	17	25	3	1	32	7	0	0	3	10	0	3	1	0	157	3	0	6	30	3	25	1490	1334	IT
KG	0	0	0	0	0	0	0	0	0	4	0	0	0	21	2	1	1	334	0	0	0	0	0	23	0	12	0	18	656	1	KG
KZT	0	0	0	0	0	3	0	1	0	173	0	0	0	2	4	2	19	39	1	1	0	0	1	16	0	7	0	4	774	11	KZT
LT	0	0	0	14	3	206	0	9	3	67	14	1	6	0	0	0	43	0	4	22	0	1	16	0	0	9	3	0	854	645	LT
LU	0	1	0	36	1	38	2	6	4	4	1	3	6	0	0	1	9	0	23	1	0	9	33	0	0	39	4	3	1407	1350	LU
LV	0	0	0	10	4	92	0	5	2	58	17	0	3	0	0	0	24	0	4	22	0	0	13	0	0	8	3	0	630	481	LV
MD	1	2	0	3	1	125	0	302	17	85	2	1	15	0	0	14	266	1	2	3	10	2	3	0	0	11	1	1	1209	604	MD
ME	245	24	0	2	0	38	0	44	305	6	1	2	11	0	0	5	18	0	1	1	1	36	2	0	2	14	1	11	1120	270	ME
MK	7	334	0	1	0	38	0	75	299	12	1	1	11	0	0	16	36	0	1	1	3	20	2	0	1	16	1	8	1429	611	MK
MT	4	6	196	1	0	14	1	17	28	4	0	2	3	0	0	14	11	0	4	0	1	525	2	0	22	19	13	51	682	559	MT
NL	0	1	0	317	4	72	2	7	5	5	3	1	5	0	0	1	11	0	36	7	0	6	143	0	0	56	10	2	1566	1513	NL
NO	0	0	0	3	51	8	0	1	0	4	7	0	0	0	0	0	1	0	6	3	0	0	8	0	0	8	4	0	129	71	NO
PL	0	1	0	19	2	744	0	35	15	25	6	4	38	0	0	1	56	0	6	13	1	3	17	0	0	21	2	1	1460	1302	PL
PT	0	0	0	1	0	2	265	1	1	0	0	0	0	0	0	0	1	0	98	0	0	19	2	0	3	29	7	2	509	503	PT
RO	2	5	0	2	1	90	0	779	70	40	1	3	20	0	0	9	137	1	2	1	9	3	3	0	0	13	1	2	1457	1121	RO
RS	22	38	0	3	1	83	0	209	700	17	1	4	31	0	0	5	55	0	3	1	3	11	4	0	1	20	1	5	1732	712	RS
RUE	0	0	0	0	1	7	0	1	0	242	1	0	0	0	1	1	16	2	1	1	0	0	1	1	0	12	0	1	370	23	RUE
SE	0	0	0	7	16	30	0	3	1	8	60	0	1	0	0	0	4	0	5	14	0	0	14	0	0	8	3	0	252	215	SE
SI	1	4	0	5	1	72	1	44	72	7	1	551	19	0	0	2	19	0	3	1	1	43	5	0	1	21	1	4	1751	1368	SI
SK	1	3	0	6	1	248	0	94	52	14	2	13	396	0	0	1	58	1	4	1	1	5	5	0	0	19	1	2	1506	1305	SK
TJ	0	0	0	0	0	0	0	0	0	4	0	0	0	153	10	2	1	269	0	0	0	0	0	36	0	16	0	25	534	1	TJ
TM	0	0	0	0	0	3	0	0	0	49	0	0	0	7	120	7	16	160	0	0	0	0	1	49	0	11	0	12	583	10	TM
TR	0	2	0	0	0	11	0	16	6	23	0	0	1	0	0	908	50	1	1	0	13	23	1	21	2	12	2	21	1082	72	TR
UA	0	1	0	3	1	118	0	60	8	138	2	1	10	0	0	13	309	1	2	3	7	1	3	1	0	10	1	1	863	301	UA
UZ	0	0	0	0	0	2	0	0	0	60	0	0	0	31	26	5	16	473	1	0	0	0	1	23	0	11	0	15	991	10	UZ
ATL	0	0	0	1	1	2	1	0	0	5	0	0	0	0	0	0	1	0	20	0	0	1	2	0	0	19	12	0	54	42	ATL
BAS	0	0	0	21	8	99	0	8	3	28	46	1	3	0	0	0	11	0	7	44	0	1	27	0	0	14	5	0	582	510	BAS
BLS	0	2	0	1	1	41	0	65	10	119	1	0	4	0	1	157	248	1	1	1	74	6	1	2	0	11	6	3	785	191	BLS
MED	4	9	3	1	0	20	1	23	28	10	0	3	4	0	0	292	35	0	5	0	7	406	2	4	16	16	13	37	832	383	MED
NOS	0	0	0	48	9	27	1	3	2	2	4	1	2	0	0	0	3	0	28	5	0	2	55	0	0	20	15	1	590	563	NOS
AST	0	0	0	0	0	2	0	1	0	24	0	0	0	3	11	74	11	27	0	0	1	10	0	167	1	21	1	15	254	11	AST
NOA	2	5	1	0	0	6	1	9	10	3	0	0	1	0	0	82	12	0	2	0	2	133	1	1	43	29	5	35	270	136	NOA
EXC	1	1	0	3	2	28	2	16	9	147	3	2	4	2	4	34	27	22	4	2	1	7	4	5	0	15	1	3	583	195	EXC
EU	1	3	0	16	3	98	9	64	19	14	9	9	15	0	0	8	24	0	19	6	1	30	18	0	1	21	4	4	962	846	EU
	ME	MK	MT	NL	NO	PL	PT	RO	RS	RUE	SE	SI	SK	TJ	TM	TR	UA	UZ	ATL	BAS	BLS	MED	NOS	AST	NOA	BIC	DMS	VOL	EXC	EU	

APPENDIX D

Explanatory note on country reports for 2011

For many years, country reports have been issued as a supplement to the EMEP status reports.

The country reports issued by EMEP MSC-W focus on chemical species that are relevant to eutrophication, acidification and ground level ozone, but also information on particulate matter is given. More specifically, these country reports provide for each country:

- horizontal maps of emissions, and modeled air concentrations and depositions in 2011
- emission trends for the years 2000 to 2011, and emissions in the year 2020 according to the revised Gothenburg Protocol
- modeled trends of air concentrations and depositions for the years 2000 to 2011, and for the year 2020
- maps and charts on transboundary air pollution in 2011, visualizing the effect of the country on its surroundings, and vice versa
- frequency analyses of air concentrations and depositions, based on measurements and model results for 2011, along with a statistical analysis of model performance
- maps on the risk of damage from ozone and particulate matter in 2011

EMEP MSC-W issues these country reports for 47 Parties to the Convention, and for Tajikistan, Turkmenistan and Uzbekistan. For the Russian Federation, the country report includes the territory of the Russian Federation, which is covered by the extended EMEP domain (see Figure 1.1b).

All 50 country reports are written in English. For the 12 EECCA countries, the reports are made available also in Russian. All country reports can be downloaded in pdf format from the MSC-W report page on the EMEP website `http://emep.int/mscw/mscw_publications.html`

This year, the country reports are found under the header 'MSC-W Data Note 1/2013'. The reports for each country can be selected conveniently from a drop-down menu.

APPENDIX E

Model Development - Performance Changes

Tables E:1-E:15 present the results of both the current model version (rv4.4) and earlier model versions as obtained from the orginal EMEP status reports. Data from these Tables underly the discussion and illustrations presented in Chapter 3 (see Section 3.4 for details).

Table E:1: Comparison of model results and observations for SO_2 [μg(S) m^{-3}] for the years 1980–2011. 'Original' results refer to evaluations as given in earlier EMEP reports, with model version as given in left column. 'Updated' results are derived from model version rv4.4 and latest EMEP CCC data-base for observations. See Chapter 3 for details.

Original Results					Year	Updated Results (rv4.4)			
Rev.	N_{stat}	Obs.	Bias(%)	Corr.		N_{stat}	Obs.	Bias(%)	Corr.
rv1.7	44	5.46	4	0.84	1980				
rv1.7	51	6.04	-8	0.76	1985				
rv1.7	60	2.82	7	0.42	1990	93	3.07	30	0.53
rv1.7	77	1.42	24	0.60	1995				
rv1.7	77	1.53	16	0.81	1996				
rv1.7	76	1.15	30	0.80	1997				
rv1.7	75	1.01	23	0.71	1998				
rv1.7	80	0.84	25	0.81	1999				
rv1.7	81	0.72	39	0.73	2000	78	0.80	29	0.73
rv1.8	76	0.81	14	0.67	2001	80	0.79	32	0.70
rv2.0	68	0.85	24	0.56	2002	70	0.78	29	0.64
rv2.3	59	0.88	32	0.59	2003	64	0.84	30	0.67
rv2.6	58	0.67	34	0.67	2004	63	0.67	26	0.69
rv2.7	58	0.80	22	0.51	2005	60	0.76	11	0.50
rv3.1	56	0.78	21	0.41	2006	61	0.74	16	0.40
rv3.4	59	0.50	27	0.62	2007	57	0.57	14	0.32
rv3.6	51	0.42	48	0.60	2008	52	0.42	38	0.65
rv3.8	48	0.42	58	0.39	2009	45	0.41	52	0.35
rv4.0	44	0.54	21	0.37	2010	44	0.54	25	0.33
rv4.4	38	0.54	21	0.59	2011	38	0.54	21	0.59

Notes: N_{stat} is the number of stations with observations that went into the calculation of this table, 'Obs.' represents the Observations, Bias(%) is the relative bias between the observation and model results in percentage and 'Corr.' represents the spatial correlation. The year in the table shows the meteorological year. Relative bias is defined as $\frac{Mod-Obs}{0.5(Mod+Obs)} \times 100\%$. Thus a negative bias indicates that the model concentrations are lower compared to the concentrations.

Table E:2: As Table E:1, but for SO_4^{2-} [μg(S) m^{-3}]

Original Results					Year	Updated Results (rv4.4)			
Rev.	N_{stat}	Obs.	Bias(%)	Corr.		N_{stat}	Obs.	Bias(%)	Corr.
rv1.7	27	1.70	6	0.94	1980				
rv1.7	34	1.57	-3	0.86	1985				
rv1.7	47	1.23	-3	0.72	1990	87	1.34	4	0.59
rv1.7	67	0.95	0	0.79	1995				
rv1.7	67	1.03	2	0.79	1996				
rv1.7	67	0.83	0	0.77	1997				
rv1.7	67	0.77	-5	0.77	1998				
rv1.7	68	0.73	-10	0.74	1999				
rv1.7	70	0.63	-4	0.71	2000	82	0.66	-7	0.75
rv1.8					2001	82	0.70	-11	0.83
rv2.0	70	0.74	-9	0.78	2002	77	0.73	-14	0.84
rv2.3	68	0.79	-5	0.71	2003	77	0.77	-14	0.82
rv2.6	56	0.61	-13	0.82	2004	63	0.60	-9	0.80
rv2.7	60	0.70	-13	0.81	2005	67	0.68	-18	0.77
rv3.1	61	0.73	-19	0.75	2006	68	0.72	-19	0.76
rv3.4	61	0.64	-41	0.64	2007	64	0.62	-22	0.74
rv3.6	58	0.56	-42	0.64	2008	59	0.56	-25	0.67
rv3.8	53	0.58	-43	0.74	2009	54	0.58	-26	0.76
rv4.0	43	0.58	-20	0.80	2010	43	0.58	-26	0.79
rv4.4	43	0.63	-27	0.85	2011	43	0.63	-27	0.85

Table E:3: As Table E:1, but for NO_2 [μg(N) m^{-3}]

Original Results					Year	Updated Results (rv4.4)			
Rev.	N_{stat}	Obs.	Bias(%)	Corr.		N_{stat}	Obs.	Bias(%)	Corr.
rv1.7					1990	54	3.09	-21	0.70
rv1.7					2000	52	2.02	19	0.56
rv1.8					2001	50	1.84	22	0.76
rv2.0					2002	49	2.05	11	0.73
rv2.3					2003	48	1.79	18	0.70
rv2.6					2004	50	1.84	20	0.52
rv2.7					2005	44	1.77	16	0.72
rv3.1					2006	44	1.83	17	0.72
rv3.4					2007	42	1.90	3	0.63
rv3.6	40	1.70	-12	0.77	2008	41	1.72	7	0.77
rv3.8	42	1.70	3	0.74	2009	44	1.68	14	0.78
rv4.0	42	1.98	-7	0.77	2010	42	1.98	3	0.79
rv4.4	37	1.79	8	0.61	2011	37	1.79	8	0.61

Table E:4: As Table E:1, but for NH_3 [μg(N) m^{-3}]

Original Results					Year	Updated Results (rv4.4)			
Rev.	N_{stat}	Obs.	Bias(%)	Corr.		N_{stat}	Obs.	Bias(%)	Corr.
rv1.7					1990	3	5.11	-87	0.98
rv1.7					2000	14	1.68	-64	0.99
rv1.8					2001	12	1.88	-64	0.97
rv2.0					2002	12	1.54	56	0.94
rv2.3					2003	12	0.85	-51	0.61
rv2.6					2004	12	0.64	-54	0.87
rv2.7	15	1.79	-20	0.94	2005	20	1.43	-41	0.89
rv3.1	14	0.90	40*	0.35	2006	20	0.76	-19	0.58
rv3.4	16	1.78	-34	0.93	2007	20	0.76	-22	0.70
rv3.6	22	1.02	-11	0.32	2008	22	0.99	-15	0.34
rv3.8	11	0.92	-10	0.29	2009	11	0.92	-12	0.40
rv4.0	11	0.72	9	0.51	2010	11	0.72	13	0.52
rv4.4	10	0.89	-5	0.48	2011	10	0.89	-5	0.48

Table E:5: As Table E:1, but for NH_4^+ [μg(N) m^{-3}]

Original Results					Year	Updated Results (rv4.4)			
Rev.	N_{stat}	Obs.	Bias(%)	Corr.		N_{stat}	Obs.	Bias(%)	Corr.
rv1.7	4	2.35	-24	0.97	1980				
rv1.7	6	2.76	-29	0.99	1985				
rv1.7	7	1.14	42	0.91	1990	20	1.38	18	0.76
rv1.7	16	0.95	37	0.83	1995				
rv1.7	16	1.17	29	0.81	1996				
rv1.7	19	1.13	15	0.80	1997				
rv1.7	20	1.03	15	0.84	1998				
rv1.7	22	0.89	17	0.75	1999				
rv1.7	21	0.79	34	0.75	2000	34	0.62	24	0.77
rv1.8					2001	21	0.76	-8	0.92
rv2.0					2002	21	0.92	5	0.79
rv2.3					2003	25	0.91	5	0.82
rv2.6	19	0.63	19	0.84	2004	24	0.71	7	0.81
rv2.7	22	0.87	26	0.79	2005	33	0.93	0	0.84
rv3.1	21	0.94	-1	0.75	2006	31	0.96	-5	0.81
rv3.4	30	0.78	-29	0.64	2007	35	0.85	2	0.86
rv3.6	37	0.67	-26	0.78	2008	39	0.85	-5	0.82
rv3.8	27	0.85	-40	0.66	2009	26	1.07	-17	0.76
rv4.0	22	1.09	-16	0.74	2010	22	1.09	-14	0.74
rv4.4	24	1.00	-18	0.75	2011	24	1.00	-18	0.75

Table E:6: As Table E:1, but for total ammonium (TNHx = $NH_3 + NH_4^+$) [μg(N) m^{-3}]

Original Results					Year	Updated Results (rv4.4)			
Rev.	N_{stat}	Obs.	Bias(%)	Corr.		N_{stat}	Obs.	Bias(%)	Corr.
rv1.7	21	1.39	-14	0.85	1990	28	1.46	-33	0.61
rv1.7	32	1.30	5	0.91	1995				
rv1.7	32	1.30	13	0.84	1996				
rv1.7	34	1.23	8	0.80	1997				
rv1.7	34	1.04	15	0.80	1998				
rv1.7	40	1.33	-2	0.78	1999				
rv1.7	38	1.31	2	0.76	2000	51	1.19	-6	0.79
rv1.8					2001	46	1.21	-5	0.82
rv2.0	42	1.20	35	0.72	2002	48	1.16	2	0.69
rv2.3	34	1.12	42	0.73	2003	48	1.26	2	0.80
rv2.6	43	1.24	25	0.63	2004	46	1.25	-7	0.80
rv2.7	36	1.46	15	0.66	2005	47	1.49	-16	0.83
rv3.1	42	1.72	12	0.57	2006	49	1.59	-19	0.81
rv3.4	38	1.48	-7	0.79	2007	48	1.43	-18	0.84
rv3.6	45	1.42	-16	0.68	2008	47	1.46	-25	0.74
rv3.8	35	1.51	-18	0.85	2009	43	1.62	-27	0.80
rv4.0	35	1.45	-14	0.85	2010	35	1.45	-25	0.81
rv4.4	29	1.48	-21	0.84	2011	29	1.48	-21	0.84

Table E:7: As Table E:1, but for NO_3^- [μg(N) m^{-3}]

Original Results					Year	Updated Results (rv4.4)			
Rev.	N_{stat}	Obs.	Bias(%)	Corr.		N_{stat}	Obs.	Bias(%)	Corr.
rv1.7					1990	16	0.60	47	0.75
rv1.7	11	0.58	61	0.88	1995				
rv1.7	15	0.60	54	0.77	1996				
rv1.7	18	0.58	47	0.71	1997				
rv1.7	17	0.52	56	0.83	1998				
rv1.7	18	0.52	45	0.73	1999				
rv1.7	19	0.43	76	0.65	2000	27	0.41	31	0.78
rv1.8					2001	26	0.38	22	0.93
rv2.0	23	0.36	33	0.76	2002	26	0.38	28	0.88
rv2.3	33	0.34	32	0.75	2003	37	0.40	25	0.78
rv2.6	23	0.31	39	0.80	2004	25	0.32	35	0.81
rv2.7	25	0.44	37	0.80	2005	31	0.41	28	0.83
rv3.1	26	0.48	-2	0.78	2006	32	0.48	12	0.71
rv3.4	25	0.41	-28	0.72	2007	29	0.38	31	0.84
rv3.6	30	0.34	8	0.68	2008	32	0.33	34	0.72
rv3.8	24	0.45	-27	0.85	2009	23	0.42	-5	0.89
rv4.0	20	0.40	-8	0.86	2010	20	0.40	-5	0.87
rv4.4	18	0.59	3	0.91	2011	18	0.59	3	0.91

Notes: In the Supplementary material to EMEP Report 1/2012, the NO_3^- concentration was reported as μg m^{-3} , here we use μg(N) m^{-3} for all years.

Table E:8: As Table E:1, but for HNO_3 [μg(N) m^{-3}]

Original Results					Year	Updated Results (rv4.4)			
Rev.	N_{stat}	Obs.	Bias(%)	Corr.		N_{stat}	Obs.	Bias(%)	Corr.
rv1.7					1990	3	0.46	-28	0.57
rv1.7					2000	16	0.13	8	0.60
rv1.8					2001	15	0.09	31	0.73
rv2.0	13	0.11	16	0.70	2002	15	0.09	26	0.72
rv2.3	14	0.13	-13	0.51	2003	16	0.13	13	0.62
rv2.6	14	0.15	-25	0.38	2004	14	0.14	-14	0.57
rv2.7	17	0.19	-28	0.27	2005	19	0.17	-17	0.46
rv3.1	15	0.19	-26	-0.01	2006	20	0.16	-7	0.38
rv3.4	13	0.17	-29	0.49	2007	17	0.14	-8	0.65
rv3.6	21	0.18	-38	0.47	2008	21	0.18	-25	0.56
rv3.8	14	0.16	-35	0.48	2009	14	0.16	-26	0.51
rv4.0	12	0.10	-16	0.46	2010	12	0.10	-16	0.47
rv4.4	12	0.14	-24	0.43	2011	12	0.14	-24	0.43

Table E:9: As Table E:1, but for total nitrate, $TNO_3 = HNO_3 + NO_3^-$ [μg(N) m^{-3}]

Original Results					Year	Updated Results (rv4.4)			
Rev.	N_{stat}	Obs.	Bias(%)	Corr.		N_{stat}	Obs.	Bias(%)	Corr.
rv1.7	24	0.51	15	0.93	1990	29	0.50	11	0.89
rv1.7	35	0.44	42	0.92	1995				
rv1.7	32	0.50	31	0.82	1996				
rv1.7	35	0.46	34	0.77	1997				
rv1.7	33	0.42	39	0.85	1998				
rv1.7	43	0.47	33	0.79	1999				
rv1.7	42	0.42	52	0.82	2000	53	0.43	38	0.80
rv1.8					2001	47	0.44	33	0.83
rv2.0	41	0.48	23	0.90	2002	47	0.47	28	0.86
rv2.3	35	0.48	22	0.88	2003	47	0.56	19	0.90
rv2.6	43	0.47	23	0.87	2004	46	0.48	23	0.86
rv2.7	41	0.55	19	0.88	2005	47	0.56	16	0.90
rv3.1	41	0.68	-16	0.80	2006	49	0.63	7	0.88
rv3.4	42	0.57	-33	0.86	2007	48	0.53	13	0.88
rv3.6	47	0.49	-11	0.81	2008	49	0.50	7	0.86
rv3.8	45	0.61	-31	0.64	2009	49	0.64	-17	0.69
rv4.0	42	0.46	2	0.83	2010	42	0.46	5	0.84
rv4.4	33	0.58	5	0.79	2011	33	0.58	5	0.79

Table E:10: As Table E:1, but for wet-deposition of SO_4^{2-} [μg(S) m^{-2}]

Original Results					Year	Updated Results (rv4.4)			
Rev.	N_{stat}	Obs.	Bias(%)	Corr.		N_{stat}	Obs.	Bias(%)	Corr.
rv1.7	23	17900	12	0.63	1980				
rv1.7	35	24877	32	0.57	1985				
rv1.7	38	23306	13	0.38	1990	83	51204	59	0.60
rv1.7	50	28275	-1	0.44	1995				
rv1.7	48	23969	6	0.71	1996				
rv1.7	50	23089	-15	0.29	1997				
rv1.7	58	23870	-4	0.82	1998				
rv1.7	44	18659	-5	0.73	1999				
rv1.7	45	18769	-6	0.62	2000	68	25971	11	0.66
rv1.8					2001	66	26187	3	0.65
rv2.0	60	21935	-4	0.65	2002	67	24012	5	0.68
rv2.3	53	15274	2	0.61	2003	65	18241	10	0.62
rv2.6	40	13309	-4	0.62	2004	57	18789	4	0.68
rv2.7	53	15552	-8	0.71	2005	56	16126	2	0.53
rv3.1	54	14490	-11	0.64	2006	58	15068	13	0.53
rv3.4	49	13873	-18	0.59	2007	59	16284	9	0.53
rv3.6	63	17673	-20	0.69	2008	62	16945	-4	0.72
rv3.8	61	14375	4	0.67	2009	62	14403	0	0.69
rv4.0	57	12677	-3	0.63	2010	57	12677	-11	0.65
rv4.4	50	11509	-26	0.53	2011	50	11509	-26	0.53

Table E:11: As Table E:1, but for SO_4^{2-} concentrations in precipitation, [μg(S) l^{-1}]

Original Results					Year	Updated Results (rv4.4)			
Rev.	N_{stat}	Obs.	Bias(%)	Corr.		N_{stat}	Obs.	Bias(%)	Corr.
rv1.7	23	0.98	21	0.85	1980				
rv1.7	35	1.00	37	0.64	1985				
rv1.7	38	0.77	27	0.55	1990	83	0.97	29	0.55
rv1.7	50	0.73	3	0.25	1995				
rv1.7	48	0.63	22	0.78	1996				
rv1.7	50	0.52	3	0.64	1997				
rv1.7	58	0.44	7	0.85	1998				
rv1.7	44	0.47	7	0.77	1999				
rv1.7	45	0.45	6	0.86	2000	68	0.54	0	0.77
rv1.8					2001	66	0.58	-12	0.54
rv2.0	60	0.50	-12	0.73	2002	67	0.52	9	0.82
rv2.3	53	0.43	3	0.74	2003	65	0.49	1	0.78
rv2.6	40	0.49	-9	0.65	2004	57	0.49	-3	0.75
rv2.7	53	0.45	-12	0.61	2005	56	0.45	-6	0.66
rv3.1	54	0.40	-10	0.74	2006	58	0.38	0	0.78
rv3.4	49	0.39	-9	0.65	2007	59	0.38	-4	0.72
rv3.6	63	0.33	-19	0.72	2008	62	0.33	-10	0.80
rv3.8	61	0.29	1	0.80	2009	62	0.29	-4	0.80
rv4.0	57	0.28	3	0.75	2010	57	0.28	-6	0.77
rv4.4	50	0.35	27	0.42	2011	50	0.35	-27	0.42

Table E:12: As Table E:1, but for wet-deposition of NH_4^+ [μg(N) m^{-2}]

Original Results					Year	Updated Results (rv4.4)			
Rev.	N_{stat}	Obs.	Bias(%)	Corr.		N_{stat}	Obs.	Bias(%)	Corr.
rv1.7	18	8344	-33	0.76	1980				
rv1.7	34	16694	-27	0.82	1985				
rv1.7	35	14959	-36	0.51	1990	82	31142	-14	0.70
rv1.7	47	19858	-38	0.72	1995				
rv1.7	41	17060	-34	0.72	1996				
rv1.7	47	16705	-29	0.71	1997				
rv1.7	58	20271	-20	0.72	1998				
rv1.7	43	14911	-24	0.80	1999				
rv1.7	44	17062	-28	0.53	2000	67	21505	-14	0.69
rv1.8					2001	65	19904	-13	0.58
rv2.0	60	18735	-16	0.74	2002	66	19858	-11	0.72
rv2.3	53	15315	-22	0.73	2003	64	17549	-19	0.72
rv2.6	43	14093	-13	0.61	2004	58	17542	-14	0.72
rv2.7	53	15467	-19	0.74	2005	56	16054	-16	0.70
rv3.1	53	15293	-22	0.78	2006	58	16092	-9	0.78
rv3.4	50	15257	-20	0.74	2007	58	17294	-9	0.60
rv3.6	63	20448	-17	0.67	2008	61	19282	-5	0.67
rv3.8	61	16960	-1	0.64	2009	62	17015	-2	0.63
rv4.0	56	14966	-14	0.68	2010	56	14966	-14	0.68
rv4.4	50	13211	-14	0.18	2011	50	13211	-14	0.18

Table E:13: As Table E:1, but for NH_4^+ concentrations in precipitation, [μg(N) l^{-1}]

Original Results					Year	Updated Results (rv4.4)			
Rev.	N_{stat}	Obs.	Bias(%)	Corr.		N_{stat}	Obs.	Bias(%)	Corr.
rv1.7	18	0.67	-34	0.87	1980				
rv1.7	34	0.71	-29	0.77	1985				
rv1.7	35	0.54	-31	0.69	1990	82	0.61	-33	0.67
rv1.7	47	0.50	-27	0.62	1995				
rv1.7	41	0.51	-23	0.62	1996				
rv1.7	47	0.42	-18	0.68	1997				
rv1.7	58	0.37	-9	0.78	1998				
rv1.7	43	0.39	-14	0.84	1999				
rv1.7	44	0.41	-15	0.64	2000	67	0.40	-19	0.68
rv1.8					2001	65	0.38	-16	0.63
rv2.0	60	0.39	-19	0.63	2002	66	0.39	-22	0.66
rv2.3	53	0.42	-18	0.52	2003	64	0.45	-23	0.60
rv2.6	43	0.42	-10	0.64	2004	58	0.41	-16	0.60
rv2.7	53	0.43	-14	0.69	2005	56	0.42	-17	0.66
rv3.1	53	0.40	-17	0.68	2006	58	0.39	-18	0.72
rv3.4	50	0.41	-9	0.68	2007	58	0.41	-24	0.54
rv3.6	63	0.38	-21	0.64	2008	61	0.38	-13	0.67
rv3.8	61	0.34	-3	0.52	2009	62	0.34	-4	0.55
rv4.0	56	0.35	-14	0.49	2010	56	0.35	-14	0.48
rv4.4	50	0.39	-12	0.20	2011	50	0.39	-12	0.20

Table E:14: As Table E:1, but for wet-deposition of NO_3^- [μg(N) m^{-2}]

Original Results					Year	Updated Results (rv4.4)			
Rev.	N_{stat}	Obs.	Bias(%)	Corr.		N_{stat}	Obs.	Bias(%)	Corr.
rv1.7	22	6862	-11	0.76	1980				
rv1.7	36	13025	-10	0.73	1985				
rv1.7	38	11892	-17	0.75	1990	83	24814	17	0.78
rv1.7	49	15456	-24	0.77	1995				
rv1.7	46	15424	-27	0.70	1996				
rv1.7	49	14088	-26	0.70	1997				
rv1.7	58	17537	-25	0.76	1998				
rv1.7	43	14683	-30	0.74	1999				
rv1.7	43	14193	-29	0.81	2000	67	19671	-7	0.72
rv1.8					2001	65	19477	-10	0.67
rv2.0	60	16908	-32	0.75	2002	66	17933	-4	0.71
rv2.3	53	12771	-28	0.76	2003	64	14853	-4	0.66
rv2.6	42	12647	-29	0.6	2004	58	16821	-11	0.80
rv2.7	53	13546	-32	0.66	2005	56	14100	-7	0.70
rv3.1	54	13236	-38	0.76	2006	59	13930	3	0.69
rv3.4	50	12524	-40	0.67	2007	59	13873	9	0.66
rv3.6	64	15928	-19	0.69	2008	62	15180	5	0.70
rv3.8	62	14693	-14	0.71	2009	63	14689	-3	0.71
rv4.0	57	12232	-11	0.75	2010	57	12232	-13	0.75
rv4.4	51	10596	-58	0.53	2011	51	10596	-14	0.50

Table E:15: As Table E:1, but for NO_3^- concentrations in precipitation, [μg(N) l^{-1}]

Original Results					Year	Updated Results (rv4.4)			
Rev.	N_{stat}	Obs.	Bias(%)	Corr.		N_{stat}	Obs.	Bias(%)	Corr.
rv1.7	22	0.43	-11	0.86	1980				
rv1.7	36	0.50	-11	0.78	1985				
rv1.7	38	0.40	-10	0.84	1990	83	0.43	0	0.82
rv1.7	49	0.38	-12	0.75	1995				
rv1.7	46	0.41	-10	0.70	1996				
rv1.7	49	0.35	-13	0.76	1997				
rv1.7	58	0.33	-15	0.78	1998				
rv1.7	43	0.38	-19	0.78	1999				
rv1.7	43	0.35	-18	0.86	2000	67	0.38	-16	0.68
rv1.8					2001	65	0.41	-23	0.52
rv2.0	60	0.36	-32	0.69	2002	66	0.36	-17	0.74
rv2.3	53	0.36	-26	0.70	2003	64	0.38	-14	0.65
rv2.6	42	0.41	-30	0.50	2004	58	0.41	-18	0.58
rv2.7	53	0.39	-31	0.55	2005	56	0.38	-14	0.60
rv3.1	54	0.36	-35	0.69	2006	59	0.34	-8	0.75
rv3.4	50	0.33	-29	0.66	2007	59	0.30	-2	0.80
rv3.6	64	0.28	-17	0.79	2008	62	0.28	-1	0.82
rv3.8	62	0.29	-15	0.66	2009	63	0.28	-6	0.66
rv4.0	57	0.27	-9	0.74	2010	57	0.27	-11	0.76
rv4.4	51	0.34	-23	0.36	2011	51	0.34	-23	0.36

APPENDIX F

Model Evaluation

The EMEP MSC-W model is regularly evaluated against various kinds of measurements, including ground-based, airborne and satellite measurements. As the main application of the EMEP MSC-W model within the LRTAP Convention is to assess the status of air quality on regional scales and to quantify long-range transboundary air pollution, the focus of the evaluation performed for the EMEP status reports is on the EMEP measurement sites.

Since 2009, only parts of this evaluation are included in the printed version of the EMEP status report (see, e.g. plots of normalized differences in Chapter 2). A comprehensive collection of maps, graphs and statistical analyses, including a more detailed discussion of model performance, are freely available as supplementary material from the MSC-W report page on the EMEP website `http://emep.int/mscw/mscw_publications.html`

This year, the evaluation report is found under the link 'Supplementary material to EMEP Status Report 1/2013'. It contains a comprehensive evaluation of the EMEP MSC-W model for air concentrations and depositions in 2011. The report is divided into two chapters, dealing with pollutants responsible for eutrophication and acidification (Nyíri et al. 2013) and ground level ozone (Gauss and Hjellbrekke 2013), respectively.

The agreement between model and measurements in 2011 is visualized as:

- scatter plots for the EMEP MSC-W model domain
- time series for each EMEP station
- horizontal maps combining model results and EMEP measurement data through kriging (also showing normalized differences)

Tables summarize common statistical measures of model score, such as bias, root mean square error, temporal and spatial correlations and the index of agreement (see Chapter 1).

This type of model evaluation is performed on an annual basis and can be downloaded from the same web page also for previous years.

References

Gauss, M. and Hjellbrekke, A.-G.: Photo-oxidants: validation and combined maps, Supplementary material to EMEP Status Report 1/2013, available online at www.emep.int, The Norwegian Meteorological Institute, Oslo, Norway, 2013.

Nyíri, Á., Gauss, M., Semeena, V. S., and Hjellbrekke, A.-G.: Acidifying and eutrophying components: validation and combined maps, Supplementary material to EMEP Status Report 1/2013, available online at www.emep.int, The Norwegian Meteorological Institute, Oslo, Norway, 2013.